2.5.2 Vibratory Ground Motion

The AP1000 is designed for an earthquake defined by a peak ground acceleration (PGA) of 0.30g and the design response spectra specified in Subsection 3.7.1.1, and Figures 3.7.1-1 and 3.7.1-2. The AP1000 design earthquake is referred to as the AP1000 Certified Seismic Design Response Spectra (CSDRS). The AP1000 CSDRS was developed using the Regulatory Guide 1.60 response spectra as the base and modified to include additional high frequency amplification at a control point at 25 Hz. The peak ground accelerations in the two horizontal and the vertical directions are equal. The CSDRS also represents the AP1000 Foundation Input Response Spectra (FIRS) at a hard rock site.

The AP1000 is evaluated for high frequency input using the response spectra specified in Appendix 3I, Figures 3I.1-1 and 3I.1-2. The seismic response spectra given in Figures 3I.1-1 and 3I.1-2 are envelope response spectra with high frequency content.

2D Analyses

Where features of the site are not within the parameters specified for the AP1000, site-specific soil structure interaction analyses may be performed using the 2D SASSI models described in Appendix 3G for variations in site conditions that can be represented in these models. Results should be compared to the results of the 2D SASSI analyses described in Appendix 3G. Such analyses may be used to demonstrate that local features, such as soil degradation properties or backfill, are well within the bounds established by the design cases. If the results are not clearly enveloped at the significant frequencies of response at the six key locations compared with the floor response spectra of the certified design at 5-percent damping, then a 3D SASSI analysis may be required.

3D Analyses

If required, a 3D evaluation will consist of a site-specific dynamic analysis and generation of in-structure response spectra at six key locations to be compared with the floor response spectra of the certified design at 5-percent damping. The certified seismic site design response spectra at the foundation level in the free-field given in Figures 3.7.1-1 and 3.7.1-2 were used to develop the floor response spectra. They were applied at foundation level for the hard rock site and at finished grade level for the soil sites. The site is acceptable if the floor response spectra from the site-specific evaluation do not exceed the AP1000 spectra for each of the locations identified below or the exceedances are justified:

Containment internal structures at elevation of reactor vessel support	Figure 3G.4-5X to 3G.4-5Z
Containment operating floor	Figure 3G.4-6X to 3G.4-6Z
Auxiliary building NE corner at elevation 116'-6"	Figure 3G.4-7X to 3G.4-7Z
Shield building at fuel building roof	Figure 3G.4-8X to 3G.4-8Z
Shield building roof	Figure 3G.4-9X to 3G.4-9Z
Steel containment vessel at polar crane support	Figure 3G.4-10X to 3G.4-10Z

Site-specific soil structure interaction analyses are performed using the 3D SASSI models described in Appendix 3G. The site-specific soil structure interaction analyses use the site-specific soil conditions (including variation in soil properties in accordance with Standard Review Plan 3.7.2 and site-specific soil degradation models). The three components of the site-specific ground motion time history must satisfy the regulatory requirements for statistical independence and enveloping of the site design spectra at 5% damping. Floor response spectra determined from the site-specific analyses should be compared against the design basis of the AP1000 described above.

If the site-specific spectra at foundation level at a rock site exceed the response spectra in Figures 3I.1-1 and 3I.1-2 at any frequency, a site-specific evaluation can be performed similar to that described in Appendix 3I.

This subsection provides a detailed description of the vibratory ground motion assessment for the Units 6 & 7 site and demonstrates compliance with 10 CFR 100.23(c). This assessment uses the guidance from RG 1.208. RG 1.208 incorporates developments in ground motion estimation models; updated models for seismic sources; methods for determining site response; and new methods for defining a site-specific, performance-based earthquake ground motion that satisfy the requirements of 10 CFR 100.23. Identification and characterization of seismic sources lead to the determination of safe shutdown earthquake (SSE) ground motion. This subsection develops the site-specific ground motion response spectrum (GMRS) characterized by horizontal and vertical response spectra determined as free-field motions on the ground surface using performance-based procedures.

The GMRS represents the first part in development of an SSE for a site as a characterization of the regional and local seismic hazard. The GMRS is used to determine the adequacy of the certified seismic design response spectra (CSDRS) for the AP1000 design (RG 1.208). The CSDRS is the SSE ground motion for the site, the vibratory ground motion for which certain structures, systems, and components are designed to remain functional, pursuant to Appendix S to 10 CFR Part 50.

The starting point for the GMRS assessment is the probabilistic seismic hazard analysis (PSHA) conducted by the Electric Power Research Institute (EPRI) for the seismicity owners group (SOG). The EPRI-SOG seismic hazard study is based on the evaluation of seismicity, seismic source models, and ground motion attenuation relationships (Reference 245).

Subsection 2.5.2.1 documents the review and update of the available EPRI earthquake catalog. The earthquake data are reviewed and used to update the EPRI earthquake catalog in Phase 1 of the seismicity update. A Phase 2 catalog of earthquakes is completed and used as a supplement to the EPRI earthquake catalog for the large, frequent, but distant earthquakes of the Caribbean region.

Subsections 2.5.2.2 through 2.5.2.4 address the new information on seismic source models and ground motion characterizations that relates to the 1989 EPRI seismic hazard model, the Cuba area, and the North America-Caribbean plate boundary region. The guidelines outlined in RG 1.208 are discussed in Subsection 2.5.2.4 and are conducted to perform an updated PSHA for the Units 6 & 7 site. The results of this updated PSHA are used to develop uniform hazard response spectra (UHRS) and to identify controlling earthquakes.

Subsection 2.5.2.5 summarizes information about the seismic wave transmission characteristics of the site, including information on the geotechnical properties used for the site response. A detailed discussion of all engineering aspects of the subsurface, including the results of initial and supplemental subsurface investigations, is provided in Subsection 2.5.4.

Subsection 2.5.2.6 describes development of the site-specific horizontal GMRS for the site following RG 1.208, which provides guidance for implementation of the risk-informed/performance-based approach. Site-specific horizontal ground motion amplification factors are developed incorporating uncertainties in site-specific estimates of subsurface soil and rock properties. These amplification factors are then used to scale the hard rock UHRS spectra to develop UHRS at the ground surface accounting for effects of the site-specific geologic/soil column on seismic wave transmission using Approach 2A of NUREG/CR-6728 (Reference 308). Note that the term “hard rock” is used throughout the remainder of this document to designate rock properties used by EPRI (Reference 242) as the basis for development of updated ground motion prediction equations for the central and eastern United States (CEUS) (Reference 242). Subsection 2.5.2.6 also describes vertical GMRS developed by scaling the horizontal GMRS by a frequency-dependent vertical-to-horizontal (V/H) factor. Additionally, results of sensitivity analyses of the GMRS to assess impacts of geotechnical properties

developed through supplemental subsurface investigations described in Subsection 2.5.4 are also addressed.

2.5.2.1 Seismicity and Earthquake Catalog

The seismic hazard analysis conducted by EPRI (Reference 245) relies, in part, on an analysis of historical seismicity in the CEUS to estimate seismicity parameters (rates of seismic activity, Gutenberg-Richter b-value, and maximum magnitude) for individual seismic sources. The historical earthquake catalog used in the EPRI seismic hazard analysis was complete through 1984.

Given the location of the Units 6 & 7 site at the southeast edge of the EPRI-SOG seismic hazard study region, the earthquake data for the site region for all time through mid-February 2008 were reviewed and used to update the EPRI earthquake catalog. These earthquakes were cataloged in Phase 1 of the seismicity update (Subsection 2.5.2.1.2). It was also recognized that there was some potential for a significant contribution to seismic hazard at the site from the large, frequent, but distant earthquakes of the Caribbean region.

The EPRI seismic hazard study did not incorporate contributions to the seismic hazard from sources in the Caribbean region and in the Gulf of Mexico except along the immediate Gulf coast. Therefore, special attention in the update of the EPRI earthquake catalog was given to earthquakes throughout the Gulf of Mexico and the Caribbean region. A Phase 2 catalog of earthquakes was completed as a supplement to the EPRI earthquake catalog for the region for moment magnitude (M_w) 3.0 and larger earthquakes occurring in the Caribbean south of the Phase 1 catalog coverage (Subsection 2.5.2.1.3).

2.5.2.1.1 1988 EPRI Regional Earthquake Catalog

Many seismic networks record earthquakes in the CEUS. An effort was made during the EPRI seismic hazard study to combine available data on historical earthquakes and to develop a homogeneous earthquake catalog that contained all recorded earthquakes for the region. “Homogeneous” means that estimates of body-wave magnitude (m_b) for all earthquakes are consistent, duplicate earthquakes have been removed, non-earthquakes (e.g., mine blasts and sonic booms) have been eliminated, and significant events in the historical record have not been missed. The EPRI earthquake catalog (Reference 246) is the basic input data source for assessing seismicity parameters such as earthquake recurrence rates and maximum magnitude.

2.5.2.1.2 Updated Seismicity Data in the Phase 1 Investigation Region

The Phase 1 earthquake catalog used in the study region (Figure 2.5.2-201) is an updated catalog to determine whether regional earthquake patterns and seismicity parameters developed from the EPRI earthquake catalog (Reference 246) remained unchanged. RG 1.206 specifies that earthquakes of modified Mercalli intensity (MMI) greater than or equal to IV or magnitude greater than or equal to 3.0 “that have been reported within 200 miles (320 kilometers) of the site” should be listed. The location of the Units 6 & 7 site was taken as 25.4241° N and 80.3332° W. In updating the EPRI earthquake catalog, a latitude-longitude window of 22° to 35° N, 100° to 65° W was used. This large window, called the Phase 1 seismicity investigation region, incorporates the 200-mile (320-kilometer) radius “site region” and all seismic sources north of the Caribbean contributing significantly to earthquake hazard at the site.

Table 2.5.2-201 lists the earthquakes for the Phase 1 investigation region of uniform magnitude (Rmb) ≥ 3.0 or maximum intensity value (I_0) ≥ IV.

Thirty-four regional earthquake catalogs were considered in the development of the Phase 1 earthquake catalog. The earthquake catalogs used for this initial update are listed below in the order of their preference for duplicate events removal and earthquake parameter characterization:

- Electric Power Research Institute (Reference 246)
- Updated Engdahl (NENG) (Reference 249)
- Engdahl and Villasenor (EV02) (Reference 250)
- Villasenor et al. (ISSv) (Reference 333)
- Villasenor and Engdahl (VE07) (Reference 332)
- Perez (PEREZ) (Reference 298)
- Wysession et al. (Reference 338)
- Cuba Catalog (CUBA) (Reference 205)
- Southeastern U.S. Seismic Network (SEUSN) (Reference 341)
- Frohlich and Davis (FD02) (Reference 253)
- Missouri-Tennessee Regional Data, 1974-1994 (SLU) (Reference 307)
- Southeast Blacksburg Catalog (BLA) (Reference 307)
- Tennessee Earthquake Information Center (TEIC) (Reference 307)
- Decade of North America Geology (DNA) (Reference 307)
- Central U.S. Catalog (OWN) (Reference 307)
- NEIC Preliminary Determination of Epicenters (PDE, PDE-W, PDE-Q) (Reference 292)
- Panamerican Institute of Geography and History (IPGH) (Reference 307)
- National Geophysical Data Center USGS “PDE” Catalog (Reference 307)
- Advanced National Seismic System (ANSS) (Reference 204)
- International Seismological Centre (ISC) (Reference 265)
- Puerto Rico Seismic Network (PRSN) (Reference 305)
- Middle America Seismograph Consortium (MIDAS) (Reference 284)
- Regional Data from Trinidad (TRN) (Reference 307)
- Earthquake History of the U.S. (EQH) (Reference 307)
- NEIC Significant U.S. Earthquakes (USHIS) (Reference 340)

- Historical U.S., 1568-1984 (STO) (Reference 307)
- U.S. Network Catalog (USN) (Reference 307)
- Gutenberg and Richter (G-R) (Reference 307)
- NEIC Eastern, Central, and Mountain States of U.S. (SRA) (Reference 288)
- NEIC Mexico, Central America and Caribbean, 1900-1979 (MCAC) (Reference 289)
- Regional Catalog for the Caribbean Sea (CARIB) (Reference 307)
- Mexico Composite Catalog (Reference 307)
- Incorporated Research Institutions for Seismology (IRIS) (Reference 264)
- Utsu Catalog (UTS) (Reference 307)

No events were found in either the MCAC (Reference 289) or VE07 (Reference 332) catalogs. In the event of duplicate entries for a given earthquake in the remaining 32 catalogs, earthquake location and size were selected with the following order of preference: first the EPRI earthquake catalog, then special studies of regional earthquakes, then routine listings from regional catalogs, and finally routine listings from global catalogs.

For the purpose of developing earthquake recurrence statistics in the Phase 1 investigation region, it was necessary to eliminate dependent events (that is, foreshocks, aftershocks, and secondary events of an apparent seismicity cluster). The EPRI earthquake catalog distinguishes MAIN (independent) events from non-MAIN (dependent) events. The few events that were judged to be dependent events, based on the EPRI criteria for MAIN vs. non-MAIN and on apparent spatial and temporal similarity between events, were removed from the Phase 1 update of the EPRI earthquake catalog. The remaining events in the Phase 1 investigation region were assessed to be equivalent to EPRI MAIN events.

2.5.2.1.2.1 Assessment of Best Estimate and Uniform Magnitude

For the EPRI-SOG methodology, two scales of magnitudes are required for each event in the catalog: (a) best, or expected, estimate of body-wave magnitude (E[m_b], also referred to as Emb in the 1988 EPRI study; Reference 246); and (b) uniform magnitude (m_b*, also referred to as Rmb in the 1988 EPRI study; Reference 246). These magnitudes were applied in the Phase 1 earthquake catalog where the EPRI earthquake catalog was considered in the development of the reevaluated earthquake catalog.

Best Estimate Magnitude Emb

Various magnitude scales may be available for a given event. Each available magnitude was considered in the evaluation of Emb for that event. If a body-wave magnitude (m_b) was available, it was adopted directly. Other magnitudes were converted to the best estimate magnitude Emb using the Equation 4-1 and Table 4-1 in the 1988 EPRI study (Reference 246):

$$Emb = 0.253 + 0.907 \cdot Md \qquad \text{Equation 2.5.2-1}$$

$$Emb = 0.655 + 0.812 \cdot ML \qquad \text{Equation 2.5.2-2}$$

$$Emb = 2.302 + 0.618 \cdot MS \qquad \text{Equation 2.5.2-3}$$

where, Md is duration (or coda) magnitude, ML is "local" magnitude, and MS is surface-wave magnitude.

If no explicit magnitudes are available for an event, an available I0 was converted to Emb, using a relationship from Table 4-1 in the 1988 EPRI study (Reference 246):

$$Emb = 0.709 + 0.599 \cdot I_0 \qquad \text{Equation 2.5.2-4}$$

The EPRI PSHA study expressed maximum magnitude (Mmax) values in terms of m_b, whereas most modern seismic hazard analyses describe Mmax in terms of moment magnitude (M_w). To provide a consistent comparison between magnitude scales, m_b was related to M_w using the arithmetic average of three equations, or their inversions, presented by Atkinson and Boore (Reference 210), Frankel et al. (Reference 252), and EPRI (Reference 244). Throughout the discussion in Subsections 2.5.2.2 and 2.5.2.3, the largest values of Mmax distributions assigned by the Earth Science Teams (ESTs) (Reference 247) to seismic sources are presented for both magnitude scales (m_b and M_w). For example, EPRI m_b values of Mmax are followed by the equivalent M_w value. Conversion values from m_b to M_w and M_w to m_b are provided in Table 2.5.2-202. Body-wave magnitudes converted from moment magnitudes in this fashion were considered the best estimate magnitude Emb. For each event, the final Emb was taken as the largest best estimate magnitude Emb.

Uniform Magnitude Rmb

The EPRI-SOG seismic hazard methodology modifies the Emb values to develop a uniform magnitude (Rmb), m_b^*, to assess an unbiased estimate of seismicity recurrence parameters. EPRI Equation 4-2 (Reference 246) indicates that the equation from which m_b^* is estimated from $E[m_b]$ and the standard deviation of m_b, σ_{mb}, (referred to as Smb in the 1988 EPRI study; Reference 246) is:

$$m_b^* = E[m_b] + (1/2) \cdot \ln(10) \cdot b \cdot \sigma^2_{mb} \qquad \text{Equation 2.5.2-5}$$

where,

$b = 1.0$

Based on an examination of the EPRI-SOG catalog, particularly σ_{mb} (Smb) values listed as related to the various size measures from which they were determined, values for σ_{mb} (Smb) were estimated for each earthquake in the updated catalog, and m_b^* (Rmb) values were calculated (Equation 2.5.2-5) for each event added to the updated earthquake catalog.

The result of the above process was a homogeneous earthquake update of the EPRI earthquake catalog (Reference 246) for earthquakes occurring within the Phase 1 seismicity investigation region (Table 2.5.2-201). For the purpose of earthquake recurrence analysis, all events added for the update are assumed to be independent events.

2.5.2.1.3 Caribbean Seismicity Data in the Phase 2 Investigation Region

Occurrence of large earthquakes in the region south of the Phase 1 coverage suggested that additional examination of earthquakes in the Caribbean region was needed (Figure 2.5.2-201). The original EPRI-SOG analysis indicated that earthquake recurrence parameters had not been evaluated for the Caribbean region. The occurrence of recent moderate to large earthquakes in the

Caribbean region indicated the potential for a significant contribution to seismic hazard at the site from sources in this region. This required a careful evaluation of Caribbean seismicity, both before and after the development of the EPRI earthquake catalog.

In order to investigate the potential of the Caribbean region to contribute to the seismic hazard of the site, it was necessary to consider a larger area of investigation. A latitude-longitude window of 15° to 24° N, 100° to 65° W was used to create a new catalog supplement to the EPRI earthquake catalog. This large window, called the Phase 2 seismicity investigation region, incorporates all events with $M_W \geq 3.0$ and all Caribbean seismic sources that would be expected to contribute significantly to the earthquake hazard of the site. Table 2.5.2-203 lists the earthquakes for the Phase 2 investigation region for the larger events of moment magnitude $M_W \geq 6.0$. The Phase 2 earthquake catalog combined with the Phase 1 earthquake catalog described in Subsection 2.5.2.1.2, allows an improved characterization of the seismicity within the project seismicity investigation window.

There are many earthquake catalogs covering the Phase 2 seismicity investigation region, but no single published catalog includes everything for assessing earthquake occurrence. Thus, several regional and global catalogs were combined to make a new catalog supplement. These catalogs cover different time, space, and magnitude ranges with varying accuracy.

For instance, the magnitudes of earthquakes in the Cuba catalog (Reference 205) have been estimated using various methods from historical macroseismic data (that is, based on non-instrumental felt and damage effects), instrumental data from international agencies, and instrumental data from the Cuban local network. The majority of earthquakes in the Cuba catalog have an estimate of intensity-based magnitude. In these cases, the magnitude scale, M_I, of Garcia et al. (Reference 254) is used, fitting the isoseismals (contour lines of equal intensity). For earthquakes recorded by the Cuban seismographic network, the surface-wave magnitudes (M_S), which is intended to be equivalent to the intensity-based magnitude (M_I), are obtained by the Alvarez et al. (Reference 237) regression relationships. The remaining magnitudes in the Cuba catalog are adopted from international agency compilations.

Note that most earthquakes in the Cuba catalog (Reference 205), whose magnitudes have been obtained from macroseismic data, do not have well-constrained locations and depend on inherently subjective information. Comparison of magnitude scales in the Cuba catalog with more recent earthquakes recorded by other seismological agencies shows that the M_I for the earthquakes reported in the Cuba catalog often appear to have been overestimated.

Therefore, reliance on reports of earthquake effects in the Cuba area has apparently resulted in an overestimate of earthquake size in some cases. Nevertheless, this Cuba Catalog (Reference 205) data is the best available and, in spite of its likely conservatism, was used to prepare a dataset for Cuba characterized by only one magnitude entry for each event (Subsection 2.5.2.1.3.1).

Besides the Cuba catalog (Reference 205), 22 significant regional earthquake catalogs were considered in the development of the Phase 2 earthquake catalog within the Phase 2 investigation region. The earthquake catalogs used for this phase of the update are listed below in the order of their preference for duplicate events removal and earthquake parameter characterization:

- Updated Engdahl (NENG) (Reference 249)
- Villasenor et al., 1997 (ISSv) (Reference 333)
- Villasenor and Engdahl, 2007 (VE07) (Reference 332)
- Engdahl and Villasenor, 2002 (EV02) (Reference 250)

- Perez (PEREZ) (Reference 298)
- Puerto Rico Seismic Network (PRSN) (Reference 305)
- International Seismological Centre (ISC) (Reference 265)
- Advanced National Seismic System (ANSS) (Reference 204)
- NEIC Preliminary Determination of Epicenters (PDE, PDE-W, PDE-Q) (Reference 292)
- National Geophysical Data Center USGS “PDE” Catalog (Reference 307)
- NEIC Mexico, Central America and Caribbean, 1900-1979 (MCAC) (Reference 289)
- NEIC Significant Worldwide Earthquakes (NOAA) (Reference 307)
- Cuba Catalog (CUBA) (Reference 205)
- Regional Catalog for the Caribbean Sea (CARIB) (Reference 307)
- Panamerican Institute of Geography and History (IPGH) (Reference 307)
- Middle America Seismograph Consortium (MIDAS) (Reference 284)
- Gutenberg and Richter (G-R) (Reference 307)
- Mexico Composite Catalog (Reference 307)
- Decade of North America Geology (DNA) (Reference 307)
- Earthquake History of the U.S. (EQH) (Reference 307)
- Regional Data from Trinidad (TRN) (Reference 307)
- U.S. Network Catalog (USN) (Reference 307)
- Wysession et al., 1995 (Reference 338)

Duplicate entries from these 23 catalogs were removed under a process that included selection of preferred entries for location and size parameters based on a regionally defined preference order for Phase 2 of the seismicity update to yield an initial earthquake catalog. As implied by the above preference order, the earthquake location and size were selected based on seismicity data from local or international seismic networks with the following order of preference: first special studies of local earthquake catalogs, then routine listings from regional catalogs, and finally routine listing from global catalogs.

After an initial uniform earthquake catalog was compiled (Subsection 2.5.2.1.3.1), foreshocks and aftershocks were eliminated using the 1974 time-distance window method of Gardner and Knopoff (Reference 256). In this method dependent events (classified as those that fall within specified time and space intervals around the mainshock and that are of smaller magnitudes) are eliminated to obtain a data set of mainshocks that is assumed to show a Poisson distribution in time.

The Gardner-Knopoff (Reference 256) method is proposed as an appropriate technique for removing dependent events for an earthquake catalog such as the Phase 2 catalog, which has variable quality

station coverage in different regions and over different time periods. That is, the method does not depend upon details of small magnitude earthquake completeness to help identify mainshocks (Reference 314).

Dependent or "related" events of a mainshock are identified within time-distance windows as a function of the time, location, and magnitude of the mainshock. The first earthquake in the catalog is declared provisionally to be a mainshock event, and then all equal or smaller magnitude related events are identified and eliminated as aftershocks from the catalog using the specified time-distance window parameters. The next earthquake in the rest of the catalog is then declared to be the next provisional mainshock event, and this cluster removal procedure is repeated, this time considering related events both before and after this mainshock. Equal or smaller magnitude related events occurring before the mainshock are marked for deletion as foreshocks—possibly including a previously assumed mainshock, that may now be identified as a foreshock of the current provisional mainshock—and equal or smaller magnitude related events occurring after the mainshock are marked for deletion as aftershocks. This procedure is repeated throughout the compilation of the entire Phase 2 earthquake catalog.

A listing of values selected for the shape of the time-distance envelope is given in Table 1 of Gardner and Knopoff (Reference 256). There is an upper-bound (enveloping) linear relationship between time and magnitude, such that all aftershocks occur at times less than the envelope value. There is also an upper-bound linear relationship between distance and magnitude that is used in a similar way to the time bounds. The original table proposed by Gardner and Knopoff (Reference 256), which gives discrete time-distance envelope values, is generalized for all magnitudes by interpolating it in the form of the following smooth linear relationships:

$$\text{Distance (km)} = 10^{(0.1238M + 0.983)} \qquad \text{Equation 2.5.2-6}$$

$$\text{Time (days)} = 10^{(0.032M + 2.7389)} \text{ for } M \geq 6.5 \qquad \text{Equation 2.5.2-7}$$

$$= 10^{(0.5409M - 0.547)} \text{ for } M < 6.5$$

where, “M” is assumed to be equivalent to M_w. As an example, any earthquake within 918 days after an $M_w = 7.0$ earthquake and with an epicenter location within about 71 kilometers of the epicenter of the $M_w = 7.0$ mainshock, is identified as an aftershock. For $M_w \geq 6.5$, the slope of the time window is less than $M_w < 6.5$ to conform with improved estimates of the shape of the envelope given by Gardner and Knopoff (Reference 256).

Figure 2.5.2-201 shows the Units 6 & 7 site and its associated site region, the defined latitude-longitude windows, both the original EPRI earthquake catalog and updated seismicity data for the Phase 1 and Phase 2 investigation regions. These earthquake catalogs are used later in Subsection 2.5.2.4 to develop earthquake recurrence parameters for the Gulf of Mexico and Caribbean region for use in the PSHA of the site.

2.5.2.1.3.1 Uniform Magnitude M_w

In this subsection, the rationale for selecting moment magnitude (M_w) as the uniform magnitude scale for the Phase 2 earthquake catalog is discussed and the magnitude conversion process adopted for all events in the Cuba and Caribbean Phase 2 earthquake catalog is described in detail.

Rationale for Selecting M_w as the Uniform Magnitude Scale for the Phase 2 Catalog

Seismologists performing conventional probabilistic seismic hazard analyses, as well as development of ground motion prediction equations (References 300 and 344), prefer the use of M_w

over other magnitude scales, including m_b scale, because it is a more direct indication of the seismic energy associated with an earthquake, particularly for both shallow and deep focus earthquakes with large fault dimensions and/or complex rupture mechanisms that occur in the Caribbean. The m_b magnitude scale saturates, or is progressively insensitive to, energy release, beginning with magnitudes greater than approximately 5.0 due to the difference in the period and the seismic-wave type used to determine the magnitude size. While the magnitudes of earthquakes within the CEUS region have generally and traditionally been adequately represented by the m_b scale, the largest events in the Caribbean are not. This rationale for selecting moment magnitude was the basis for its use in developing the Phase 2 earthquake catalog.

Also, the update of the Phase 1 earthquake catalog, as discussed in Subsection 2.5.2.1.2, was constrained to maintain the magnitude scale in m_b because both the EPRI-SOG seismicity catalog and recurrence characterization of the EPRI-SOG seismic sources use the m_b scale.

NUREG-0800 Section 2.5.2 and RG 1.206 specify that the earthquake catalog should include all earthquakes having Modified Mercalli Intensity (MMI) greater than or equal to IV, or magnitude greater than or equal to 3.0 that have been reported within 320 kilometers (200 miles) of the site. Large earthquakes outside of this area that would impact the SSE (in NUREG-0800) or the GMRS (in RG 1.206) should be reported. The Phase 1 and Phase 2 catalogs were developed to meet these requirements. The magnitude scale is not explicitly specified in these requirements, although both documents later state that "magnitude designations such as m_b, M_L, M_s, M_w should be identified." There is no specification of the magnitude scale for the earthquake catalog given in RG 1.208.

The magnitude conversion relations between the moment magnitude scale and many other scales, such as m_b scale, show that the magnitudes less than about 4.5 (very short fault lengths) are assumed to be numerically equivalent to M_w and that the conversion relations are nonlinear at large magnitude values to reflect the saturation of some magnitude scales, specifically m_b scale (Reference 346). Therefore, in the development of the Phase 2 catalog, all small earthquakes of any magnitude scale less than 4.5 were assumed to be numerically equivalent to M_w. As a result of this assumption for small events, the selected threshold magnitude scale $M_w \geq 3.0$ for the Phase 2 earthquake catalog and m_b (or (E)m_b) ≥ 3.0 for the Phase 1 earthquake catalog presents no inconsistency in terms of minimum size or minimum seismic energy of a given earthquake considered in the two catalogs. Therefore, under the process used to develop moment magnitudes for the Phase 2 catalog, all earthquakes of magnitude 3.0 and larger, regardless of characterization as moment magnitude or body-wave magnitude, are included in both Phase 1 and Phase 2 earthquake catalogs, and there is no impact on the number of earthquakes in the two earthquake catalogs associated with the different magnitude scales used in the two earthquake catalogs.

Magnitude Conversion Process for Earthquakes in the Caribbean Region

The differences that exist among published seismotectonic region-specific magnitude conversion relations make the selection of appropriate relations for a given region important and, if such relations are not available, difficult. Seismic network operational histories are such that catalogs of events in a given region contain earthquakes located with different location programs. These programs use different station configurations and different crustal-velocity models with magnitudes calculated using different calibration. Therefore, conversions of diverse best estimates of magnitudes determined in different regions to a given uniform magnitude scale may show notable differences, depending on tectonic setting (Reference 240).

In contrast to the CEUS tectonic environment considered for the Phase 1 earthquake catalog, the Caribbean region with its (1) different tectonic environments (e.g., plate boundary and near plate boundary shallow crustal faults and subduction zones), (2) different magnitude scales, and (3) different seismic network instrumentation and operational histories, required consideration of different global or regional magnitude conversion relationships for the Phase 2 earthquake catalog development.

To contrast the nature of earthquakes from the Caribbean region to the CEUS region, a magnitude conversion process was developed to consider the various magnitude scales used in the original source catalogs considered in the development of the Phase 2 earthquake catalog, and these various magnitude scales were converted to M_w.

Among the various earthquake source catalogs used for compiling the Phase 2 catalog, there were 19 different magnitude types that needed to be converted to moment magnitude. These different magnitude scale conversions are discussed further below based on the following simplified process. First, magnitudes of any type less than 4.5, with reference to the Heaton et al. (Reference 346) correlation plot described below, were assumed to be equivalent to M_w directly. For magnitudes of any type of 4.5 and larger, the following simplified process was followed:

- Moment magnitudes were already moment magnitudes, so no conversion was necessary.
- Surface-wave magnitudes M_s were converted to M_w considering the Ekstrom and Dziewonski relations (Reference 240) and the Kanamori relation (Reference 269).
- Body-wave magnitudes m_b were converted to M_s considering the Garcia et al. relation (Reference 254) and then the above process of conversion from M_s to M_w was followed.
- Intensity-based magnitudes in the Cuba catalog were considered equivalent to M_s magnitudes (Reference 254) and then the above process of conversion from M_s to M_w was followed.
- All other magnitude types were considered equivalent to m_b and then the above process to convert from m_b to M_s to M_w was followed.

The Heaton et al. (Reference 346) magnitude correlations, following similar work by Kanamori (Reference 347), plot various magnitude scales relative to M_w for a seismotectonic setting more similar to the Caribbean than the CEUS region (e.g., western U.S. region or other active plate boundary regions), allowing conversion of Caribbean earthquake magnitudes in other scales into moment magnitude. These magnitude-scale plots graphically show relationships between the moment magnitude scale and several other magnitude scales, applicable magnitude ranges, and how they are nonlinear to reflect the saturation of some of the magnitude scales.

Following is a detailed summary of the approach that was used to provide specific magnitude scale conversions to estimate M_w for the Phase 2 earthquake catalog.

Specific Magnitude Scales Used in the Phase 2 Earthquake Catalog

The Phase 2 earthquake catalog developed for the Caribbean region contains 19 different measures of size for earthquakes that have occurred in notably different tectonic regions as compared to the CEUS region.

- Moment magnitudes (M_w)

The moment magnitude scale, which provides an estimation of total energy released in an earthquake, was the preferred magnitude scale in the Caribbean Phase 2 catalog under the rationale given above. Therefore, for all earthquakes in Phase 2 earthquake catalog that were originally reported in the M_w magnitude scale, these M_w values were directly included in the catalog.

- Surface-wave magnitudes (M_s)

The surface-wave magnitude (M_s) scale is commonly used for shallow events larger than M_s 5.0 (References 347 and 350) which, by definition, are earthquakes where surface waves may have

been generated. Since the surface-wave magnitude gives the poorest results for small earthquakes or those deep or at intermediate depth, there are relatively few earthquakes of this type of magnitude scale in the Phase 2 catalog. For those reported earthquakes with M_s less than 4.5, these M_s magnitude scales were considered to be numerically equivalent to M_w. For M_s values equal to or greater than 4.5, the 1988 global surface-wave magnitude to average seismic moment (M_o) conversion relations of Ekstrom and Dziewonski (Reference 240) and then the seismic moment-to-moment magnitude conversion relation of Kanamori (Reference 269) was used to convert surface-wave magnitudes to M_w in the Phase 2 earthquake catalog development.

- Body-wave magnitudes (m_b)

The Heaton et al. (Reference 346) m_b-M_w magnitude correlation plot suggests that body-wave magnitude (m_b) less than about 4.5 are consistent with M_w, and thus, they were assumed to be numerically equivalent to M_w for the Caribbean region. This consideration is also consistent with USGS Open File Report 97-464 (Reference 350) for body-wave magnitudes in the western U.S. region.

As may also be seen in the Heaton et al. (Reference 346) magnitude correlation plot, there is an issue of saturation of the m_b scale beginning with magnitudes larger than approximately 5.0. The m_b scale stops increasing with increasing earthquake size at about magnitude 6.4 corresponding to a moment magnitude of approximately 7.5. Therefore, for m_b magnitudes of 4.5 and larger the magnitude conversion relation for m_b to M_s from the Garcia et al. study (Reference 254) was used, and then the M_s to M_w scaling, discussed above, was applied for these larger m_b values in the Caribbean Phase 2 catalog.

- Intensity-based magnitudes (M_I and M_k) in the Cuba catalog

The majority of earthquakes in the Cuba catalog have an estimate of intensity-based magnitude, M_I and M_k, as discussed in the Garcia et al. study (Reference 254). Both of these magnitude types are considered to be correlated to coda or duration magnitudes [see below]. For the magnitude conversion process, where there were no region-specific magnitude conversion relations for intensity-based magnitudes, as well as none for coda- or duration-magnitudes, to M_w, these M_I and M_k magnitudes were taken as equivalent to M_w for magnitudes less than 4.5, following Heaton et al. (Reference 346), and equivalent to M_s for magnitudes 4.5 and larger, following the Garcia et al. study (Reference 254). The M_s magnitude scale values were then converted to M_w as described above.

- Local, Duration, and Coda magnitudes (M_L, M_d, DR and M_c)

The local magnitude (M_L), duration magnitude (M_d), sometimes designated “DR” or “M_D” in the National Geophysical Data Center (NGDC) database, and coda magnitude (M_c) are three types of measurements for earthquakes that are used to determine the local magnitudes and are conventionally considered equivalent. The instrumental M_c and M_d are typically reported for small and moderate magnitude earthquakes less than approximately 6.0, while it is found that M_L is also reported for larger earthquakes up to about 7.0. These three magnitude scales in the Phase 2 earthquake catalog, which are provided by different seismic networks with varying operational histories and different station calibrations, are comparable on average to M_w for magnitudes less than 4.5 in the Phase 2 earthquake catalog (References 346 and 350). Nuttli and Herrmann (Reference 351) report that M_L and m_b values are nearly equal in the western United States. Given the common equivalence of M_L, M_d, and M_c magnitudes and the Nuttli and Herrmann observation, these magnitudes when larger than 4.5 are considered equivalent to m_b and converted to M_w as detailed above.

- Broadband body-wave magnitudes (m_B)

There are also some earthquakes larger than 6.0 in the Phase 2 catalog that are designated broadband body-wave magnitude (m_B). The main advantage of m_B magnitude scale rather than M_S is its applicability to both shallow and deep earthquakes. These m_B magnitude-scale events in the Phase 2 catalog are considered to be equivalent to M_S over the applicable magnitude range of events between about 6.0 and 8.0 (References 346 and 347), and then converted to M_W as described above.

- Intensity-based magnitudes ($M(I_o)$), not in the Cuba catalog

These magnitudes are estimated from maximum intensity (I_o) using the Gutenberg-Richter (Reference 345) relationship, which correlates to local magnitude M_L. Therefore, these earthquakes are converted from M_L to M_W as described above.

- Equivalent local and coda-duration magnitudes (m_1, m_2, fm, xm, MA, and m_t)

The PRSN earthquake catalog, which locally collects the events in the Caribbean region, has recorded earthquakes whose magnitudes are determined using different local magnitude relations (m_1 and xm), as well as different magnitude-coda duration relations (m_2 and fm) – the xm and fm magnitudes are determined using the earthquake location program Hypoellipse (Reference 348). An event less than magnitude 3.0, excluded from the Phase 2 catalog, is reported as a type MA magnitude, attributed to PRSN – it may be expected that this small magnitude is one of or an average of the other PRSN magnitudes. Also reported in the PRSN catalog are earthquakes from the Jamaica Seismic Network (JSN), which determines average coda magnitudes (m_t) based on the regression between standard m_b and log of the signal duration (Reference 352). As for local, duration, and coda magnitudes described above when greater than 4.5 these magnitudes are considered equivalent to m_b and are converted to M_W.

- Unspecified magnitudes (nk and MG)

Finally, there are some earthquakes in the Phase 2 catalog with unknown magnitude scale labeled “nk” or “ ” (e.g., the computational method was unknown and could not be determined from published sources) as well as an unspecified magnitude scale labeled “MG” (e.g., magnitudes either have been reported by the contributor without listing the type [e.g., "MG 3.5"] or have been computed using procedures which are not defined by the magnitude types routinely reported). These types of earthquakes were considered to be equivalent to m_b for small ($3 \le M_W < 4.5$) and moderate ($4.5 \le M_W < 6$) earthquake magnitudes in the Phase 2 catalog. Lamarre and Shah (Reference 349) have plotted the unspecified magnitude scales versus M_L for the NGDC database used in the Phase 2 earthquake catalog, and have indicated that it is very closely approximated by the M_L and m_b for earthquakes in magnitude range less than about 5.0. Taken as equivalent to m_b, these magnitudes were converted to M_W as described above.

Since the types of data used in determination of these magnitude scales are very different from region to region (e.g., observational errors and intrinsic variations in source properties), it is important to establish tectonically-similar regional magnitude scale correlations (Reference 347). Therefore, it should be emphasized that this magnitude conversion process was not incorporated into Phase 1 earthquake catalog that includes all events in the CEUS region with a notably different tectonic environment as compared to the Caribbean region (Subsection 2.5.1).

2.5.2.1.4 Final Earthquake Catalogs

The objective of compiling earthquake catalogs for the Units 6 & 7 site was to develop an improved characterization of seismicity for all time within the seismicity investigation region (15° to 35° N, 100° to 65° W), which is used to not only compare to the EPRI-SOG earthquake catalog, as it had been used in the development of the seismic source characterization for the EPRI-SOG seismic hazard

study, but also to suggest and facilitate characterization of possible additional seismic sources to the south of the original EPRI-SOG CEUS study region.

The final earthquake catalog consists of two separate catalogs. The earthquake catalog for the Phase 1 seismicity investigation region (22° to 35° N, 100° to 65° W) is primarily the earthquakes in the EPRI-SOG catalog supplemented by earthquakes from several additional earthquake catalogs. Table 2.5.2-201 lists the earthquakes for the Phase 1 investigation region for which the events are Rmb ≥ 3.0 or intensity I_0 ≥ IV through mid-February 2008. The earthquake catalog for the Phase 2 seismicity investigation region (15° to 24° N, 100° to 65° W) is a composite of several earthquake catalogs appropriate for Cuba and the Caribbean for events that have moment magnitude M_w ≥ 3.0 for all years through mid-March 2008. Table 2.5.2-203 lists the earthquakes for the Phase 2 investigation region for the larger events of moment magnitude M_w ≥ 6.0.

It should be noted that there is a 2-degree overlap in the Phase 1 and Phase 2 regions of the Units 6 & 7 seismicity investigation—the region between 22° N and 24° N. As elaborated later in discussions about the seismic sources, different magnitude scales were required for characterization of the EPRI-SOG sources in the northern portion of the investigation region, as compared to the Caribbean sources in the southern portion. The 2-degree overlap of the coverage of the two phases of seismicity update allowed for completeness and consistency of seismicity characterization of each subregion. In the plot of seismicity for the investigation region in Figure 2.5.2-201, the seismicity of Phase 2 is presented in the 2-degree overlay area to fully encompass Cuba seismicity.

The distribution of epicenters indicated that the largest density of earthquakes was located along the Caribbean transform fault zones. Within the updated earthquake catalog there are two moderate seismic events in the Gulf of Mexico that are significant for an updated characterization of the regional seismicity. These are (1) a possible M_w 5.1 (m_b 5.6) earthquake or a possible landslide event that occurred on February 10, 2006, offshore of the Louisiana coast within the Gulf of Mexico (Subsection 2.5.2.4.3.1.2), and (2) a M_w 5.8 (m_b 5.9) earthquake that occurred on September 10, 2006, off the Florida coast within the Gulf of Mexico (Subsection 2.5.2.4.3.1.1).

A moment-tensor source can be used to model the surface waves generated by the possible February 10, 2006, earthquake if the earthquake centroid is placed within a few miles of the earth's surface in a medium with a very low shear modulus. The explanation for the February 10 earthquake that is currently in best agreement with the observed seismic data is a gravity-driven displacement surface within a thick shallow sedimentary wedge (Reference 293).

The focal mechanism for the September 10, 2006, earthquake indicates a reverse sense of motion, and the earthquake depth is reported as 14 to 19 miles (22 to 31 kilometers) (Reference 290). This mechanism is that of an earthquake caused by tectonically driven stresses within the earth's crust.

2.5.2.1.5 Periods of Completeness for the Offshore Florida Earthquakes

The EPRI seismic hazard methodology (Reference 246) uses estimates of periods of completeness for the reporting of earthquakes as a function of magnitude. This methodology employs a matrix of probability of detection of earthquakes for an area for selected ranges of time-before-present and magnitude. The purpose of this subsection is to develop detection probability matrices for the areas in the Gulf of Mexico and off the coast of Florida where such information is not available in the original EPRI parameterization (Reference 243), but is necessary for the complete characterization of updated EPRI-SOG seismic sources (Figure 2.5.2-202). Matrices for three regions—referred to as “Gulf of Mexico,” “Near Florida,” and “Near Atlantic”—are used later in Subsection 2.5.2.4 to develop EPRI-consistent earthquake recurrence parameters for use in the PSHA of the site.

Gulf of Mexico

Table 2.5.2-204 lists the 26 earthquakes within the Gulf of Mexico seismicity recurrence region, considered EPRI MAIN or independent events that were used to develop the matrix of detection probability for this area. This matrix was prepared to be consistent with the 1988 EPRI seismic hazard methodology. Generation of the matrix of detection probability used, as a conservative guideline, the adjacent EPRI matrices of detection probability available onshore. The 1988 EPRI seismic hazard study used a detailed analysis of United States demographics and history, number, quality, and distribution of seismographic instruments to develop matrices of probability of completeness as a function of time period, gridded area, and magnitude interval. Given uneven population distributions over time and uneven deployment of seismographic networks these completeness probability matrices also vary by location. EPRI “Incompleteness Regions” 2 and 3 are closest to the Gulf of Mexico seismicity recurrence region (Reference 243, Table 5-1) — Figure 2.5.2-202.

It was assumed that the probabilities of earthquake detection for the Gulf of Mexico are less than those given for onshore coastal locations for comparable time periods. The procedure followed for estimating detection probabilities for the Gulf of Mexico was, therefore, to start with an available EPRI matrix, suggesting the lowest probabilities along the shoreline—that is, EPRI Incompleteness Region 2, as it has lower detection probabilities than Incompleteness Region 3—and to assume lower probabilities of detection within the Gulf of Mexico.

The first matrix shown in Table 2.5.2-205 is a version of the EPRI Incompleteness Region 2 matrix, modified to add additional years since 1984 (the last complete year in the 1988 EPRI earthquake catalog). The latest bin time period of the Incompleteness Region 2 matrix (1975–1983) has detection probabilities of 1.00 for all magnitude bins. Therefore, given that detection probability would not be expected to decrease with time, additional time bins with detection probabilities of 1.00 for all magnitudes were appended to the Incompleteness Region 2.

The first matrix of detection probability shown in Table 2.5.2-205 is appropriate for much of the on, or very near onshore sites of seismic activity of the Gulf of Mexico. This matrix may be used for seismicity occurring through the year 2007.

In developing the detection probability of matrix appropriate for the Gulf of Mexico region, the modified Incompleteness Region 2 matrix in Table 2.5.2-205 was qualitatively modified in consideration of the following constraints:

- For a given magnitude bin, detection probability for a given time bin would be expected to be the same or more than the detection probability of an adjacent earlier time bin. That is, the overall trend is for detection probabilities for a given magnitude interval to increase with time.

- For a given time bin, the probability of earthquake detection for a given magnitude bin would be the same or more than the detection probability for an adjacent smaller magnitude bin. That is, the overall trend is for detection probabilities for a given time interval to increase with magnitude.

- Given the lack of regional seismographic stations in the Gulf of Mexico, as well as the obvious lack of felt or damage reports in the Gulf, detection probabilities for the Gulf of Mexico are expected to be no higher for any magnitude and time bin than that corresponding to the nearest onshore location of lowest detection probabilities.

- It was assumed that after the advent of the World-Wide Standardized Seismograph Network in the mid-1960s most earthquakes of magnitude 5.5 and greater would be detectable and recorded (Reference 250).

- In general, global b-values tend to average about 0.8 to 1.2 (Table 2 of the 2002 Engdahl and Villasenor study [Reference 250] and Table 4-7 of the 1994 Johnston et al. study [Reference 268] for stable continental regions). It was assumed that a value within this range is reasonable for the Gulf of Mexico.

The time intervals of the matrix of detection probabilities for Incompleteness Region 2 were subdivided to allow for refinement of the probabilities of detection for the Gulf of Mexico region—the second matrix shown in Table 2.5.2-205. Following the elements of expert judgment noted above, the EPRI Incompleteness Region 2 matrix of detection probability was modified for the Gulf of Mexico region, as given in Table 2.5.2-206. Using the detection probability matrix with the seismicity of the Gulf of Mexico region results in a reasonable test b-value of 0.84.

Near Atlantic

The Near Atlantic region may be considered to have reduced probabilities of detection for reasons similar to those for the Gulf of Mexico region, however, the Near Atlantic region is most proximal to the Incompleteness Region 13 (Figure 2.5.2-202).

To estimate the probability of detection matrix for the Near Atlantic region, the reduction in probabilities developed for the Gulf of Mexico region as a fraction of the probabilities for Incompleteness Region 2 may be applied as a scaling factor to the probabilities of detection for Incompleteness Region 13, shown as the third matrix in Table 2.5.2-205. The results of this scaling gives the same probability of detection matrix for the Near Atlantic region, as was developed for the Gulf of Mexico region, and considered for the Near Atlantic region because of the distribution of the unity [1.00] and zero [0.00] values in both of the probabilities of detection matrices for Incompleteness Regions 2 and 13.

Seismicity is actually too sparse within the Near Atlantic region to determine a test calculation of b-value to assess the probability of detection matrix for the Near Atlantic region.

Near Florida

For the Near Florida region, the appropriate probability of detection matrix would be transitional between those values in Florida, given by the matrix for the Incompleteness Region 13, and those developed for Near Atlantic region. Therefore, the probability of detection matrix for Near Florida region was developed as simply the average of the detection probabilities for Incompleteness Region 13 (Table 2.5.2-205, third matrix) and Near Atlantic region (Table 2.5.2-206). These average values are listed in Table 2.5.2-206.

Again, seismicity is too sparse within the Near Florida region to determine a test calculation of b-value to assess the probability of detection matrix for the Near Florida region.

2.5.2.2 Updating the EPRI Seismic Source Model for the Site Region

RG 1.208 provides guidance on methods acceptable to the NRC to satisfy the requirements of 10 CFR 100.23 for assessing the appropriate SSE ground motion levels for new nuclear power plants. RG 1.208 states that an acceptable starting point for this assessment at sites in the CEUS is the PSHA conducted by the EPRI in the 1980s (References 243 and 247). RG 1.208 further specifies that the adequacy of the EPRI source model must be evaluated in light of more recent data and evolving knowledge pertaining to seismic hazard evaluation in the CEUS. As described in Subsection 2.5.1, a comprehensive review of available geological, seismological, and geophysical data has been performed for the site region and adjoining areas.

Subsection 2.5.2.2 summarizes seismic source interpretations from the original EPRI PSHA study (References 243 and 247). Modifications and updates to the original EPRI model are required for the following reasons:

- Recent earthquakes in the Gulf of Mexico and U.S. Gulf Coast region require updates to Mmax distributions and weights for the original EPRI model. Subsection 2.5.2.4.3 describes these Mmax updates.
- The original EPRI model (Reference 243) does not cover the entire 200-mile radius site region. As such, supplemental source zones are defined to cover the entire site region. Subsection 2.5.2.4.4.1 describes these supplemental source zones.
- New seismic source characterizations of seismic sources beyond the site region, including the Cuba area, the North America-Caribbean plate boundary region, and the Charleston seismic source, should be included. Subsections 2.5.2.4.4.2 and 2.5.2.4.4.3 describe the Charleston source characterization and the Cuba and northern Caribbean source characterization, respectively.

2.5.2.2.1 Summary of EPRI Seismic Sources

This subsection summarizes the seismic sources and parameters used in the original EPRI project (References 243 and 247). The description of seismic sources includes those sources located at least partially within 200 miles of the Units 6 & 7 site (i.e., the site region).

In the original EPRI project, six independent ESTs evaluated geological, geophysical, and seismological data to develop a model of seismic sources in the CEUS. These sources were used to model the occurrence of future earthquakes and evaluate earthquake hazards at nuclear power plant sites across the CEUS. The six ESTs involved in the original EPRI project were Bechtel Group, Dames & Moore, Law Engineering, Rondout Associates, Weston Geophysical, and Woodward-Clyde Consultants. Each team produced a report (volumes 5 through 10 of Reference 247) providing detailed descriptions of how they identified and defined seismic sources. The results were implemented into a PSHA study (Reference 243).

For the computation of hazard in the 1989 study, a few seismic source parameters were modified or simplified from the original parameters determined by the six ESTs. EPRI (Reference 243) summarizes the parameters used in the final PSHA calculations, and this reference is the primary source for the seismicity parameters. Each EST provides more detailed descriptions of the rationale and methodology used in evaluating tectonic features and establishing the seismic sources (volumes 5 through 10 of Reference 247).

Figures 2.5.2-203 through 2.5.2-209 show the EPRI source zones located at least partially within the site region. These figures also show earthquakes from the Phase 1 seismicity update (Subsection 2.5.2.1.2) to show the spatial relationships between seismicity and seismic sources.

The Mmax, interdependencies, and probability of activity for each EST's seismic sources are presented in Table 2.5.2-207. This table presents the parameters assigned to each source. Table 2.5.2-207 also indicates whether new information has been identified that would lead to a revision of the source's geometry, Mmax, or recurrence parameters.

The EPRI PSHA study expressed Mmax values in terms of m_b, whereas most modern seismic hazard analyses describe Mmax in terms of moment magnitude M_W. To provide a consistent comparison between magnitude scales, Subsection 2.5.2.1.2.1 relates body-wave magnitude to moment magnitude using the arithmetic average of three equations, or their inversions, presented in Atkinson and Boore (Reference 210), Frankel et al. (Reference 252), and EPRI TR-102293

(Reference 244). The conversion relations are consistent for magnitudes ≥4.5, but begin to show divergence at lower magnitudes.

Table 2.5.2-202 lists m_b and M_w equivalences developed from these relations over the range of interest for this study. Throughout this subsection, the values of Mmax distributions assigned by the ESTs to seismic sources are presented for both magnitude scales (m_b and M_w) to give perspective on the maximum earthquakes that were considered possible in each seismic source. For example, EPRI m_b values of Mmax are followed by the equivalent M_w value.

The following subsections describe the most significant EPRI sources for each EST with respect to the site. For all EPRI sources located within the site region, recent, post-EPRI-catalog earthquakes exceed the minimum Mmax bound assigned by the ESTs, thereby requiring Mmax updates for all EPRI sources within the site region. Subsection 2.5.2.4.3 describes these Mmax updates.

2.5.2.2.2 Sources Used for EPRI PSHA — Bechtel Group

Bechtel Group characterized only one seismic source within the site region, the Gulf Coast (BZ1) source zone. Table 2.5.2-207 summarizes the source parameters for this and other EPRI-ESTs' source zones within the site region. Figures 2.5.2-203 and 2.5.2-204 show the location and geometry of Bechtel Group's Gulf Coast (BZ1) seismic source zone.

The Units 6 & 7 site is located within Bechtel Group's Gulf Coast (BZ1) source zone. This background source extends from east Texas to the continental shelf east of Florida, including all of Louisiana and the southern portions of Mississippi, Alabama, and Georgia. The Bechtel Group assigned a maximum Mmax value of m_b 6.6 (M_w 6.5) to this zone.

2.5.2.2.3 Sources Used for EPRI PSHA — Dames & Moore

Dames & Moore characterized only one seismic source within the site region, the Southern Coastal Margin (20) source zone. Table 2.5.2-207 summarizes the source parameters for this and other EPRI-ESTs' source zones within the site region. Figures 2.5.2-203 and 2.5.2-205 show the location and geometry of Dames & Moore's Southern Coastal Margin (20) seismic source zone.

The Units 6 & 7 site is located within Dames & Moore's Southern Coastal Margin (20) source zone. This source roughly parallels the Paleozoic rifted continental margin from Texas to Alabama and also includes most of Florida. This source represents the down-warping wedge of continental margin sediments that has been accumulating since the Cretaceous Period and is characterized by diffuse seismicity (Reference 247). The Dames & Moore team assigned a maximum Mmax value of m_b 7.2 (M_w 7.5) to this zone, reflecting its assumption of the possibility for moderate to large earthquakes within this area.

2.5.2.2.4 Sources Used for EPRI PSHA — Law Engineering

Law Engineering characterized only one seismic source within the site region, the South Coastal block (126) source zone. Table 2.5.2-207 summarizes the source parameters for this and other EPRI-ESTs' source zones within the site region. Figures 2.5.2-203 and 2.5.2-206 show the location and geometry of Law Engineering's South Coastal block (126) seismic source zone.

The Units 6 & 7 site is located within Law Engineering's South Coastal block (126) source zone. This source represents an area of low amplitude, broad wavelength magnetic anomalies extending from the Texas/Mexico border to the continental shelf east of Florida. Law Engineering interprets the northern portion of the zone from Texas to Alabama as the Paleozoic edge of the North American craton (Reference 247). The Law Engineering team assigned a maximum Mmax value of m_b 4.9 (M_w 4.5) to this zone.

2.5.2.2.5 Sources Used for EPRI PSHA — Rondout Associates

Rondout Associates characterized two seismic sources within the site region. These two sources are:

- Appalachian Basement (49-05)
- Gulf Coast to Bahamas Fracture Zone (51)

Table 2.5.2-207 summarizes the source parameters for these two Rondout Associates source zones, as well as other EPRI-ESTs' source zones within the site region. Figures 2.5.2-203 and 2.5.2-207 show the locations and geometries of the Rondout seismic sources 49-05.

The Units 6 & 7 site is located within the Gulf Coast to Bahamas Fracture Zone (51) source zone. This roughly coast-parallel background source extends from the Texas/Mexico border to southern Florida. Source zone 51 comprises Paleozoic crust that is separated from Appalachian crust of roughly the same age based on differing stress regimes (Reference 247). The Rondout Associates team assigned a maximum Mmax value of m_b 5.8 (M_w 5.4) to this zone.

At its nearest point, the Appalachian Basement (49-05) source zone is located about 115 kilometers (70 miles) northeast of the Units 6 & 7 site. This source zone incorporates crust located east of the Precambrian cratonic edge and represents a complex accretionary terrane that may not have uniform seismic potential (Reference 247). The Rondout Associates team assigned a maximum Mmax value of m_b 5.8 (M_w 5.4) to this zone.

2.5.2.2.6 Sources Used for EPRI PSHA — Weston Geophysical

Weston Geophysical characterized only one seismic source within the site region, the Gulf Coast (107) source zone. Table 2.5.2-207 summarizes the source parameters for this and other EPRI-ESTs' source zones within the site region. Figures 2.5.2-203 and 2.5.2-208 show the location and geometry of Weston Geophysical's Gulf Coast (107) seismic source zone.

The Units 6 & 7 site is located within Weston Geophysical's Gulf Coast (107) source zone. This background source extends from eastern Texas to Florida, including all of Louisiana and the southern portions of Mississippi, Alabama, and Georgia. The Weston Geophysical team assigned a maximum Mmax value of m_b 6.0 (M_w 5.7) to this zone.

2.5.2.2.7 Sources Used for EPRI PSHA — Woodward-Clyde Consultants

The Woodward-Clyde Consultants team characterized only one seismic source within the site region, the Turkey Point Background (BG-35) source zone. Table 2.5.2-207 summarizes the source parameters for this and other EPRI-ESTs' source zones within the site region. Figures 2.5.2-203 and 2.5.2-209 show the location and geometry of Woodward-Clyde's Turkey Point Background (BG-35) seismic source zone.

The Turkey Point Background (BG-35) source is a large rectangle containing the Units 6 & 7 site and covering most of southern Florida and extending offshore to include parts of the Atlantic continental shelf, the Gulf Coast, and northern Cuba. This source is a background zone defined as a rectangular area centered on the Units 6 & 7 site, and its geometry is not based on any geological, geophysical, or seismological features. The largest Mmax assigned by the Woodward-Clyde Consultants team to this zone is m_b 6.6 (M_w 6.5).

2.5.2.3 Correlation of Seismicity with Geologic Structures and Seismic Sources

Seismic sources used in the Turkey Point Units 6 & 7 PSHA include updated EPRI seismic sources (Subsection 2.5.2.4.3.2), supplemental seismic sources (Subsection 2.5.2.4.4.1), Charleston, South Carolina seismic sources (Subsection 2.5.2.4.4.2), and Cuba and northern Caribbean seismic sources (Subsection 2.5.2.4.4.3). The EPRI earthquake catalog covers earthquakes in the CEUS through 1984, as described in Subsection 2.5.2.1. Figures 2.5.2-203 through 2.5.2-209 show the distribution of earthquake epicenters from both the EPRI (pre-1985) and Phase 1 update (through mid-February 2008) earthquake catalogs in comparison to the seismic sources identified by each of the EPRI ESTs. Seismicity is sparse and appears evenly distributed throughout each EPRI source zone that is located within the site region. There is no clear association of seismicity with any known geologic structure in these sources.

Comparison of the additional events of the updated Phase 1 earthquake catalogs to the EPRI earthquake catalog shows:

- There are no new earthquakes within the site region that can be associated with a known geologic structure.
- There are no unique clusters of seismicity that suggest a new seismic source not captured by the EPRI seismic source model.
- The updated earthquake catalog does not show a pattern of seismicity that requires revision to the geometry of any of the EPRI seismic sources.
- The Phase 1 earthquake catalog does not imply a significant change in seismicity parameters (rate of activity, b-value) for any of the EPRI seismic sources.

The Phase 1 earthquake catalog does indicate that Mmax updates are required for most of EPRI seismic sources located within the site region. Subsection 2.5.2.4.3 describes these Mmax updates.

The correlation of seismicity from the Phase 1 earthquake catalog with supplemental seismic sources is described in Subsection 2.5.2.4.4.1. The correlation of seismicity from the Phase 1 earthquake catalog with the Charleston, South Carolina seismic source is described in Subsection 2.5.2.4.4.2. The correlation of seismicity from the Phase 2 earthquake catalog with Cuba and northern Caribbean seismic sources is described in Subsection 2.5.2.4.4.3.

2.5.2.4 Probabilistic Seismic Hazard Analysis and Controlling Earthquakes

This subsection describes the PSHA conducted for the Units 6 & 7 site following the guidelines outlined in RG 1.208. Subsections 2.5.2.4.1 through 2.5.2.4.4 address the potential significance of new information on seismic source characterization, as that new information relates to the 1989 EPRI seismic hazard model (Reference 245), the Cuba area, and the North America-Caribbean plate boundary region. Subsection 2.5.2.4.5 summarizes the methods used to characterize ground motions within the original EPRI-SOG seismic sources in the CEUS region, and develops new attenuation models for the Caribbean seismic sources.

Subsection 2.5.2.4.6 describes the results of PSHA sensitivity analyses used to test the impact of the new information on the seismic hazard and the procedure conducted to perform an updated PSHA for the site. The results of this updated PSHA are used to develop UHRS and to identify controlling earthquakes. Development of GMRS for the Units 6 & 7 site in terms of the site-specific UHRS is described in Subsections 2.5.2.5 and 2.5.2.6.

2.5.2.4.1 1989 EPRI Seismic Hazard Study

The starting point of the PSHA calculations for the site was the 1989 EPRI study (Reference 245). The 1989 EPRI study used expert opinion on alternative, competing models of earthquake occurrences (size, location, and rates of occurrence) and ground motion amplitude and its variability to weight alternative hypotheses. PSHA calculations are conducted for these alternative hypotheses. The result is a family of weighted seismic hazard curves from which mean and fractile seismic hazard can be derived.

There were no PSHA results published in the 1989 EPRI study (Reference 245) for the Units 6 & 7 site. Therefore, as a starting point for calculations, the seismic hazard for the Crystal River site was replicated, because those hazard results were available from the 1989 EPRI study. The Crystal River site is on the west coast of Florida, near the northern end of the Florida Peninsula, and is the closest site for which 1989 EPRI study results are available. The purpose of this replication was to use the same assumptions on seismic sources and ground motion attenuation relationships, to calculate seismic hazard, and to compare results to the 1989 EPRI study.

Table 2.5.2-208 compares individual team and total annual frequencies of exceedance calculated in the 1989 EPRI study for the Crystal River site (labeled “EPRI-SOG”) to annual frequencies of exceedance calculated in the Units 6 & 7 study for peak ground acceleration (PGA) amplitudes of 100, 250, and 500 centimeters/second^2. All results are for hard rock. The “% diff” columns show the percent difference between the 1989 calculations and the current hazard calculations at the Crystal River site. Comparisons are shown for mean PGA hazard and for the 15th fractile, median, and 85th fractile hazard curves. Note that the minimum magnitude (Mmin) for these hazard calculations was m_b = 5.0, which was the assumption made in the 1989 EPRI study (Reference 245). Observations for these comparisons are as follows:

- Bechtel team — comparison showed similar results, with current results slightly higher than for 1989 EPRI study (Reference 245).

- Dames & Moore team — comparison showed similar results except for 85th fractile hazard values, with current PGA results being +43 percent to -30 percent different from 1989 EPRI study (Reference 245). The 85th fractile hazard values show a larger difference, but the overall comparison is considered acceptable because the main concern is with replication of mean hazard. For mean hazard at three amplitudes 100, 250, and 500 centimeters/second^2, the current PGA results are within 2 percent of the 1989 EPRI results.

- Law Engineering — current results are well below 1989 EPRI study results (Reference 245). The host source (LAW-126) has Mmax values that are all below the value of Mmin = 5.0 used in the 1989 EPRI study, so it is reasonable that the current calculation shows very low hazard for the Law team (the host source contributes zero hazard in the current calculation).

- Rondout — comparison showed similar results except for the 15 percent fractile, where the current results are much lower than the 1989 EPRI results (Reference 245). Rondout sources RND-51 and RND-C01 (the host sources) have a Mmax distribution that includes a value of 4.8 (weight 0.2), which is below Mmin = 5.0, so it is reasonable that the 15 percent fractile hazard would be very low for the Rondout team, as the current calculations show.

- Weston — comparison showed similar results, with current results slightly higher than for the 1989 EPRI study (Reference 245).

- Woodward-Clyde — comparison showed similar results except for the 15 percent fractile, where the current results are much lower than the 1989 EPRI results (Reference 245). Woodward-Clyde source WGC-B36 (the background host source) has a Mmax distribution

that includes a value of 4.9 (weight 0.17), which is below Mmin = 5.0, so it is logical that the 15 percent fractile hazard would be very low for the Woodward-Clyde team, as the current calculations show.

- Total — comparison of mean hazard showed similar results, with agreement being between 0 percent and 4 percent for PGA amplitudes of 100, 250, and 500 centimeter/second^2. The agreement for specific fractiles is not as good, for reasons discussed above, but this is less of a concern because (a) mean hazards are used to derive recommendations for design spectra, and (b) differences related to Mmax distributions are resolved since Mmax distributions for the EPRI team sources are updated as described below.

The conclusion from this comparison is that the overall mean seismic hazard from the 1989 EPRI study (Reference 245) can be replicated accurately, but unstated assumptions and different treatment of Mmax distributions below a value of 5.0 lead to somewhat different fractile hazards for individual team results. Given that mean hazards are used to derive recommendations for design spectra, the comparison is considered acceptable.

At the Units 6 & 7 site, updates to the inputs to PSHA lead to changes in the level of seismic hazard compared to what would have been calculated based on the 1989 EPRI model (Reference 245). Seismic source characterization data and ground motion assessments that could affect the calculated level of seismic hazard include:

- Updates in the characterization of the rate of earthquake occurrence as a function of magnitude for one or more seismic sources.
- Updates in the characterization of the maximum magnitude for seismic sources.
- Extension of seismic sources to additional regions not covered in the EPRI 1989 study.
- Modeling of new seismic sources to the south, outside the original 1989 EPRI study region.
- Updates to models used for estimating strong ground shaking and its variability in the CEUS.

Possible changes to seismic hazard caused by changes in these areas are addressed in the following subsections.

2.5.2.4.2 Effect of Updated Earthquake Catalog

Subsection 2.5.2.1.2 describes the development of an updated earthquake catalog. This updated catalog involves the addition of earthquakes that have occurred after completion of the EPRI evaluation development (post-1984). The impact of the new catalog information was assessed by evaluating the effect of the new data on earthquake recurrence estimates for the Florida Peninsula, as described below.

The 1989 EPRI study (Reference 245) defined completeness regions for the entire CEUS, within the boundaries of a study region that approximately followed the Atlantic and Gulf of Mexico coasts. In the Florida region only the Florida Peninsula was defined to be within the boundaries of the EPRI study region because the earthquake catalog was thought to be incomplete in the Gulf of Mexico and in the Atlantic region east of Florida. Figure 2.5.2-210 shows the boundary of the EPRI region and also shows the “Florida test region” used here to examine the effects of an updated earthquake catalog. Earthquake locations are shown for both the original EPRI earthquake catalog and for the updated catalog (south of latitude 35° N), as given in Table 2.5.2-201.

The effect of the updated earthquake catalog on earthquake occurrence rates was assessed by computing earthquake recurrence parameters for the Florida test region shown in Figure 2.5.2-210. The truncated exponential recurrence model was fit to the seismicity data using the EPRI EQPARAM program, which uses the maximum likelihood technique. Earthquake recurrence parameters were computed first using the original EPRI earthquake catalog and periods of completeness, and then using the updated earthquake catalog and extending the periods of completeness to 2007, assuming that the probability of detection for all magnitudes is unity for the time period 1985 to 2007.

The resulting earthquake recurrence rates for the Florida test region are compared in Figure 2.5.2-211. This comparison shows that the updated earthquake catalog results in lower estimated earthquake recurrence rates. On the basis of the comparison shown in Figure 2.5.2-211, it is concluded that the earthquake occurrence rate parameters developed in the 1989 EPRI evaluation (Reference 245) have not increased in the period 1985-2007.

Therefore, on the basis of earthquake occurrences alone, the seismicity rates of all EPRI team sources were not updated. Note that the EPRI analysis assumed that the EPRI earthquake catalog was complete for all magnitudes during the period 1975–1984 (probability of detection is 1.0, Table 2.5.2-205), so this was an extension of that assumption to cover the updated catalog period.

2.5.2.4.3 New Maximum Magnitude Information

The updated earthquake catalog described in Subsection 2.5.2.1 indicates that increases in Mmax values are required for all source zones within the site region except for Woodward-Clyde source BG-35. Post-EPRI earthquakes in the updated earthquake catalog require Mmax increases because recent earthquakes have occurred in each site region source zone with magnitudes exceeding the original EPRI lower bound Mmax values (Table 2.5.2-207). Subsection 2.5.2.4.3.1 describes these earthquakes, and Subsection 2.5.2.4.3.2 and Table 2.5.2-207 present rationale for, and updates of, the original EPRI source parameters.

With the exception of earthquakes in the Cuba area and the North America-Caribbean plate boundary region, the updated earthquake catalog does not indicate any post-EPRI seismicity patterns indicative of new seismic sources. Assessment of seismicity in the Cuba area and the North America-Caribbean plate boundary region was not included in the original EPRI study. Subsection 2.5.2.4.4.3 presents details of the Cuba and northern Caribbean seismic source model.

2.5.2.4.3.1 Earthquakes Significant to EPRI Mmax Values

A total of four post-EPRI earthquakes from the updated earthquake catalog (Table 2.5.2-201) have magnitudes greater than the lower bound Mmax value for the source zone within which they occurred. These new data require revision to the Mmax distributions for all seven EPRI seismic source zones within the site region except for Woodward-Clyde source BG-35. The following subsections describe these four earthquakes. In the following discussion, magnitude estimates are presented in units of either body-wave magnitude, m_b, or the “best estimate” of body-wave magnitude, Emb. For the purposes of this subsection, m_b and Emb are considered equivalent.

2.5.2.4.3.1.1 September 10, 2006, Emb 5.90 Gulf of Mexico Earthquake

The September 10, 2006, earthquake occurred in the Gulf of Mexico, roughly equidistant from the Florida and Alabama coasts. The event was felt throughout the southeastern U.S., including Louisiana, Arkansas, Missouri, Alabama, Georgia, South Carolina, and Florida. Maximum felt intensities were MMI IV (Reference 330). Focal mechanisms indicate reverse faulting and hypocentral depth estimates indicate a source located beneath the Gulf of Mexico sedimentary section (Reference 330).

The updated earthquake catalog compiled for the Units 6 & 7 site assigns Emb 5.90 to the September 10, 2006, Gulf of Mexico earthquake (Figures 2.5.2-204 through 2.5.2-209). Based on preliminary data, however, previous studies assigned Emb 6.11 to this same earthquake. The Emb 6.11 estimate is adopted for the purpose of updating EPRI Mmax ranges. The difference in magnitude estimates for this event reflects the uncertainty in magnitude determination and the older and slightly larger estimate is used.

The magnitude of the September 10, 2006, earthquake exceeds the original EPRI Mmax lower bound magnitudes, and thereby requires upward revision of the Mmax distributions for the following sources (Table 2.5.2-207):

- Bechtel source BZ1 (Gulf Coast)
- Rondout Associates source 51 (Gulf Coast to Bahamas Fracture Zone)
- Weston Geophysical source 107 (Gulf Coast)

2.5.2.4.3.1.2 February 10, 2006, Emb 5.58 Gulf of Mexico Earthquake

The February 10, 2006, earthquake occurred in the Gulf of Mexico south of Louisiana. This Emb 5.58 event was felt in coastal Louisiana, Texas, and Florida with a maximum intensity of MMI III (Reference 291). The event occurred along the Sigsbee Escarpment offshore of Louisiana. Nettles (Reference 293) and Dellinger et al. (Reference 228) suggest that this event may be the result of a gravity-driven landslide. This interpretation is based on the lack of high-frequency energy in the waveforms, slow rise time, preliminary focal mechanism determinations, and the location of the event on the Sigsbee Escarpment.

Dewey and Dellinger (Reference 239) suggest that this event represents either: (a) faulting within crystalline basement at a depth beneath approximately 13 kilometers; (b) faulting within the sedimentary section above approximately 13 kilometers; or (c) a landslide within the sedimentary section. Based on seismic waveform characteristics, Dewey and Dellinger (Reference 239) consider a source within the crystalline basement unlikely for this event, and therefore favor either a shallow earthquake or landslide mechanism. Regardless of mechanism, Dewey and Dellinger (Reference 239) suggest a focal depth of 5 kilometers for this event, but they indicate that the depth could not be calculated reliably and most likely is between 1 and 15 kilometers. If the event occurred near the deep end of this range, then a landslide origin is precluded.

Based on available data, there is the possibility that the February 10, 2006, event was nontectonic in origin. Because this is not a consensus conclusion within the seismological community and to capture uncertainty associated with this event, it is assumed to be of tectonic origin and Mmax values are updated for source zones containing the event.

The magnitude of the February 10, 2006, event exceeds the original EPRI Mmax lower bound magnitudes, and thereby requires upward revision of the Mmax distributions for the following sources (Table 2.5.2-207):

- Dames & Moore source 20 (Southern Coastal Margin)
- Law Engineering source 126 (South Coastal block)

While this event also is located within Rondout Associates source 51 (Gulf Coast to Bahamas Fracture Zone) and Weston Geophysical source 107 (Gulf Coast) and has a larger magnitude than the lower bound Mmax value for both zones, updates to Rondout Associates source 51 and Weston Geophysical source 107 are based on the larger September 10, 2006, earthquake described above.

The February 10, 2006, event is located about 22 miles south of Law Engineering source 126 (Figure 2.5.2-206). This event was poorly located by traditional land-based seismograph networks, and the epicentral location is uncertain.

Therefore, it is assumed that the February 10, 2006, Emb 5.58 event occurred within Law Engineering source 126 based on positional uncertainty and the lack of any known seismotectonic boundaries that would suggest a change in seismotectonic behavior across the southern source boundary.

2.5.2.4.3.1.3 October 24, 1997, Emb 4.96 Southwestern Alabama Earthquake

The October 24, 1997, Escambia County, Alabama earthquake occurred in southwestern Alabama. This Emb 4.96 event was felt throughout southwestern Alabama and westernmost Florida with a maximum intensity of MMI VI to VII (Reference 259). This earthquake occurred within or at the perimeter of an active oil and gas extraction field, suggesting the possibility of a causal relationship between hydrocarbon recovery and the October 24, 1997, earthquake (Reference 259). Therefore, it is possible that this earthquake is non-tectonic in origin. Regardless, this event is assumed to be tectonic in origin, and Mmax values are updated for source zones containing the event as appropriate.

The magnitude of the October 24, 1997, earthquake exceeds the original EPRI Mmax lower bound magnitude, and thereby requires upward revision of the Mmax distributions for the following sources (Table 2.5.2-207):

- Rondout Associates source 49-05 (Appalachian Basement)
- Law Engineering source 126 (South Coastal block)

However, as described in the preceding subsection, it is assumed that the poorly located and larger February 10, 2006, Emb 5.58 earthquake also occurred within Law Engineering source 126. Therefore, the Mmax distribution for Law Engineering source 126 is updated based on the February 10, 2006, earthquake.

2.5.2.4.3.1.4 January 23, 1880, Emb 6.09 West Cuba Earthquake

The largest earthquake in Woodward-Clyde seismic source BG-35 is the January 23, 1880, Emb 6.09 San Cristobal-Candelaria, Cuba earthquake in west Cuba (Figures 2.5.2-203 and 2.5.2-214). The magnitude of this earthquake exceeds the minimum Mmax value (m_b 5.8) defined by Woodward-Clyde for its source BG-35 (Table 2.5.2-207). However, as described in Subsection 2.5.2.4.4.3, the southern margin of Woodward-Clyde source BG-35 is truncated by the northern boundary of the new Cuba and northern Caribbean seismic source model to avoid double-counting of earthquakes.

As such, the January 23, 1880 west Cuba earthquake is located outside of the truncated Woodward-Clyde source and within the area modeled by the new Cuba and northern Caribbean seismic source model. Therefore, the January 23, 1880, earthquake does not provide rationale for updating the original EPRI Mmax distribution for Woodward-Clyde source BG-35.

The largest earthquake in the truncated Woodward-Clyde source is the June 2, 1990, Emb 4.09 earthquake, north of Cuba (Figure 2.5.2-209). Subsection 2.5.2.4.4.3 describes the geometry of the truncated Woodward-Clyde source zone. Because this earthquake is smaller than the minimum value of the original EPRI Mmax distribution (m_b 5.8), no change to the original Mmax distribution is required for the truncated Woodward-Clyde seismic source.

2.5.2.4.3.2 EPRI Site Region Source Zone Mmax Revisions

The following subsections describe Mmax modifications to the original EPRI source zones within 200 miles of the Units 6 & 7 site. Review of published literature does not indicate any new information that requires revision to the existing EPRI source zone geometries. Post-EPRI earthquakes in the updated earthquake catalog, however, require Mmax increases for five of the six ESTs because recent earthquakes have occurred in each site region source zone with magnitudes larger than the original EPRI lower bound Mmax values (Table 2.5.2-207).

Modifications to the original EPRI seismic source zones in the site region are limited to:

- Revising Mmax distributions based on updated seismicity data.
- Truncating the southern extent of Woodward-Clyde source BG-35 to prevent overlap with the Cuba and northern Caribbean seismic source model. Subsection 2.5.2.4.4.3 describes the Cuba and northern Caribbean source model.

Mmax distribution revisions follow the individual EST methodologies as described in the original EPRI team reports (Reference 247). These recommended changes are described in the subsections below.

2.5.2.4.3.2.1 Mmax Update — Bechtel Group

Source BZ1 (Gulf Coast) is the only Bechtel source within 200 miles of the Units 6 & 7 site (Figure 2.5.2-204) (Table 2.5.2-207). The only post-EPRI information that requires revision to this source zone is the September 10, 2006, Emb 5.90 earthquake that occurred within the Gulf Coast source zone. As described in Subsection 2.5.2.4.3.1.1, Emb 6.11 is adopted for this earthquake.

The original EPRI Mmax distribution for Bechtel source BZ1 (with weights in brackets) is: m_b 5.4 [0.1], 5.7 [0.4], 6.0 [0.4], and 6.6 [0.1] (Table 2.5.2-207) (Reference 243). Because the September 10, 2006, earthquake has a larger magnitude than the lower bound Mmax magnitude, the original EPRI Mmax distribution is updated.

The following summarizes the Bechtel Group's methodology for defining Mmax distributions, as described within their EST volume (Reference 247), and its application to update Source BZ1.

- The lower-bound magnitude of the distribution is defined as the greater of either the largest observed earthquake magnitude within the zone, or m_b 5.4 with a weight of 0.1. For Source BZ1 this lower-bound Mmax value is m_b 6.1 with a weight of 0.1.
- The next higher magnitude is 0.3 magnitude units greater then the lower-bound Mmax value and is given a weight of 0.4. For Source BZ1 this results in a Mmax value of m_b 6.4 with a weight of 0.4.
- A third magnitude is 0.6 magnitude units above the lower-bound Mmax value and is given a weight of 0.4. For Source BZ1 this results in a Mmax value of m_b 6.7 with a weight of 0.4.
- A fourth magnitude is m_b 6.6 interpreted by the Bechtel EST as the largest intraplate earthquake in the CEUS with specific exceptions, and is given a weight of 0.1.

Applying this methodology to account for the Emb 6.11 earthquake results in updated Mmax values, listed in increasing magnitude order, of 6.1, 6.4, 6.6, and 6.7 with weights of 0.1, 0.4, 0.1, and 0.4, respectively, for Source BZ1 (Table 2.5.2-207).

It is noted, however, that a different initial interpretation of the Bechtel methodology was used in the development of the rock UHRS shown in Tables 2.5.2-210 and 2.5.2-227. The resultant Mmax distribution and weights for BZ1 based on this initial distribution was 6.1, 6.4, and 6.6 with weights of 0.1, 0.4, and 0.5, respectively. A sensitivity study has been performed showing that the effect of adopting the updated BZ1 Mmax distribution shown in Table 2.5.2-207 would, over the entire frequency range of interest (0.5 to 100 Hz) and in the 10^{-4} to 10^{-5} mean annual frequency of exceedance range used to determine ground motion design response spectrum values, result in an increase of 0.18 percent or less. Based on these results, it is concluded that this increase is insignificant, and that the design ground motions derived from the response spectra in Tables 2.5.2-210 and 2.5.2-227 remain appropriate for the Units 6 & 7 site.

2.5.2.4.3.2.2 Mmax Update — Dames & Moore

Source 20 (Southern Coastal Margin) is the only Dames & Moore source within 200 miles of the Units 6 & 7 site (Figure 2.5.2-205) (Table 2.5.2-207). The only post-EPRI information that requires revision to this source zone is the February 10, 2006, Emb 5.58 earthquake that occurred within the southern boundary of the Southern Coastal Margin source zone.

The original EPRI Mmax distribution for Dames & Moore source 20 (with weights in brackets) is: m_b 5.3 [0.8] and 7.2 [0.2] (Reference 243) (Table 2.5.2-207). The February 10, 2006, earthquake was poorly recorded by traditional land-based seismograph networks. Despite the potential uncertainty in location, it is assumed that this event is correctly positioned within the source zone. Because the earthquake's Emb 5.58 magnitude is larger than the lower bound Mmax value, the original EPRI Mmax distribution is updated.

The Mmax distribution for Dames & Moore source 20 presented here results from increasing the lower-bound Mmax to match the magnitude of the observed Emb 5.58 earthquake (and rounding to the nearest tenth of a magnitude unit), while maintaining the same upper bound and weightings as the original EPRI Mmax distribution for the source zone. The updated Mmax values are (with weights in brackets) m_b 5.6 [0.8] and 7.2 [0.2] (Table 2.5.2-207).

Moreover, Dames & Moore did not prescribe any smoothing in determining seismicity parameters for their source 20 (Reference 243). The revised smoothing options shown in Table 2.5.2-207 are based on the range of smoothing options provided to the EPRI ESTs. The smoothing options vary between moderate to strong smoothing on a- and b-values, and all the options have a strong prior of 1.04 on b-value based on the Dames & Moore preference of that option (Reference 243).

2.5.2.4.3.2.3 Mmax Update — Law Engineering

Source 126 (South Coastal block) is the only Law Engineering source within 200 miles of the Units 6 & 7 site (Figure 2.5.2-206) (Table 2.5.2-207). The only post-EPRI information that requires revisions to this source zone is the February 10, 2006, Emb 5.58 earthquake that occurred about 22 miles south of the South Coastal block source zone. The February 10, 2006, earthquake was poorly recorded by traditional land-based seismograph networks and is assumed to have occurred within Law Engineering source 126.

The original EPRI Mmax distribution for Law Engineering source 126 (with weights in brackets) is: m_b 4.6 [0.9] and 4.9 [0.1] (Table 2.5.2-207) (Reference 243). Based on the inclusion of the earthquake within the source zone and the observation that the earthquake's Emb 5.58 magnitude is larger than the lower bound Mmax value, the original EPRI Mmax distribution for this source zone is revised.

The updated Mmax distribution of m_b 5.6 [0.90] and 5.7 [0.10] (Table 2.5.2-207) is determined using Law Engineering's methodology for developing Mmax distributions, as follows (Reference 247):

- The lower bound Mmax is the magnitude of the maximum observed earthquake in the zone.
- The upper bound Mmax magnitude defined by Law Engineering for regions with earthquakes occurring within 6.2 miles (10 kilometers) of the surface is m_b 5.7.

Weights for the original Mmax distribution (0.9 on the lower bound Mmax and 0.1 on the upper bound Mmax) (References 243 and 247) are retained in the updated Mmax distribution.

2.5.2.4.3.2.4 Mmax Update — Rondout Associates

Source 51 (Gulf Coast to Bahamas Fracture Zone) and source 49-05 (Appalachian Basement) are the only Rondout Associates source zones within 200 miles of the Units 6 & 7 site (Figure 2.5.2-207) (Table 2.5.2-207). Two sources of post-EPRI information require revisions to the Mmax distributions of these source zones: (1) the October 24, 1997, Emb 4.96 earthquake that occurred within source 49-05, and (2) the September 10, 2006, Emb 5.90 earthquake that occurred within source 51. As described in Subsection 2.5.2.4.3.1.1, Emb 6.11 is adopted for the September 10, 2006, earthquake.

The original EPRI Mmax distribution for sources 51 and 49-05 (with weights in brackets) is: m_b 4.8 [0.2], 5.5 [0.6], and 5.8 [0.2] (Reference 243) (Table 2.5.2-207). Because the October 24, 1997, and September 10, 2006, earthquakes have larger magnitudes than the lower bound Mmax magnitude, the original EPRI Mmax distributions for sources 51 and 49-05 are updated.

For Rondout Associates source 51, the updated Mmax values of m_b 6.1 [0.3], 6.3 [0.55], and 6.5 [0.15] (Table 2.5.2-207) follow from reclassifying the source zone as one capable of producing moderate earthquakes instead of the original classification of the source zone as one only capable of producing smaller than moderate earthquakes (Reference 247). The original Rondout Associates Mmax distribution for moderate earthquake source zones is m_b 5.2 [0.3], 6.3 [0.55], and 6.5 [0.15]. The updated Mmax distribution follows this distribution with the exception of an increase in the lower bound of the distribution to m_b 6.1 to account for the observed September 10, 2006, earthquake within this zone.

For Rondout Associates source 49-05, the updated Mmax values of m_b 5.0 [0.2], 5.5 [0.6], and 5.8 [0.2] (Table 2.5.2-207) result from increasing the lower Mmax bound to match the magnitude of the observed October 24, 1997, Emb 4.96 earthquake while maintaining the same upper bound and weightings of the original Mmax distribution for the source zone.

2.5.2.4.3.2.5 Mmax Update — Weston Geophysical Corporation

Source 107 (Gulf Coast Background) is the only Weston Geophysical source within 200 miles of the Units 6 & 7 site (Figure 2.5.2-208 and Table 2.5.2-207). The only post-EPRI information requiring revisions to any of these source zones is the September 10, 2006, Emb 5.90 earthquake that occurred within the Gulf Coast source zone. As described in Subsection 2.5.2.4.3.1.1, Emb 6.11 is adopted for this earthquake to be consistent with earlier studies.

The original EPRI Mmax distribution for Weston Geophysical source 107 (with weights in brackets) is: m_b 5.4 [0.71] and 6.0 [0.29] (Table 2.5.2-207) (Reference 243). Because the September 10, 2006, earthquake has a larger magnitude than the lower bound Mmax magnitude, the original EPRI Mmax distribution is updated.

Weston Geophysical's methodology for defining Mmax is based on developing discrete distributions for the probability of Mmax being a particular value (Reference 247). For source 107, these Mmax values and probabilities determined by the Weston Geophysical EST are: m_b 3.6 [0.04628], 4.2 [0.11982], 4.8 [0.27542], 5.4 [0.34415], 6.0 [0.16169], 6.6 [0.04461], and 7.2 [0.00553] (Reference 247). Following a conservative interpretation of Weston Geophysical's methodology, this

discrete probability distribution is truncated at the magnitude that is closest to, yet greater than, the maximum observed earthquake within the source zone.

For this study the distribution is truncated at 6.6 because the September 10, 2006, Emb 5.90 earthquake (for which Emb 6.11 is adopted) occurred within the source zone, and the next highest discrete magnitude in the distribution is 6.6. The truncated distribution is then renormalized so that the sum of all the probabilities is 1.0. The final Mmax values are the truncated distribution, and the weightings are the renormalized probabilities. For source 107, the updated Mmax distribution is: m_b 6.6 [0.89], 7.2 [0.11] (Table 2.5.2-207).

2.5.2.4.3.2.6 Mmax Update — Woodward-Clyde Consultants

Woodward-Clyde Consultants originally defined large background zones that cover the majority of the CEUS and a small set of source zones to represent tectonic features (Reference 247). These large background zones were simplified in later stages of the EPRI project to individual, rectangular background zones centered on plant sites. Source BG-35 (Turkey Point Background) is a roughly 400 x 400 miles rectangle centered on the Turkey Point site that extends southward into northern Cuba (Figure 2.5.2-203). The original EPRI Mmax distribution for source BG-35 is the same as those for the other Woodward-Clyde East Coast backgrounds: m_b 5.8 [0.33], 6.2 [0.34], 6.6 [0.33] (Table 2.5.2-207) (Reference 243).

To update Woodward-Clyde source BG-35, this source is truncated at the northern margin of the new Cuba and northern Caribbean seismic source model. Subsection 2.5.2.4.4.3 describes the new Cuba and northern Caribbean source model. Southward truncation of Woodward-Clyde source BG-35 is required to avoid double-counting of earthquakes in the northern portion of the new Cuba and northern Caribbean seismic source model.

The largest earthquake in the truncated Woodward-Clyde BG-35 source zone is the June 2, 1990, Emb 4.09 earthquake located off the north coast of Cuba (Figure 2.5.2-209 and Table 2.5.2-207). Because this earthquake is smaller than the minimum value of the original EPRI Mmax distribution (m_b 5.8), no change to the original Mmax distribution is required for the truncated Woodward-Clyde source.

2.5.2.4.4 New Seismic Source Characterizations

To complement the updated EPRI seismic source model described above, three new seismic source characterizations are included for analysis. These three new source characterizations are:

- Supplemental seismic source zones that fill the area of the site region beyond the area covered by the original EPRI source model (Subsection 2.5.2.4.4.1).
- New, post-EPRI characterization of the Charleston seismic source (Subsection 2.5.2.4.4.2).
- New, post-EPRI characterization of seismic sources located in the Cuba area and the North America-Caribbean plate boundary region (Subsection 2.5.2.4.4.3).

An additional post-EPRI model is the USGS National Seismic Hazard Mapping Project (NSHMP) (Reference 300), which characterizes seismic sources throughout the continental United States using multiple classes of earthquake source models. While the NSHMP source model is described below, source parameters from this model are not included in the updated PSHA for the Turkey Point Units 6 & 7 site. The general approach used by the USGS for modeling distributed seismicity in the CEUS is based on gridded, spatially smoothed seismicity in large background zones. Seismic sources within the CEUS most relevant to the Turkey Point Units 6 &7 site are modeled with: (1) a regional uniform background source model dividing the Extended Margin of the CEUS from the

Craton; (2) special zones accounting for variability in catalog completeness, seismicity, maximum magnitude, and b-value, such as the uniform source zones for the Eastern Tennessee and New Madrid seismic zones; and (3) finite fault sources, such as those included for the New Madrid and Charleston seismic sources.

The 2008 NSHMP earthquake sources are depicted in Figure 2.5.2-276. Significant changes from the 2002 NSHMP model of seismic hazard in the CEUS (Reference 251) include: (1) uncertainty in the maximum magnitude (Mmax) assigned to Mmax zones (e.g., extended margin); (2) revised geometry of the Charleston seismic source zones; and (3) revised magnitudes, rates, and geometry for the New Madrid seismic source. As a result of these updates, the 2008 NSHMP characterizes Mmax for the Extended Margin and Craton as weighted distributions ranging between M7.1-7.7 and M6.6-7.2, respectively. The two areal zones defining the Charleston source are both assigned Mmax distributions of M6.8-7.5 with a recurrence interval of 550 years, unchanged from the 2002 NSHMP. The USGS NSHMP Charleston seismic source update is discussed in Subsections 2.5.2.4.4.2.2 and 2.5.2.4.4.2.3.

2.5.2.4.4.1 Supplemental Source Zones

In all but one case, the Woodward-Clyde Consultants team, the EPRI ESTs' source zones do not cover the entire 200-mile radius site region (Figure 2.5.2-203). In general, the EPRI Gulf Coast seismic source zones do not extend much beyond the site to either the south or east, thus leaving large portions of the site region without any seismic source zones. This subsection provides the rationale for adding supplemental source zones to account for potential seismic sources within the remainder of the site region north of the northern border of the new Cuba and northern Caribbean seismic source model (Subsection 2.5.2.4.4.3), consistent with current knowledge of the geologic, geophysical, and seismic characteristics of the crust in this region.

The areas of the site region not covered by the original EPRI model are largely devoid of seismicity (Figures 2.5.2-203 through 2.5.2-209). Based on this observation, new supplemental sources within the site region are added to represent the extension of Gulf Coast seismic sources, instead of expanding the existing EPRI source zones to cover the site region. By simply expanding existing EPRI Gulf Coast source zones to offshore areas devoid of historical earthquake activity, the site hazard may be unduly decreased due to seismicity smoothing options detailed for these zones. Adding new source zones (with similar parameters to the updated EPRI Gulf Coast zones) instead is an appropriate approach, the details of which are described below. The combination of a Gulf Coast zone and a new supplemental source zone with similar parameters provides source zones covering the entire site region to account for future earthquakes.

In general, the EPRI ESTs provide minimal documentation describing the data and interpretations that define the southern and eastern boundaries of their Gulf Coast source zones (Reference 247). The eastern and southern boundaries of the Gulf Coast source zones are largely arbitrary and are often not tied to any specific geologic, seismologic, or geophysical features. The southern boundary of five of the six original EPRI ESTs' Gulf Coast source zones appear to have been arbitrarily truncated at about 25° N latitude (Figure 2.5.2-203). The sixth team, Woodward-Clyde Consultants, defines its Turkey Point Background (BG-35) source as a rectangular area centered on the Turkey Point site and is not based on any geological, geophysical, or seismological features.

The new supplemental source zones are based on an assessment after evaluating the existing data that the entire site region is potentially seismogenic. The geometries of these supplemental zones, which were created by using the original EPRI Gulf Coast source zone geometries and filling in the remainder of the site region north of the northern boundary of the new Cuba and northern Caribbean seismic source model, are shown in Figures 2.5.2-204 through 2.5.2-208. As shown in Table 2.5.2-211, this process results in five new source zones (one for each EPRI EST except Woodward-Clyde). A sixth, modified source, shown in Figure 2.5.2-209, is the result of truncating

existing Woodward-Clyde source BG-35 by the northern boundary of the new Cuba and northern Caribbean seismic source model. This truncated source is intended to replace the original EPRI Woodward-Clyde source BG-35. Table 2.5.2-212 provides geographic coordinates of the corner points of the five supplemental source zones and the truncated Woodward-Clyde source.

The new supplemental source zones also are based on the evaluation that the crust within the site region between southern Florida and the northern boundary of the newly assessed Cuba and northern Caribbean seismic source model is similar and has similar earthquake potential. The EPRI Gulf Coast sources are broad, regional seismic source zones that include predominantly extended continental crust characterized by low rates of seismicity. While individual seismic source zones characterizing this crust from each EST differ, they generally extend from Texas to Florida (Figures 2.5.2-203 through 2.5.2-209). Basement rock within the Gulf of Mexico region has been divided by Sawyer et al. (Reference 315) into four major types: oceanic, thin transitional, thick, transitional, and continental crust (Figure 2.5.1-238). These gross characteristics and boundaries between various types of crust in the Gulf of Mexico region are based on reflection and refraction seismic profiles, gravity, magnetic, and subsidence data and reflect the manner in which crust was created or modified by Mesozoic rifting. Based on mapping of crust in this region (e.g., References 258 and 315), the majority of these regional Gulf seismic source zones comprise thick transitional crust, however the northeast area of northern Florida, Georgia, and Alabama is considered continental crust by Sawyer et al. (Reference 315). These zones also include significant amounts of thin transitional crust as well as minor amounts of oceanic crust near their southern boundary (Figure 2.5.1-238). Additional discussion is provided in Subsection 2.5.1.1.1.2.2.

Implementation of this method involves the following:

- No changes to the geometries of the original EPRI Gulf Coast source zones (except Woodward-Clyde seismic source BG-35, which is truncated at the northern boundary of new Cuba and northern Caribbean seismic source model).

- Add five additional source zones (one for each EST except Woodward-Clyde) to fill in the site region, truncated at the northern boundary of new Cuba and northern Caribbean seismic source model (Figures 2.5.2-204 through 2.5.2-209) (Tables 2.5.2-211 and 2.5.2-212).

- Reassess Mmax distributions and weights for original EPRI source zones within the site region based on the updated earthquake catalog, as described in Subsection 2.5.2.4.3.2.

- Assess Mmax distributions and weights for five new source zones based on the updated earthquake catalog. These five new source zones are largely devoid of historical seismicity (Table 2.5.2-211), thus Mmax distributions are based on Mmax estimates for their respective updated EPRI EST Gulf Coast zones (Table 2.5.2-207). Due to the similarity of the crust between the supplemental source zones and the original EPRI Gulf Coast source zones, the new zones reflect the same Mmax distributions as their updated Gulf Coast source zone counterpart for each EST.

Figures 2.5.2-204 through 2.5.2-208 show the supplemental seismic source zones and epicenters from the Phase 1 earthquake catalog. Seismicity within each of the supplemental sources is very sparse, with a total of just one or two earthquakes in each (Figures 2.5.2-204 through 2.5.2-208). The largest magnitude earthquake from the Phase 1 earthquake catalog in each supplemental source zone is Emb 4.09.

Given the paucity of earthquakes in 1 x 1 degree cells offshore of Florida, the following steps were used to assign a- and b-values to the updated EPRI sources and new supplemental source zones:

- Average a- and b-values were calculated for peninsular Florida using the updated earthquake catalog and original completeness matrices (extended to 2007) and full smoothing. The average values for the 15-degree cells are a = -2.28 and b = 1.03.

- These average a- and b-values were used to represent seismicity in 1 x 1 degree cells for the five new supplemental source zones.

- These average a- and b-values also were used to represent seismicity in 1 x 1 degree cells in the updated EPRI team sources representing Gulf Coast seismicity outside of the original EPRI completeness regions. One x one degree cells more than 200 miles from the Units 6 & 7 site were not modeled.

- The original a- and b-values were used for the updated EPRI team sources, where they are defined.

2.5.2.4.4.2 Updated Charleston Seismic Source (UCSS) Model

The Units 6 & 7 site is located roughly 500 miles from Charleston, South Carolina (Figure 2.5.2-203). The original EPRI seismic source model (References 243 and 247) includes assessments of the Charleston seismic source. However, several studies that post-date the EPRI EST assessments demonstrate that the source parameters for geometry, Mmax, and recurrence of Mmax in the Charleston seismic source need to be updated to capture a more current understanding of both the 1886 Charleston earthquake and the seismic source that produced this earthquake. Therefore, this subsection presents an update of the Charleston seismic source.

The Updated Charleston Seismic Source (UCSS) model presented in this subsection was developed through use of a Senior Seismic Hazard Analysis Committee (SSHAC) Level 2 process (Reference 318) for the Vogtle site in Georgia. Subsections 2.5.2.4.4.2.1 through 2.5.2.4.4.2.3 describe the UCSS model.

2.5.2.4.4.2.1 UCSS Model Geometry

The UCSS model includes four mutually exclusive source zone geometries (A, B, B', and C; Figure 2.5.2-212). Table 2.5.2-213 presents the latitude and longitude coordinates that define these four source zones. The four geometries of the UCSS model are defined based on current understanding of geologic and tectonic features in the 1886 Charleston earthquake epicentral region: the 1886 Charleston earthquake shaking intensity; distribution of seismicity; and geographic distribution, age, and density of liquefaction features associated with both the 1886 and prehistoric earthquakes. These features strongly suggest that the majority of evidence for the Charleston source is concentrated in the Charleston area and is not widely distributed throughout South Carolina.

Geometry A - Charleston

Geometry A is an about 100 x 50 kilometers, northeast-oriented area centered on the 1886 Charleston meizoseismal area (Figure 2.5.2-212). Geometry A is intended to represent a localized source area that generally confines the Charleston source to the 1886 meizoseismal area (i.e., a stationary source in time and space). Geometry A completely envelops the 1886 earthquake MMI X isoseismal (Reference 216), the majority of identified Charleston-area tectonic features and inferred fault intersections, and the majority of reported 1886 liquefaction features. Geometry A excludes the northern extension of the southern segment of the postulated East Coast Fault system because this system extends well north of the meizoseismal zone and is included in its own source geometry (Geometry C).

Geometry A also excludes outlying liquefaction features because liquefaction occurs as a result of strong ground shaking that may extend well beyond the areal extent of the tectonic source. Geometry

A also envelops instrumentally located earthquakes spatially associated with the Middleton Place-Summerville Seismic Zone (MPSSZ), which is located in the meizoseismal zone of the 1886 Charleston earthquake (References 272, 324, and 325). The preponderance of these moderately abundant earthquakes is thought to be aftershocks of the historical 1886 Emb 6.75 event (References 272, 324, and 325). The largest magnitude earthquake from the Phase 1 earthquake catalog in Geometry A is the historical 1886 Emb 6.75 event.

The preponderance of evidence strongly supports the conclusion that the seismic source for the 1886 Charleston earthquake is located in a relatively restricted area defined by Geometry A. These observations show that future earthquakes having magnitudes comparable to the Charleston earthquake of 1886 most likely would occur within the area defined by Geometry A. The UCSS model assigns a weight of 0.70 to Geometry A (Figure 2.5.2-213). To confine the rupture dimension to within the source area and to maintain a preferred northeast fault orientation, Geometry A is represented in the model by a series of closely spaced, northeast-striking faults parallel to the long axis of the zone.

Geometries B, B', and C

Whereas the preponderance of evidence supports the assessment that the 1886 Charleston meizoseismal area and Geometry A defines the area where future events would most likely be centered, it is possible that the tectonic feature responsible for the 1886 earthquake either extends beyond or lies outside of Geometry A. Therefore, the remaining three geometries (B, B', and C) are assessed to capture the uncertainty that future events may not be restricted to Geometry A.

The distribution of liquefaction features along the entire coast of South Carolina and observations from the paleoliquefaction record that a few events were localized (moderate earthquakes to the northeast and southwest of Charleston) suggest that the Charleston source could extend well beyond Charleston proper. Geometries B and B' represent a larger source zone, while Geometry C represents the southern segment of the postulated East Coast Fault system as a possible source zone.

The UCSS model assigns a weight of 0.20 to the combined geometries of B and B', and a weight of 0.10 to Geometry C. Geometry B' is a subset of B, and formally defines the onshore coastal area as a source that restricts earthquakes to the onshore region. Geometry B, which includes the onshore and offshore regions, and Geometry B' are mutually exclusive. The UCSS model assigns equal weights of 0.10 to Geometries B and B'.

Geometry B — Coastal and Offshore Zone

Geometry B is a coast-parallel, approximately 260 x 100 kilometers source area that (a) incorporates all of Geometry A, (b) is elongated to the northeast and southwest to capture other, more distant liquefaction features in coastal South Carolina (References 207, 208, and 323), and (c) extends to the southeast to include the offshore Helena Banks fault zone (Reference 213) (Figure 2.5.2-212). Seismicity within Geometry B, outside of the area of overlap with Geometry A, is sparse. The largest magnitude earthquake from the Phase 1 earthquake catalog in Geometry B is the historical 1886 Emb 6.75 event (Figure 2.5.2-212). The elongation and orientation of Geometry B is roughly parallel to the regional structural grain as well as roughly parallel to the elongation of 1886 isoseismals. The mapped extent of paleoliquefaction features (References 207, 208, and 323) defines the northeastern and southwestern extents of Geometry B.

The location and timing of paleoliquefaction features in the Georgetown and Bluffton areas to the northeast and southwest of Charleston suggest to some researchers that the earthquake source may not be restricted to the Charleston area (References 207, 295, 296, and 323). Geometry B accounts for the possibility that there may be an elongated source or multiple sources along the South Carolina coast. Paleoliquefaction features in the Georgetown and Bluffton areas may be explained by an earthquake source both northeast and southwest of Charleston, as well as possibly offshore.

Geometry B extends southeast to include an offshore area and the Helena Banks fault zone. The Helena Banks fault zone is clearly shown by multiple seismic reflection profiles and has demonstrable late Miocene offset (Reference 213). Offshore earthquakes in 2002 (m_b 3.5 and 4.4) suggest a possible spatial association of seismicity with the mapped trace of the Helena Banks fault system. Whereas these two events in the vicinity of the Helena Banks fault system do not provide a positive correlation with seismicity or demonstrate recent fault activity, these small earthquakes are new data that post-date the EPRI studies.

The UCSS model assigns a low weight of 0.10 to Geometry B (Figure 2.5.2-213) because the preponderance of evidence indicates that the seismic source that produced the 1886 earthquake lies onshore in the Charleston meizoseismal area and not in the offshore region. To confine the rupture dimension to within the source area and to maintain a preferred northeast fault orientation, the UCSS model represents Geometry B as a series of closely spaced, northeast-striking faults parallel to the long axis of the zone.

Geometry B' — Coastal Zone

Geometry B' is a coast-parallel, approximately 260 x 50 kilometers source area that incorporates all of Geometry A, as well as the majority of reported paleoliquefaction features (References 207, 208, and 323). Unlike Geometry B, however, Geometry B' does not include the offshore Helena Banks fault zone (Figure 2.5.2-212). Seismicity within Geometry B', outside of the area of overlap with Geometry A, is sparse. The largest magnitude earthquake from the Phase 1 earthquake catalog in Geometry B' is the historical 1886 Emb 6.75 event.

The Helena Banks fault system is excluded from Geometry B' because the preponderance of data and evaluations support the assessment that the fault system is not active and because evidence strongly suggests that the 1886 Charleston earthquake occurred onshore in the 1886 meizoseismal area and not on an offshore fault. Whereas there is little uncertainty regarding the existence of the Helena Banks fault, there is a lack of evidence that this feature is still active. Isoseismal maps documenting shaking intensity in 1886 indicate an onshore meizoseismal area (Figure 2.5.2-212). An onshore source for the 1886 earthquake and prehistoric events is supported by the instrumentally recorded seismicity in the MPSSZ and the corresponding high-density cluster of 1886 and prehistoric liquefaction features.

Similar to Geometry B above, the UCSS model assigns a weight of 0.10 to Geometry B', reflecting the assessment that Geometry B' has a much lower probability of being the source zone for Charleston-type earthquakes than Geometry A (Figure 2.5.2-213). To confine the rupture dimension to within the source area and to maintain a preferred northeast fault orientation, the UCSS model represents Geometry B' as a series of closely spaced, northeast-striking faults parallel to the long axis of the zone.

Geometry C — East Coast Fault System-South

Geometry C is about 200 x 30 kilometers, north-northeast-oriented source area (Figure 2.5.2-212) enveloping the southern segment of the proposed East Coast Fault system shown in Figure 3 of Reference 278. The area of Geometry C is defined to envelop the original depiction of the postulated East Coast Fault System-South by Marple and Talwani in Reference 278. The largest magnitude earthquake from the Phase 1 earthquake catalog in Geometry C is Emb 4.31. The location of the 1886 Emb 6.75 earthquake from the Phase 1 earthquake catalog plots just outside of Geometry C, but, given the uncertainty in the location of this earthquake, it is considered to have possibly occurred within Geometry C. There is partial overlap between Geometries A and C. Within the area of overlap, seismicity in Geometry C is moderately abundant. To the north, outside the area of overlap, seismicity in Geometry C is very sparse.

The UCSS model assigns a low weight of 0.10 to Geometry C to reflect the assessment that Geometries B, B', and C all have equal, but relatively low, likelihoods of producing large-magnitude earthquakes (Figure 2.5.2-213). As with the other UCSS alternative geometries, the UCSS model represents Geometry C as a series of parallel, vertical faults oriented northeast-southwest and parallel to the long axis of the narrow rectangular zone. The faults and extent of earthquake ruptures are confined within the rectangle depicting Geometry C.

UCSS Model Parameters

Based on studies by Bollinger et al. (References 214 and 215) and Bollinger (Reference 217), the UCSS model assumes a 20-kilometer thick seismogenic crust. To model the occurrence of earthquakes in the characteristic part of the Charleston distribution ($M_w \geq 6.7$), the model uses a series of closely-spaced, vertical faults parallel to the long axis of each of the four source zones (A, B, B', and C). Faults and earthquake ruptures are limited to within each respective source zone and are not allowed to extend beyond the zone boundaries, and ruptures are constrained to occur within the depth range of 0 to 20 kilometers.

The UCSS model assumes fault rupture areas have a width-to-length aspect ratio of 0.5, conditional on the assumed maximum fault width of 20 kilometers. To obtain Mmax earthquake rupture lengths from magnitude, the UCSS model uses the Wells and Coppersmith (Reference 334) empirical relationship between surface rupture length and magnitude for earthquakes of all slip types.

To maintain as much similarity as possible with the original EPRI model, the UCSS model treats earthquakes in the exponential part of the distribution ($M_w < 6.7$) as point sources uniformly distributed within the source area (full smoothing), with a constant depth fixed at 10 kilometers.

2.5.2.4.4.2.2 UCSS Model Mmax

Mmax estimates for the Charleston seismic source are based on published literature and previous source characterizations. Given the large uncertainties in working with the paleoliquefaction record and methods for estimating magnitudes from these data, the best representation of the Mmax for the Charleston seismic source should be based on estimates of the size of the 1886 earthquake.

Based on assessment of the currently available data and interpretations regarding the range of modern Mmax estimates, the UCSS model modifies the 2008 U.S. Geological Survey (USGS) hazard model magnitude distribution (Reference 300) to include a total of five discrete magnitude values, each separated by 0.2 M_w units (Figure 2.5.2-213). The UCSS Mmax distribution is based on recent studies, as summarized in Table 2.5.2-214.

The UCSS Mmax distribution includes a discrete value of M_w 6.9 to represent the Bakun and Hopper (Reference 211) best estimate of the 1886 Charleston earthquake magnitude, as well as a lower value of M_w 6.7 to capture a low probability that the 1886 earthquake was smaller than the Bakun and Hopper (Reference 211) mean estimate of M_w 6.9. Bakun and Hopper (Reference 211) do not explicitly report a 1-sigma range in magnitude estimate of the 1886 earthquake, but do provide a 2-sigma range of M_w 6.4 to 7.2.

The UCSS magnitudes and weights are as follows:

M_w	Weight	
6.7	0.10	
6.9	0.25	Bakun and Hopper (Reference 211) mean
7.1	0.30	
7.3	0.25	Johnston (Reference 267) mean
7.5	0.10	

This results in a weighted Mmax mean magnitude of M_W 7.1 for the UCSS, slightly lower than the mean magnitude of M_W 7.2 in the 2008 USGS model (Reference 300).

2.5.2.4.4.2.3 UCSS Model Recurrence of Mmax

In the 1989 EPRI study (Reference 243), the six EPRI ESTs use an exponential magnitude distribution to represent earthquake sizes for their Charleston sources. Parameters of the exponential magnitude distribution are estimated from historical seismicity in the respective source areas. This results in recurrence intervals for Mmax earthquakes (at the upper end of the exponential distribution) of several thousand years.

The UCSS model for earthquake recurrence is a composite model consisting of two distributions. The first is an exponential magnitude distribution used to estimate recurrence between the lower-bound magnitude used for hazard calculations and M_W 6.7. The parameters of this distribution are estimated from the earthquake catalog, as they were for the 1989 EPRI study. This is the standard procedure for smaller magnitudes and is the model used, for example, by the USGS 2002 national hazard maps (Reference 251).

The second distribution treats Mmax earthquakes ($M_W \geq 6.7$) according to a characteristic model, with discrete magnitudes and mean recurrence intervals estimated through analysis of geologic data, including paleoliquefaction studies. The term Mmax is used to describe the range of largest earthquakes in both the characteristic portion of the UCSS recurrence model and the EPRI exponential recurrence model.

This composite model achieves consistency between the occurrence of earthquakes with $M_W < 6.7$ and the earthquake catalog and between the occurrence of large earthquakes ($M_W \geq 6.7$) with paleoliquefaction evidence. It is a type of "characteristic earthquake" model, in which the recurrence rate of large events is higher than what would be estimated from an exponential distribution inferred from the historical seismic record.

Mmax Recurrence

This subsection describes how the UCSS model determines mean recurrence intervals for Mmax earthquakes. The UCSS model incorporates geologic data to characterize the recurrence intervals for Mmax earthquakes. As described earlier, identifying and dating paleoliquefaction features provides a basis for estimating the recurrence of large Charleston area earthquakes. Most of the available geologic data pertaining to the recurrence of large earthquakes in the Charleston area were published after 1990 and therefore were not available to the six EPRI ESTs. In the absence of geologic data, the six EPRI EST estimates of recurrence for large, Charleston-type earthquakes are based on a truncated exponential model using historical seismicity (References 243 and 247).

The truncated exponential model also provides the relative frequency of all earthquakes greater than m_b 5.0 up to Mmax in the EPRI PSHA. The recurrence of Mmax earthquakes in the EPRI models is on the order of several thousand years, which is significantly greater than more recently published estimates of about 500 to 600 years, based on paleoliquefaction data (Reference 323).

Paleoliquefaction Data

Strong ground shaking during the 1886 Charleston earthquake produced extensive liquefaction, and liquefaction features from the 1886 event are preserved in geologic deposits at numerous locations in the South Carolina coastal region. Documentation of older liquefaction-related features in geologic deposits provides evidence for prior strong ground motions during prehistoric large earthquakes. Estimates of the recurrence of large earthquakes in the UCSS are based on dating paleoliquefaction features.

Many potential sources of ambiguity and/or error are associated with dating and interpreting paleoliquefaction features. This assessment does not reevaluate field interpretations and data; rather, it reevaluates criteria used to define individual paleoearthquakes in the published literature. In particular, the UCSS model reevaluates the paleoearthquake record interpreted by Talwani and Schaeffer (Reference 323) based on that study's compilation of sites with paleoliquefaction features.

Talwani and Schaeffer (Reference 323) compile radiocarbon ages from paleoliquefaction features along the coast of South Carolina. These data include ages that provide contemporary, minimum, and maximum limiting ages for liquefaction events. Radiocarbon ages are corrected for past variability in atmospheric ^{14}C using well-established calibration curves and converted to “calibrated” (approximately calendar) ages. From their compilation of calibrated radiocarbon ages from various geographic locations, Talwani and Schaeffer (Reference 323) correlate individual earthquake episodes.

Talwani and Schaeffer (Reference 323) identify individual earthquake episodes based on samples with “contemporary” age constraints that have overlapping calibrated radiocarbon ages at approximately 1-sigma confidence interval. The estimated age of each earthquake is calculated from the “weighted averages of overlapping contemporary ages” (Reference 323, p. 6632). They define as many as eight events (named 1886, A, B, C, D, E, F, and G, in order of increasing age) from the paleoliquefaction record, and offer two scenarios to explain the distribution and timing of paleoliquefaction features (Table 2.5.2-215). The two scenario paleoearthquake records proposed by Talwani and Schaeffer (Reference 323) have different interpretations for the size and location of prehistoric events (Table 2.5.2-215).

In their Scenario 1, the four prehistoric events, A, B, E, and G, that produced widespread liquefaction features similar to the large 1886 Charleston earthquake are interpreted to be large, 1886 Charleston-type events. Three events, C, D, and F, are defined by paleoliquefaction features that are more limited in geographic extent than other events and are interpreted to be smaller, moderate-magnitude events (approximately M_W 6). Events C and F are defined by features found north of Charleston in the Georgetown region, and Event D is defined by sites south of Charleston in the Bluffton area.

In their Scenario 2, all events are interpreted as large, 1886 Charleston-type events. Furthermore, Events C and D are combined into a large Event C'. Talwani and Schaeffer (Reference 323) justify the grouping of the two events based on the observation that the calibrated radiocarbon ages that constrain the timing of Events C and D are indistinguishable at the 95 percent (2-sigma) confidence interval.

The length and completeness of the paleoearthquake record based on paleoliquefaction features is a source of epistemic uncertainty in the UCSS model (epistemic uncertainty is the result of inaccurate or incomplete information and can be reduced or eliminated given better models or additional observations, as opposed to aleatory uncertainty that results from randomness and cannot be reduced with more or better observations). The paleoliquefaction record along the South Carolina coast extends from 1886 to the mid-Holocene (Reference 323).

There is uncertainty regarding the length of completeness of the paleoliquefaction record in the Charleston region. There is general agreement that the paleoliquefaction record is complete for the past approximately 2000 years and that liquefaction events may be missing from the older portions of the geologic record (Reference 323). The suggested incompleteness of the older portions of the record is based on the argument that past fluctuations in sea level have produced time intervals of low water table conditions (and thus low liquefaction susceptibility), during which large earthquake events may not have been recorded in the paleoliquefaction record (Reference 323). While this assertion may be true, it is possible that the paleoliquefaction record may be complete back to the mid-Holocene.

2-Sigma Analysis of Event Ages

The Talwani and Schaeffer (Reference 323) data compilation of liquefaction is the basis for analysis of the coastal South Carolina paleoliquefaction record performed in support of Subsection 2.5.2. As described previously, Talwani and Schaeffer (Reference 323) use calibrated radiocarbon ages with 1-sigma error bands to define the timing of past liquefaction episodes in coastal South Carolina. The standard in paleoseismology, however, is to use calibrated ages with 2-sigma (95.4 percent confidence interval) error bands (Reference 261). Likewise, in paleoliquefaction studies, to more accurately reflect the uncertainties in radiocarbon dating, Tuttle (Reference 328) advises the use of calibrated radiocarbon dates with 2-sigma error bands (as opposed to narrower 1-sigma error bands).

Talwani and Schaeffer's (Reference 323) use of 1-sigma error bands may lead to over-interpretation of the paleoliquefaction record such that more episodes are interpreted than actually occurred. In recognition of this possibility, the conventional radiocarbon ages presented in Talwani and Schaeffer (Reference 323) are recalibrated and reported with 2-sigma error bands. The recalibration of individual radiocarbon samples and estimation of age ranges for paleoliquefaction events show broader age ranges with 2-sigma error bands that are used to obtain broader age ranges for paleoliquefaction events in the Charleston area.

Event ages based on overlapping 2-sigma ages of paleoliquefaction features are presented in Table 2.5.2-215. Paleoearthquakes are distinguished based on grouping paleoliquefaction features that have contemporary radiocarbon samples with overlapping calibrated ages. Event ages are defined by selecting the age range common to each of the samples. For example, an event defined by overlapping 2-sigma sample ages of 100 to 200 calendar years before present and 50 to 150 calendar years before present has an event age of 100 to 150 calendar years before present. The UCSS model considers these “trimmed” ages to represent the approximately 95 percent confidence interval, with a “best estimate” event age as the midpoint of the approximately 95 percent age range.

The UCSS model 2-sigma analysis identifies six distinct paleoearthquakes in the data presented by Talwani and Schaeffer (Reference 323). As noted by that study, Events C and D are indistinguishable at the 95 percent confidence interval, and in the UCSS, those samples define Event C' (Table 2.5.2-215). Additionally, the UCSS 2-sigma analysis suggests that Talwani and Schaeffer Events F and G (Reference 323) are a single, large event, defined in the UCSS as F'.

One important difference between the UCSS result and that of Talwani and Schaeffer (Reference 323) is that the three Events C, D, and F in their Scenario 1, which are inferred to be smaller, moderate-magnitude events, are grouped into more regionally extensive Events C' and F' (Table 2.5.2-215). Therefore, in the UCSS, all earthquakes in the 2-sigma analysis are interpreted to represent large, Charleston-type events.

The incorporation of large Events C' and F' into the UCSS model is, in effect, a conservative approach. In the effort to estimate the recurrence of Mmax events (M_W 6.7 to 7.5), moderate-magnitude (about M_W 6) earthquakes C and D would be eliminated from the record of large (Mmax) earthquakes in the UCSS model, thereby increasing the calculated Mmax recurrence interval and lowering the hazard without sufficient justification.

For these reasons the UCSS model uses a single, large Event C' (instead of separate, smaller Events C and D) and a single, large Event F' (instead of separate, smaller Events F and G). Analysis suggests that there have been four large earthquakes in the most-recent, about 2000-year portion of the record (1886 and Events A, B, and C'). In the entire 5000-year paleoliquefaction record, there is evidence for six large, Charleston-type earthquakes (1886, A, B, C', E, F'; Table 2.5.2-215). Figure 2.5.2-212 shows the geographic distribution of liquefaction features. The distributions of paleoliquefaction sites for Events A, B, C', E, and F' are all very similar to the coastal extent of the liquefaction features from the 1886 earthquake.

Recurrence intervals developed from the earthquakes recorded by paleoliquefaction features assume that these features were produced by large Mmax events and that both the 2000-year and 5000-year records are complete. However, the UCSS model highlights at least two concerns regarding the use of the paleoliquefaction record to characterize the recurrence of past Mmax events.

First, it is possible that multiple, moderate-sized earthquakes closely spaced in time produced the paleoliquefaction features associated with one or more of the pre-1886 events. If this is the case, then the calculated recurrence interval would yield artificially short recurrence for Mmax, because it is calculated using repeat times of both large (Mmax) events and smaller earthquakes. Limitations of radiocarbon dating and limitations in the stratigraphic record often preclude identifying individual events in the paleoseismologic record that are closely spaced in time (i.e., separated by only a few years to a few decades). Several seismic sources have demonstrated tightly clustered earthquake activity in space and time that are indistinguishable in the radiocarbon and paleoseismic record:

- New Madrid (December 1811, January 1812, and February 1812)
- North Anatolian fault (August 1999 and November 1999)
- San Andreas fault (December 1812 and January 1857)

Therefore, the UCSS acknowledges the distinct possibility that Mmax occurs less frequently than what is calculated from the paleoliquefaction record.

A second concern is that the recurrence behavior of the Mmax event may be highly variable through time. For example, the UCSS considers it unlikely that M_W 6.7 to 7.5 events have occurred on a Charleston source at an average repeat time of about 500 to 600 years (Reference 323) throughout the Holocene Epoch. Such a moment release rate would likely produce tectonic landforms with clear geomorphic expression, such as are present in regions of the world with comparably high rates of moderate to large earthquakes (for example, faults in the Eastern California shear zone with sub-millimeter per year slip rates and recurrence intervals on the order of about 5000 years have clear geomorphic expression [Reference 309]).

Perhaps it is more likely that the Charleston source has a recurrence behavior that is highly variable through time, such that a sequence of events spaced about 500 years apart is followed by quiescent intervals of thousands of years or longer. This sort of variability in inter-event time may be represented by the entire mid-Holocene record, in which both short interevent times (e.g., about 400 years between Events A and B) are included in a record with long inter-event times (e.g., about 1900 years between Events C' and E).

Recurrence of Mmax

The UCSS model calculates two average recurrence intervals covering two different time intervals. The UCSS model represents these two recurrence intervals as separate branches on the logic tree (Figure 2.5.2-213). The first average recurrence interval is based on the four events that occurred within the past about 2000 years. This time period is considered to represent a complete portion of the paleoseismic record (Reference 323). These events include 1886, A, B, and C' (Table 2.5.2-215). The average recurrence interval calculated for the most recent portion of the paleoliquefaction record (four events over the past about 2000 years) is given 0.80 weight on the logic tree (Figure 2.5.2-213).

The second average recurrence interval is based on events that occurred within the past about 5000 years. This time period represents the entire paleoseismic record based on paleoliquefaction data (Reference 323). These events include 1886, A, B, C', E, and F' as listed in Table 2.5.2-215. Published literature and questioned researchers suggest that the older part of the record (older than about 2000 years ago) may be incomplete. Whereas this assertion may be true, it is also possible that the older record, which exhibits longer inter-event times, is complete.

The UCSS model assigns a weight of 0.20 to the average recurrence interval calculated for the 5000-year record (six events) (Figure 2.5.2-213). The 0.80 and 0.20 weighting of the 2000-year and 5000-year paleoliquefaction records, respectively, reflects incomplete knowledge of both the short- and long-term recurrence behavior of the Charleston source.

The mean recurrence intervals for the most recent 2000-year and 5000-year records represent the average time interval between earthquakes attributed to the Charleston seismic source. The mean recurrence intervals and their parametric uncertainties are calculated according to the methods outlined by Savage (Reference 313) and Cramer (Reference 227). The methods provide a description of mean recurrence interval, with a best estimate mean and an uncertainty described as a lognormal distribution with a median and parametric lognormal shape factor.

The lognormal distribution is one of several distributions, including the Weibull, Double Exponential, and Gaussian, among others, used to characterize earthquake recurrence (Reference 248). Ellsworth et al. (Reference 248) and Matthews et al. (Reference 280) propose a Brownian-passage time model to represent earthquake recurrence, arguing that it more closely simulates the physical process of strain build-up and release. This Brownian-passage time model is currently used to calculate earthquake probabilities in the greater San Francisco Bay region (Reference 337).

Analyses show that the lognormal distribution is very similar to the Brownian-passage time model of earthquake recurrence for cases where the time elapsed since the most recent earthquake is less than the mean recurrence interval (References 225 and 248). This is the case for Charleston, where 120 years have elapsed since the 1886 earthquake and the mean recurrence interval determined over the past 2000 years is about 548 years. The UCSS model calculates average recurrence intervals using a lognormal distribution because its statistics are well known (Reference 294) and numerous other studies use this method (References 227, 313, and 336).

The average interval between earthquakes is expressed as two continuous lognormal distributions. The average recurrence interval for the 2000-year record, based on the three most recent inter-event times (1886—A, A-B, and B-C'), has a best estimate mean value of 548 years, an uncertainty distribution described by a median value of 531 years, and a lognormal shape factor of 0.25. The average recurrence interval for the 5000-year record, based on five inter-event times (1886—A, A-B, B-C', C'-E, and E-F'), has a best estimate mean value of 958 years, an uncertainty distribution described by a median value of 841 years, and a lognormal shape factor of 0.51.

At one standard deviation, the average recurrence interval for the 2000-year record is between 409 and 690 years; for the 5000-year record, it is between 452 and 1564 years. Combining these mean values of 548 and 958 years with their respective logic tree weights of 0.8 and 0.2 results in a weighted mean of 630 years for Charleston Mmax recurrence.

The UCSS model uses mean recurrence values that are similar to those determined by earlier studies. Talwani and Schaeffer (Reference 323) consider two possible scenarios to explain the distribution in time and space of paleoliquefaction features. In their Scenario 1, large earthquakes have occurred with an average recurrence of 454 ±21 years over about the past 2000 years; in their Scenario 2, large earthquakes have occurred with an average recurrence of 523 ±100 years over the past 2000 years.

Talwani and Schaeffer (Reference 323) state that, “In anticipation of additional data we suggest a recurrence rate [sic] between 500 and 600 years for M 7+ earthquakes at Charleston.” For the 2000-year record, the 1-standard-deviation range of 409 to 690 years completely encompasses the range of average recurrence interval reported by Talwani and Schaeffer (Reference 323). The best-estimate mean recurrence interval value of 548 years is comparable to the midpoint of the Talwani and Schaeffer (Reference 323) best-estimate range of 500 to 600 years.

The best estimate mean recurrence interval value from the 5000-year paleoseismic record of 958 years is outside the age ranges reported by Talwani and Schaeffer (Reference 323), although they did not determine an average recurrence interval based on the longer record.

The 2008 USGS updated seismic hazard maps for the conterminous United States use a mean recurrence value of 550 years for characteristic earthquakes in the Charleston region (Reference 300). This value is based on the above-quoted 500 to 600 year estimate from Talwani and Schaeffer (Reference 323). The updated USGS seismic hazard maps for the conterminous United States do not incorporate uncertainty in mean recurrence interval in their calculations.

For computation of seismic hazard, discrete values of activity rate (inverse of recurrence interval) are required as input to the PSHA code (Reference 224). To evaluate PSHA based on mean hazard, the mean recurrence interval and its uncertainty distribution should be converted to mean activity rate with associated uncertainty. The final discretized activity rates used to model the UCSS in the PSHA reflect a mean recurrence of 548 years and 958 years for the 2000-year and 5000-year branches of the logic tree, respectively. Lognormal uncertainty distributions in activity rate are obtained by the following steps:

1. Invert the mean recurrence intervals to get mean activity rates.

2. Calculate median activity rates using the mean rates and lognormal shape factors of 0.25 and 0.51 established for the 2000-year and 5000-year records, respectively.

3. Determine the lognormal distributions based on the calculated median rate and shape factors.

The lognormal distributions of activity rate can then be discretized to obtain individual activity rates with corresponding weights.

2.5.2.4.4.3 Cuba and Northern Caribbean Source Model

This subsection describes the seismic source characterization developed for Units 6 & 7 of the Cuba area and the North America-Caribbean plate boundary region. Subsections 2.5.1.1.2 and 2.5.1.1.1.3.2.4 describe the geologic and seismic information assessed in support of the development of this seismic source characterization. The original EPRI study did not model this region, despite the presence of major active earthquake sources (Figures 2.5.2-214 and 2.5.2-215).

In order to evaluate contributions to seismic hazards from all portions of the 200-mile radius site region, and contributions from more distant but potentially significant seismic sources, additional seismic sources in the Cuba area and the North America-Caribbean plate boundary region are required to supplement the updated EPRI source model.

The seismic source characterization of Cuba and the North America-Caribbean plate boundary region was performed through the use of a Senior Seismic Hazard Analysis Committee (SSHAC) Level 2 process. This process involves input from recognized experts and a Technical Integrator (TI) team to characterize specific seismic source parameters and associated parametric uncertainty and to assess an overall regional seismic source model that captures the hazard contributed from each seismic source (Reference 318).

A SSHAC Level 2 study is required to develop a seismic source model because there is no seismic source model approved by the NRC (e.g., EPRI) that covers the Cuba area and the North America-Caribbean plate boundary region. The SSHAC process has been approved by the NRC in RG 1.208 as an acceptable approach for developing a seismic source model outside the CEUS and

the SSHAC Level 2 assessment is considered acceptable for a site-specific application. A detailed discussion of the SSHAC Level 2 process is provided in Subsection 2.5.2.4.4.3.1.

The northern boundary of the new Cuba and northern Caribbean seismic source model lies north of, and roughly parallel to, northern Cuba, partially within the Units 6 &7 site region. To avoid double-counting earthquakes between the new supplemental sources described in Subsection 2.5.2.4.4.1 and the new Caribbean seismic sources, the supplemental sources have all been truncated southward by the northern boundary of the new Cuba and northern Caribbean seismic source model (Figures 2.5.2-204 through 2.5.2-209).

There are many earthquake catalogs that list historical and instrumental earthquakes within portions of the Cuba area and the North America-Caribbean plate boundary region, but no single earthquake catalog includes sufficient coverage for assessing earthquake occurrence within this region. Data were compiled from regional and global catalogs into the Phase 2 earthquake catalog that covers the region 15° and 24° N, and 100° to 65° W for all time through mid-March 2008 (Figure 2.5.2-216). Subsection 2.5.2.1.3 describes in detail the development of the Phase 2 earthquake catalog. The Phase 2 earthquake catalog, along with earthquake descriptions from the published literature, was used to constrain maximum magnitude estimates for seismic sources within the Cuba area and the North America-Caribbean plate boundary region.

2.5.2.4.4.3.1 Implementation of the SSHAC Level 2 Process

A SSHAC Level 2 study was performed to incorporate current literature, data, and the understanding of experts into a new Cuba and northern Caribbean seismic source model. SSHAC (Reference 318) outlines this methodology and provides guidance on incorporating uncertainty and the use of experts in PSHA studies. The goal of the SSHAC process is to represent the range of current understanding of seismic source parameters by the informed technical community.

SSHAC (Reference 318) describes four levels of study (Levels 1 through 4), in increasing order of sophistication and effort. The choice of the level of a PSHA is driven by two factors: (1) the degree of uncertainty and contention associated with the particular project, and (2) the amount of resources available for the study (Reference 318). SSHAC (Reference 318, Table 3-1) suggests that a Level 2 study is appropriate for issues with “significant uncertainty and diversity,” and for issues that are “controversial” and “complex.”

The SSHAC Level 2 process utilizes an individual, team, or company to act as the TI. In a SSHAC Level 2 study, the TI is responsible for reviewing data and literature and contacting experts who have developed interpretations or who have specific knowledge of the seismic sources. The TI interacts with experts to identify issues and interpretations, and to assess the body and range of informed expert opinion.

This TI team: (1) compiled and reviewed literature pertaining to the geology, tectonics, and seismicity of Cuba and the Northern Caribbean; (2) contacted scientists familiar with recent and ongoing research in the study region; and (3) integrated this information to develop a seismic source characterization of the Cuba area and the North America-Caribbean plate boundary region that captures the body and range of views of the informed technical community. Table 2.5.2-216 provides a tabulation of the experts contacted as part of the SSHAC Level 2 process.

The experts listed in Table 2.5.2-216 were provided with a standard questionnaire pertaining to key issues regarding seismic sources in Cuba and the northern Caribbean. This survey was not a formal process of interrogation to obtain from each expert all of the specific parameters and weights to be used in the model. Instead, the experts were asked to speak to their own areas of expertise. It was then the TI's responsibility to combine these responses with data from the published literature to

capture the body and range of expert opinion and judgment regarding parameters and weights to be used in the seismic source model.

The seismic source model presented herein represents the TI's assessment of the body and range of informed expert opinion regarding seismic sources in Cuba and the northern Caribbean. The seismic source model parameters for geometry, Mmax, and recurrence of Mmax are the TI's assessment of the body and range of expert interpretations.

2.5.2.4.4.3.2 Seismic Source Characterization

The seismic source characterization of the Cuba and North America-Caribbean plate boundary region comprises ten seismic sources, including one areal source for Cuba and nine fault sources that represent tectonic elements of the North America-Caribbean plate boundary region to a distance of approximately 900 miles from the Units 6 & 7 site. Taken together, these seismic sources represent an appropriate model of earthquake recurrence on and near the North America-Caribbean plate boundary. Given that these sources are all located at significant distances from the Units 6 & 7 site (approximately 140 to 760 miles), some generalization of the source model geometry is justified to compute contributions to ground motion at the Units 6 & 7 site. The seismic sources, identified in Figure 2.5.2-217, are as follows:

- Cuba areal source zone
- Oriente fault – western
- Oriente fault – eastern
- Septentrional fault
- Northern Hispaniola fault – western
- Northern Hispaniola fault – eastern
- Swan Islands fault – western
- Swan Islands fault – eastern
- Walton-Duanvale fault
- Enriquillo-Plantain Garden fault

These ten seismic sources are based on geologic, geophysical, and seismic data described in Subsections 2.5.1.1.1.3.2.4 (Cuba) and 2.5.1.1.2.3 (Active Tectonic Structures of the Northern Caribbean Plate). Subsection 2.5.1.1.2.3 also describes tectonic features that are too distant from the Units 6 & 7 site to contribute to the ground motion hazard, even from the largest earthquakes that could occur in them. These distant tectonic features are not included in the seismic source characterization, and include the Muertos Trough, Mona Passage extensional zone, eastern portion of the Puerto Rico Trench, and the Beata Ridge (Figure 2.5.1-202). The decision to exclude these tectonic features from this seismic source characterization is based on the assessment that these tectonic features would not significantly contribute to ground motion hazard at the Units 6 & 7 site. Specifically, this assessment is based on the great site-to-source distances for these tectonic features.

Table 2.5.2-217 presents a summary of source parameters for the ten seismic sources in the seismic source characterization. Geographic coordinates of the Cuba areal source zone and the nine fault sources are presented in Tables 2.5.2-218 and 2.5.2-219, respectively.

The seismic source characterization presented in this subsection appropriately generalizes source geometries. Earthquake occurrence, derived from slip rates and Mmax earthquakes, sufficiently captures the hazard contribution of these sources at the Units 6 & 7 site. This reflects the intention of the source characterization to capture the contribution to ground motions at the Units 6 & 7 site due to large-magnitude earthquakes on distant sources.

Cuba Areal Source Zone

The Cuba areal source zone is characterized with a maximum magnitude (Mmax) earthquake distribution determined by historical seismicity, published values, fault lengths, and the TI team's assessment of the body and range of informed technical knowledge. An exponential recurrence model describes Mmax earthquake behavior for the areal source zone, with calculated recurrence parameters (a- and b-values) based on observed seismicity. For Cuba, which is partially inside the 200-mile radius site region, an areal source model is adopted because of the lack of knowledge about fault behavior and slip rates for Cuban faults with which to support assessment of fault-specific sources.

North America-Caribbean Fault Sources

Major faults along the North America-Caribbean plate boundary are represented in the source model by fault sources. For the North America-Caribbean plate boundary faults, generalized source geometry is acceptable because of the distances (about 420 miles or more) from the Units 6 & 7 site to the sources. Thus, generalized source models and recurrence models that capture the hazard contributions of the largest earthquakes are sufficient for evaluating sensitivity of these sources to the ground-motion hazards at the site.

Earthquake activity is modeled based on assessments of fault slip rate (based on geodetic and paleoseismic data, as well as plate boundary reconstruction data), effective seismic coupling (the fraction or ratio of slip rate accommodated during large, main-shock earthquakes), and Mmax. Mmax, in turn, is determined based on estimates of fault source geometry (fault length, fault width, and fault area) and published empirical relations between earthquake magnitude and fault area or earthquake magnitude and fault length.

The fault sources are characterized by fault slip rate, effective seismic coupling (the fraction or ratio of slip rate accommodated during large, main-shock earthquakes), and Mmax, with logic trees containing values and weights that integrate the knowledge base described in published literature and the informed opinions of scientists familiar with recent and ongoing research in the study region (Table 2.5.2-216). The rupture model assumes pure characteristic behavior. Because the attenuation model developed for the region does not require inputs of fault depth, dip direction, and slip type, those parameters are not reviewed here. In most cases, fault slip rate is determined from published geodetic rates using network Global Positioning System (GPS) geodetic data, with additional information provided by geologic and paleoseismic studies.

Seismic coupling ratios are estimated based on historical seismicity rates, published modeling experiments, analogs with similar tectonic environments, and judgment. For the two modeled thrust fault sources with non-vertical dips (the western and eastern portions of the Northern Hispaniola fault), earthquakes are assumed to occur on the fault's surface trace. This is a conservative modeling decision because the two thrust fault sources dip to the south. By constraining earthquake locations to the surface traces of these two thrust faults, source-to-site distances are minimized. Mmax is determined based on consideration of historical seismicity and empirical moment-area and moment-length scaling relationships. Fault length and fault area are defined either by the total source

length or, where a single source can arguably be divided into several rupture segments, the length of the longest rupture segment.

For all fault sources in the model regardless of slip type, consideration is given to:

- The empirical rupture area-magnitude relation of Wells and Coppersmith (Reference 334) for all slip types.
- The empirical rupture area-magnitude relation of Wyss (Reference 339).
- The rupture length-magnitude relation of Wells and Coppersmith (Reference 334) for all slip types.

For strike-slip fault sources in the model, additional consideration is given to the empirical rupture area-magnitude relations of:

- Hanks and Bakun (Reference 262).
- Working Group on California Earthquake Predictions (WGCEP) (Reference 337).

For subduction zone fault sources in the model (i.e., western and eastern portions of the Northern Hispaniola fault), additional consideration is given to:

- The empirical rupture area-magnitude relation of Abe (References 201 and 202).
- The empirical rupture area-magnitude relation of Geomatrix (Reference 257).
- The empirical rupture length-magnitude relation of Geomatrix (Reference 257).

Table 2.5.2-220 presents a summary of these empirical relations. The range of results from the various empirical relations guided assessment of the final magnitudes and weights on the logic trees.

2.5.2.4.4.3.2.1 Cuba Areal Source Zone

The single areal source zone representing Cuba (Figure 2.5.2-217) encompasses the major tectonic elements on the island and the majority of the historical seismicity. Subsection 2.5.1.1.1.3.2.4 provides discussion of geologic, geophysical, and seismic data for Cuba. The northern and eastern boundary of the source zone is drawn near the base of the submarine escarpment that marks the location of the Nortecubana fault suture and the geologic boundary between the relatively undeformed North American crust of the Bahama Platform and the highly attenuated crust of the former leading edge of the plate boundary zone (Figures 2.5.1-210 and 2.5.1-202). To account for uncertainty in the position of the boundary, a buffer of 12.5 miles from the base of the escarpment toward the north and east was added to the Cuba areal source zone. This buffer was added to account for poorly located earthquakes that probably occurred within the Cuba island arc region and/or a zone of fractured and faulted crust beyond the suture zone that formed during early Cenozoic subduction. The western boundary of the Cuba areal source zone is based on bathymetry and the locations and density of historical seismicity. This boundary approximately follows the boundary between the Yucatan Basin and the continental shelf surrounding Cuba. The southern boundary of the Cuba source zone coincides with the southern boundary of Cuba and the steep submarine escarpment that borders the Oriente fault. At closest approach, the Cuba areal source zone is located about 140 miles from the Units 6 & 7 site. The Cuba areal source is associated with moderately abundant seismicity that is distributed throughout the source (Figure 2.5.2-217). There appears to be higher concentration of epicenters in the southeastern portion of the Cuba areal source, near the active plate boundary and the eastern and western Oriente fault sources. Also, there

appears to be a higher concentration of epicenters distributed along the northern coast and near-shore portions of Cuba within the Cuba areal source. Although Figure 2.5.2-217 shows mainshock seismicity only, these observations hold for the dependent seismicity (foreshocks, aftershocks, and cluster events) and earthquakes with M_W < 3.0 as well (Figure 2.5.1-368). The largest earthquakes from the Phase 2 catalog associated with this source are the 1551 M_W 5.98 event in southeastern Cuba, the 1880 M_W 6.13 event in western Cuba, and 1914 M_W 6.29 event offshore northeastern Cuba.

For Cuba, which is partially inside the 200-mile radius site region, an areal source model is adopted because of the lack of knowledge about specific fault behavior and slip rates for Cuban faults. As described in Subsection 2.5.1.1.1.3.2.4 there are several major crustal faults mapped in Cuba. However, these faults and the earthquake activity in Cuba are insufficiently described in the literature to warrant fault sources in the seismic source characterization. Specifically:

- No fault is characterized with a late Quaternary slip-rate.
- No fault has unambiguous data to constrain the recurrence of large earthquakes.
- Poorly located earthquakes and the limited number of focal mechanisms preclude the association of earthquakes with mapped faults in Cuba.
- Subsection 2.5.1.1.1.3.2.4 describes the most detailed available geologic maps of Cuba, including the 1:500,000-scale Mapa Geológico de Republica de Cuba (Reference 231), the 1:250,000-scale Mapa Geológico de Cuba (Reference 233), and the 1:500,000-scale Mapa Tectonico de Cuba (Reference 234). The scale and quality of these geologic and tectonic maps of Cuba are inadequate to support an assessment of potential activity, geometry, and segmentation of faults.

Recent peer-reviewed literature provides support for the assessment of the lack of knowledge regarding the state of fault mapping in Cuba. For example, Cotilla- Rodríguez et al. (Reference 321) states, “...the detailed association between destructive earthquakes and active tectonic features is extremely complex and not known in depth [...] there is not a close correlation of seismic events with individual faults in Cuba.” Furthermore, Cotilla-Rodríguez et al. (Reference 321) states, “...most [historical, pre-instrumental earthquakes] have scarce data and do not permit a clear association to a seismic zone. There is no uniform knowledge about the historical seismicity of Cuba...”

Garcia et al. (Reference 254) present seismic hazard maps for Cuba that are based on seismogenic zone (SZ) source zones. Their SZs are narrow, elongated, areal seismic sources intended to represent potentially active faults. Seismicity rates for these “fault-like” SZs are not based on geologic- or geodetic-based fault slip rates because these data do not appear to exist. Instead, Garcia et al.’s (Reference 254) SZs are large enough to envelop sufficient numbers of earthquakes to estimate separate rates of seismicity for each source from the earthquakes observed within that source. In a subsequent publication, Garcia et al. (Reference 255) compare the results of their earlier SZ approach with those obtained by their implementation of a smoothed seismicity approach to hazard. Relative to the results obtained from their smoothed seismicity approach, Reference 255 concludes that the seismotectonic zone approach tends to result in slightly higher PGA values in northwestern Cuba. They indicate that “an improvement of the seismicity data collection would be welcome for a better knowledge of the seismicity in northwestern Cuba” (Reference 255). Moreover, they indicate that “although the definition of SZs is positive because it focuses on understanding the regional tectonics, this exercise could be misleading when not supported by data. Consequently, a mixture of the two approaches would probably be the best solution: a seismotectonic approach for the more seismic areas and only seismicity elsewhere” (Reference 255). According to Garcia et al. (Reference 255), “the northern intraplate region [of Cuba] is related to a moderate to low seismicity.” This observation of low to moderate rates of seismicity in northern Cuba is consistent with

observations made from the Phase 2 earthquake catalog (mainshock and dependent events), which indicates a higher concentration of earthquakes and higher magnitudes in southernmost Cuba at and near the modern plate boundary relative to the rest of the island. Therefore, Garcia et al.'s (Reference 254) seismotectonic zone approach may not be applicable to the moderate to low seismicity areas of northern Cuba.

As described in Subsection 2.5.1.1.1.3.2.4, the available GPS geodetic data are from Cuba (from only one station, which is located at Guantanamo Bay, near the plate boundary) and from nearby stations in Florida and the Caribbean. These data indicate deformation rates across Cuba relative to North America of <3 millimeters/year, and likely much less. However, data are insufficient to determine which faults or tectonic structures in Cuba accommodate this low deformation budget.

Hence, the island of Cuba is represented in the model as an areal source zone modeled with mainshock catalog seismicity representing earthquake activity. Earthquake rates within the Cuba areal source zone are determined from an analysis of completeness and an evaluation of earthquake magnitude-frequency for the source zone, and a Gutenberg-Richter relation is tested and represented by the parameters a- and b-values. Maximum magnitude values for Cuba are based on previous Cuba source models, historical seismicity, published literature, and estimates of fault capability based on assessments of possible fault dimensions and empirical moment-area and moment-length scaling relationships.

Table 2.5.2-217 summarizes source parameters for the Cuba areal source zone. The distribution of Mmax shows equal weight to branches with M_W = 7.0 and M_W = 7.25. This magnitude distribution is larger than the maximum instrumented earthquake in the catalog (February 1914 M_W ~6.3) and larger than the maximum historical earthquake (January 1880 M_W ~6.1) (Table 2.5.2-221). Our Mmax distribution is consistent with a recently published source model for Cuba, the Garcia et al. study (Reference 254), that shows a Mmax upper limit of M_S 7.0 for intraplate Cuba sources. The Garcia et al. study (Reference 254) is based on previous source characterizations of Cuba's historical seismicity, and assessment of fault capability. Garcia et al.'s study (Reference 255) assigns M_S 6.5 to their intraplate Cuba zone. The M_W 7 to 7.25 range of Mmax for Cuba presented herein is consistent with rupture lengths of about 50 to 80 kilometers and rupture thicknesses of about 12 to 18 kilometers. These rupture dimensions are reasonable given the lengths of major crustal faults in Cuba such as the Pinar, Nortecubana, and Cauto-Nipe faults (Reference 226) and estimates of Cuban crustal thickness (Reference 327).

2.5.2.4.4.3.2.2 Oriente Fault — Western

At closest approach, the western Oriente fault source is located about 420 miles from the Units 6 & 7 site (Figure 2.5.2-217). Subsection 2.5.1.1.1.1.1.2 provides discussion of the geologic, geodetic, and seismic characteristics of the Oriente fault. Table 2.5.2-217 summarizes source parameters for this fault source.

The western Oriente fault source is associated with abundant seismicity along its length, with an apparent concentration of epicenters at its western end near the Cayman trough (Figure 2.5.2-217). Seismicity also appears concentrated near its eastern end near where the western and eastern segments of the Oriente fault form a transtensional step-over (Figure 2.5.2-217). The largest earthquakes from the Phase 2 catalog associated with this source are the 1917 M_W 7.20 and 1992 M_W 6.80 events.

The slip rate distribution [and weights] for the western Oriente fault is 8 [0.1], 11 [0.7], and 13 [0.2] millimeters/year based on the GPS results of DeMets et al. (Reference 230) and DeMets and Wiggins-Grandison (Reference 229). The significant weight (0.4) given to seismic coupling ratios less than 1.0 is based on the thin, warm crust of the Cayman Trough that typifies the south side of the

fault for most of its length (Reference 326), low seismic coupling ratios noted globally for oceanic transform faults (Reference 299), and the lack of large earthquakes historically (Table 2.5.2-221).

The Mmax distribution [and weights] for the western Oriente fault is M_w 7.5 [0.3], 7.7 [0.4], and 8.0 [0.3] (Table 2.5.2-217). These values are based on rupture dimensions 300 to 490 kilometers long and 6 to 10 kilometers wide. Values higher than M_w 8.0 are obtained using empirical magnitude-rupture length relations for lengths greater than about 300 kilometers. However, these higher values are countered by the fact that longer rupture lengths involve very warm and thin crust near the mid-Cayman spreading center. The Mmax distribution exceeds the historical maximum magnitude earthquakes recorded near the eastern portion of this source in 1917 (M_w 7.2) and 1992 (M_w 6.8) (Subsection 2.5.2.1.3).

2.5.2.4.4.3.2.3 Oriente Fault — Eastern

At closest approach, the eastern Oriente fault source is located about 445 miles from the Units 6 & 7 site (Figure 2.5.2-217). Subsection 2.5.1.1.2.3.1.2 provides discussion of the geologic, geodetic, and seismic characteristics of the Oriente fault. Table 2.5.2-217 summarizes source parameters for this fault source.

The eastern Oriente fault source is associated with abundant seismicity along its length, with an apparent concentration of epicenters along its west-central portion, just offshore of southernmost Cuba near the city of Santiago de Cuba (Figure 2.5.2-217). The largest earthquake from the Phase 2 catalog associated with this source is the historical 1766 M_w 7.53 event.

The slip rate distribution and weighting for the eastern Oriente fault are identical to the western Oriente fault source. The seismic coupling ratio on the eastern Oriente fault is assigned a value of 1.0 given the repeated large earthquakes on the fault historically (Table 2.5.2-221).

The Mmax distribution [and weights] for the eastern Oriente fault is M_w 7.5 [0.2], 7.7 [0.6], and 7.9 [0.2] (Table 2.5.2-217). These values are based on rupture dimensions about 140 to 200 kilometers long (from mapped segments on the Oriente fault and Santiago deformed belt in Reference 222) and 15 to about 40 kilometers wide (References 326, 327, and 331). Values higher than M_w 7.9 are obtained using the empirical strike-slip magnitude-area relations of Hanks and Bakun (Reference 262) and WGCEP (Reference 337) for rupture widths greater than about 20 kilometers. These higher values are not used given the recognition that rupture dimensions involving widths greater than 20 kilometers would likely occur on the Santiago deformed belt with a strong reverse-oblique component, and this style of faulting is not captured in the strike-slip empirical databases. Instead, empirical values for the “all slip type” relation of Wells and Coppersmith (Reference 334) that yield an upper limit of M_w 7.9 are preferred for the larger rupture dimensions. The Mmax distribution exceeds the historical maximum magnitude earthquake of M_w 7.53 in June 1766 (Table 2.5.2-221).

2.5.2.4.4.3.2.4 Septentrional Fault

At closest approach, the Septentrional fault source is located about 545 miles from the Units 6 & 7 site (Figure 2.5.2-217). Subsection 2.5.1.1.2.3.2.1 provides discussion of the geologic, geodetic, and seismic characteristics of the Septentrional fault. Table 2.5.2-217 summarizes source parameters for this fault source.

The Septentrional fault source is associated with abundant seismicity along its entire length (Figure 2.5.2-217). The largest earthquakes from the Phase 2 catalog associated with this source are the historical 1842 M_w 8.23 and 1887 M_w 7.93 events.

The slip rate distribution [and weights] for the Septentrional fault is 6 [0.2], 9 [0.6], and 12 [0.2] millimeters/year based on the geologic slip rate of Prentice et al. (Reference 304) and GPS-based results of Manaker et al. (Reference 273). The seismic coupling ratio on the Septentrional fault is assigned a value of 1.0 given the repeated large to great earthquakes on the fault historically (Table 2.5.2-221).

The Mmax distribution [and weights] for the Septentrional fault is M_w 8.0 [0.5] and 8.25 [0.5] (Table 2.5.2-217). These values are based on the magnitude estimates of the historical 1842 rupture (Table 2.5.2-221). Equal weight is given to the lower magnitude estimate for this earthquake partially based on recognizing that strike-slip earthquakes greater than magnitude M_w 7.9 to 8.0 are exceedingly rare in the instrumental record globally. These values are consistent with rupture dimensions of about 350 kilometers long and 15 to 18 kilometers wide.

2.5.2.4.4.3.2.5 Northern Hispaniola Fault — Western

At closest approach, the western Northern Hispaniola fault source is located about 550 miles from the Units 6 & 7 site (Figure 2.5.2-217). Subsection 2.5.1.1.2.3.2.2 provides discussion of the geologic, geodetic, and seismic characteristics of the Northern Hispaniola fault. Table 2.5.2-217 summarizes source parameters for this fault source.

The western Northern Hispaniola fault source is associated with abundant seismicity along its entire length, with an especially high concentration of epicenters along its central and eastern portions (Figure 2.5.2-217). The largest earthquake from the Phase 2 catalog associated with this source is the 1953 M_w 6.93 event.

The slip rate distribution [and weights] is 4 [0.2], 6 [0.7], 8 [0.1] millimeters/year based on the GPS results of Calais et al. (Reference 220) and Manaker et al. (Reference 273). The source is modeled with a seismic coupling ratio of 1.0 based on goodness-of-fit with elastic block and fault modeling (Reference 273).

The Mmax distribution [and weights] for the western portion of the Northern Hispaniola fault is M_w 7.8 [0.2], 8.0 [0.6], and 8.3 [0.2] (Table 2.5.2-217). These values are based on rupture dimensions of 200 to 350 kilometers long and 30 to 60 kilometers wide (assumed locking depth of 12 to 20 kilometers and fault dip of 20° to 25°). The Mmax distribution exceeds the historical maximum magnitude earthquake of M_w 6.93 in May 1953 recorded at the eastern end of this source (Table 2.5.2-221). Earthquakes on the south-dipping western Northern Hispaniola fault are assumed to occur on the fault's surface trace.

2.5.2.4.4.3.2.6 Northern Hispaniola Fault — Eastern

At closest approach, the eastern Northern Hispaniola fault source is located about 760 miles from the Units 6 & 7 site (Figure 2.5.2-217). Subsection 2.5.1.1.2.3.2.2 provides discussion of the geologic, geodetic, and seismic characteristics of the Northern Hispaniola fault. Table 2.5.2-217 summarizes source parameters for this fault source.

The eastern Northern Hispaniola fault source is associated with abundant seismicity along its entire length, much of which appears in map view to the south of the surface trace of this south-dipping fault (Figure 2.5.2-217). The largest earthquake from the Phase 2 catalog associated with this source is the 1946 M_w 7.90 event.

The slip rate distribution and weighting for the eastern fault source are identical to the western fault source. Similarly, the seismic coupling ratio on the eastern portion of the Northern Hispaniola fault is 1.0 given the modeling results of Manaker et al. (Reference 273) and the historical great earthquake on the fault in August 1946 (Table 2.5.2-221).

The Mmax distribution (and weights) for the eastern Northern Hispaniola fault is M_W 8.0 [0.2], 8.3 [0.6], and 8.6 [0.2] (Table 2.5.2-217). These values are based on the 1946 M_W 7.90 historical event and rupture dimensions about 200 to 400 kilometers long and 50 to about 100 kilometers wide (assumed locking depths of 20 to 35 kilometers and fault dip of 20° to 25°). Earthquakes on the south-dipping eastern Northern Hispaniola fault are assumed to occur on the fault's surface trace.

2.5.2.4.4.3.2.7 Swan Islands Fault — Western

At closest approach, the western Swan Islands fault source is located 620 miles from the Units 6 & 7 site (Figure 2.5.2-217). Subsection 2.5.1.1.2.3.1.1 provides discussion of the geologic, geodetic, and seismic characteristics of the Swan Islands fault. Table 2.5.2-217 summarizes source parameters for this fault source.

The western Swan Islands fault source is associated with abundant seismicity along its entire length (Figure 2.5.2-217). The largest earthquake from the Phase 2 catalog associated with this source is the historical 1856 M_W 7.69 event.

The slip rate distribution [and weights] is 18 [0.2], 19 [0.6], and 20 [0.2] millimeters/year based on the GPS-derived relative plate motion rate of DeMets et al. (Reference 230). The seismic coupling ratio on the western Swan Islands fault is assigned a value of 1.0 given the possible repeated great earthquakes on the fault historically (Table 2.5.2-221).

The Mmax distribution [and weights] for the western Swan Islands fault is M_W 7.8 [0.2], 8.0 [0.7], and 8.3 [0.1] (Table 2.5.2-217). These values are based on the magnitude estimate of the historical M_W 7.69 1856 earthquake (Table 2.5.2-221). These values are consistent with rupture dimensions of about 350 to 500 kilometers long and 10 to 15 kilometers wide. The low weight assigned to the historical estimate of M 8.3 is based on recognizing that strike-slip earthquakes greater than magnitude M_W 7.9 to 8.0 are exceedingly rare in the instrumental record globally, and that only the largest rupture dimensions considered for the western Swan Islands fault source results in an empirical estimate of M_W 8.3.

2.5.2.4.4.3.2.8 Swan Islands Fault — Eastern

At closest approach, the eastern Swan Islands fault source is located 540 miles from the Units 6 & 7 site (Figure 2.5.2-217). Subsection 2.5.1.1.2.3.1.1 provides discussion of the geologic, geodetic, and seismic characteristics of the Swan Islands fault. Table 2.5.2-217 summarizes source parameters for this fault source.

The eastern Swan Islands fault source is associated with abundant seismicity along its entire length, with an apparent concentration of epicenters located near its eastern end near the Cayman trough (Figure 2.5.2-217). No earthquakes from the Phase 2 catalog greater than or equal to M_W 6.75 are associated with this source.

The slip rate distribution and weighting are identical to the western Swan Islands fault source. The significant weight of 0.4 to seismic coupling ratios less than 1.0 is based on the thin, warm crust of the Cayman Trough that typifies the north side of the fault source for most of its length (Reference 326), low seismic coupling ratios noted globally for oceanic transform faults (Reference 299), and the lack of large earthquakes historically (Table 2.5.2-221).

The Mmax distribution [and weights] for the eastern Swan Islands fault is M_W 7.2 [0.4], 7.5 [0.5], and 7.7 [0.1] (Table 2.5.2-217). These values are based on rupture dimensions of 130 to 200 kilometers long (from mapping by Rosencrantz and Mann, Reference 310) and 8 to 15 kilometers wide. The low weight on the highest magnitude reflects the recognition that a rupture length of 200 kilometers would at least partially involve very warm and thin crust near the mid-Cayman spreading center, and thus a

15-kilometer wide average fault rupture is unlikely. No historical earthquakes greater than or equal to M_w 6.75 are recorded near this source (Reference 331) (Table 2.5.2-221).

2.5.2.4.4.3.2.9 Walton-Duanvale Fault

At closest approach, the Walton-Duanvale fault source is located 490 miles from the Units 6 & 7 site (Figure 2.5.2-217). Subsection 2.5.1.1.2.3.2.3 provides discussion of the geologic, geodetic, and seismic characteristics of the Walton-Duanvale fault. Table 2.5.2-217 summarizes source parameters for this fault source.

The Walton-Duanvale fault source is associated with moderately abundant seismicity along its length, with an apparent concentration of epicenters located near its western end near the Cayman trough (Figure 2.5.2-217). Seismicity also appears concentrated at the eastern end of this source near Jamaica, where the left-lateral Walton-Duanvale and Enriquillo-Plantain Garden faults form a restraining bend. The largest earthquakes from the Phase 2 catalog associated with this source are the two approximately M_w 6.6 events that occurred in 1907 and 1957.

The slip rate distribution [and weights] is 6 [0.2], 8 [0.6], 10 [0.2] millimeters/year based on the GPS data of DeMets and Wiggins-Grandison (Reference 229). The weight of 0.3 for a seismic coupling ratio less than 1.0 is based on the thin, warm crust of the Cayman Trough that typifies the north side of the fault for much of its length (Reference 326), low seismic coupling ratios noted globally for oceanic transform faults (Reference 299), and the lack of large earthquakes historically (Table 2.5.2-221).

The Mmax distribution [and weights] for the Walton-Duanvale fault source is M_w 7.3 [0.3], 7.6 [0.6], and 7.8 [0.1] (Table 2.5.2-217). These values are based on rupture dimensions of 140 to 215 kilometers long and 6 to 10 kilometers wide. The Mmax distribution exceeds the historical maximum magnitude earthquakes of about M_w 6.6 in January 1907 and March 1957 recorded near the eastern portion of this source (Table 2.5.2-221).

2.5.2.4.4.3.2.10 Enriquillo-Plantain Garden Fault

At closest approach, the western Enriquillo-Plantain Garden fault source is located 560 miles from the Units 6 & 7 site (Figure 2.5.2-217). Subsection 2.5.1.1.2.3.2.3 provides discussion of the geologic, geodetic, and seismic characteristics of the Enriquillo-Plantain Garden fault. Table 2.5.2-217 summarizes source parameters for this fault source.

The Enriquillo-Plantain Garden fault source is associated with abundant seismicity along its length, with apparent concentrations of epicenters at its western and eastern ends (Figure 2.5.2-217). Multiple large historical earthquakes have ruptured along the Enriquillo-Plantain Garden fault (Reference 282), including from the Phase 2 catalog the 1692 M_w 7.78 earthquake near Jamaica and the 1751 M_w 7.28 and 1770 M_w 7.53 earthquakes near Port-au-Prince, Haiti.

The slip rate distribution and weighting are identical to the Walton-Duanvale fault source. The seismic coupling ratio on the Enriquillo-Plantain Garden fault source is assigned a value of 1.0 given the repeated large earthquakes on the fault historically (Table 2.5.2-221) and the goodness-of-fit with elastic block and fault modeling (Reference 273).

The Mmax distribution [and weights] for the Enriquillo-Plantain Garden fault is M_w 7.5 [0.2], 7.7 [0.6], and 7.9 [0.2] (Table 2.5.2-217). These values are based on rupture dimensions of about 120 to 250 kilometers long (from mapping by Mann et al., Reference 276) and 15 to about 18 kilometers wide. The Mmax distribution is comparable to the upper estimates of historical earthquakes attributed to this source, including the June 1692 M_w 7.78, the October 1751 M_w 7.28, the June 1770 M_w 7.53, and the April 1860 M_w 6.73 earthquakes (Table 2.5.2-221).

Based on the slip rates and maximum magnitudes considered for this fault source, the 2010 M_w 7.0 Haiti earthquake, which occurred within the Enriquillo fault zone, is predictable (Subsection 2.5.1.1.2.3.2.3) and completely within the magnitude and recurrence assessments incorporated into the updated PSHA for the Units 6 & 7 site.

2.5.2.4.4.3.3 Comparison of Seismic Source Parameters with USGS Initial Seismic Hazard Maps for Haiti

The USGS initial seismic hazard maps for Haiti by Frankel et al. (Reference 235) are based on the available information on seismic source parameters and seismicity data obtained immediately following the M_w 7.0 January 12, 2010, Haiti earthquake (Reference 235). They emphasize the preliminary nature of their model, indicating that it was developed in response to the urgent need for earthquake hazard information and that, “more extensive logic trees will be developed to better capture the uncertainty in key parameters” (Reference 235, p. 1).

Frankel et al. (Reference 235) characterize a total of seven fault sources, four of which also are included in the seismic source characterization of Cuba and the North America-Caribbean plate boundary region developed as part of the updated PSHA for the Units 6 & 7 site. The four seismic sources common to both Frankel et al.'s model (Reference 235) and the model developed for the 6 & 7 site study include the following sources: the Enriquillo-Plantain Garden fault, Septentrional fault, Northern Hispaniola fault – eastern, and Northern Hispaniola fault – western (Subsection 2.5.2.4.4.3.2). The three seismic sources included in Frankel et al.'s model (Reference 235) that are not included in the PSHA update at the Units 6 & 7 site are: the Muertos Trough Neiba segment, the Muertos Trough central segment, and the Matheux Neiba fault sources. The Muertos Trough segments are not included in the Units 6 & 7 site characterization because of their great distance from the site (about 1210 kilometers [750 miles] at their nearest approach). Likewise, the Matheux Neiba fault is not included in the Units 6 & 7 site characterization because of its great distance from the site (1045 kilometers [650 miles] at its nearest approach) and its estimated slip rate of 1 millimeter/year (Reference 235) is an order of magnitude lower than other included sources more proximal to the site with equivalent or greater Mmax values.

Table 2.5.2-222 presents a comparison of seismic source parameters from the Frankel et al. (Reference 235) and the Units 6 & 7 site characterizations. In general, there is good agreement between source parameters from these two characterizations. The assigned range of Mmax values equals or exceeds the characteristic magnitude (M_{char}) values defined for the equivalent Frankel et al. (Reference 235) sources. The assigned range of slip rate values to the Enriquillo-Plantain Garden fault and Northern Hispaniola fault – western sources envelops or exceeds the equivalent values from Frankel et al.'s characterization (Reference 235). The assigned range of slip rate values to the Septentrional fault and Northern Hispaniola fault – eastern sources is less than the values defined for the equivalent Frankel et al.'s sources (Reference 235). However, Frankel et al.'s slip rate estimates for the Septentrional and eastern Northern Hispaniola faults (Reference 235) exceed recently published geodetic and geologic estimates (Subsection 2.5.2.4.4.3.2).

2.5.2.4.4.3.4 Hazard Sensitivity Calculations

Hazard sensitivity calculations were performed to assess the significance of certain aspects of the PSHA for the Turkey Point Units 6 & 7 site. Calculations were performed to assess the potential impact of: (1) the Walkers Cay fault, (2) several faults within Cuba, and (3) different approaches to modeling the Cuba areal source zone.

2.5.2.4.4.3.4.1 Walkers Cay Fault Hazard Sensitivity Calculation

The Walkers Cay fault lies northeast of the Turkey Point Units 6 & 7 site and straddles the 200-mile site region boundary (Figure 2.5.1-366). Subsection 2.5.1.1.1.3.2.2 describes geologic and seismic

reflection data for the Walkers Cay fault. Based on the available data that suggest possible faulting of the seafloor, Quaternary activity on the Walkers Cay fault cannot be precluded. For this reason, a hazard sensitivity calculation was performed to assess the potential impact of a Walkers Cay fault source on the PSHA for the Turkey Point Units 6 & 7 site.

The geometry of the Walkers Cay fault source is based on the mapping of Mullins and Van Buren (Reference 355). For the purposes of the hazard sensitivity calculation, the Walkers Cay fault is assumed to have a vertical dip angle and a rupture depth from 0–15 kilometers (0-9 miles). The characteristic magnitude for the Walkers Cay fault source is based on the empirical surface rupture length-magnitude regression from Wells and Coppersmith (Reference 334) for all fault types, assuming a surface rupture length equal to the 33-kilometer (21-mile) mapped length of the fault. This regression provides a median value of M_W 6.8. Uncertainty associated with this value is accounted for in the hazard sensitivity calculation by allowing earthquakes of 0.2 magnitude units larger or smaller than the characteristic event. The characteristic magnitude distribution [and weights] assigned to the Walkers Cay fault source is: M_W 6.6 [0.2], 6.8 [0.6], 7.0 [0.2].

There are no data with which to directly determine the late Quaternary slip rate on the Walkers Cay fault. There are, however, data and observations that can be used to constrain possible slip rate values for the Walkers Cay fault source. The slip rate distribution in millimeters/year [and weights] assigned to the Walkers Cay fault source for the hazard sensitivity calculation is: 0.001 [0.2], 0.01 [0.6], 0.05 [0.2]. The largest weight in this distribution is accorded to a slip rate of 0.01 millimeters/year, which appears to represent a limiting rate beyond which there would be a significant likelihood that vertical separations of Quaternary and Pliocene deposits would be sufficiently large to be observable within the presently available data. Also, the lack of perturbations observed in structure contours of Miocene- and Cretaceous-age contacts in the vicinity of the Walkers Cay fault suggests that the total amount of vertical separation across the fault likely is on the order of tens of meters or less.

For the purpose of the hazard sensitivity calculation, a characteristic earthquake recurrence model (Reference 356) but with no contribution from an exponential portion of the recurrence curve at lower magnitudes is assumed for the Walkers Cay fault source. Walkers Cay fault hazard is calculated using the Mid-Continent crustal model and non-rifted coefficients from the EPRI 2004 attenuation relations.

The results of the sensitivity study indicate that adding the Walkers Cay fault to the total hazard results in 10^{-4} mean annual frequency of exceedance (MAFE) amplitudes that are 0.3 percent higher at 1 Hz and 0.5 percent higher at 10 Hz, and annual frequencies of exceedance, at the FSAR 10^{-4} MAFE amplitudes, that are 0.7 percent higher at 1 Hz and 1.0 percent higher at 10 Hz. As such, the results of the hazard sensitivity calculation based on the conservative seismic source characterization of the Walkers Cay fault indicate that further consideration of the Walkers Cay fault for the Turkey Point Units 6 & 7 site hazard is unwarranted due to its insignificant contribution to site hazard.

2.5.2.4.4.3.4.2 Cuba Hazard Sensitivity Calculations

This subsection describes the characterization and results of intraplate Cuba seismic sources for use in a hazard sensitivity calculation performed to assess the potential impact on the Turkey Point Units 6 & 7 PSHA. As described in Subsection 2.5.1.1.1.3.2.4, it is unclear which, if any, of the faults in intraplate Cuba are capable tectonic sources. For this reason, hazard sensitivity calculations were performed to assess the potential impact of intraplate Cuba seismic sources. The seismic source parameters for both areal and fault sources used in these hazard sensitivity calculations were developed through the use of the SSHAC Level 2 methodology (Reference 318). Subsection 2.5.2.4.4.3.1 describes the SSHAC Level 2 methodology.

For the SSHAC Level 2 study of Cuba seismic sources, the TI team comprised Dean Ostenaa, Roland LaForge, Scott Lindvall, and Ross Hartleb. Participatory peer review was provided by Robert Creed. A total of eleven experts were contacted by the TI team with questions regarding the sensitivity calculations. These experts include geologists, seismologists, and hazard analysts from Cuba, the U.S., and elsewhere (Table 2.5.2-232). The level of detail provided to the TI team by the experts varies (Table 2.5.2-232). Some experts provided detailed responses and interacted with the TI team, whereas other experts provided only terse responses. Four experts either declined to participate or did not respond at all.

2.5.2.4.4.3.4.2.1 Cuba Seismic Sources for Hazard Sensitivity Calculation

Based on review of published literature and interaction with experts, the TI team developed a seismic source characterization for intraplate Cuba seismic sources for use in a hazard sensitivity calculation to assess the impact on hazard at the Turkey Point Units 6 & 7 site. This subsection describes the characterization of both areal sources and fault sources for the hazard sensitivity calculations.

Three scenarios by which areal source zones are implemented in the hazard sensitivity calculations are summarized below and in Table 2.5.2-233.

- Single areal source zone scenario (Z1) — In the single areal source zone model, a single areal source for Cuba is used, with a uniform seismicity rate throughout the zone that is based on observed seismicity from the Phase 2 earthquake catalog (Figure 2.5.2-271). This is the base case for the hazard sensitivity calculations and is the seismic source characterization for intraplate Cuba used in the PSHA (Subsection 2.5.2.4.6). The Z1 model results in a contribution to hazard that is intermediate between the Z6 and Z11% zone scenarios (Table 2.5.2-233).

- Elevated rate areal source zone scenario (Z11%) — In the elevated rate zone scenario, a single areal source for Cuba is used, with a uniform seismicity rate throughout the zone that is based on observed seismicity from the Phase 2 earthquake catalog. The geometry of this zone is equivalent to that in the Z1 scenario. Unlike the Z1 scenario, however, the uniform rate for the Z11% scenario is based on a small subzone in northern Cuba (the “northern Cuba subzone” shown in Figure 2.5.2-271) that is located partially within the site region and that exhibits a higher rate of seismicity than surrounding regions. The seismicity rate from the northern subzone is approximately 11 percent higher than that for the entire Cuba areal source zone, and this higher rate is applied to the Z1 scenario. The Z11% scenario results in the highest contribution to hazard from the three zone scenarios (Table 2.5.2-233).

- Six areal source zones scenario (Z6) — In the six areal source zones scenario, Cuba is divided into six zones largely on the basis of observed patterns in seismicity (Figure 2.5.2-271). The seismicity *b*-value is constant across all six zones and equivalent to that used in the Z1 scenario; the seismicity *a*-values vary from zone to zone, are uniform within each zone, and are based on the observed seismicity within each zone. For the six-zone scenario (Z6), the *a*-values were determined by counting the number of events in each subzone greater than or equal to M_W 3.0. The *b*-value in base case Z1 is used for all six subzones. The Z6 scenario results in the lowest contribution to hazard from the three zone scenarios (Table 2.5.2-233).

All areal source scenarios are given equally weighted maximum moment magnitudes, M_W, of 7.0 and 7.3 with uniformly distributed seismicity parameters (complete smoothing) determined from the earthquakes within each zone. Values for Z1 and Z11% are shown in Table 2.5.2-234, using the completeness table for Cuba from Garcia et al. (Reference 255) (Table 2.5.2-235). Focal depth for all areal sources is the same as was implemented in Subsection 2.5.2.4.6, which uses a three-point

distribution to represent the 0-15 kilometer (0–9 mile) seismogenic thickness: 2.5, 7.5, and 12.5 kilometers (1.6, 4.7, and 7.8 miles), equally weighted.

The input parameters for the Cuba sensitivity fault sources are described below and are summarized in Table 2.5.2-236 and Figure 2.5.2-272:

- Fault sources and geometries — Intraplate Cuba fault sources include Cotilla-Rodríguez et al.'s (Reference 321) seismoactive faults in Cuba plus the Pinar fault (Figure 2.5.2-272). For the purpose of the hazard sensitivity calculation, it is assumed that all of these faults are capable tectonic sources. The Nortecubana fault is divided into three sensitivity fault sources, the Nortecubana West, Nortecubana Central, and Nortecubana East fault sources. The Baconao fault is divided into two sensitivity fault sources, the Baconao Northwest and the Baconao Southeast fault sources. Seismogenic depth for all fault sources in the hazard sensitivity calculation extends from 0- 15 kilometers (0-9 miles). All fault sources are modeled with vertical dip angle, except the three Nortecubana fault sources, all of which are modeled as dipping 30 degrees to the south.

- Probability of activity — For the purpose of the hazard sensitivity calculation, it is assumed that each of the Cuba faults listed in Table 2.5.2-236 is a capable tectonic source with a probability of activity of 1.0. This is a conservative decision given the available geologic data.

- Maximum magnitude assessment — Modeled magnitude distribution [and weight] for all of the Cuba sensitivity fault sources is M_W 7.0 [0.5], 7.3 [0.5]. These values and weights are the same as those used in the Cuba areal source zone (Subsection 2.5.2.4.4.3.2.1). The maximum magnitude (Mmax) values for the sensitivity fault sources are higher than those presented in published literature. For example, Garcia et al.'s (Reference 254) Table 4 shows the range of Mmax values for fault sources in intraplate Cuba (their sources 1 through 24) from their study and previous studies, which range from M_W 5.0 to 7.0, with many at the middle to low end of this range.

- Slip rate assessment — There are no data to directly determine late Quaternary slip rates for potential Cuba sensitivity fault sources. For most sensitivity fault sources, slip rates in millimeters/year [and weights] are assigned as 0.001 [0.33], 0.01 [0.34], 0.1 [0.33]. For the three sensitivity fault sources most proximal to the modern plate boundary, higher slip rates are assigned as 0.01 [0.1], 0.1 [0.5], 1.0 [0.4]. These slip rate distributions span orders of magnitude, reflecting the lack of data and considerable uncertainty. It is assumed that all slip is seismogenic (i.e., fully coupled).

- Recurrence model — For the purpose of the hazard sensitivity calculation, a characteristic earthquake recurrence model is assumed for the Cuba sensitivity fault sources, but with no contribution from the exponential portion of the recurrence curve at lower magnitudes.

For the hazard sensitivity calculations, there are three scenarios for fault sources, as shown in Table 2.5.2-233 and summarized below:

- No fault sources scenario — This scenario excludes fault sources from the hazard sensitivity calculations. This is consistent with the seismic source characterization used for the PSHA presented in Subsection 2.5.2.4.6.

- Full fault model scenario (FF) — The full fault model scenario includes 15 fault sources, as summarized in Table 2.5.2-236.

- Scaled fault model scenario (SF) — The SF scenario is derived from the FF scenario such that the total seismic moment rate from the fault sources is equivalent to the seismic moment rate from the observed seismicity (Z1 scenario). The SF scenario results in a contribution to hazard that is lower than that from the FF fault source scenario (Table 2.5.2-233).

A total of eleven possible combinations of areal and fault scenarios are shown in Table 2.5.2-233. The results of hazard sensitivity calculations using these scenarios is presented in Subsection 2.5.2.4.4.3.4.2.2. The hazard sensitivity calculations for both the areal and fault source scenarios use ground motion attenuation relationships developed for Caribbean crustal seismic sources described in Subsection 2.5.2.4.5.2.

2.5.2.4.4.3.4.2.2 Results of Cuba Hazard Sensitivity Calculations

This section describes the results of hazard sensitivity calculations for individual areal and fault source scenarios as well as scenarios that combine areal and fault sources. A total of eleven possible combinations of areal and fault scenarios are shown in Table 2.5.2-233. One of these (Z1) is the base case used in the PSHA (Subsection 2.5.2.4.6). In addition to Z1, five of these scenarios are evaluated quantitatively (Z6, Z11%, SF, Z1+SF, and FF) and are described below in this subsection. Figures 2.5.2-273 and 2.5.2-274 present 1 Hz and 10 Hz hazard curves for these five scenarios. These figures also present the corresponding total hazard curves that include each of these Cuba scenarios.

- The Z6 scenario results in a decrease in hazard relative to the Z1 base case.
- The Z11% scenario results in an increase in hazard relative to the Z1 base case.
- The SF scenario results in a lower hazard relative to the Z1 base case.
- The Z1+SF scenario results in a higher hazard relative to the Z1 base case.
- The FF scenario results in a higher hazard relative to the Z1 base case.

Of these five scenarios, four are judged by the TI team to be most likely to encompass the center, body, and range of the views of the informed technical community (Z6, Z11%, SF, and Z1+SF). In contrast, the FF scenario is judged as overly conservative and therefore technically indefensible. The rationale for this assessment is based on the discrepancy between the observed historical rate of large earthquakes in Cuba and that predicted by the moment rate for the FF scenario. The moment rate for the FF scenario is derived from the weighted mean of slip rate distributions for the 15 Cuba fault sources. The bottom row of Table 2.5.2-237 illustrates that the moment rate for the weighted mean slip rate (FF model) yields a return period of 124 years for M_W 7.0 events. The completeness period for earthquakes in Cuba in the M_W 6.0 to 7.0 range is given as about 500 years according to Garcia et al. (Reference 255) (Table 2.5.2-235). In the approximately 500-year record of observed seismicity in Cuba, there are no magnitude 7 events, and the largest earthquake in that time in the Phase 2 earthquake catalog from intraplate Cuba is approximately M_W 6.3 (Subsection 2.5.2.4.4.3.2.1). Another way to examine the overly conservative rate derived from the FF scenario is to compare the ratio of moment rate derived from the assumed fault slip rates to the moment rate derived from seismicity in the middle column of Table 2.5.2-237. That comparison shows that the FF scenario moment rate is 267 percent greater (3.6657 ratio in Table 2.5.2-237) than the moment rate derived from historical seismicity. While the individual FF scenario is presented in Figures 2.5.2-273 and 2.5.2-274, it is not considered further. Likewise, combinations involving the FF scenario are also eliminated and not presented, as they would be overly conservative and technically indefensible.

The remaining five combination scenarios (Z6+FF, Z1+FF, Z11%+FF, Z6+SF, and Z11% +SF) are discarded from further consideration based on the rationale provided below:

- Three combination scenarios, Z6+FF, Z1+FF, and Z11%+FF, are discarded due to the inclusion of the FF scenario as described above.

- The Z6+SF combination scenario is judged to lie within the likely center, body, and range of the views of the informed technical community, but would result in an intermediate hazard not useful for this sensitivity analyses because SF is also combined with the Z1 scenario. The Z1+SF scenario results in higher hazard (Figures 2.5.2-273 and 2.5.2-274).

- The Z11%+SF combination scenario includes an areal zone scenario that is based on an arbitrary activity rate increase applied to the entire zone.

To assess the impact of various Cuba sensitivity scenarios on the Turkey Point Units 6 & 7 site hazard, based on the evaluation of the hazard results presented in Figures 2.5.2-273 and 2.5.2-274, four sensitivity scenarios (Z6, Z11%, SF, and Z1+SF) were selected to represent the Cuba hazard in lieu of the Z1 base case scenario used for the original base case hazard total. Total hazard curves that include these four scenarios are presented in Figure 2.5.2-275, along with the original total hazard.

Detailed comparisons of the differences in total hazard for the four scenarios with respect to the base case total hazard are compiled in Tables 2.5.2-238 and 2.5.2-239. Two acceleration spectral response frequencies (1 Hz and 10 Hz) and two MAFE levels (10^{-4} and 10^{-5}) are considered. Table 2.5.2-238 shows the percent differences in MAFE for each scenario at the respective base case amplitudes. Negative values indicate lower hazard levels than the base case levels, positive values are higher. The base case values are shown in the first pair of columns, and the subsequent four scenarios increase in hazard level from left to right. Differences for the Z6 scenario range from -8.8 percent to -1.1 percent of the base case total. Differences for the SF scenario range from -12 percent to 1.0 percent. The Z11% scenario is based on an increased seismicity rate for the entire areal zone compared to the base case and results in differences which range from -0.1 percent to 2.5 percent. For the Z1+SF scenario, differences are the greatest, ranging from 1.4 percent to 13.1 percent. Note that the apparent decrease (0.1 percent) in 10 Hz MAFE at the 10^{-5} MAFE amplitudes for scenario Z11% is due to the limited number of significant digits presented in the base case for total mean hazard, the process of interpolation, and rounding. That this is only an apparent decrease is supported by the fact that the 10^{-5} MAFE amplitudes for scenario Z11% match the base case amplitudes exactly to three significant figures (Table 2.5.2-239).

Table 2.5.2-239 shows the changes in rock motion amplitude for the four scenarios. The largest of these changes is negative relative to the base case amplitudes. These are shown as absolute and percent differences in amplitudes. The largest percent increase is 4.4 percent and results from the Z1+SF scenario and the greatest decrease is -6.9 percent from the SF scenario. Of greater importance than the percentages is the maximum increase in rock motion amplitude from the different scenarios. None of the increases in rock motions from all scenarios exceeds 0.004 g.

The scenarios presented in Figure 2.5.2-275 are derived from a reasonable range of technically defensible seismic source characterizations for intraplate Cuba. As shown in Table 2.5.2-239, this range of seismic source characterizations results in only small changes in hazard at the Turkey Point Units 6 & 7 site. Based on the results of these hazard sensitivity calculations, it is concluded that the use of a single areal source zone and the parameters used to characterize it as presented in Subsection 2.5.2.4.6 gives a reasonably conservative estimate of the contribution to site hazard from intraplate Cuba seismic sources.

2.5.2.4.4.3.4.3 Santaren Anticline Fault Source Hazard Sensitivity Calculation

A seismic source characterization for a potential fault underlying the Santaren anticline for use in a hazard sensitivity calculation was performed to assess the impact on hazard at the Turkey Point Units 6 & 7 site.

Masaferro et al. (Reference 362) interpret the Santaren anticline in the southern Santaren Channel as a detachment fold with possible Quaternary activity. For the purpose of this sensitivity analysis, it is conservatively assumed that the anticline is cored by a seismogenic fault. Figure 2.5.2-272 shows the location of the Santaren anticline fault source, based on Masaferro et al. (Reference 362). A Santaren anticline fault is assumed to have the same surface trace as the anticline. Table 2.5.2-240 shows the surface rupture dimensions, assumed dip, uplift rate (from Masaferro et al. [Reference 363]), slip rate (uplift rate divided by sine of the dip), and distance of the fault endpoints to the site. The fault is assumed to reach the surface.

As part of the PSHA sensitivity calculations for hypothetical active faults in Cuba (Subsection 2.5.2.4.4.3.4.2), hazard curves for 1 Hz and 10 Hz spectral acceleration were developed for the 15 faults shown in Figure 2.5.2-272. One of these, the Hicacos fault source, lies about 15 miles (about 25 kilometers) closer to the site than the Santaren anticline fault source, and was thus used as a proxy for the Santaren anticline fault source. The same magnitude distribution was assumed for the Santaren anticline fault source as for the Hicacos fault source (M_W 7.3 and 7.0, equally weighted [Table 2.5.2-236]). The Hicacos hazard curve annual frequencies of exceedance were then scaled by the ratio of the Santaren anticline fault source slip rate (0.071 millimeters/year) to the mean Hicacos slip rate (0.037 mm/yr, from Table 2.5.2-236), or 1.92. This strategy is conservative in that the Hicacos fault is closer to the site than the Santaren anticline fault source.

The Santaren anticline fault source hazard curves were added to those for the FSAR total hazard (from Table 2.5.2-223), and the increases in hazard and ground motion at annual frequencies of exceedance of 10^{-4} and 10^{-5} were computed.

Figure 2.5.2-286 shows the Santaren anticline fault source hazard curves, the FSAR total hazard curves, and the effect of summing the two. As depicted in Figure 2.5.2-286, adding the Santaren anticline fault source clearly has a small effect on the total hazard.

Table 2.5.2-241 shows the change in hazard at MAFE of 10^{-4} and 10^{-5}. The hazard increases range from 1.42% to 8.80%. Table 2.5.2-242 shows the change in ground motions at these hazard levels. The ground motion increases range from 0.77% to 3.48%. The maximum ground motion increase is less than 0.003g.

2.5.2.4.4.4 Implementation Notes on Incorporation of New Seismic Source Parameterization into PSHA

Subsections 2.5.2.2 through 2.5.2.4 review new geological, geophysical, and seismological information from Subsection 2.5.1 as related to seismic source characterization as the basis for updating the PSHA at the Units 6 & 7 site. New seismic sources (or extensions of existing seismic sources) were developed as follows:

Gulf of Mexico and Atlantic

Seismicity was added in degree cells offshore of the Florida Peninsula (west in the Gulf of Mexico and east in the Atlantic), using seismicity rates smoothed over the Florida Peninsula (Figure 2.5.2-210) using the updated earthquake catalog through mid-February 2008. The completeness of earthquake catalogs offshore is problematic and based on similar crust and tectonic history the rates of activity offshore appear identical to average rates onshore. The degree cells for which seismicity was added are discussed in Subsection 2.5.2.2.

Caribbean South of Florida

Seismicity was added in degree cells south of Florida, because latitude 25° N was the southernmost extent of the EPRI completeness regions (Figure 2.5.2-210). As for the Gulf of Mexico and Atlantic Ocean, the seismicity in these degree cells was assigned the same rate as calculated for the Florida Peninsula, using the updated earthquake catalog through mid-February 2008. The supplemental source for each EPRI team was given a geometry that completely filled the region between that team's Florida source and the Cuba area (described below).

Cuba Areal Source Zone

A single areal source zone represents earthquake occurrences on the island of Cuba and slightly offshore. Parameters of this source are described in Subsection 2.5.2.4.4.3.2.

North America-Caribbean Fault Sources

Nine faults were identified in the North America-Caribbean plate boundary region, and the geometries and parameters of these faults are described in Subsection 2.5.2.4.4.3.2.

Charleston Seismic Source

An updated model for the Charleston seismic zone was adopted that reflects current scientific evidence on recurrence rates for large magnitude earthquakes in the Charleston, South Carolina region and on the magnitudes of those earthquakes. This Charleston source was used rather than the EPRI team sources for Charleston because if reflects current thinking on both recurrence rates and magnitude values. The Charleston source is summarized in Subsection 2.5.2.4.4.2.

2.5.2.4.5 Ground Motion Attenuation Models

The PSHA was conducted by combining the hazard from EPRI-SOG seismic sources with the hazard from Cuban and Caribbean sources to the south. The location of the Units 6 & 7 site at the very southeastern extremity of EPRI-SOG study region and the occurrence of recent moderate-large earthquakes in the Caribbean region indicate the potential for contributions to seismic hazard at the site from sources in both the CEUS and Caribbean regions. This subsection provides a review of the methods used to characterize ground motions within the original EPRI-SOG seismic sources in the CEUS region, and then summarizes the new attenuation models that were developed for the Caribbean seismic sources as the basis for updating the PSHA at the Units 6 & 7 site.

2.5.2.4.5.1 Attenuation Models for the CEUS Region

Since the 1989 EPRI study (Reference 245), researchers have continued to evolve ground motion attenuation models for the CEUS and a number of alternative models have been published. An EPRI project was conducted to summarize these studies regarding CEUS ground motions, and results were published in a 2004 EPRI report (Reference 242). These updated attenuation equations estimate median spectral acceleration and its uncertainty as a function of earthquake magnitude and distance.

Epistemic uncertainty is modeled using multiple ground motion attenuation relationships with weights, and multiple estimates of aleatory uncertainty, also with weights. Different sets of equations are recommended for seismic sources that represent rifted vs. non-rifted regions of the earth's crust. Equations are available for hard rock site conditions at spectral frequencies of 100 Hz (which is equivalent to peak ground acceleration, PGA), 25 Hz, 10 Hz, 5 Hz, 2.5 Hz, 1 Hz, and 0.5 Hz. All ground motion estimates are for spectral acceleration with 5 percent of critical damping.

Aleatory uncertainties published in the 2004 EPRI (Reference 242) model were reexamined by Abrahamson and Bommer (Reference 203) because it was thought that the 2004 EPRI aleatory

uncertainties were probably too large, resulting in over-estimates of seismic hazard. The Abrahamson and Bommer (Reference 203) study recommends a revised set of aleatory uncertainties and weights that can be used to replace the original 2004 EPRI (Reference 242) estimates of aleatory uncertainty.

The ground motion attenuation models used in the seismic hazard calculations for CEUS seismic sources consisted of the median equations from 2004 EPRI (Reference 242) combined with the updated aleatory uncertainties of the Abrahamson and Bommer study (Reference 203).

2.5.2.4.5.2 New GMPE Models for the Cuba and Caribbean Region

The incorporation of additional seismic sources developed for the Caribbean region in the PSHA requires applicable ground motion prediction equation (GMPE) models. Although much of the Caribbean has experienced large, damaging earthquakes, there are very few recorded strong ground motion data from the region, and this has prevented the development of a regional empirical GMPE, specifically one for attenuation of ground motion between sources in the northern Caribbean and the Turkey Point Units 6 & 7 site location in southern Florida. Moreover, the use of ground motion prediction equations (GMPEs) from other regions, such as the 2004 EPRI (Reference 242) GMPEs, cannot be uncritically adopted for PSHA analysis because of the observed differences in crustal properties between the CEUS and Caribbean.

No studies have been found modeling attenuation of strong ground motion between earthquakes in the Caribbean and sites in the CEUS so that no experts could be identified who could be characterized as a proponent, which SSHAC (Reference 318) defines as “an expert who advocates a particular hypothesis or technical position.” The absence of a proponent or proponents made it difficult to categorize the level of the study in accordance with the SSHAC (Reference 318) guidelines. However, what has been done in this regard is otherwise fully consistent with industry practice in general and the SSHAC (Reference 318) guidelines in particular.

Initial development of a suite of specific GMPEs was performed by, what in SSHAC (Reference 318) nomenclature would be called the TI team of two Bechtel seismologists: Drs. Nick Gregor and Behrooz Tavakoli, both with significant experience in generating and evaluating GMPEs. Peer review was provided by a Technical Advisory Group (TAG) at several points throughout the GMPE development process. A resource expert, Dr. Dariush Motazedian of Carleton University, Ottawa, Canada, was also consulted during this time.

The GMPE development reflects the uniquely challenging situation that exists with regard to the seismic characterization of Cuba and the adjacent northern Caribbean region in that, for this region, empirical ground motion data is limited or unavailable, there are no calibrated GMPEs predicting ground motions in southern Florida arising from earthquakes in Cuba or the northern Caribbean, and there are no experts identified that can be characterized as proponents as defined in SSHAC (Reference 318).

SSHAC (Reference 318) characterizes a Level 2 study as one in which the TI reviews the literature and then interacts with proponents and resource experts to identify issues and interpretations and, on the basis of these interactions, “estimates community distribution,” that is, develops “a representation . . . of the diversity of interpretations and their uncertainties” (see Table 3-1 and Sections 3.1.3.5 and 3.2.1 of Reference 318). SSHAC (Reference 318) also acknowledges (in Section 3.1.3.3) that the “choice of the level of [study] is often driven by . . . the amount of resources available for the study.”

Initially, a literature review was performed with the goal of retrieving acceptable GMPEs for the Cuba and Caribbean region. However, this literature review only retrieved one GMPE developed recently by Motazedian and Atkinson (Reference 287). In addition to the interaction with the TAG members,

correspondence was conducted with Professor Motazedian during the initial development of the Caribbean GMPEs. These initial technical discussions were for the possible application of the published Motazedian and Atkinson (Reference 287) GMPE for the PSHA study. However, based on the limitations of this GMPE (e.g., incomplete suite of necessary spectral frequencies, limited application for distances greater than 500 kilometers [311 miles], and site-specific ground conditions of soft rock), it was determined that the published GMPE was not directly acceptable for use in the PSHA.

The process described is generally consistent with a Level 2 study as described in SSHAC (Reference 318) where it states (in Section 3.2.1): ". . . the TI would communicate with the authors of published studies and other local experts who have expertise in the region or in regional ground motions . . . to hear and understand the technical positions taken by various proponents of particular hypotheses . . . In effect, the TI is . . . attempting to provide an overall assessment that would represent the informed scientific community's view of the subject, if the community were to make such an assessment."

Motazedian and Atkinson (Reference 287) analyzed a dataset of approximately 300 earthquakes recorded by stations in Puerto Rico. This dataset spanned the M_W range of 3 to 5.5 and distances from about 20 to 500 kilometers. Motazedian and Atkinson acknowledge that their ground motion dataset consisted of recorded ground motions from both crustal and subduction zone earthquakes and that the separation of the earthquakes used in their dataset into crustal and subduction events was not possible because of the limited station coverage for the region. Based on these data, Motazedian and Atkinson developed a set of regional anelastic attenuation and source parameters. Finally, Motazedian and Atkinson used these regional parameters within a stochastic simulation process to create an artificial dataset for larger earthquakes at near distances to fit a GMPE to these generated data.

To address this possible concern about the influence of using both subduction and crustal events to estimate the regional attenuation and source parameters, Motazedian and Atkinson (Reference 287) provide a comparison of their GMPE with representative GMPEs for the CEUS (Reference 210), California (Reference 357), and an empirically based GMPE based on the global ground motion dataset for subduction zones (Reference 358). They conclude that, overall, the Puerto Rico relations agree well with the stochastic relations for California and eastern North America and are quite different from those calculated by the global subduction relations. This comparison and noted results provide a technical justification for using the source and attenuation parameters from the Puerto Rico ground motion dataset (Reference 287) as the starting point for the development of applicable GMPEs for the Caribbean seismic sources.

The Motazedian and Atkinson (Reference 287) study focused on GMPEs most useful for the evaluation of PSHA results for Puerto Rico. For the purposes of an evaluation of potential contributions to PSHA at the Turkey Point Units 6 & 7 site from Caribbean earthquakes, GMPE results from somewhat larger and significantly more distant earthquakes are needed.

Beginning with the suite of regional anelastic attenuation and source parameters of Motazedian and Atkinson, and following the stochastic simulation methodology, region-specific GMPE models for the Cuba and Caribbean region were developed. Ground motions were estimated for seven spectral frequencies on hard rock for earthquakes with magnitudes between M_W 4.75 and 8.75 and for a distance range of 150 to 2000 kilometers.

To account for the expected uncertainty associated with the application of regional attenuation and source parameters estimated from earthquakes in and around Puerto Rico and their application to other regions within the Caribbean (e.g., Cuba), the stress parameter of the source and the anelastic attenuation models from Motazedian and Atkinson (Reference 287) were varied in the stochastic ground motion simulation analysis. The regional attenuation and source parameters from the

Motazedian and Atkinson (Reference 287) study and the specific values used for the development of the suite of applicable GMPE models are listed in Table 2.5.2-231. The variation of the stress parameter was defined to be normally distributed with a standard deviation (sigma value) of 0.7 (in natural log units) given in the EPRI 1993 study (Reference 244). The variation of the regional anelastic attenuation constant term was based on an assumed sigma value of 0.4 (in natural log units) given in the 2003 Silva et al. study (Reference 342). In addition, three separate seismic source models were used in the analysis: single corner with constant stress parameter (1CC model), single corner with magnitude dependent stress parameter (1CV model), and double corner source (2C model) based on the analysis of CEUS ground motion data. These three seismic source models are part of the larger set of source models that are included in the 2004 EPRI (Reference 242) ground motion models.

A linear regression was performed on the simulated datasets to estimate the regression coefficients for the Caribbean regional GMPEs for use in the PSHA. A nonlinear GMPE functional form and regression, generally needed to successfully predict saturation of strong ground motion at small distances, were not required because of the large minimum distance of 150 kilometers separating Caribbean earthquakes from the Turkey Point Units 6 & 7 site. An aleatory sigma value of 0.645 (in natural log units) was selected following the Motazedian and Atkinson study (Reference 287) and was assigned to each Caribbean GMPE model for use in the PSHA for all frequencies.

To capture the epistemic uncertainty in ground motion models in the hazard analysis, a number of GMPEs from the different seismic source models were included along with model-dependent weights. The weights for these new GMPE models were assessed based on the family class weights used in the 2004 EPRI ground motion model study and the family class (that is, 1CC, 1CV, or 2C) of the seismic source model (Reference 242). Figure 2.5.2-255 shows the suite of Caribbean PGA GMPE curves for a magnitude M_W 7 earthquake over the applicable distance range of 150–2000 kilometers. Within a given seismic source model type (e.g., single corner constant stress parameter), the difference between the GMPE models based on the low, base, and high stress parameter values resulted in a constant scaling of the GMPE curves. This scalar variation was captured by combining the datasets from these stress parameter values for the regression analysis leading to a combined suite of nine ground motion GMPE models (i.e., heavy lines) that were adopted for use in the PSHA with the Caribbean seismic sources. As a check, the complete suite of GMPE curves is shown in Figure 2.5.2-255 and the resulting nine adopted GMPE curves span the general range of values from the complete suite of curves. Figures 2.5.2-256 and 2.5.2-257 plot the GMPE curves for the periods of 0.1 and 1.0 seconds, respectively.

At the suggestion of TAG members over the course of the three TAG meetings, a sensitivity analysis was performed to examine the effect on epistemic uncertainty of alternative GMPEs for use in the PSHA. The alternative relationships considered adopted a double corner (2C) seismic source model, such as might be expected to occur in a more active tectonic environment such as the western United States (WUS) rather than the double corner seismic source model of the less active tectonic environment of the CEUS, and a Gulf Coast region lower amplitude but higher (less rapidly attenuating) anelastic attenuation factor (Q) model rather than the Puerto Rico region-specific (higher amplitude but more rapidly attenuating) Q model from Motazedian and Atkinson (Reference 287) recognizing that much of the propagation path from the Caribbean sources to the Turkey Point Units 6 & 7 site is through the Gulf Coast crust. It was found that adoption of these alternatives (i.e., different suite of regional attenuation and seismic source parameter values) led to ground motion values that were equal to (at large distances based on the anelastic attenuation rates) or lower than (based on the different magnitude scaling from the WUS-based double corner model) the suite of original nine new GMPE models adopted for the Cuba and Caribbean region. A comparison of the weighted combination of the original nine GMPE models and the inclusion of these additional sensitivity models resulted in a slightly lower weighted mean GMPE curve over the magnitude and distance range needed for the PSHA. Therefore, their incorporation into the final PSHA results would have slightly lowered the already low hazards, and, thus, the use of the original nine GMPE models

was accepted by the TAG members because the inclusion of these additional GMPE models would be expected to lead to lower, and less conservative, ground motion results.

After the suite of GMPEs was developed, two additional sensitivity analyses were performed to further validate the technical assessment of the stochastic Caribbean GMPE models developed for Turkey Point Units 6 & 7. These analyses sought additional empirical data with which to compare the GMPEs for Turkey Point Units 6 & 7 and examined the effect of alternate suites of GMPEs on the PSHA results at the site. The results of these two additional sensitivity studies are presented here.

The first supplemental sensitivity analysis compared the suite of GMPEs used in the Turkey Point Units 6 & 7 PSHA with empirical regional ground motion data. To assist in the technical evaluation of the current Caribbean GMPE models developed for Turkey Point Units 6 & 7, a comparison of empirical ground motions from five regional earthquakes occurring since 2004 in the Gulf of Mexico and northern Caribbean region were analyzed. These earthquakes were selected from among those available as being most representative of earthquakes whose tectonic settings and locations might be expected to be like those of future earthquakes contributing to the overall PSHA at the site under the source model adopted. Specifically, these were shallow crustal earthquakes in the northern Caribbean or Gulf of Mexico.

Regional broadband empirical data from selected Incorporated Research Institutions for Seismology (IRIS) stations were obtained, processed and compared to the suite of Caribbean GMPE models and the suite of EPRI (References 242 and 203) GMPE models for both the mid-continent and Gulf Coast regional models. Based on these comparisons, a technical assessment can be made on the applicability of using the Caribbean GMPE for the Turkey Point Units 6 & 7 PSHA.

Note that the current PSHA results were developed using the suite of EPRI (References 242 and 203) mid-continent GMPE models for other non-Caribbean sources. In this comparison, all of the GMPE curves are for the assumed CEUS hard rock site conditions with *Vs*= 2.83 kilometers/second (1.76 miles/second), whereas the empirical IRIS data are for the individual unknown site conditions of each station which is expected to be less than *Vs*= 2.83 kilometers/second (1.76 miles/second). Based on a simplified site response analysis, it was computed that adjustment factors for the station-specific site conditions to the more stable CEUS hard rock site conditions required a reduction factor in the observed empirical ground motion values, especially for the longer spectral frequencies of interest (e.g., 1 or 2.5 Hz).

The current deaggregation of seismic hazard at the Turkey Point Units 6 & 7 site from all sources—Cuban, Caribbean, and southeast United States—is shown in Figures 2.5.2-226 and 2.5.2-228 for longer period motions (for which the relative contribution of the larger, more distant Cuban and Caribbean sources would be expected to have their greatest relative contribution) and for the 10^{-4} and 10^{-5} mean annual frequency of occurrence probabilities used to develop design ground motions under NRC regulatory guidance. The relative contribution for the higher frequency cases of 5 Hz and 10 Hz (Figures 2.5.2-227 and 2.5.2-229) from the more distant Caribbean sources is significantly reduced relative to the closer local seismic sources. For this sensitivity comparison, the empirical ground motions for 1 Hz and 2.5 Hz are presented for each of the five regional earthquakes and ground motion prediction equations.

For each event, acceleration response spectra for a spectral damping of 5 percent at each station were computed. The geometric mean of the two horizontal components was computed and amplitudes for the 1 Hz and 2.5 Hz spectral frequencies were generated and compared to the suite of GMPE models (i.e., both of the EPRI 2004 GMPE models (Reference 242) and the Caribbean GMPE models).

Note that based on the hypocentral location and geographical location relative to tectonic plate boundary, all five of these earthquakes are considered to be shallow crustal events and are not

associated with any regional subduction zones. For each event, a standard time history processing methodology was applied with the final results being a dataset of the acceleration response spectra for a spectral damping of 5 percent at each station. The geometric mean of the two horizontal components was computed and comparison plots for the 1 Hz and 2.5 Hz spectral frequencies were generated showing the empirical data (both as recorded and adjusted for consistent CEUS hard rock site conditions) and the suite of GMPE models (i.e., both of the EPRI 2004 GMPE models [Reference 242] and the Caribbean GMPE models). Both the individual GMPE curves and the weighted mean GMPE curve for a given set are shown in the comparison plots for each spectral frequency and earthquake.

These five events were as follows:

- December 14, 2004 - Caribbean Sea Region (M_W6.8, 19.05 N, -81.52 W, hypocenter depth 12.0 kilometers), Fault Plane 1 (Strike, Dip, Rake): 258.0, 84.0, -2.0; Fault Plane 2 (Strike, Dip, Rake): 349.0, 88.0, -174.0. The fault plane solution implies almost pure strike-slip motion on a nearly vertically dipping fault.

  This event occurred in the Caribbean Sea region and its epicenter is shown in Figure 2.5.2-258a along with the Turkey Point Units 6 & 7 site location and the location of the IRIS stations that recorded this earthquake. Based on the observed station distribution, the IRIS station DWPF located in central Florida has the most applicable source to site path for this comparison. The GMPE curves and empirical data are shown in Figures 2.5.2-258b and 2.5.2-258c for the 1 Hz and 2.5 Hz spectral frequencies. The data point from the DWPF station is highlighted as a solid blue symbol. Overall, the empirical data falls below the median Caribbean GMPE curve (heavy red line) and has values that are in the lower distribution range of Caribbean GMPE curves.

- September 10, 2006 - Gulf of Mexico (M_W5.9, 26.32 N, -86.84 W, hypocenter depth 29.6 kilometers), Fault Plane 1 (Strike, Dip, Rake): 324.0, 28.0, 117.0; Fault Plane 2 (Strike, Dip, Rake): 114.0, 65.0, 77.0. The fault plane solution implies composite strike-slip and reverse-slip motion on a moderately steeply dipping fault.

  This event occurred in the Gulf of Mexico and its epicenter is shown in Figure 2.5.2-259a along with the Turkey Point Units 6 & 7 site location, and the location of the IRIS stations that recorded this earthquake and were analyzed. Based on the observed station distribution, the IRIS station DWPF located in central Florida has the most applicable source to site path for this comparison. Out of the five earthquakes considered in this analysis, this event has the most consistent tectonic structure between the earthquake and the Turkey Point Units 6 & 7 site and can be considered as the best representative event for events occurring in and around the island of Cuba and being observed in southern Florida. The distribution of stations in the central United States has a less applicable travel path azimuth and may show different attenuation properties based on these different tectonic travel paths. The GMPE curves and empirical data are shown in Figures 2.5.2-259b and 2.5.2-259c for the 1 Hz and 2.5 Hz spectral frequencies. The data point from the DWPF station is highlighted as a solid blue symbol. In general, the empirical observations fall within the range of the Caribbean GMPE curves with the single exception of station LRAL (i.e., at a distance of approximately 750 kilometers [466 miles]) for 2.5 Hz in which the unadjusted empirical data exceeds the highest Caribbean GMPE curve. For this station and frequency, however, the CEUS hard rock adjusted ground motions fall within the range of Caribbean GMPE models which are defined for CEUS hard rock site conditions. It can also be concluded from the comparison plots in Figures 2.5.2-259b and 2.5.2-259c that the distribution of the current Caribbean GMPE curves adequately captures the range of the empirical data. In addition, the observation from the DWPF station is in the lower range of the Caribbean GMPE curves.

- February 4, 2007 - Cuba Region (M_w6.2, 19.49 N, -78.34 W, hypocenter depth 12.0 kilometers), Fault Plane 1 (Strike, Dip, Rake): 257.0, 76.0, -9.0; Fault Plane 2 (Strike, Dip, Rake): 349.0, 81.0, -166.0. The fault plane solution implies almost pure strike-slip motion with a small normal component on a steeply dipping fault.

  This event occurred south of the island of Cuba and its epicenter is shown in Figure 2.5.2-260a along with the Turkey Point Units 6 & 7 site location and the location of the IRIS stations that recorded this earthquake and were analyzed. Only three IRIS stations were analyzed from this earthquake and their station locations are shown in Figure 2.5.2-260a. Based on the observed station distribution, the IRIS station DWPF located in central Florida has the most applicable source to site path for this comparison. The GMPE curves and empirical data are shown in Figures 2.5.2-260b and 2.5.2-260c for the 1 Hz and 2.5 Hz spectral frequencies. The data point from the DWPF station is highlighted as a solid blue symbol. Overall, the empirical data falls below the median Caribbean GMPE curve (heavy red line) and has values that are in the lower distribution range of Caribbean GMPE curves. In addition, the observation from the DWPF station is similar to the lowest Caribbean GMPE curve or lower.

- May 28, 2009 - North of Honduras (M_w7.3, 16.50 N, -87.17 W, hypocenter depth 12.0 kilometers), Fault Plane 1 (Strike, Dip, Rake): 63.0, 60.0, -7.0; Fault Plane 2 (Strike, Dip, Rake): 156.0, 84.0, -150.0. The fault plane solution implies predominantly strike-slip with a smaller normal component on a moderately to steeply dipping fault.

  This event occurred north of Honduras in Central America and is the largest earthquake in the suite of five events analyzed in this sensitivity study. The location of its epicenter is shown in Figure 2.5.2-261a along with the Turkey Point Units 6 & 7 site location and the location of the three IRIS stations that were analyzed. Based on the azimuths from the earthquake to the three IRIS stations, none of the associated seismic ray travel paths are ideal for this comparison study. The attenuation curves and empirical data are shown in Figures 2.5.2-261b and 2.5.2-261c for the 1 Hz and 2.5 Hz spectral frequencies. The comparisons provided in the figures indicate that the empirical data from this earthquake are lower than any of the Caribbean attenuation curves.

- January 12, 2010 - Haiti (M_w7.0, 18.61 N, -72.62 W, hypocenter depth 12.0 kilometers), Fault Plane 1 (Strike, Dip, Rake): 250.0, 71.0, 22.0; Fault Plane 2 (Strike, Dip, Rake): 152.0, 69.0, 159.0. The fault plane solution implies composite strike-slip with a moderate reverse component on a steeply dipping fault.

  The Haiti earthquake is the most recent event in this suite of five earthquakes analyzed. The epicentral location and the suite of IRIS stations analyzed are shown in Figure 2.5.2-262a. Note that the data from the DWPF was not available for this earthquake. For the SDV station, only one single horizontal component was available and thus was not included in the comparison which was based on the geometric mean of two horizontal component ground motions. The large distance and undesirable azimuthal direction away from southern Florida for this station from this earthquake provides an additional justification for not including this station in the comparison. The GMPE curves and empirical data are shown in Figures 2.5.2-262b and 2.5.2-262c for the 1 Hz and 2.5 Hz spectral frequencies. Overall, the empirical data falls in the lower range or lower than the Caribbean attenuation curves.

The results of these comparisons demonstrated that the suite of Caribbean GMPE models used in the current PSHA predicts larger ground motions on average than the observed empirical data from these five earthquakes for the spectral frequencies of 1 Hz and 2.5 Hz, especially when considering the adjustment to a common CEUS hard rock site condition. In addition, for the subset of data from just those stations that have a more appropriate source to site travel paths in particular, this conclusion can be extended to state that the use of the Caribbean GMPE models should provide

conservative (i.e., higher) ground motion predictions compared to the available empirical data from the region.

The second supplemental sensitivity determined the sensitivity of the GMRS at the Turkey Point Units 6 & 7 site to the GMPEs used for the Caribbean seismic sources, which include the Cuba areal source plus nine fault sources. Five sets of seismic hazard calculations for five different GMPE suites were used to develop the corresponding GMRS. The GMPEs used for Caribbean seismic sources are: those of the base case which is (1) the Caribbean GMPE models developed for Turkey Point Units 6 & 7 (Subsection 2.5.2.4.5.2), (2) EPRI mid-continent region (References 242 and 203) equations, (3) EPRI mid-continent region "mod1" (References 242 and 203) equations, (4) EPRI Gulf region (References 242 and 203) equations, and (5) EPRI Gulf region "mod 1" (References 242 and 203) equations. The modification of the EPRI GMPEs for both the mid-continent and Gulf Coast cases was to exclude the GMPE which predicts significantly higher ground motions for large distance, such as those from the contributing Cuba and Caribbean sources. All seismic hazard calculations were made for the hard rock site conditions and include the other non-Caribbean sources in the PSHA. Thus, the observed differences are based solely on the use of different GMPE models for the Caribbean seismic sources. For each of the five cases, ground motion values were estimated from the mean hazard curves for the seven standard spectral frequencies. Site-specific horizontal GMRS are plotted in
Figure 2.5.2-263 and are developed using the site amplification factors. In general, the GMRS results using the EPRI Gulf Coast GMPEs are equal to or lower than the results using the Caribbean GMPE (i.e., indicated as Base Case in Figure 2.5.2-263). For the EPRI Mid-Continent GMPE, the opposite result is concluded in which the GMRS values exceed the GMRS values using the Caribbean GMPE models. However, based on the previous additional sensitivity, the EPRI Mid-Continent models predict higher ground motions than the empirical ground motions and, as such, may not be applicable for the modeling of ground motion attenuation for seismic sources in this Caribbean region and the Turkey Point Units 6 & 7 site location in southern Florida. In addition, the tectonic structure and potential attenuation of ground motions for Caribbean sources might be more consistent with the EPRI Gulf Coast GMPE models based on the southern region of Florida being located in the Gulf Coast tectonic region of the eastern United States, especially for events that would occur in and around the island of Cuba and the Gulf of Mexico. For events occurring further south of the island of Cuba, the tectonic regime and subsequent seismic ray travel paths and associated attenuation may be more complex based on the more complex tectonic environment located south of the island of Cuba and may not be as consistent with the Gulf Coast GMPE. However, based on the results of the first sensitivity analysis, the empirical data indicates that the Caribbean GMPE is conservative in its estimation of ground motions and, based on the results shown in Figure 2.5.2-263, the use of the EPRI Gulf Coast GMPE for the PSHA gives similar or lower GMRS values.

These two supplemental sensitivity analyses indicate that the suite of GMPEs used to characterize contributions to hazard at the site from Caribbean earthquakes, and the resulting GMRS at the site from these earthquakes, are conservative.

Next, six ground motion attenuation experts were asked to review and comment on both the methodology and results of the Caribbean GMPE models. These six experts were:

- Dr. Norman Abrahamson (Consultant)
- Dr. Yousef Bozorgnia (University of California, Berkeley, PEER)
- Dr. Kenneth Campbell (EQECAT)
- Dr. Shahram Pezeshk (University of Memphis)
- Dr. Paul Somerville (URS Corporation)

- Dr. Robert Youngs (AMEC-Geomatrix)

In reviewing and summarizing the responses from the experts, it is concluded that the use of the Caribbean GMPE models in the PSHA is acceptable. As noted by the six experts, based on the comparison between the Caribbean GMPE model and the empirical IRIS data, these GMPE models may be conservative in their estimation of ground motions in the region. In addition, the assignment of an aleatory uncertainty value of 0.645 in natural log units was acceptable based on the consensus of the six experts.

When asked about the applicability of the EPRI Mid-Continent or Gulf Coast models, the consensus of the six experts was that the suite of Gulf Coast GMPE models are closer to the empirical data than the Mid-Continent suite. However, this did not indicate that the EPRI Gulf Coast models are preferable over the Caribbean GMPE models. Based on the polling and summary of the responses from the six experts, the ultimate use of the specific Caribbean GMPEs in the PSHA for the Turkey Point Units 6 & 7 site location for seismic sources in the Cuba and Caribbean region falls within the range of the informed technical community and actually may produce slightly larger ground motions than would be estimated from the center, body, and range of the informed technical community. The experts' opinions support the development of the final Caribbean GMPEs. There were no conflicting opinions among the experts regarding the suitability of the final Caribbean GMPEs for use in the PSHA analysis for Turkey Point Units 6 & 7.

Mean GMPE plots are provided for the EPRI Mid-Continent (References 242 and 203) and Caribbean GMPEs in Figures 2.5.2-264 through 2.5.2-270 for the seven defined frequencies. Note that EPRI (Reference 203) is only a recommendation for the associated aleatory uncertainty and therefore does not impact the comparison plots of the weighted mean GMPE curve. The plotted mean GMPE curve is the weighted mean of the individual median GMPE curves as defined in EPRI 2004 (Reference 242) and for the Caribbean GMPE models. These GMPE plots are provided for three specific M_w values: 6, 7, and 8 for distances between 200 kilometers (124 miles) and 1000 kilometers (621 miles). Note that the EPRI 2004 GMPE model (Reference 242) is defined as a function of epicentral distance, whereas the Caribbean GMPE model is defined as a function of hypocentral distance. For these comparison plots, the GMPE curves are plotted as a function of epicentral distance and for the Caribbean GMPE curves an assumed hypocentral depth of 8 kilometers (5 miles) was used.

2.5.2.4.6 Updated Probabilistic Seismic Hazard Analysis and Deaggregation for Rock

An updated PSHA for the Units 6 & 7 site was conducted using as inputs the following:

- EPRI team sources with extended regions in the Gulf of Mexico and Atlantic
- Supplemental sources between Florida Peninsula and Cuba
- Cuba areal source zone
- North America-Caribbean fault sources
- Updated Charleston source
- Updated ground motion attenuation models for the CEUS
- New ground motion attenuation models for the Cuba and Caribbean region

The site-specific PSHA was for hard rock site conditions consistent with the 2004 EPRI ground motion attenuation models (Reference 242).

A PSHA consists of calculating annual frequencies of exceeding various ground motion amplitudes at a site for all possible earthquakes that can occur within the parameters of the seismic hazard model for the site. The seismic sources model incorporates the rates of occurrence of earthquakes as a function of magnitude and location, and the regional ground motion model estimates the distribution of ground motions at the site for each earthquake.

Multiple weighted hypotheses on seismic sources characteristics, including rates of occurrence and magnitude distribution, and ground motions (characterized by the median ground motion amplitude and its uncertainty) result in multiple weighted seismic hazard curves. From this family of weighted curves, the mean and fractile seismic hazard can be determined. The calculation is made separately for each of the six EPRI teams, and the seismic hazard distribution for the teams is combined, weighting each team equally. This combination gives the overall mean and distribution of seismic hazard at the site.

Figures 2.5.2-218 through 2.5.2-224 show mean and fractile (5th, 16th, median, 84th, and 95th) seismic hazard curves for hard rock from this calculation for the spectral frequencies of 100, 25, 10, 5, 2.5, 1, and 0.5 Hz, respectively. Table 2.5.2-223 documents the digital fractile and mean seismic hazard curves for the seven spectral frequencies. Table 2.5.2-209 documents the UHRS values for this calculation. Figure 2.5.2-225 plots the mean and median UHRS for 1E-04, 1E-05, and 1E-06 annual frequencies of exceedance.

As a sensitivity check, the potential contribution of the New Madrid seismic source to seismic hazard was examined for 1 Hz spectral acceleration. It was determined that the New Madrid seismic source's mean hazard was less than 0.1 percent of the mean hazard from other sources, so the New Madrid seismic source was not included in the overall hazard calculations.

Also, the potential contribution of small earthquakes (smaller than the characteristic earthquakes, that is up to m_b 6.8) in the Charleston seismic source was examined for 1 Hz spectral acceleration. It was determined that these earthquakes (which are modeled with an exponential magnitude distribution) contributed a mean hazard that was less than 0.1 percent of the mean hazard from other sources. As a result, the smaller magnitude earthquakes were not included in the overall hazard calculations.

The rock hazard was deaggregated to identify the magnitudes and distances appropriate to represent rock spectral shapes for site response calculations. This deaggregation procedure followed the guidelines of RG 1.208. Specifically, the mean contributions to seismic hazard for 1 Hz and 2.5 Hz spectral accelerations (low frequencies, or LF) were deaggregated by magnitude and distance for the mean 1E-04 ground motion amplitude at 1 Hz and at 2.5 Hz, and these deaggregations were combined (contributions for each magnitude and distance bin were averaged). Figure 2.5.2-226 shows this combined deaggregation. Similar deaggregations of the mean hazard were performed for 5 and 10 Hz spectral accelerations (high frequencies, or HF), and the combined deaggregation is shown in Figure 2.5.2-227.

Deaggregations of the HF and LF mean hazard for 1E-05 and 1E-06 ground motions are shown in Figures 2.5.2-228 through 2.5.2-231. Table 2.5.2-224 shows the percent contributions for various magnitude and distance bins for the six deaggregations, and Table 2.5.2-225 summarizes the mean magnitudes and distances resulting from these deaggregations, for all contributions to hazard and for contributions with distances exceeding 100 kilometers.

For the HF controlling earthquakes, the magnitudes and distances from all distances are used (the light grey shaded cells in Table 2.5.2-225). For the LF controlling earthquakes, the magnitudes and distances from distances greater than 100 kilometers are used (the dark grey shaded cells in Table 2.5.2-225), because the contribution to hazard for distances greater than 100 kilometers is more than 5 percent of the total hazard. This follows the guidelines in RG 1.208. For

Figures 2.5.2-226 through 2.5.2-231 and Tables 2.5.2-224 and 2.5.2-225, deaggregation results are given in terms of moment magnitude.

The deaggregation plots in Figures 2.5.2-226 through 2.5.2-231 indicate that local earthquakes are a contributor to seismic hazard at the site for high frequencies, but that distant sources also make an important contribution. Distant sources contribute because the seismicity rate of local earthquakes in the Florida Peninsula is very low. For LF, distant sources have the major contribution to seismic hazard, with the Cuba areal source zone, Caribbean faults, and Charleston source contributing most of the hazard.

Smooth rock UHRS were developed from the UHRS amplitudes in Table 2.5.2-209, using controlling earthquake M and R values shown in Table 2.5.2-225 and using the hard rock spectral shapes for CEUS earthquake ground motions recommended in NUREG/CR-6728 (Reference 308). Separate spectral shapes were developed for HF and LF. In creating these spectral shapes, the single-corner and double-corner source models recommended in NUREG/CR-6728 (Reference 308) were weighted equally.

In order to reflect accurately the UHRS values calculated by the PSHA as shown in Table 2.5.2-209, the HF spectral shape was anchored to the UHRS values from Table 2.5.2-209 at 100 Hz, 25 Hz, 10 Hz, and 5 Hz. In between these frequencies, the spectrum was interpolated using shapes anchored to the next higher and lower frequency and using weights on the two shapes equal to the inverse logarithmic difference between the intermediate frequency and the next higher or lower frequency. Below 5 Hz, the HF shape was extrapolated from 5 Hz. For the LF spectral shape a similar procedure was used except that the LF spectral shape was anchored to the UHRS values at all seven frequencies for which UHRS values are available from Table 2.5.2-209 (100 Hz, 25 Hz, 10 Hz, 5 Hz, 2.5 Hz, 1 Hz, and 0.5 Hz).

The reason that the LF spectral shape was anchored to all seven frequencies, including the HF, was that, if this anchoring were not done, the LF spectrum would exceed the HF spectrum at high frequencies, which would not be realistic. The UHRS at all frequencies accounts for all earthquakes, small and large, close and distant, and the UHRS amplitudes should not be exceeded by spectra representing the controlling earthquakes.

For frequencies below 0.5 Hz, the spectral shapes for both the HF and LF spectra were extrapolated from the value at 0.5 Hz assuming a constant spectral velocity (i.e., spectral accelerations were assumed to scale linearly with frequency) down to 0.125 Hz (8 seconds). From 0.125 Hz to 0.1 Hz, spectral accelerations were assumed to scale as $(\text{frequency})^2$. This follows the recommendation of Building Seismic Safety Council (Reference 219) for long periods.

Figures 2.5.2-232 through 2.5.2-231 show the horizontal HF and LF spectra calculated in this way for 1E-04, 1E-05, and 1E-06 annual frequencies of exceedance, respectively. As mentioned previously, these spectra were appropriately anchored to accurately reflect the rock UHRS amplitudes in Table 2.5.2-209 that were calculated for the seven spectral frequencies at which PSHA calculations were done.

2.5.2.4.7 Hazard Sensitivity Analyses Using the CEUS SSC Model

This subsection describes sensitivity analyses performed using the CEUS SSC seismic source model presented in NUREG-2115 (Reference 353) and presents comparisons of the CEUS hard rock hazards and UHRS computed using the CEUS SSC model with the results presented in Subsection 2.5.2.4.6.

2.5.2.4.7.1 Summary of CEUS SSC Model Sources

This section summarizes the CEUS SSC model. Details are provided in NUREG-2115 (Reference 353). The model for seismic sources in the CEUS consists of two types of seismic sources. The first type is seismic source zones used to model future distributed seismicity throughout the CEUS. As shown on Figures 2.5.2-280 and 2.5.2-281, two approaches are used to define the distributed seismicity sources. The seismotectonic approach (Figure 2.5.2-280) subdivides the CEUS into different source zones on the basis of differences in geology and tectonic history. The Mmax Zones approach (Figure 2.5.2-281) subdivides the CEUS into regions that are expected to have different values of the maximum magnitude that can occur. The second type of seismic source is used to model the recurrence of repeated large magnitude earthquakes (RLMEs) that have been identified from the historical and paleoseismic record. The RLME sources are additional sources of large magnitude earthquakes added to the hazard computed from the distributed seismicity sources—either the Mmax source zones or the Seismotectonic source zones. The location of the RLME sources is shown on Figure 2.5.2-282. The nearest RLME source to the Turkey Point Units 6 & 7 site is the Charleston RLME source.

2.5.2.4.7.2 Description of CEUS SSC Model Sensitivity Analysis

Comparison of the areal extent of the CEUS SSC model shown on Figures 2.5.2-280 and 2.5.2-281 with the region encompassed by the updated EPRI-SOG seismic sources shown on Figures 2.5.2-204 through 2.5.2-209 indicates that the two source models cover the same region. In addition, Charleston RLME source in the CEUS SSC model, shown on Figure 2.5.2-282 occupies the same general location as the UCSS shown on Figure 2.5.2-212. Thus, the CEUS SSC model can be considered as a replacement for the updated EPRI-SOG model, including the UCSS source and the supplemental sources between Florida and Cuba in their entirety. As a consequence, an assessment of the effect of the CEUS SSC model on the total hazard for the site can be evaluated by subtracting from the total mean hazard presented in Subsection 2.5.2.4.6 and Table 2.5.2-223 the contributions of the updated EPRI-SOG sources and then adding the hazard contributed by the CEUS SSC model sources. Comparing the resulting values against the total hazard listed in Table 2.5.2-223 shows the sensitivity of the site rock hazard to use of the CEUS SSC model sources in place of the updated EPRI-SOG sources.

The CEUS SSC model was used to compute hard rock hazard at the Turkey Point site. The hazard was computed using the contributions from those portions of all of the CEUS SSC seismic source zones within 1000 kilometers (620 miles) of the site. In addition, the hazard from the Charleston RLME source (Figure 2.5.2-282) was included. Consistent with the calculations presented in Subsection 2.5.2.4, the hazard calculations for the seismic source zones and the Charleston RLME used the mid-continent versions of the EPRI (Reference 242) ground motion models. Similar to the analyses presented in Subsection 2.5.2.4, the contribution from the New Madrid RLME (Figure 2.5.2-282) was found to be negligible, and this source was not included in the hazard calculations. Also, as documented in Chapter 8 of NUREG-2115 (Reference 353), the other RLME sources in the vicinity of the New Madrid RLME were found to have negligible contribution to the hazard at the Chattanooga demonstration site, and thus would not contribute to the hazard at Turkey Point, which is much further way from these sources. Therefore, only the Charleston RLME source was included in the sensitivity calculations. Corrected maximum magnitude (Mmax) distributions for the CEUS SSC seismotectonic model zones PEZ-N and PEZ-W as reported in (Reference 361) are used in the hazard calculations.

Calculations were performed for PGA and spectral accelerations at structural frequencies of 25, 10, 5, 2.5, 1, and 0.5 Hz using the CEUS SSC model sources. These results were used to develop total mean hazard for the site by adding the hazard from the Caribbean sources described in Subsection 2.5.2.4.6.

2.5.2.4.7.3 CEUS SSC Model Sensitivity Analysis Results

Figures 2.5.2-283 and 2.5.2-284 compare the hazard results obtained using the CEUS SSC model with those presented in Subsection 2.5.2.4.6 using the updated EPRI-SOG model for 10 Hz and 1 Hz spectral accelerations, respectively. The solid curves show the total mean hazard for the combined updated EPRI-SOG plus Caribbean sources and the mean hazard from the three major source types: the EPRI-SOG distributed seismicity sources, the Charleston (UCSS) source, and the Caribbean sources. The dashed curves show the total hazard for the combined CEUS SSC plus Caribbean sources and the mean hazard from the CEUS SSC distributed seismicity sources and the Charleston RLME source (the hazard from the Caribbean sources is the same for the two analyses).

The results for 10 Hz (Figure 2.5.2-283) indicate that the total hazard computed using the CEUS SSC sources is lower than that computed using the updated EPRI-SOG sources in the important annual exceedance frequency range of 1E-04 to 1E-06. As shown on the figure, the hazard computed using the Charleston RLME source is essentially the same as that computed using the Charleston UCSS source. Thus, the difference in the hazard is due to differences in the characterization of the distributed seismicity sources in the CEUS. As the hazard in both models is computed using the same ground motion models, difference in hazard is due to a difference in the predicted frequency of earthquakes in the site region with the CEUS SSC model predicting a lower rate of earthquakes than the updated EPRI-SOG model.

The results for 1 Hz (Figure 2.5.2-284) indicate that the total hazard computed using the CEUS SSC sources is slightly higher than that computed using the updated EPRI-SOG sources in the important annual exceedance frequency range of 1E-04 to 1E-06. The increase in computed hazard is about 3 percent at 1E-04 and about 11 percent at 1E-06. Again, as shown on the figure, the hazard computed using the Charleston RLME source is essentially the same as that computed using the Charleston UCSS source and the difference in the hazard is due to differences in the characterization of the distributed seismicity sources in the CEUS. The larger hazard at low structural frequencies from the CEUS SSC distributed seismicity sources is attributed to the larger on average maximum magnitudes for these sources in the CEUS SSC model as compared to the values for the distributed seismicity sources in the updated EPRI-SOG model. The differences in hazard for 1 Hz spectral accelerations shown on Figure 2.5.2-284 are less than the suggested tolerances for hazard accuracy presented in Chapter 9 of NUREG-2115 (Reference 353).

The total mean hazard obtained by combining the hazard from the CEUS SSC model with that from the Caribbean sources was used to compute hard rock UHRS. Figure 2.5.2-285 compares these UHRS to those computed using the updated EPRI-SOG source model presented in Table 2.5.2-209. For structural frequencies of 2 Hz and higher, the UHRS based on the CEUS SSC sources are lower than those based on the updated EPRI-SOG source model. At lower structural frequencies, the UHRS based on the CEUS SSC source model are about 1 percent higher at 1E-04 mean annual exceedance frequency, about 2 to 2.5 percent higher at 1E-05 mean annual exceedance frequency, and 3 to 5 percent higher at 1E-06 mean annual exceedance frequency. These small differences at low structural frequencies are considered to be negligible because they are similar in magnitude to differences in computed ground motions that are obtained from implementation of the CEUS SSC model by two different software packages, as documented in hazard calculation for the seven NUREG-2115 (Reference 353) demonstration sites documented in Table 2.5.2-232 of Attachment C to the Progress Energy supplemental response for Levy Nuclear Units 1 and 2 to the RAI concerning the Fukushima Near-Term Task Force recommendations contained in SECY-12-0025 (Reference 354).

Thus, the conclusion of the sensitivity calculations is that ground motions for the site computed using the CEUS SSC seismic source model presented in NUREG-2115 (Reference 353) are similar to or enveloped by ground motions computed using the updated EPRI-SOG seismic source model presented in Subsection 2.5.2.4.6.

2.5.2.5 Seismic Wave Transmission Characteristics of the Site

The UHRS described in the previous subsection are defined on hard rock. Hard rock is characterized with minimum shear-wave velocity (V_S) = 9200 feet per second (fps), which at the site is located at about 10,000 feet (3050 meters) below the ground surface. This subsection describes the development of the site amplification factors that result from the transmission of the seismic waves through the thick site-specific geologic column above hard rock, referred to as "soil column" thereafter. The effect of variability in material properties of the geologic column is modeled by randomizing over the range of properties and layer thicknesses extending from the finished ground surface (including structural fill) to randomized hard rock depths varying between 7400 feet (2256 meters) and 11,400 feet (3476 meters), and randomizing over the range of shear modulus reduction and damping within the column, as well as an adjustment to the soil column damping to represent the anelastic attenuation of ground motion by the entire column (the "kappa" value).

The development of the site amplification factors is performed in the following steps:

1. Develop a model of the base case soil column, using site-specific geotechnical and geophysical data to a depth of about 636 feet (194 meters), and from 636 feet to a depth of about 12,000 feet (3658 meters) using deep velocity profiles taken from industry, as described in Subsection 2.5.2.5.1. The model for the upper 636 feet (194 meters) is based on mean shear-wave velocities measured at the site, except for the upper 30.5 feet (9.3 meters) of structural fill. Strain-dependent in situ shear modulus and damping are obtained from generic curves based on Resonant Column Torsional Shear (RCTS) of in situ samples of the native soils (Subsection 2.5.4.7). The deeper layers are assumed to behave linearly. This model provides the base case representation for evaluation of the dynamic behavior of materials beneath the site to hard rock with V_S = 9200 fps under seismic loading.

2. Calculate strain-independent (linear-elastic) material damping values for the deep strata (between 636 feet and 9200 fps hard rock), which experience small levels of strain during the earthquake, to ensure that the base case model accurately accounts for the dissipation of energy in this depth interval. This is done by constraining the damping within these deeper strata to replicate the estimate of the kappa for the site.

3. Generate a set of 60 randomized profiles by using the base soil column, and develop a probabilistic model that includes the uncertainties in the above material properties, location of layer and hard rock boundaries, correlation between the velocities in adjacent layers, and the overall dissipation of energy in the site-specific column.

4. Use the 1E-04 and 1E-05 annual-frequency-of-exceedance smooth LF and HF hard rock spectra of Subsection 2.5.2.4 for input into the base of the randomized profiles, calculate dynamic response of the site for each of the 60 randomized profiles by using an equivalent-linear site-response formulation together with Random Vibration Theory (RVT), and calculate the mean site response. Time histories for the site response analysis are not required for the frequency-domain RVT approach to site response analysis. This step is repeated for each of the four input motions (1E-04 and 1E-05 annual frequencies, HF and LF smooth spectra). Note that the GMRS horizon is defined at elevation -35 feet. To calculate the site response at GMRS horizon, two consecutive site response analyses are conducted. In the first analysis, the randomized profiles with full column height up to finished grade at elevation +25.5 feet are analyzed. In the second analysis, the strain-compatible properties of the columns, provided by the first analysis, are used without iteration, the layers above the GMRS horizon are omitted, and the amplification factors at elevation -35 feet (corresponding to zero depth in this case) are calculated.

Details of the implementation of these steps are described in the following subsections. The resulting site-specific amplification factors are used with the hard rock spectra of Subsection 2.5.2.4 to develop the GMRS in Subsection 2.5.2.6.

2.5.2.5.1 Base Case Site-specific Column and Uncertainties

Development of a base case site-specific column is described in detail in Subsection 2.5.4. Summaries of the low strain shear-wave velocity, material damping, and strain-dependent properties of the base case strata based on the initial subsurface investigation are provided below in this subsection. These parameters serve as input for the generation of randomized profiles and for site response analyses.

The Units 6 & 7 site is a limestone and sand site covered with an approximate 5-foot thick layer of muck. The existing upper approximately 611 feet (186 meters) of the site-specific column were investigated using test borings, Cone Penetration Testing (CPT), test pits, and geophysical methods. The soil layers and approximate thicknesses encountered during the initial subsurface investigation at the boring and CPT locations consist of, in descending order:

- Five feet of muck, consisting of peat and silt (during construction, structural fill is designed to replace the 5 feet of muck)
- Miami Limestone (25 feet)
- Key Largo Limestone (20 feet)
- Fort Thompson Formation (70 feet)
- Tamiami Formation (100 feet)
- Upper Hawthorn sand (230 feet)
- Lower Hawthorn Group consisting of limestone, mudstone, dolomite, dolosilt, shells, quartz sand, clay, and mixtures of these materials.

The GMRS, at elevation -35 feet, is located near the top of the Key Largo Limestone, below the Miami Limestone. The Primary-Secondary (P-S) suspension measurements and CPT results provided shear and compression wave velocities of the soil and rock at 1.6 feet (0.5 meters) intervals. These data were used to develop a mean shear-wave profile for the upper 611 feet (186 meters) of in situ materials. Note that the estimated mean shear-wave velocity values of 650 fps at the ground surface to 1100 fps at a depth of 30.5 feet were assigned to the structural fill layer (uppermost 30.5 feet, 9.3 meters) (Subsection 2.5.4). The initial S-wave velocity profiles are shown in Figure 2.5.4-220.

In order to capture the uncertainty in this estimate, a coefficient of variation of 1.5 applied to the shear modulus was used to provide upper and lower bounds. These values are based on an assumed unit weight of 130 pounds per cubic foot (pcf) and a Standard Penetration Test (SPT) resistance (normalized with respect to overburden pressure) of N_1 = 30 blows per foot for the fill.

Information used for defining the site-specific geologic column for depths exceeding 636 feet (194 meters) below top of fill was obtained from available industry resources (Subsection 2.5.4). A total of eight deep sonic logs of compression wave velocity were located within about a 115-mile radius of the Units 6 & 7 site: six were obtained in digitized format at 0.5 feet (0.15 meters) intervals, and two were digitized manually at 10 feet (3 meters) intervals. The compression wave velocities were converted to shear-wave velocities using values of Poisson ratios based on near surface

measurements taken at the site and values published by the U.S. Army Corps of Engineers (Subsection 2.5.4). In this manner, shear-wave velocity data at varying depths ranging from 500 feet to 11,920 feet were determined. Unit weights of the deep strata (below approximately 636 feet [194 meters]) were assumed to be 130 pcf (Subsection 2.5.4).

As part of the construction of the Class V exploratory well EW-1 at the Turkey Point Units 6 & 7 site, additional sonic log data was collected after the conclusion of the site response analysis (Subsection 2.5.4.2.1.2.10). This data provides additional shear-wave velocities for depths between 1100 feet and 3200 feet. An evaluation was conducted with the aim of assessing the impact of the new shear-wave velocity information on the site amplification. The evaluation concludes that the newly acquired data does not change the site amplification results documented in this section and that the site response analysis results are not affected.

As described in Subsection 2.5.4.2.3, RCTS testing was conducted on seven samples obtained during the initial subsurface investigation. These samples are from the Tamiami Formation sands. These results were matched to the closest fitting generic EPRI material shear modulus and damping degradation curves for sandy soils (Reference 244). The remaining materials consist of hard limestones, which are treated as elastic materials with 1 percent damping. Analyses for the development of site-specific amplification factors were therefore conducted using measured shear wave velocity profiles combined with shear modulus and damping degradation curves for the sands and elastic properties for the limestone.

Generic EPRI curves (Reference 244) were adopted to describe the strain dependencies of shear modulus and damping for the sands occurring between depths of about 120 feet (37 meters) and 450 feet (137 meters). The structural fill materials, forming the uppermost 30.5-foot (9.3-meter) layer (from final grade at El. +25.5 feet to the top of the Miami Limestone at El. –5 feet), are to be derived from crushed limestone during construction. EPRI shear modulus and damping degradation curves for gravel (Reference 317) are used to model the fill layers, as shown in Subsection 2.5.4.7.

Damping values were developed for the linear deep layers to maintain the total kappa (κ) for the site-specific geologic column as described below. Low-strain kappa value, a near surface damping parameter for modeling site-dependent effects, is used as a measure of the total dissipation of energy in the soil column during the small strain events. The site-specific kappa value accounts for damping of the layers and scattering of the waves at layer interface boundaries. The kappa representing soil layer damping is additive for all layers. The following expression shows the relationship between kappa (κ_i) and the damping coefficient, (ζ_i) of the layer (i):

$$\kappa_i = \frac{2H_i\xi_i}{V_{Si}}$$ Equation 2.5.2-11

where, H_i is the thickness and V_{Si} is the shear-wave velocity of the layer (i).

Total kappa value of the site associated with material damping equals the sum of the κ_i values of all layers included in the model:

$$\kappa = \sum_i \kappa_i$$ Equation 2.5.2-12

Total kappa is directly evaluated from recordings of earthquakes (Reference 209), of which there are too few in the site vicinity to obtain an explicit site-specific estimate of kappa. Therefore, when total kappa is not available from near or applicable earthquake recordings, an alternative is to estimate

total kappa directly using the correlation with average rock shear-wave velocity, V_S, from Reference 241:

$$\log(\kappa) = 2.2189 - 1.0930 \times \log(V_S[ft/\sec]) \qquad \text{Equation 2.5.2-13}$$

Based on review of EPRI, (Reference 241), the average shear-wave velocity to use with Equation 2.5.2-13 appears to be representative of the uppermost approximate 100 feet of rock. The average velocity of the Key Largo Limestone and Fort Thompson Formation (which totals about 86 feet thick) is used for this analysis. The average shear-wave velocity of the 86 feet of Key Largo Limestone and Fort Thompson Formation was calculated to be 4239 fps, which, using Equation 2.5.2-13, corresponds to a total kappa of 0.018 second. By inspection of Figure 2.5.2-235, the shear-wave velocities determined in the upper 1000 feet of rock vary between about 4000 fps and 5000 fps, which correspond to total kappa values of 0.019 second and 0.015 second, respectively. Therefore, a total kappa value of 0.018 second is used for the soil/rock column with a standard deviation of 0.4 natural log units.

A kappa value of 0.006 second applies to the CEUS hard rock (Reference 244), leaving a total kappa value of 0.012 second for the damping of the full depth of the soil column.

EPRI, 1993 (Reference 244) recommends a standard deviation of 0.4 natural log units to be appropriate for total kappa values of sites within the eastern U.S. This is consistent with EPRI, 2005 (Reference 241) in considering 50 percent variation about the base case value of kappa for Mississippi Embayment sites.

Therefore, a base case kappa value of 0.012 second is used for the Units 6 & 7 site-specific geologic column with a standard deviation of 0.4 natural log units.

The following procedure is used to assign the damping to the models of the materials at depths below 636 feet (194 meters) in order to match the assigned kappa value:

1. From Equations 2.5.2-11 and 2.5.2-12, kappa associated with material damping is calculated for the top approximately 600 feet (183 meters) of strata, i.e., excluding top fill, by using small strain damping for each layer.

2. The kappa value of the top approximately 600 feet (183 meters) of soil/rock is deducted from the total kappa value, and a constant damping value is assigned to deep layers. The process of the randomization of velocity profiles introduces additional scattering of upward propagating shear waves (S-waves) in such a manner that the median response of all randomized profiles is lower than the response obtained from the analyses of the median profile. These scattering effects are accounted for by decreasing the damping value of the deep layers in the randomized profiles, and therefore reduce total kappa for the site. In this case, however, because damping in the deep layers was very small (median of 0.3 percent), no reduction was applied.

3. The damping of each deep layer is randomized with consideration given to the mean and variation of the total kappa.

The input motion for site amplification analysis was specified at the bottom of the site-specific geologic column, below which the halfspace was modeled with shear-wave velocity of 9200 fps and a damping ratio of 1 percent, hard rock.

As described in Subsection 2.5.2.5.2, the properties for each layer in the column were randomized to account for the inherent natural variability, as well as the (epistemic) uncertainty associated with the choice of curves to capture the variation of shear modulus and damping with strain level. Therefore,

the actual site response analysis comprised a range of properties for each layer, and in particular, a range of initial small strain shear modulus and degradation curves. Because of different properties in each of the randomized profiles, the site response analysis generated a range of results, as reported in Subsection 2.5.2.5.3.

2.5.2.5.2 Capturing Site-Specific Geologic Column Properties, Uncertainties, and Correlations

To account for variations in shear-wave velocity across the site, 60 randomized profiles were generated using the stochastic model discussed in Reference 319, with some modifications to account for the site-specific conditions at the Units 6 & 7 site. These randomized profiles represent the truncated column from the top of hard rock with shear-wave velocity of 9200 fps to the ground surface. This model uses as inputs the following quantities:

1. A shear-wave velocity profile, which is equal to the base-case profile described above.

2. The standard deviation of ln(V_S) (the natural logarithm of the shear-wave velocity) as a function of depth.

3. The correlation coefficient between ln(V_S) in adjacent layers, which is taken from generic studies using the inter-layer correlation model for category USGS “A” soils (Reference 319), with modifications to some of the parameters to increase the correlation in order to reduce the number of V_S reversals.

4. The probabilistic characterization of layer thickness is accomplished using a function that describes the rate of layer boundaries as a function of depth. This study used a form of this function, taken from Reference 319, but modified to allow for sharp changes and discontinuities in the adopted base-case velocity profile, especially near the surface.

5. The profiles of the median and plus/minus one standard deviation of the shear-wave velocity profile are shown in Figure 2.5.2-236. The variation was used in the randomization of the shear-wave velocity profile.

6. For each randomized profile, hard rock is defined to occur at the depth where the randomization algorithm calculates a V_S that exceeds 9200 fps (excluding depths shallower than 7000 feet).

7. Median value of shear stiffness (G/G_{max}) and damping for each geologic unit are provided in Table 3JJ-214. Uncertainties in the strain-dependent properties for each unit are characterized using the values in Reference 320. Figures 2.5.2-237 and 2.5.2-238 illustrate the shear stiffness and damping curves generated for natural materials found at elevation less than 150-foot depth, described in Subsection 2.5.2.5.1.

Figure 2.5.2-239 illustrates the 60 V_S random profiles generated, using the median, logarithmic standard deviation, and correlation model described above. The same figure compares the median of these 60 V_S profiles (randomized median) to the input median V_S profile described in the previous subsection, indicating good agreement. At depths greater than 7000 feet, the randomized median appears lower than the input median because, when a random V_S profile exceeds 9200 fps, the profile is truncated at that depth. The randomized median curve in Figure 2.5.2-239 does not include these truncated profiles but shows the median of only the remaining profiles (with V_S < 9200 fps) at each depth. Therefore, the median of these filtered profiles (with V_S < 9200 fps) is lower than the overall median at deep locations in the profile.

This set of 60 random profiles, consisting of V_S versus depth, depth to hard rock, stiffness, and damping, are used to calculate and quantify site response and its uncertainty, as described in the following subsections.

2.5.2.5.3 Site Response Analysis

The site response analysis performed for the Units 6 & 7 site is conducted using the program P-SHAKE, which uses a procedure based on RVT (References 232 and 306) with the following assumptions:

- Vertically propagating shear waves are the dominant contributor to site response.
- An equivalent-linear formulation of nonlinearity is appropriate for the characterization of site response.

These are the same assumptions that are implemented in the SHAKE program (Reference 263). With respect to RVT implementation, the major steps used in P-SHAKE are as follows:

1. The input motion is provided in terms of an acceleration response spectrum (ARS) and associated spectral damping instead of spectrum-compatible acceleration time histories. The input ARS is converted to an acceleration power spectral density (PSD) using the RVT based procedure with the peak factor function.
2. From the frequency domain computation (following SHAKE approach), the transfer function for shear strain in each layer of the profile is obtained and convolved with the PSD of input motion to get the PSD and the maximum strain in each layer. The effective strain is obtained from the maximum strain and is used to obtain new properties (shear modulus and damping) for the next iteration.
3. The iterations are repeated until convergence limit set by the analyst is reached in all layers.
4. Once the final frequency domain solution is obtained, the ARS at each layer interface can be computed from the solution using an inverse process of obtaining PSD from the ARS.

The site-response analysis procedure, as described above, requires the following additional parameters:

- Strong-motion duration — The RVT methodology requires this parameter, but results are not very sensitive to it. These are calculated from the mean magnitudes from the deaggregation. Table 2.3.1 in ASCE 4-98 (Reference 206) provides strong motion duration values as a function of magnitude. Accordingly, strong motion durations were assigned for each of the cases considered (1E-04 and 1E-05 annual frequencies, HF and LF smooth spectra) and are presented in Table 2.5.2-226.
- Effective strain ratio — A value of 0.65 is used. Effective strain ratio is defined as the ratio between the peak acceleration of earthquake time history and the equivalent harmonic wave going through the layers (Reference 316).

As discussed earlier, the GMRS horizon is defined at elevation -35 feet. To calculate the site response at the GMRS horizon, two consecutive site response analyses are conducted. In the first analysis, the full soil column height up to finished grade at elevation +25.5 feet is analyzed. In the second analysis, the strain-compatible properties of the column, provided by the first analysis, are used without iteration after omitting the layers above the GMRS horizon, and the amplification factors at elevation -35 feet (corresponding to zero depth in this case) are calculated.

Figure 2.5.2-240 shows as a thick red line the logarithmic mean (median) of site amplification factors at the GMRS horizon from the analysis of the 60 random profiles with the 1E-04 LF input motion. Amplifications are largest at low frequencies (below 6.0 Hz) and de-amplification occurs at high frequencies because of damping. The maximum strains in the column are low for this motion. This is shown in Figure 2.5.2-241, which plots the maximum strains versus depth that are calculated for the 60 profiles and their logarithmic mean (as a red thick line).

The median of maximum strains does not exceed 0.020 percent. The maximum strain calculated from the analyses of all 60 profiles is 0.070 percent in the structural fill layers. The maximum strains in the deep strata at depths below 636 feet (194 meters) are very small and do not exceed a value of 0.005 percent.

Figures 2.5.2-242 and 2.5.2-243 show similar plots of amplification factors and maximum strains obtained from the analyses with 1E-04 HF motion. The maximum strain results show that the site-specific column exhibits a lower level of straining under this motion with maximum strains being less than 0.04 percent.

Figures 2.5.2-244 through 2.5.2-247 show comparable plots of amplification factors and maximum strains from the analyses performed with the 1E-05 input motion, both LF and HF. For this higher motion, larger maximum strains are observed, but the maximum median does not exceed 0.045 percent. From all of 1E-05 analyses, a maximum strain of 0.23 percent is calculated at the top structural fill layers. The maximum strain in the deep layers, below 636 feet (194 meters), is very small, less than 0.01 percent.

Comparison of the profiles of median maximum strains for the full site-specific column and the upper 800 feet in Figure 2.5.2-248 clearly shows that strains under the LF motions are larger than under HF motions. Figure 2.5.2-249 shows the median profiles for the strain-compatible damping resulting from the four input rock motions as well as the low-strain damping, for the full site-specific geologic column and the upper 800 feet.

Damping is a measure of energy dissipation in the profile during the shaking. Corresponding to the strains, a maximum damping value of 5 percent for depths above 636 feet (194 meters) are calculated for the analyses with the 1E-05 LF motion. The strain compatible damping calculated for 1E-04 LF motion is small and does not exceed 3 percent.

A comparison of the envelopes of median site amplification factors at GMRS horizon for LF and HF 1E-04 and 1E-05 input motions is shown in Figure 2.5.2-250. The amplifications at 1E-04 level of input motion are larger due to LF input motion than the ones due to HF input motion. De-amplification occurs at higher frequencies and is smaller for the LF input motion, followed by amplification of the peak ground acceleration starting at about 80 Hz and reaching about 1.3 at 100 Hz. The amplification due to 1E-05 level of input motion is smaller than for the 1E-04 level of input motion at frequencies larger than 3 Hz, due to the higher strain levels and nonlinearity in the column. At these higher frequencies, amplification factors for the LF and HF 1E-05 motions are very close.

The corresponding numerical values of the site amplification factors are tabulated in Tables 2.5.2-210 and 2.5.2-227. These tables show values for just 38 frequencies, but site amplification factors and site spectra were calculated for 301 frequencies between 0.1 and 100 Hz.

2.5.2.6 Performance-based Ground Motion Response Spectra

This subsection presents the development of performance-based ground motion response spectra (GMRS) for the Units 6 & 7 site. The site-specific horizontal GMRS are developed for the site following the guidelines described in RG 1.208, and then the vertical GMRS are constructed from the horizontal spectra using V/H response spectral ratios appropriate for the site.

2.5.2.6.1 Horizontal Spectra

With the site-specific amplification calculations described in the previous subsection, the site GMRS were determined as follows.

Figure 2.5.2-251 shows the 1E-04 and 1E-05 horizontal HF and LF spectra, obtained at -35 feet plotted on a linear spectral acceleration scale. These HF and LF 1E-04 and 1E-05 horizontal spectra were enveloped and smoothed to remove small frequency-to-frequency variations, using smoothing function that averaged over spectral accelerations at adjacent frequencies. Figure 2.5.2-252 shows the smoothed, enveloped spectra calculated in this way plotted on a linear spectral acceleration scale.

The horizontal GMRS was calculated at each frequency using the following equations:

$$A_R = SA(10^{-5})/SA(10^{-4}) \qquad \text{Equation 2.5.2-14}$$

$$DF = 0.6 \times A_R^{0.8} \qquad \text{Equation 2.5.2-15}$$

$$GMRS = max[SA(10^{-4}) \times max(1.0, DF), 0.45 \times SA(10^{-5})] \qquad \text{Equation 2.5.2-16}$$

where, $SA(10^{-4})$ is the spectral acceleration for the 1E-04 envelope spectrum at each spectral frequency (and similarly for 1E-05), and GMRS is the Ground Motion Response Spectrum at that spectral frequency. These equations follow the procedure in RG 1.208 to determine the GMRS from the 1E-04 and 1E-05 spectra.

Figure 2.5.2-253 shows the GMRS calculated with the above equations at each spectral frequency, and shows the 1E-04 and 1E-05 horizontal spectra, plotted on a logarithmic spectral acceleration scale. At low spectral frequencies (2 Hz and below), the hazard curves are steep, so A_R in Equation 2.5.2-14 above is low, and the GMRS from Equation 2.5.2-16 is equal to the 1E-04 UHRS.

Tables 2.5.2-210 and 2.5.2-227 document the 1E-04 and 1E-05 spectra, respectively, including the hard rock spectra, site amplification factors, and site spectra.

The method described above corresponds to Approach 2A in Reference 308. Thus hazard curves were not generated for the GMRS elevation; only the 1E-04, 1E-05, and 1E-06 site spectra were generated at the GMRS elevation. Table 2.5.2-228 documents the 1E-04 and 1E-05 spectral amplitudes, the calculation of A_R and DF from Equations 2.5.2-14 and 2.5.2-15, and the GMRS calculated according to Equation 2.5.2-16. Table 2.5.2-229 documents the 1E-04, 1E-05, and 1E-06 site spectra, with smoothing for the 1E-06 spectrum conducted with the same function as described above for the 1E-04 and 1E-05 spectra.

2.5.2.6.2 Vertical Spectra

To calculate vertical spectra, V/H ratios from RG 1.60 were adopted. The V/H ratios were applied to the 1E-04 and 1E-05 horizontal spectra to calculate 1E-04 and 1E-05 vertical spectra, and Equations 2.5.2-14 through 2.5.2-16 were applied to the 1E-04 and 1E-05 vertical spectral accelerations to calculate a vertical GMRS. The resulting vertical 1E-04 and 1E-05 spectra and GMRS are plotted in Figure 2.5.2-254.

Table 2.5.2-230 documents the V/H ratios, the 1E-04 and 1E-05 vertical spectra, values of A_R and DF from Equations 2.5.2-14 and 2.5.2-15, and the calculated vertical GMRS from Equation 2.5.2-16.

2.5.2.6.3 GMRS Sensitivity Analyses

The supplemental subsurface investigation described in Subsection 2.5.4, which updated the initial characterization of subsurface material properties, invited consideration of the effect on the site-specific GMRS. To investigate this possibility, and to provide insight into its potential significance, sensitivity analyses were performed. These sensitivity analyses evaluated the effect of the updated site properties on the horizontal GMRS based on a simplified methodology to capture the variability of the subsurface properties as compiled from site investigations. That is, this variability was captured by using UB, BE, and LB soil column models rather than 60 randomized soil columns as was done to calculate the performance-based GMRS described in Subsection 2.5.2.6.2.

The GMRS sensitivity analyses were conducted in a manner consistent with the approach used for parallel sensitivity analyses performed to evaluate the potential effect of updated soil column profiles on both the NI and FAR FIRS and SSI input properties. Further details on these sensitivity analyses and their conclusions on the FIRS and SSI input properties are documented in Subsection 3JJ.7.

The results of the GMRS sensitivity analyses are summarized as follows:

1. The sensitivity result (developed using the updated site characteristics and the simplified procedure outlined above to capture the variability of the subsurface material properties) was determined to give a spectrum slightly higher than the horizontal GMRS (see Figure 2.5.2-253a). At a frequency of 100 Hz, the sensitivity result spectrum increased from the 0.058g value of the GMRS to 0.062g (about seven percent). The maximum horizontal ground-motion change (from 0.0635g to 0.0698g, about 10 percent) occurred at a frequency of 45 Hz. The ground-motion differences of 0.004g at a frequency of 100 Hz and 0.006g at a frequency of 45 Hz are well within the confidence bounds of the PSHA and seismic site response.

2. The vertical GMRS is developed, following the guidance of RG 1.60, from the horizontal GMRS by applying a scalar ranging from 1.0 for high frequencies to 0.67 for low frequencies. Applying the same scalars to the horizontal spectrum resulting from the sensitivity analyses would lead to the same conclusions about present change and significance for the vertical spectrum as for the horizontal spectrum.

3. As shown on Figure 2.5.2-253a, both the horizontal GMRS and the sensitivity result spectra lead to a characterization of the Turkey Point Units 6 & 7 site as a site with low seismic hazard.

The results show that the horizontal spectrum, resulting from the above sensitivity analyses, is only modestly higher than the GMRS, as shown in Figure 2.5.2-253a. Further, as described in Subsection 3JJ.7, similar sensitivity analyses performed in a manner consistent with the sensitivity analyses of this section demonstrate that the increase in the NI and FAR control point horizon horizontal design response spectra remain enveloped by RG 1.60 spectrum values that define the FIRS for these facilities. Therefore, the GMRS presented in Subsection 2.5.2.6.2 remains an adequate characterization of the free field site-specific ground motion.

2.5.2.7 References

201. Abe, K., *Complements to Magnitudes of Large Shallow Earthquakes from 1904 to 1980*, Physics of the Earth and Planetary Interiors, Vol. 34, No. 1-2, pp. 17–23, 1984.

202. Abe, K., *Magnitudes of Large Shallow Earthquakes from 1904 to 1980*, Physics of the Earth and Planetary Interiors, Vol. 27, No. 1, pp. 72–92, 1981.

203. Abrahamson, N. and J. Bommer, *Program on Technology Innovation: Truncation of the Lognormal Distribution and Value of the Standard Deviation for Ground Motion Models in the Central and Eastern United States*, EPRI TR-1014381, Electric Power Research Institute, August 2006.

204. Advanced National Seismic System, *ANSS/CNSS Worldwide Earthquake Catalog*. Available at http://www.ncedc.org/anss/catalogsearch.html, accessed February 14, 2008.

205. Alvarez, L., T. Chuy, J. García, B. Moreno, H. Alvarez, M. Blanco, O. Expósito, O. González, and A. Fernández, *An Earthquake Catalogue of Cuba and Neighboring Areas*, internal report from the United Nations Educational, Scientific and Cultural Organization, International Atomic Energy Agency, and The Abdus Salam International Centre for Theoretical Physics, Trieste, Italy, January 1999.

206. American Society of Civil Engineers, *Seismic Analysis of Safety-Related Nuclear Structures and Commentary*, ASCE 4-98, 2000.

207. Amick, D., R. Gelinas, G. Maurath, R. Cannon, D. Moore, E. Billington, and H. Kemppinen, *Paleoliquefaction Features along the Atlantic Seaboard*, U.S. NRC Report, NUREG/CR-5613, 1990.

208. Amick, D., G. Maurath, and R. Gelinas, *Characteristics of Seismically Induced Liquefaction Sites and Features Located in the Vicinity of the 1886 Charleston, South Carolina Earthquake,* Seismological Research Letters, Vol. 61, No. 2, pp. 117–130, 1990.

209. Anderson, J. and S. Hough, *A Model for the Shape of the Fourier Amplitude Spectrum of Acceleration at High Frequencies*, Bulletin of the Seismological Society of America, Vol. 74, 1969–1993, 1984.

210. Atkinson, G. and D. Boore, *Ground-Motion Relations for Eastern North America*, Bulletin of the Seismological Society of America, Vol. 85, No. 1, pp. 17–30, 1995.

211. Bakun, W. and M. Hopper, *Magnitudes and Locations of the 1811–1812 New Madrid, Missouri, and the 1886 Charleston, South Carolina, Earthquakes*, Bulletin of the Seismological Society of America, Vol. 94, No. 1, pp. 64–75, 2004.

212. Not Used.

213. Behrendt, J. and A. Yuan, *The Helena Banks Strike-Slip (?) Fault Zone in the Charleston, South Carolina Earthquake Area: Results from a Marine, High-Resolution, Multichannel, Seismic-Reflection Survey*, Geological Society of America Bulletin, Vol. 98, pp. 591–601, 1987.

214. Bollinger, G., M. Chapman, M. Sibol, and J. Costain, *An Analysis of Earthquake Focal Depths in the Southeastern U.S.*, Geophysical Research Letters, Vol. 12, No. 11, pp. 785–788, 1985.

215. Bollinger, G., A. Johnston, P. Talwani, L. Long, K. Shedlock, M. Sibol, and M. Chapman, *Seismicity of the Southeastern United States; 1698–1986*, D. Slemmons, E. Engdahl, M. Zoback, and D. Blackwell, (eds.), Neotectonics of North America, Decade Map Volume to Accompany the Neotectonic Maps, Geological Society of America, 1991.

216. Bollinger, G., *Reinterpretation of the Intensity Data for the 1886 Charleston, South Carolina, Earthquake: in Studies Related to the Charleston, South Carolina, Earthquake of 1886 — A Preliminary Report*, U.S. Geological Survey, Professional Paper 1028, pp. 17–32, 1977.

217. Bollinger, G., *Specification of Source Zones, Recurrence Rates, Focal Depths, and Maximum Magnitudes for Earthquakes Affecting the Savannah River Site in South Carolina*, U.S. Geological Survey, Bulletin 2017, 1992.

218. Boore, D., *SMSIM — Fortran Programs for Simulating Ground Motions from Earthquakes Version. 2.3 — A Revision of OFR 96-80-A*, U.S. Geological Survey, Open-File Report 00-509, 2005.

219. Building Seismic Safety Council, *NEHRP Recommended Provisions and Commentary for Seismic Regulations for New Buildings and Other Structures*, 2003 ed. (FEMA 450), p. 752, 2004.

220. Calais, E., Y. Mazabraud, B. Mercier de Lepinay, and P. Mann, *Strain Partitioning and Fault Slip Rates in the Northeastern Caribbean from GPS Measurements*, Geophysical Research Letters, Vol. 29, pp. 1856–1859, 2002.

221. Not Used.

222. Calais, E. and B. Mercier de Lepinay, *Strike-Slip Tectonics and Seismicity along the Northern Caribbean Plate Boundary from Cuba to Hispaniola*, J. Dolan and P. Mann (eds.), Active Strike-Slip and Collisional Tectonics of the Northern Caribbean Plate Boundary Zone, Geological Society of America, Special Paper 326, pp. 125–141, 1998.

223. Chapman, M. and P. Talwani, *Seismic Hazard Mapping for Bridge and Highway Design in South Carolina*, South Carolina Department of Transportation Report, 2002.

224. Cornell, C., *Engineering Seismic Risk Analysis*, Bulletin of the Seismological Society of America, Vol. 58, No. 5, pp. 1583–1606, 1968.

225. Cornell, C. and S. Winterstein, *Temporal and Magnitude Dependence in Earthquake Recurrence Models*, Bulletin of the Seismological Society of America, Vol. 79, pp. 1522–1537, 1988.

226. Cotilla-Rodríguez, M., H. Franzke, and D. Cordoba Barba, *Seismicity and Seismoactive Faults of Cuba*, Russian Geology and Geophysics, Vol. 48, pp. 505–522, 2007.

227. Cramer, C., *A Seismic Hazard Uncertainty Analysis for the New Madrid Seismic Zone*, Engineering Geology, Vol. 62, pp. 251–266, 2001.

228. Dellinger, J., J. Dewey, J. Blum, and M. Nettles, *Relocating and Characterizing the 10 Feb 2006 Green Canyon Gulf of Mexico Earthquake Using Oil-Industry Data*, Eos, Transactions, Vol. 88, No. 52, Fall Meeting Supplement, Abstract S13F-01, 2007.

229. DeMets, C. and M. Wiggins-Grandison, *Deformation of Jamaica and Motion of the Gonave Microplate from GPS and Seismic Data*, Geophysical Journal International, Vol. 168, pp. 362–378, 2007.

230. DeMets, C., P. Jansma, G. Mattioli, T. Dixon, F. Farina, R. Bilham, E. Calais, and P. Mann, *GPS Geodetic Constraints on Caribbean-North America Plate Motion*, Geophysical Research Letters, Vol. 27, pp. 437–440, 2000.

231. Perez-Othon, J. and V. Yarmoliuk, (eds), Geologic Map of the Republic of Cuba, (Mapa Geológico de Republica de Cuba), 1:500,000 scale (5 sheets), Ministry of Basic Industry, Center for Geologic Investigations, 1985.

232. Der Kiureghian, A., *Structural Response to Stationary Excitation*, Journal of the Engineering Mechanics Division ASCE, Vol. 106, No. EM6, pp. 1195–1213, December 1980.

233. Pushcharovskiy, Y., M. Borkowska, G. Hamor, J. Suarez, I. Velinov, (eds), Geologic Map of the Republic of Cuba, (Mapa Geológico de Cuba), 1:250,000 scale (40 sheets), Academy of Sciences of Cuba, Institute of Geology and Paleontology, 1988 (based on geologic information current through 1985).

234. Pushcharovskiy, Y. (ed.), Tectonic Map of the Republic of Cuba, (Mapa Tectonico de Cuba), 1:500,000 scale (4 sheets), 1987.

235. Frankel, A., S. Harmsen, C. Mueller, E. Calais, and J. Haase, *Documentation for Initial Seismic Hazard Maps for Haiti*, U.S. Geological Survey, Open-File Report 2010–1067, p. 12, 2010.

236. Dolan, J. and D. Wald, *The 1943-1953 North-Central Caribbean Earthquakes: Active Tectonic Setting, Seismic Hazards, and Implications for Caribbean-North American Plate Motions*, J. Dolan and P. Mann (eds.), Active Strike Slip and Collisional Tectonics of the Northern Caribbean Plate Boundary Zone, Geological Society of America, Special Paper 326, pp. 143–169, 1998.

237. Alvarez, L., R. Mijailova, E. Vorobiova, T. Chuy, G. Zhakirzhanova, E. Perez, L. Rodionova, H. Alvarez, and K. Mirzoev, *Terremotos de Cuba y Area Aledanas*, Internal Report, Fondos del CENAIS, pp. 1–78, 1990.

238. U.S. Geological Survey, USGS Earthquake Hazards Program: Significant Earthquakes of the World 2010, January 12 Haiti Region record. Available at http://earthquake.usgs.gov/earthquakes/eqarchives/significant/sig_2010.php, accessed April 28, 2010.

239. Dewey, J. and J. Dellinger, *Location of the Green Canyon (Offshore Southern Louisiana) Seismic Event of February 10, 2006*, U.S. Geological Survey, Open-File Report 2008-1184, p. 30, 2008.

240. Ekstrom, G. and A. Dziewonski, *Evidence of Bias in Estimations of Earthquakes Size*, Nature, Vol. 332, pp. 319–323, 1988.

241. Electric Power Research Institute and U.S. Department of Energy, *Program on Technology Innovation: Assessment of a Performance-Based Approach for Determining Seismic Ground Motions for New Plant Sites*, Vol. 2, Seismic Hazard Results at 28 Sites, Final Report, EPRI Report TR-1012045, August 2005.

242. Electric Power Research Institute, *CEUS Ground Motion Project Final Report*, EPRI Report TR-1009684, December 2004.

243. Electric Power Research Institute, *EQHAZARD Primer*, prepared by Risk Engineering for Seismicity Owners Group and Electric Power Research Institute, EPRI Report NP-6452-D, June 1989.

244. Electric Power Research Institute, *Guidelines for Determining Design Basis Ground Motions*, Vol. 1–5, EPRI Report TR-102293, November 1993.

245. Electric Power Research Institute, *Probabilistic Seismic Hazard Evaluation at Nuclear Plant Sites in the Central and Eastern United States, Resolution of the Charleston Earthquake Issue*, EPRI Report NP-6395-D, 1989.

246. Electric Power Research Institute, *Seismic Hazard Methodology for the Central and Eastern United States*, Vol. 1, part 2, Methodology (Rev. 1), EPRI Report NP-4726-A, Rev. 1, 1988.

247. Electric Power Research Institute, *Seismic Hazard Methodology for the Central and Eastern United States*, Vol. 5-10, Tectonic Interpretations, EPRI Report NP-4726, July 1986.

248. Ellsworth, W., M. Matthews, R. Nadeau, S. Nishenko, P. Reasenberg, and R. Simpson, *A Physically-Based Earthquake Recurrence Model for Estimation of Long-Term Earthquake Probabilities,* U.S. Geological Survey, Open-File Report 99-522, p. 22, 1999.

249. Engdahl, E., R. Hilst, and R. Buland, *Global Teleseismic Earthquake Relocation with Improved Travel Times and Procedures for Depth Procedures*, Bulletin of the Seismological Society of America, Vol. 88, No. 3, pp. 722–743, 1998.

250. Engdahl, E. and A. Villasenor, *Global Seismicity: 1900–1999, International Handbook of Earthquake & Engineering Seismology*, International Association of Seismology and Physics of the Earth's Interior, Academic Press, pp. 665–690, 2002.

251. Frankel, A., M. Petersen, C. Mueller, K. Haller, K.R. Wheeler, E. Leyendecker, R. Wesson, S. Harmsen, C. Cramer, D. Perkins, and K. Rukstales, *Documentation for the 2002 Update of the National Seismic Hazard Maps*, U.S. Geological Survey, Open-File Report 02-420, 2002.

252. Frankel, A., C. Mueller, T., Barnhard, D. Perkins, E. Leyendecker, N. Dickman, S. Hanson, and M. Hopper, *National Seismic-Hazard Maps; Documentation*, U.S. Geological Survey, Open-File Report 96-532, p. 110, 1996.

253. Frohlich, C. and S. Davis, *Texas Earthquakes*, pp. 240–255, 2002.

254. Garcia, J., D. Slejko, L. Alvarez, L. Peruzza, and A. Rebez, *Seismic Hazard Maps for Cuba and Surrounding Areas*, Bulletin of the Seismological Society of America, Vol. 93, No. 6, pp. 2563–2590, 2003.

255. Garcia, J., D. Slejko, A. Rebez, M. Santulin, and L. Alvarez, *Seismic Hazard Map for Cuba and Adjacent Areas Using the Spatially Smoothed Seismicity Approach*, Journal of Earthquake Engineering, Vol. 12, pp. 173–196. 2008.

256. Gardner, J. and L. Knopoff, *Is the Sequence of Earthquakes in Southern California, with Aftershocks Removed, Poissonian?* Bulletin of Seismological Society of America, Vol. 64, pp.1363–1367, 1974.

257. Geomatrix, *Seismic Design Mapping, State of Oregon*, Final report prepared for the Oregon Department of Transportation, Salem, Oregon, 1995.

258. Dunbar, J. and D. Sawyer, *Implications of Continental Crust Extension for Plate Reconstruction: An Example from the Gulf of Mexico*, Tectonics, Vol. 6, No. 6, pp. 739–755, 1987.

259. Gomberg, J. and L. Wolf, *Possible Cause for an Improbable Earthquake: the 1997 Mw 4.9 Southern Alabama Earthquake and Hydrocarbon Recovery*, Geology, Vol. 27, No. 4, pp. 367–370, 1999.

260. Pacific Disaster Center, *Haiti Earthquake Shake Map Overview*, January 12, 2010. Available at http://www.pdc.org/geodata/download/Haiti_eq_shakemap.pdf, accessed June 23, 2010.

261. Grant, L. and K. Sieh, *Paleoseismic Evidence of Clustered Earthquakes on the San Andreas Fault in the Carrizo Plain, California*, Journal of Geophysical Research, Vol. 99, No. B4, pp. 6819–6841, 1994.

262. Hanks, T. and W. Bakun, *A Bilinear Source-Scaling Model for M-log A Observations of Continental Earthquakes*, Bulletin of the Seismological Society of America, Vol. 92, No. 5, pp. 1841–1846, 2002.

263. Idriss, I. and J. Sun, *SHAKE91: A Computer Program for Conducting Equivalent Linear Seismic Response Analyses of Horizontally Layered Soil Deposits*, Department of Civil and Environmental Engineering, Center for Geotechnical Modeling, University of California, 1992.

264. Incorporated Research Institutions for Seismology, *Event Search*. Available at http://www.iris.edu/quakes/eventsrch.htm, accessed February 14, 2008.

265. International Seismological Centre, Bulletin, *United Kingdom*. Available at http://www.isc.ac.uk, accessed February 28, 2008.

266. Not Used.

267. Johnston, A., *Seismic Moment Assessment of Earthquakes in Stable Continental Regions — III. New Madrid 1811-1812, Charleston 1886 and Lisbon 1755*, Geophysical Journal International, Vol. 126, pp. 314–344, 1996.

268. Johnston, A., K. Coppersmith, L. Kanter, and C. Cornell, *The Earthquakes of Stable Continental Regions*, Vol. 1, Assessment of Large Earthquake Potential, Final Report, TR-102261-V1, EPRI, 1994.

269. Kanamori, H., *The Energy Release in Great Earthquakes*, Journal of Geophysical Research, Vol. 82, No. 20, pp. 2981–2987, 1977.

270. Not Used.

271. Not Used.

272. Madabhushi, S. and P. Talwani, *Fault Plane Solutions and Relocations of Recent Earthquakes in Middleton Place-Summerville Seismic Zone near Charleston, South Carolina*, Bulletin of the Seismological Society of America, Vol. 83, No. 5, pp. 1442–1466, 1993.

273. Manaker, D., E. Calais, A. Freed, S. Ali, P. Przybylski, G. Mattioli, and P. Jansma, *Interseismic Plate Coupling and Strain Partitioning in the Northeastern Caribbean*, Geophysical Journal International, in press 2008.

274. Not Used.

275. Not Used.

276. Mann, P., F. Taylor, R. Edwards, and T. Ku, *Actively Evolving Microplate Formation by Oblique Collision and Sideways Motion Along Strike-Slip Faults: an Example from the Northeastern Caribbean Plate Margin*, Tectonophysics, Vol. 246, pp. 1–69, 1995.

277. Not Used.

278. Marple, R. and P. Talwani, *Evidence for a Buried Fault System in the Coastal Plain of the Carolinas and Virginia-Implications for Neotectonics in the Southeastern United States*, Geological Society of America Bulletin, Vol. 112, No. 2, pp. 200–220, 2000.

279. Martin, J. and G. Clough, *Seismic Parameters from Liquefaction Evidence*, Journal of Geotechnical Engineering Vol. 120, No. 8, pp. 1345–1361, 1994.

280. Matthews, M., W. Ellsworth, and P. Reasenberg, *A Brownian Model for Recurrent Earthquakes*, Bulletin of the Seismological Society of America, Vol. 92, pp. 2233–2250, 2002.

281. Not Used.

282. McCann, W., *Estimating The Threat of Tsunamigenic Earthquakes and Earthquake Induced Landslide Tsunami the Caribbean*, Caribbean Tsunami Hazard, Proceedings of the National Science Foundation Caribbean Tsunami Workshop, March 2004, pp.43–65, World Scientific Publishing Co., Singapore, 2006.

283. Not Used.

284. Middle America Seismograph Consortium, *MIDAS Catalog*. Available at http://midas.uprm.edu, accessed January 22, 2008.

285. Not Used.

286. Not Used.

287. Motazedian, D. and G. Atkinson, *Ground-Motion Relations for Puerto Rico*, Geological Society of America, Special Paper 385, pp. 61–80, 2005.

288. National Earthquake Information Center, *Eastern, Central, and Mountain States of the United States, 1350–1986 (SRA)*, Earthquake Search. Available at http://neic.usgs.gov/neis/epic/epic_rect.html, accessed February 14, 2008.

289. National Earthquake Information Center, *NEIC Mexico, Central America and Caribbean, 1900–1979 (MCAC),* Earthquake Search. Available at http://neic.usgs.gov/neis/epic/epic_rect.html, accessed February 14, 2008.

290. National Earthquake Information Center, *Information Regarding Technical and Scientific Information on the September 10, 2006 Earthquake in the Gulf of Mexico*. Available at http://earthquake.usgs.gov/eqcenter/eqinthenews/2006/usslav/#scitech, accessed September 13, 2006.

291. National Earthquake Information Center, *PDE-W Earthquake Summary for 10 February 2006 041717 Event*, U.S. Geological Survey. Available at http://neic.usgs.gov/cgi-bin/epic/epic.cgi?SEARCHMETHOD=2&CLAT=0.0&CLON=0.0&CRAD=0.0&FILEFORMAT=1&SEARCHRANGE=HH&SLAT2=28&SLAT1=27&SLON2=-90&SLON1=-91&SUBMIT=Submit+Search&SYEAR=&SMONTH=&SDAY=&EYEAR=&EMONTH=&EDAY=&LMAG=&UMAG=&NDEP1=&NDEP2=&IO1=&IO2, accessed August 23, 2007.

292. National Earthquake Information Center, *Preliminary Determination of Epicenter (PDE)*. Available at http://neic.usgs.gov/neis/epic/code_catalog.html, accessed February 14, 2008.

293. Nettles, M., *Analysis of the 10 February 2006 Gulf of Mexico Earthquake from Global and Regional Seismic Data*, 2007 Offshore Technology Conference: Houston, Texas, p. OTC 19099, 2007.

294. NIST/SEMATECH, *E-Handbook of Statistical Methods*. Available at http://www.itl.nist.gov/div898/handbook/, accessed January 11, 2006.

295. Obermeier, S., R. Weems, R. Jacobson, and G. Gohn, *Liquefaction Evidence for Repeated Holocene Earthquakes in the Coastal Region of South Carolina*, Annals of the New York Academy of Sciences, Vol. 558, pp. 183–195, 1989.

296. Obermeier, S., *Liquefaction-Induced Features*, J. McCalpin (ed.), Paleoseismology, Academic Press, San Diego, 1996.

297. Not Used.

298. Perez, O., *Revised World Seismicity Catalog (1950-1997) for Strong (Ms > 6) Shallow (H < 70 Km) Earthquakes*, Bulletin of the Seismological Society of America, Vol. 89, No. 2, pp. 335–341, 1999.

299. Perrot, J., E. Calais, and B. Mercier de Lepinay, *Tectonic and Kinematic Regime along the Northern Caribbean Plate Boundary: New Insights from Broad-Band Modeling of the May 25, 1992, MS = 6.9 Cabo Cruz, Cuba, Earthquake*, Pure and Applied Geophysics, Vol. 149, pp. 475–487, 1997.

300. Petersen, M., A. Frankel, S. Harmsen, C. Mueller, K. Haller, R. Wheeler, R. Wesson, Y. Zeng, O. Boyd, D. Perkins, N. Luco, E. Field, C. Wills, and K. Rukstales, *Documentation for the 2008 Update of the National Seismic Hazard Maps*, U.S. Geological Survey, Open-File Report 2008-1128, 2008.

301. Not Used.

302. Not Used.

303. Not Used.

304. Prentice, C., P. Mann, L. Pea, and G. Burr, *Slip Rate and Earthquake Recurrence along the Central Septentrional Fault, North American-Caribbean Plate Boundary, Dominican Republic*, Journal of Geophysical Research, Vol. 108, No. B3, 2003.

305. Puerto Rico Seismic Network, Available at http://temblor.uprm.edu/cgi-bin/new-search.cgi, accessed February 8, 2008.

306. Rathje, E. and C. Ozbey, *Site-Specific Validation of Random Vibration Theory-Based Seismic Site Response Analysis*, Journal of Geotechnical and Geoenvironmental Engineering, Vol. 132, No. 7, pp. 911–922, July 2006.

307. National Geophysical Data Center. The Seismicity Catalog CD-ROM Collection: Volume 1: North America, 1492–1996 A.D., Volume 2: Global and Regional, 2150 B.C.–1996 A.D., National Oceanic and Atmospheric Administration/National Geophysical Data Center, World Data Center-A Solid Earth Geophysics, 325 Broadway, E/GC1, Boulder, Colorado, 2 volume CD-ROM, 1996. Available at http://www.ngdc.noaa.gov/hazard/fliers/se-0208.shtml.

308. Risk Engineering, Inc., *Technical Basis for Revision of Regulatory Guidance on Design Ground Motions: Hazard- and Risk-Consistent Ground Motion Spectra Guidelines*, NUREG/CR-6728, U.S. NRC, Washington, D.C., 2001.

309. Rockwell, T., S. Lindvall, M. Herzberg, D. Murbach, T. Dawson, and G. Berger, *Paleoseismology of the Johnson Valley, Kickapoo, and Homestead Valley Faults: Clustering of Earthquakes in the Eastern California Shear Zone*, Bulletin of the Seismological Society of America, Vol. 90, No. 5, pp. 1200–1236, 2000.

310. Rosencrantz, E. and P. Mann, *SeaMARC II Mapping of Transform Faults in the Cayman Trough, Caribbean Sea*, Geology, Vol. 19, pp. 690–693, 1991.

311. Not Used.

312. Not Used.

313. Savage, J., *Criticism of Some Forecasts of the National Earthquake Evaluation Council*, Bulletin of the Seismological Society of America, Vol. 81, No. 3, pp. 862–881, 1991.

314. Savage, M. and M. Depolo, *Foreshock Probabilities in the Western Great-Basin Eastern Sierra Nevada*, Bulletin of Seismological Society of America, Vol. 83, pp.1910–1938, 1993.

315. Sawyer, D., R. Buffler, and R. Pilger, Jr., *The Crust Under the Gulf of Mexico Basin*, The Geology of North America, Vol. J, The Gulf of Mexico Basin, The Geological Society of America, pp. 53–72, 1991.

316. Schnabel, S. and H. Seed, *Shake — A Computer Program for Earthquake Response Analysis of Horizontally Layered Sites*, Report No. 72-12, Earthquake Engineering Research Center, December 1972.

317. Seed, H., R. Wong, I. driss, and K. Tokimatsu, *Moduli and Damping Factors for Dynamic Analysis of Cohesionless Soils*, Journal of Soil Mechanics and Foundations Division, Vol. SM11, No. 112, pp. 1016–1032, ASCE, 1986.

318. Senior Seismic Hazard Analysis Committee, *Recommendations for Probabilistic Seismic Hazard Analysis — Guidance on Uncertainty and Use of Experts*, Prepared by SSHAC, NUREG/CR-6372, 1997.

319. Silva, W., N. Abrahamson, G. Toro, and C. Costantino, *Probabilistic Models of Site Velocity Profiles for Generic and Site-Specific Ground Motion Amplification Studies,* (appendix), Description and Validation of the Stochastic Ground Motion Model, Associated Universities, Inc., Upton, New York. Report submitted to Brookhaven National Laboratory, Contract No. 770573, 1996.

320. Silva, W., N. Abrahamson, G. Toro, and C. Costantino, *Recommendations for Uncertainty Estimates in Shear Modulus Reduction and Hysteretic Damping Relationships,* (appendix), Description and Validation of the Stochastic Ground Motion Model, 1996.

321. Cotilla-Rodríguez, M., *An Overview on the Seismicity of Cuba*, Journal of Seismology, Vol. 2, pp. 323–335, 1998.

322. Not Used.

323. Talwani, P. and W. Schaeffer, *Recurrence Rates of Large Earthquakes in the South Carolina Coastal Plain Based on Paleoliquefaction Data*, Journal of Geophysical Research, Vol. 106, No. B4, pp. 6621–6642, 2001.

324. Tarr, A., P. Talwani, S. Rhea, D. Carver, and D. Amick, *Results of Recent South Carolina Seismological Studies*, Bulletin of the Seismological Society of America, Vol. 71, No. 6, pp. 1883–1902, 1981.

325. Tarr, A. and B. Rhea, *Seismicity Near Charleston, South Carolina, March 1973 to December 1979*, Studies Related to the Charleston, South Carolina Earthquake of 1886 Tectonics and Seismicity, U.S. Geological Survey, Professional Paper 1313:R1-R17, 1983.

326. ten Brink, U., D. Coleman, and W. Dillon, *The Nature of the Crust under Cayman Trough from Gravity, Marine and Petroleum Geology*, Vol. 19, pp. 971–987, 2002.

327. Toiran, B., *The Crustal Structure of Cuba Derived from Receiver Function Analysis*, Journal of Seismology, Vol. 7, pp. 359–375, 2003.

328. Tuttle, M., *The Use of Liquefaction Features in Paleoseismology: Lessons Learned in the New Madrid Seismic Zone, Central United States*, Journal of Seismology, Vol. 5, pp. 361–380, 2001.

329. Not Used.

330. U.S. Geological Survey, *Preliminary Earthquake Report Magnitude 6.0 —Gulf of Mexico,* 2006 September 10 14:56:07 UTC. Available at http://earthquake.usgs.gov/eqcenter/eqinthenews/2006/usslav/index.php, accessed May 4, 2007.

331. Van Dusen, S. and D. Doser, *Faulting Processes of Historic (1917–1962) M 6.0 Earthquakes along the North-Central Caribbean Margin*, Pure and Applied Geophysics, Vol. 157, pp. 719–736, 2000.

332. Villasenor, A. and E. Engdahl, *Systematic Relocation of Early Instrumental Seismicity: Earthquakes in the International Seismological Summary for 1960-1963*, Bulletin of the Seismological Society of America, Vol. 97, No. 6, pp. 1820–1832, December 2007.

333. Villasenor, A., E. Bergman, T. Boyd, E. Engdahl, D. Frazier, M. Harden, J. Orth, R. Parkes, and K. Shedlock, *Toward a Comprehensive Catalog of Global Historical Seismicity, Eos*, Transactions, Vol. 78, No. 50, 1997.

334. Wells, D. and K. Coppersmith, *New Empirical Relationships Among Magnitude, Rupture Length, Rupture Width, Rupture Area, and Surface Displacement*, Bulletin of the Seismological Society of America, Vol. 84, No. 4, pp. 974–1002, 1994.

335. Not Used.

336. Working Group on California Earthquake Probabilities, *Seismic Hazards in Southern California: Probable Earthquakes, 1994 to 2024*, Bulletin of the Seismological Society of America, Vol. 85, pp. 379–439, 1995.

337. Working Group on California Earthquake Probabilities, *Earthquake Probabilities in the San Francisco Bay Region: 2002-2031*, U.S. Geological Survey, Open-File Report 03-2134, 2003.

338. Wysession, M., J. Wilson, L. Bartko, and R. Sakata, *Intraplate Seismicity in the Atlantic Ocean Basin: A Teleseismic Catalog,* Bulletin of Seismological Society of America, Vol. 85, No. 3, pp. 755–774, June 1995.

339. Wyss, M., *Estimating Maximum Expectable Magnitude of Earthquakes from Fault Dimensions*, Geology, Vol. 7, No. 7, pp. 366–340, 1979.

340. National Earthquake Information Center, *Significant U.S. Earthquakes, 1568-1989 (USHIS),* Earthquake Search. Available at http://neic.usgs.gov/neis/epic/epic_rect.html, accessed February 14, 2008.

341. Chapman, M., E. Mathena, and J. Snoke (eds.), January 1, 2004–December 31, 2004, Southeastern United States Seismic Network Bulletin, No. 39, June 2006.

342. Silva, W., N. Gregor, and R. Darragh, *Development of Regional Hard Rock Attenuation Relations For Central and Eastern North America, Mid-Continent and Gulf Coast Areas*, Pacific Engineering. Available at http://www.pacificengineering.org/gulf/Development%20ENA%20Midcontinent%20Gulf.pdf, accessed August 13, 2010.

343. Chen, S. and G. Atkinson, *Global Comparisons of Earthquake Source Spectra,* Bulletin of the Seismological Society of America, Vol. 92, No. 3, pp. 885–895, 2002.

344. Chiou, B., R. Darragh, N. Gregor, and W. Silva, *NGA Project Strong-Motion Database*, Earthquake Spectra, Vol. 24, pp. 23–44, 2008.

345. Gutenberg, B. and C. Richter, *Earthquake Magnitude, Intensity, Energy and Acceleration*, Bulletin of the Seismology Society of America, Vol. 46, pp. 105–145, 1956.

346. Heaton, T., F. Tajima, and A. Mori, *Estimating Ground Motions Using Recorded Accelerograms,* Surveys in Geophysics, Vol. 8, pp. 25–83, 1986.

347. Kanamori, H., *Magnitude Scale and Quantification of Earthquakes,* S. Duda and K. Aki (eds), Quantification of Earthquakes, Tectonophysics, Vol. 93, pp. 185–199, 1983.

348. Lahr, J., HYPOELLIPSE: a Computer Program for Determining Local Earthquake Hypocentral Parameters, Magnitude, and First-Motion Pattern: U.S. Geology Survey, Open-File Report 99-23, Ver. 1, 1999.

349. Lamarre, M. and H. Shah, *Seismic Hazard Evaluation for Sites in California: Development of an Expert System*, Report No. 85, 1988.

350. Mueller, C., M. Hopper, and A. Frankel, Preparation of Earthquake Catalogs for the National Seismic Hazard Maps-Contiguous 48 States: U.S. Geological Survey, Open-File Report 97-464, 1997.

351. Nutti, I. and R. Hermann, *Earthquake Magnitude Scales*, J. Geotech, Eng. Div. ASCE, Vol. 108, pp. 783–786, 1982.

352. Wiggins-Grandison, M., *Preliminary Results from the New Jamaica Seismograph Network*. Seismological Research Letters, Vol. 72, pp. 525–537, 2001.

353. Electric Power Research Institute, U.S. DOE, and U.S. NRC, *Technical Report: Central and Eastern United States Seismic Source Characterization for Nuclear Facilities*, published as NUREG-2115 by the U.S. NRC, 2012.

354. Progress Energy, Letter NPD-NRC-2012-029 to the U.S. Nuclear Regulatory Commission, Levy Nuclear Plant, Units 1 and 2, Docket Nos. 52-029 and 52-030 Supplement 2 To Response To NRC RAI Letter 108 — *Implementation of Fukushima Near-Term Task Force Recommendations,* NRC ADAMS Accession No. ML12258A469, August 1, 2012.

355. Van Buren, H., and H. Mullins, *Seismic Stratigraphy and Geologic Development of an Open-Ocean Carbonate Slope: the Northern Margin of Little Bahama Bank, Initial Reports of Deep Sea Drilling Project,* Vol. 76, pp. 749–762, 1983.

356. Youngs, R. and K. Coppersmith, *Implications of Fault Slip Rates and Earthquake Recurrence Models to Probabilistic Seismic Hazard Estimates*, Bulletin of the Seismological Society of Americas, Vol. 75, No. 4, pp. 939–964, 1985.

357. Atkinson, G. and W. Silva, *Stochastic Modeling of California Ground Motions*, Bulletin of the Seismological Society of America, Vol. 90, No. 2, pp. 255–274, 2000.

358. Atkinson, G. and D. Boore, *Empirical Ground Motion Relation for Subduction Zone Earthquakes and their Application to Cascadia and other Regions,* Bulletin of the Seismological Society of America, Vol. 93, No. 4, pp. 1703–1729, 2003.

359. Atkinson, G. and D. Boore, *Modifications to Existing Ground-Motion Prediction Equations in Light of New Data*, Bulletin of the Seismological Society of America, Vol. 101, No. 3, pp. 1121–1135, 2011.

360. Boore, D. and G. Atkinson, *Boore-Atkinson NGA Ground Motion Relations for the Geometric Mean Horizontal Component of Peak and Spectral Ground Motion Parameters*, Pacific Earthquake Engineering Research Center, PEER Report 2007/01, University of California, Berkeley, May 2007.

361. Richards, J., *Central and Eastern United States Seismic Source Characterization (CEUS SSC) for Nuclear Facilities*, EPRI Report Number 1021097, Letter to Utility Seismic Hazard and GMRS Contacts,RSM-111414-090, December 1, 2014.

362. Masaferro, J., J. Poblet, M. Bulnes, G. Eberli, T. Dixon, and K. McClay, *Palaeogene-Neogene/Present Day(?) Growth Folding in the Bahamian Foreland of the Cuban Fold and Thrust Belt*, Journal of the Geological Society, Vol. 156, pp. 617–631, 1999.

363. Masaferro, J., M. Bulnes, J. Poblet, and G. Eberli, *Episodic Folding Inferred from Syntectonic Carbonate Sedimentation: the Santaren Anticline, Bahamas Foreland*, Sedimentary Geology, Vol. 146, No. 1-2, pp. 11–24, 2002.

Table 2.5.2-201 (Sheet 1 of 24)
Earthquake Catalog for the Phase 1 Investigation Region [22°N to 35°N, 100°W to 65°W] for which the Events are Rmb Magnitude Greater than or Equal to 3.0 or Intensity [Int] Greater than or Equal to IV(4)

Catalog Reference[a]	Year	Month	Day	Hour	Min	Sec	Lat	Lon	Depth (km)	Int	Emb	Smb	Rmb	Epicenter (km)[b]
SEUSN	1698	3	5	0	0	00.00	32.900	–80.000	0	3	2.70	0.56	3.06	828
SEUSN	1699	12	25	19	0	00.00	34.900	–90.300	0	4	3.10	0.56	3.46	1421
SEUSN	1754	5	19	16	0	00.00	32.900	–80.000	0	3	2.70	0.56	3.06	828
SEUSN	1755	11	0	0	0	00.00	33.400	–79.300	0	3	2.70	0.56	3.06	888
SEUSN	1757	2	7	0	0	00.00	32.900	–80.000	0	3	2.70	0.56	3.06	828
CUBA	1762	11	13	0	0	00.00	22.980	–82.370	10	—	3.97	0.56	4.33	339
CUBA	1777	7	7	9	29	00.00	22.830	–82.030	10	—	4.41	0.56	4.77	333
EPRIm	1780	2	6	0	0	00.00	30.400	–87.200	0	6	4.30	0.55	4.65	869
EPRIm	1799	4	4	0	0	00.00	32.900	–80.000	0	5	3.70	0.56	4.06	828
CUBA	1810	0	0	0	0	00.00	23.130	–82.400	10	—	3.97	0.56	4.33	328
CUBA	1812	0	0	0	0	00.00	23.050	–81.580	10	—	3.97	0.56	4.33	290
EPRIm	1820	9	3	8	30	00.00	33.400	–79.300	0	4	3.11	0.56	3.47	888
CUBA	1824	0	0	0	0	00.00	22.810	–80.080	10	—	3.97	0.56	4.33	289
SEUSN	1843	2	7	15	0	00.00	32.900	–80.000	0	3	2.70	0.56	3.06	828
CUBA	1843	2	21	0	0	00.00	23.130	–82.400	10	—	4.41	0.56	4.77	328
CUBA	1843	3	5	0	0	00.00	23.050	–81.580	10	—	3.53	0.56	3.89	290
SEUSN	1843	4	11	0	0	00.00	34.200	–80.600	0	3	2.70	0.56	3.06	972
CUBA	1846	10	10	0	0	00.00	23.000	–82.080	10	—	3.75	0.56	4.11	320
FD02	1847	2	14	2	0	00.00	29.600	–98.000	0	5	3.60	0.56	3.96	>1609
CUBA	1849	0	0	0	0	00.00	22.710	–83.060	15	—	4.12	0.56	4.48	407
CUBA	1849	8	30	0	0	00.00	22.150	–80.450	10	—	3.97	0.56	4.33	361
CUBA	1852	0	0	0	0	00.00	23.050	–81.580	10	—	4.41	0.56	4.77	290
CUBA	1852	7	7	14	59	00.00	22.420	–79.970	10	—	3.97	0.56	4.33	333
EPRIm	1853	5	20	0	0	00.00	34.000	–81.200	0	6	4.30	0.55	4.65	953
CUBA	1854	9	9	0	0	00.00	23.050	–81.580	10	—	4.41	0.56	4.77	290
CUBA	1857	7	7	0	0	00.00	22.810	–80.080	10	—	3.75	0.56	4.11	289
EPRIm	1857	12	19	14	4	00.00	32.900	–80.000	0	5	3.70	0.56	4.06	828
CUBA	1858	3	7	12	29	00.00	22.480	–79.550	10	—	4.26	0.56	4.62	334
CUBA	1858	8	14	6	29	00.00	22.480	–79.550	10	—	4.26	0.56	4.62	334

Table 2.5.2-201 (Sheet 2 of 24)
Earthquake Catalog for the Phase 1 Investigation Region [22°N to 35°N, 100°W to 65°W] for which the Events are Rmb Magnitude Greater than or Equal to 3.0 or Intensity [Int] Greater than or Equal to IV(4)

Catalog Reference[a]	Year	Month	Day	Hour	Min	Sec	Lat	Lon	Depth (km)	Int	Emb	Smb	Rmb	Epicenter (km)[b]
CUBA	1859	8	15	2	59	00.00	22.480	–79.550	10	—	3.97	0.56	4.33	334
CUBA	1859	10	4	0	0	00.00	23.130	–82.400	10	—	3.97	0.56	4.33	328
EPRIm	1860	1	19	23	0	00.00	32.900	–80.000	0	5	3.70	0.56	4.06	828
SEUSN	1860	10	0	0	0	00.00	32.900	–80.000	0	3	2.70	0.56	3.06	828
SEUSN	1860	10	22	0	0	00.00	34.200	–82.400	0	3	2.70	0.56	3.06	992
SEUSN	1860	12	19	0	0	00.00	32.900	–80.000	0	3	2.70	0.56	3.06	828
CUBA	1861	5	27	13	59	00.00	22.810	–80.080	10	—	3.75	0.56	4.11	289
CUBA	1861	6	27	0	0	00.00	22.810	–80.080	10	—	4.48	0.56	4.84	289
CUBA	1862	0	0	0	0	00.00	23.130	–82.400	10	—	3.53	0.56	3.89	328
CUBA	1862	8	0	0	0	00.00	23.130	–82.400	10	—	3.53	0.56	3.89	328
CUBA	1868	3	25	0	0	00.00	23.130	–82.400	10	—	4.41	0.56	4.77	328
CUBA	1868	5	1	0	0	00.00	22.360	–79.580	10	—	3.97	0.56	4.33	346
EPRIm	1869	0	0	0	0	00.00	32.900	–80.000	0	4	3.11	0.56	3.47	828
EPRIm	1871	4	16	5	0	00.00	34.300	–78.000	0	5	3.70	0.56	4.06	1008
CUBA	1872	0	0	0	0	00.00	22.910	–81.860	10	—	3.53	0.56	3.89	317
CUBA	1872	0	0	0	0	00.00	22.710	–83.060	15	—	3.68	0.56	4.04	407
CUBA	1872	6	0	0	0	00.00	22.510	–79.470	10	—	4.77	0.56	5.13	333
EPRIm	1872	6	17	20	0	00.00	33.100	–83.300	0	5	3.70	0.56	4.06	896
EPRIm	1873	5	1	4	30	00.00	30.200	–97.700	0	4	2.81	0.56	3.17	>1609
CUBA	1873	8	12	3	29	00.00	22.480	–79.550	10	—	4.99	0.56	5.35	334
SEUSN	1875	7	28	23	5	00.00	33.100	–83.300	0	3	2.70	0.56	3.06	896
EPRIm	1875	11	2	2	55	00.00	33.800	–82.500	0	6	4.30	0.55	4.65	950
SEUSN	1876	10	0	0	0	00.00	32.900	–80.000	0	3	2.70	0.56	3.06	828
EPRIm	1876	12	12	0	0	00.00	32.900	–80.000	0	4	3.11	0.56	3.47	828
EPRIm	1879	1	13	4	45	00.00	29.500	–82.000	0	6	4.30	0.55	4.65	479
CUBA	1879	9	21	0	0	00.00	22.710	–83.060	15	—	4.12	0.56	4.48	407
SEUSN	1879	10	27	1	0	00.00	34.400	–81.100	0	3	2.70	0.56	3.06	997
CUBA	1880	1	23	4	39	00.00	22.700	–83.000	15	—	6.09	0.56	6.45	404
CUBA	1880	6	12	1	29	00.00	22.420	–79.630	10	—	3.97	0.56	4.33	339
EPRIm	1882	1	8	22	10	00.00	34.600	–76.500	0	4	3.11	0.56	3.47	1081

Table 2.5.2-201 (Sheet 3 of 24)
Earthquake Catalog for the Phase 1 Investigation Region [22°N to 35°N, 100°W to 65°W] for which the Events are Rmb Magnitude Greater than or Equal to 3.0 or Intensity [Int] Greater than or Equal to IV(4)

Catalog Reference[a]	Year	Month	Day	Hour	Min	Sec	Lat	Lon	Depth (km)	Int	Emb	Smb	Rmb	Epicenter (km)[b]
EPRIm	1882	10	22	22	15	00.00	33.600	–95.600	0	8	5.39	0.28	5.48	>1609
EPRIm	1884	1	18	13	0	00.00	34.300	–78.000	0	5	3.70	0.56	4.06	1008
SEUSN	1884	3	31	10	0	00.00	33.100	–83.300	0	3	2.70	0.56	3.06	896
EPRIm	1885	10	17	22	30	00.00	33.000	–83.000	0	4	3.11	0.56	3.47	877
CUBA	1886	0	0	0	0	00.00	22.810	–80.080	10	—	3.97	0.56	4.33	289
EPRIm	1886	2	5	1	0	00.00	32.800	–88.000	0	5	3.70	0.56	4.06	1104
CUBA	1886	8	31	22	20	00.00	22.940	–80.010	15	—	4.48	0.56	4.84	276
EPRIm	1886	9	1	0	0	00.00	30.400	–81.700	0	4	3.11	0.56	3.47	565
EPRIm	1886	9	1	2	51	00.00	32.900	–80.000	0	X[c]	6.75	0.20	6.80	828
CUBA	1886	9	3	0	0	00.00	22.940	–80.010	15	—	4.19	0.56	4.55	276
CUBA	1887	0	0	0	0	00.00	22.900	–83.330	20	—	4.77	0.56	5.13	411
SEUSN	1887	1	5	17	57	00.00	30.150	–97.060	0	5	3.60	0.56	3.96	>1609
SEUSN	1887	1	31	22	14	00.00	30.530	–96.300	0	4	3.10	0.56	3.46	>1609
CUBA	1889	4	12	2	19	00.00	22.810	–80.080	10	—	3.97	0.56	4.33	289
EPRIm	1891	1	8	6	0	00.00	31.700	–95.200	0	7	3.70	0.30	3.80	1606
EPRIm	1891	10	13	5	55	00.00	32.900	–80.000	0	4	3.11	0.56	3.47	828
EPRIm	1893	6	21	7	7	00.00	30.400	–81.700	0	4	3.11	0.56	3.47	565
EPRIm	1893	7	5	8	10	00.00	32.900	–80.000	0	4	3.11	0.56	3.47	828
CUBA	1894	7	29	0	0	00.00	22.020	–75.840	15	—	4.19	0.56	4.55	590
EPRIm	1895	10	6	6	25	00.00	32.900	–80.000	0	4	3.11	0.56	3.47	828
CUBA	1896	0	0	0	0	00.00	22.750	–83.560	20	—	4.77	0.56	5.13	440
CUBA	1896	4	25	0	0	00.00	22.510	–79.470	10	—	4.55	0.56	4.92	333
SEUSN	1897	5	9	0	0	00.00	33.900	–81.600	0	3	2.70	0.56	3.06	946
EPRIm	1898	1	27	1	35	00.00	34.600	–90.600	0	4	3.11	0.56	3.47	1417
EPRIm	1899	3	10	5	45	00.00	32.900	–80.000	0	4	3.11	0.56	3.47	828
CUBA	1899	9	16	0	0	00.00	22.710	–83.060	15	—	4.12	0.56	4.48	407
SEUSN	1899	11	4	0	0	00.00	34.300	–82.800	0	3	2.70	0.56	3.06	1011
EPRIm	1899	12	4	12	48	00.00	32.900	–80.000	0	4	3.11	0.56	3.47	828
SEUSN	1899	12	19	0	0	00.00	34.300	–81.400	0	3	2.70	0.56	3.06	988
EPRIm	1900	10	31	16	15	00.00	30.400	–81.700	0	5	3.70	0.56	4.06	565

Table 2.5.2-201 (Sheet 4 of 24)
Earthquake Catalog for the Phase 1 Investigation Region [22°N to 35°N, 100°W to 65°W] for which the Events are Rmb Magnitude Greater than or Equal to 3.0 or Intensity [Int] Greater than or Equal to IV(4)

Catalog Reference[a]	Year	Month	Day	Hour	Min	Sec	Lat	Lon	Depth (km)	Int	Emb	Smb	Rmb	Epicenter (km)[b]
EPRIm	1901	12	2	0	26	00.00	32.900	–80.000	0	4	3.11	0.56	3.47	828
SEUSN	1902	6	10	0	0	00.00	34.200	–81.700	0	3	2.70	0.56	3.06	981
FD02	1902	10	9	19	0	00.00	30.100	–97.600	0	5	3.90	0.56	4.26	>1609
CUBA	1903	0	0	0	0	00.00	22.680	–81.110	18	—	4.70	0.56	5.06	312
EPRIm	1903	1	24	1	0	00.00	32.900	–80.000	0	4	3.11	0.56	3.47	828
SEUSN	1903	1	24	1	15	00.00	32.100	–81.100	0	6	4.10	0.56	4.46	742
CUBA	1905	0	0	0	0	00.00	22.750	–83.700	20	—	4.26	0.56	4.62	450
EPRIm	1905	2	3	0	0	00.00	30.500	–91.100	0	5	3.70	0.56	4.06	1194
SEUSN	1905	9	4	9	0	00.00	27.500	–82.600	0	3	2.70	0.56	3.06	321
CUBA	1905	10	12	0	0	00.00	23.050	–82.010	10	—	3.97	0.56	4.33	312
CUBA	1906	0	0	0	0	00.00	22.650	–83.200	15	—	3.53	0.56	3.89	421
CUBA	1906	1	15	0	0	00.00	22.600	–80.330	10	—	4.04	0.56	4.40	311
CUBA	1906	5	6	20	29	00.00	22.710	–83.060	15	—	3.68	0.56	4.04	407
CUBA	1906	5	8	0	0	00.00	22.710	–83.060	15	—	3.68	0.56	4.04	407
CUBA	1906	5	26	20	29	00.00	22.710	–83.060	15	—	3.68	0.56	4.04	407
CUBA	1906	6	5	5	59	00.00	22.880	–80.380	10	—	4.48	0.56	4.84	280
CUBA	1906	10	0	0	0	00.00	22.200	–84.090	20	—	4.12	0.56	4.48	521
CUBA	1907	2	19	0	0	00.00	23.130	–82.400	10	—	4.41	0.56	4.77	328
CUBA	1907	4	15	0	0	00.00	23.130	–82.400	10	—	3.97	0.56	4.33	328
EPRIm	1907	4	19	8	30	00.00	32.900	–80.000	0	5	3.70	0.56	4.06	828
CUBA	1908	1	0	0	0	00.00	22.480	–79.550	10	—	3.82	0.56	4.19	334
EPRIm	1909	10	8	10	0	00.00	34.900	–85.000	0	4	3.11	0.56	3.47	1142
CUBA	1910	0	0	0	0	00.00	22.630	–83.370	15	—	3.90	0.56	4.26	435
FD02	1910	5	8	17	18	00.00	30.100	–96.000	0	4	3.80	0.56	4.16	>1609
EPRIm	1911	3	31	16	57	00.00	34.000	–91.800	0	7	4.10	0.30	4.20	1458
EPRIm	1911	3	31	18	10	00.00	33.800	–92.200	0	4	3.70	0.30	3.80	1474
CUBA	1912	5	6	0	0	00.00	22.510	–79.690	10	—	3.97	0.56	4.33	328
EPRIm	1912	6	12	10	30	00.00	32.900	–80.000	0	7	4.90	0.56	5.26	828
EPRIm	1912	6	20	0	0	00.00	32.000	–81.000	0	5	3.70	0.56	4.06	730
EPRIm	1912	10	23	1	15	00.00	32.700	–83.500	0	4	3.11	0.56	3.47	861

Table 2.5.2-201 (Sheet 5 of 24)
Earthquake Catalog for the Phase 1 Investigation Region [22°N to 35°N, 100°W to 65°W] for which the Events are Rmb Magnitude Greater than or Equal to 3.0 or Intensity [Int] Greater than or Equal to IV(4)

Catalog Reference[a]	Year	Month	Day	Hour	Min	Sec	Lat	Lon	Depth (km)	Int	Emb	Smb	Rmb	Epicenter (km)[b]
CUBA	1913	0	0	0	0	00.00	22.340	–84.390	0	—	4.26	0.56	4.62	533
CUBA	1913	0	0	0	0	00.00	22.150	–80.450	10	—	3.97	0.56	4.33	361
EPRIm	1913	1	1	18	28	00.00	34.700	–81.700	0	8	4.94	0.30	5.04	1036
EPRIm	1913	3	13	5	0	00.00	34.500	–85.000	0	4	3.11	0.56	3.47	1101
CUBA	1914	0	0	0	0	00.00	22.150	–80.450	10	—	4.26	0.56	4.62	361
EPRIm	1914	3	5	20	5	00.00	33.500	–83.500	0	6	4.30	0.55	4.65	945
EPRIm	1914	3	7	1	20	00.00	34.200	–79.800	0	4	3.11	0.56	3.47	973
CUBA	1914	5	27	6	59	00.00	22.710	–82.280	10	—	3.97	0.56	4.33	358
CUBA	1914	5	28	3	29	00.00	22.710	–82.280	10	—	4.41	0.56	4.77	358
EPRIm	1914	12	30	1	0	00.00	30.500	–95.900	0	4	3.40	0.30	3.50	>1609
EPRIm	1916	3	2	5	2	00.00	34.500	–82.700	0	4	3.11	0.56	3.47	1031
EPRIm	1916	10	18	22	3	40.00	33.500	–86.200	0	7	4.90	0.56	5.26	1059
EPRIm	1917	6	30	1	23	00.00	32.700	–87.500	0	5	3.70	0.56	4.06	1063
EPRIm	1918	10	4	9	21	00.00	35.000	–91.100	0	4	4.30	0.30	4.40	1482
CUBA	1920	0	0	0	0	00.00	22.510	–79.710	10	—	3.82	0.56	4.19	327
CUBA	1921	9	23	0	0	00.00	22.910	–82.610	10	—	3.97	0.56	4.33	360
EPRIm	1923	3	27	8	0	00.00	34.600	–89.700	0	4	3.80	0.30	3.90	1358
SEUSN	1923	10	28	16	15	00.00	34.900	–88.100	0	3	2.90	0.56	3.26	1288
EPRIm	1923	12	31	20	6	00.00	34.800	–82.500	0	4	3.11	0.56	3.47	1060
EPRIm	1924	10	20	8	30	00.00	35.000	–82.600	0	5	3.70	0.56	4.06	1084
CUBA	1925	0	0	0	0	00.00	22.350	–83.500	10	—	3.97	0.56	4.33	466
CUBA	1926	0	0	0	0	00.00	22.600	–80.330	10	—	4.04	0.56	4.40	311
CUBA	1927	1	0	0	0	00.00	22.770	–81.020	18	—	4.34	0.56	4.70	301
EPRIm	1927	6	16	12	0	00.00	34.700	–86.000	0	5	3.70	0.30	3.80	1163
EPRIm	1927	10	8	12	56	00.00	35.000	–85.300	0	5	3.70	0.56	4.06	1164
EPRIm	1927	11	13	16	21	00.00	32.300	–90.200	0	4	3.80	0.30	3.90	1224
EPRIm	1927	11	23	0	50	00.00	33.900	–78.000	0	4	3.11	0.56	3.47	965
EPRIm	1927	12	15	4	30	00.00	28.900	–89.400	0	4	3.80	0.30	3.90	973
SEUSN	1928	5	23	10	15	00.00	30.800	–83.300	0	3	2.70	0.56	3.06	661
CUBA	1928	6	5	0	0	00.00	22.770	–81.020	18	—	3.90	0.56	4.26	301

Table 2.5.2-201 (Sheet 6 of 24)
Earthquake Catalog for the Phase 1 Investigation Region [22°N to 35°N, 100°W to 65°W] for which the Events are Rmb Magnitude Greater than or Equal to 3.0 or Intensity [Int] Greater than or Equal to IV(4)

Catalog Reference[a]	Year	Month	Day	Hour	Min	Sec	Lat	Lon	Depth (km)	Int	Emb	Smb	Rmb	Epicenter (km)[b]
CUBA	1929	0	0	0	0	00.00	22.290	–84.290	20	—	3.82	0.56	4.19	529
EPRIm	1929	1	3	12	5	00.00	33.900	–80.300	0	4	3.11	0.56	3.47	938
SEUSN	1929	6	13	14	44	00.00	30.700	–88.000	0	3	2.90	0.56	3.26	950
EPRIm	1929	7	28	17	0	00.00	28.900	–89.400	0	4	3.80	0.30	3.90	973
EPRIm	1929	10	28	2	15	00.00	34.300	–82.400	0	4	3.11	0.56	3.47	1003
EPRIm	1930	7	19	18	53	00.00	25.800	–81.400	0	5	3.70	0.56	4.06	114
EPRIm	1930	10	19	12	12	00.00	30.100	–91.000	0	6	4.20	0.30	4.30	1167
EPRIm	1930	11	16	12	30	00.00	34.300	–92.800	0	5	3.20	0.30	3.30	1552
EPRIm	1930	12	10	0	2	00.00	34.300	–82.400	0	4	3.11	0.56	3.47	1003
EPRIm	1930	12	26	3	0	00.00	34.500	–80.300	0	4	3.11	0.56	3.47	1005
CUBA	1931	0	0	0	0	00.00	22.230	–79.330	10	—	3.97	0.56	4.33	366
EPRIm	1931	5	5	12	18	00.00	33.700	–86.600	0	6	4.30	0.55	4.65	1098
CUBA	1931	8	12	18	0	00.00	22.810	–80.080	10	—	3.97	0.56	4.33	289
ISSv	1931	8	16	8	6	18.00	28.800	–65.200	0	—	5.76	0.10	5.77	1538
EPRIm	1931	12	17	3	36	00.00	34.100	–89.800	0	6	4.60	0.30	4.70	1325
CUBA	1932	0	0	0	0	00.00	22.980	–80.590	10	—	3.75	0.56	4.11	270
CUBA	1932	0	0	0	0	00.00	23.130	–82.400	10	—	3.97	0.56	4.33	328
EPRIm	1932	4	9	10	15	00.00	31.700	–96.400	0	6	3.50	0.30	3.60	>1609
CUBA	1933	0	0	0	0	00.00	22.050	–79.460	10	—	3.97	0.56	4.33	382
EPRIm	1933	6	9	11	30	00.00	33.300	–83.500	0	4	3.11	0.56	3.47	924
EPRIm	1933	12	23	9	40	00.00	32.900	–80.000	0	5	3.70	0.56	4.06	828
CUBA	1934	0	0	0	0	00.00	22.660	–80.190	10	—	3.97	0.56	4.33	305
EPRIm	1934	4	11	17	40	00.00	33.900	–95.500	0	5	3.80	0.30	3.90	>1609
EPRIm	1935	11	14	3	10	00.00	29.600	–81.700	0	4	3.11	0.56	3.47	480
CUBA	1936	0	19	15	30	00.00	22.340	–79.340	15	—	4.26	0.56	4.62	354
EPRIm	1936	3	14	17	20	00.00	34.000	–95.200	0	5	3.50	0.30	3.60	>1609
CUBA	1936	12	19	15	30	00.00	22.340	–79.340	15	—	4.26	0.56	4.62	354
CUBA	1937	1	1	16	0	00.00	22.290	–79.200	10	—	3.97	0.56	4.33	364
CUBA	1937	1	8	0	0	00.00	22.330	–79.260	10	—	3.97	0.56	4.33	358
CUBA	1937	4	17	0	0	00.00	22.710	–83.060	15	—	3.68	0.56	4.04	407

Table 2.5.2-201 (Sheet 7 of 24)
Earthquake Catalog for the Phase 1 Investigation Region [22°N to 35°N, 100°W to 65°W] for which the Events are Rmb Magnitude Greater than or Equal to 3.0 or Intensity [Int] Greater than or Equal to IV(4)

Catalog Reference[a]	Year	Month	Day	Hour	Min	Sec	Lat	Lon	Depth (km)	Int	Emb	Smb	Rmb	Epicenter (km)[b]
CUBA	1937	5	14	0	0	00.00	22.780	–80.080	10	—	4.34	0.56	4.70	293
CUBA	1937	5	20	15	35	00.00	22.710	–83.060	15	—	4.99	0.56	5.35	407
CUBA	1937	12	20	15	35	00.00	22.710	–83.060	15	—	4.99	0.56	5.35	407
CUBA	1937	12	21	16	30	00.00	22.710	–83.060	15	—	4.12	0.56	4.48	407
CUBA	1938	1	0	0	0	00.00	22.300	–79.730	10	—	3.82	0.56	4.19	350
EPRIm	1938	4	26	5	42	00.00	34.200	–93.500	0	4	3.11	0.56	3.47	1598
SEUSN	1938	6	24	9	0	00.00	34.700	–86.600	0	—	3.00	0.10	3.01	1191
CUBA	1938	6	30	0	0	00.00	22.510	–79.470	10	—	3.75	0.56	4.11	333
CUBA	1938	7	29	0	0	00.00	22.480	–79.550	10	—	3.75	0.56	4.11	334
CUBA	1938	10	0	0	0	00.00	22.300	–79.730	10	—	3.82	0.56	4.19	350
CUBA	1938	11	0	0	0	00.00	22.310	–79.240	10	—	3.97	0.56	4.33	361
CUBA	1939	1	1	14	0	00.00	22.310	–79.240	10	—	3.82	0.56	4.19	361
CUBA	1939	1	13	9	20	00.00	22.510	–79.470	10	—	4.48	0.56	4.84	333
CUBA	1939	1	13	9	30	00.00	22.420	–79.350	10	—	4.04	0.56	4.40	346
CUBA	1939	1	13	9	35	00.00	22.310	–79.240	10	—	3.75	0.56	4.11	361
CUBA	1939	2	15	0	0	00.00	22.310	–79.240	10	—	3.97	0.56	4.33	361
CUBA	1939	2	15	16	45	00.00	22.600	–83.300	15	—	3.68	0.56	4.04	432
ISSv	1939	3	5	15	12	09.00	23.100	–69.400	160	—	5.80	0.10	5.81	1133
CUBA	1939	5	0	0	0	00.00	22.510	–79.470	10	—	3.97	0.56	4.33	333
EPRIm	1939	5	5	2	45	00.00	33.700	–85.800	0	5	3.70	0.56	4.06	1057
EPRIm	1939	6	1	7	30	00.00	35.000	–96.400	0	4	4.30	0.30	4.40	>1609
EPRIm	1939	6	19	21	43	12.00	34.100	–92.600	0	5	4.30	0.30	4.40	1524
EPRIm	1939	6	24	10	27	00.00	34.700	–86.600	0	4	3.40	0.30	3.50	1191
CUBA	1939	8	15	3	50	00.00	22.720	–75.550	10	—	3.75	0.56	4.11	568
ISSv	1939	8	15	3	52	31.00	22.500	–79.000	0	—	5.80	0.10	5.81	349
EPRIm	1940	10	19	5	54	00.00	34.700	–85.100	0	4	3.40	0.30	3.50	1125
EPRIm	1940	12	2	16	16	00.00	33.000	–94.000	0	4	3.11	0.56	3.47	1567
CUBA	1941	0	0	0	0	00.00	22.080	–78.500	10	—	3.97	0.56	4.33	413
CUBA	1941	0	0	0	0	00.00	23.130	–82.400	10	—	3.97	0.56	4.33	328
CUBA	1941	4	24	20	30	00.00	22.810	–80.080	10	—	3.97	0.56	4.33	289

Table 2.5.2-201 (Sheet 8 of 24)
Earthquake Catalog for the Phase 1 Investigation Region [22°N to 35°N, 100°W to 65°W] for which the Events are Rmb Magnitude Greater than or Equal to 3.0 or Intensity [Int] Greater than or Equal to IV(4)

Catalog Reference[a]	Year	Month	Day	Hour	Min	Sec	Lat	Lon	Depth (km)	Int	Emb	Smb	Rmb	Epicenter (km)[b]
CUBA	1941	4	25	2	15	00.00	22.850	–80.100	15	—	4.12	0.56	4.48	285
EPRIm	1941	6	28	18	30	00.00	32.300	–90.800	0	4	2.81	0.56	3.17	1270
CUBA	1942	0	0	0	0	00.00	22.410	–83.720	15	—	4.12	0.56	4.48	477
EPRIm	1942	1	19	0	0	00.00	26.500	–81.000	0	4	3.11	0.56	3.47	136
CUBA	1942	3	9	18	10	00.00	22.940	–80.010	15	—	4.19	0.56	4.55	276
CUBA	1942	4	11	5	40	00.00	22.480	–79.550	10	—	3.97	0.56	4.33	334
CUBA	1942	6	4	6	0	00.00	22.810	–80.080	10	—	3.75	0.56	4.11	289
CUBA	1942	8	0	0	0	00.00	22.340	–80.560	10	—	4.26	0.56	4.62	341
CUBA	1942	8	18	0	0	00.00	23.130	–82.400	10	—	3.97	0.56	4.33	328
CUBA	1942	12	18	0	0	00.00	23.130	–82.400	10	—	3.97	0.56	4.33	328
CUBA	1943	0	0	0	0	00.00	22.810	–80.080	10	—	3.82	0.56	4.19	289
CUBA	1943	1	1	0	0	00.00	22.810	–80.080	10	—	3.82	0.56	4.19	289
CUBA	1943	7	0	0	0	00.00	22.210	–79.240	10	—	3.82	0.56	4.19	371
CUBA	1943	7	31	2	0	00.00	22.150	–79.970	10	—	3.97	0.56	4.33	363
CUBA	1943	7	31	3	15	00.00	22.110	–79.720	10	—	3.75	0.56	4.11	370
CUBA	1943	12	0	0	0	00.00	22.210	–79.240	10	—	3.82	0.56	4.19	371
EPRIm	1943	12	28	10	25	00.00	33.000	–80.200	0	4	3.11	0.56	3.47	838
CUBA	1944	0	0	0	0	00.00	22.060	–79.400	10	—	4.04	0.56	4.40	383
CUBA	1944	1	0	0	0	00.00	22.350	–79.230	10	—	3.97	0.56	4.33	357
CUBA	1944	1	1	3	0	00.00	22.330	–79.260	10	—	4.48	0.56	4.84	358
CUBA	1944	1	1	19	0	00.00	22.800	–80.100	10	—	4.04	0.56	4.40	290
CUBA	1944	10	12	15	0	00.00	22.710	–83.060	15	—	4.63	0.56	4.99	407
CUBA	1945	0	0	0	0	00.00	22.680	–79.710	10	—	3.97	0.56	4.33	309
EPRIm	1945	6	14	3	25	00.00	35.000	–84.500	0	5	3.90	0.30	4.00	1134
EPRIm	1945	7	26	10	32	16.40	33.750	–81.380	5	4	4.30	0.30	4.40	927
SEUSN	1945	12	22	15	25	00.00	25.800	–80.000	0	3	2.70	0.56	3.06	53
CUBA	1946	0	0	0	0	00.00	22.000	–79.360	10	—	4.04	0.56	4.40	390
CUBA	1946	0	0	0	0	00.00	22.600	–83.310	15	—	4.12	0.56	4.48	433
CUBA	1947	5	9	0	0	00.00	22.660	–76.030	10	—	4.04	0.56	4.40	531
CUBA	1947	9	0	0	0	00.00	22.030	–78.300	10	—	3.97	0.56	4.33	427

Table 2.5.2-201 (Sheet 9 of 24)
Earthquake Catalog for the Phase 1 Investigation Region [22°N to 35°N, 100°W to 65°W] for which the Events are Rmb Magnitude Greater than or Equal to 3.0 or Intensity [Int] Greater than or Equal to IV(4)

Catalog Reference[a]	Year	Month	Day	Hour	Min	Sec	Lat	Lon	Depth (km)	Int	Emb	Smb	Rmb	Epicenter (km)[b]
EPRIm	1947	9	20	21	30	00.00	31.900	–92.600	0	4	3.40	0.56	3.76	1392
EPRIm	1947	11	2	4	30	00.00	32.900	–80.000	0	4	3.11	0.56	3.47	828
EPRIm	1947	12	27	19	0	00.00	35.000	–85.300	0	4	3.11	0.56	3.47	1164
CUBA	1948	9	0	0	0	00.00	22.810	–80.080	10	—	3.97	0.56	4.33	289
EPRIm	1948	11	8	17	44	00.00	26.500	–82.200	0	4	3.11	0.56	3.47	221
EPRIm	1949	2	2	10	52	00.00	32.900	–80.000	0	4	3.11	0.56	3.47	828
EPRIm	1949	7	9	18	44	43.00	32.250	–70.750	0	—	5.61	0.20	5.66	1199
CUBA	1950	0	0	0	0	00.00	22.800	–80.280	10	—	3.97	0.56	4.33	289
CUBA	1950	1	1	0	0	00.00	22.800	–80.280	10	—	3.97	0.56	4.33	289
EPRIm	1950	3	20	13	24	00.00	33.500	–97.100	0	4	3.11	0.56	3.47	>1609
CUBA	1951	1	12	11	0	00.00	22.480	–79.550	10	—	3.97	0.56	4.33	334
EPRIm	1951	3	4	2	55	00.00	32.900	–80.000	0	4	3.11	0.56	3.47	828
EPRIm	1951	12	30	7	55	00.00	32.900	–80.000	0	4	3.11	0.56	3.47	828
CUBA	1952	2	3	6	30	00.00	22.790	–80.160	10	—	4.26	0.56	4.62	291
CUBA	1952	2	3	16	30	00.00	22.880	–80.280	15	—	4.63	0.56	4.99	280
SEUSN	1952	2	6	15	12	00.00	33.500	–86.900	0	4	3.30	0.56	3.66	1096
CUBA	1952	3	10	14	0	00.00	22.110	–78.630	15	—	4.63	0.56	4.99	404
EPRIm	1952	10	17	15	48	00.00	30.100	–93.700	0	4	3.11	0.56	3.47	1409
EPRIm	1952	11	18	20	12	00.00	30.600	–84.600	0	4	3.11	0.56	3.47	708
EPRIm	1952	11	19	0	0	00.00	32.900	–80.000	0	5	3.70	0.56	4.06	828
CUBA	1953	0	0	0	0	00.00	22.410	–83.720	15	—	4.12	0.56	4.48	477
CUBA	1953	0	0	0	0	00.00	22.980	–80.590	10	—	3.82	0.56	4.19	270
CUBA	1953	1	1	11	20	00.00	22.150	–78.600	15	—	4.85	0.56	5.21	401
CUBA	1953	1	1	15	0	00.00	22.980	–80.590	10	—	3.82	0.56	4.19	270
CUBA	1953	1	2	15	0	00.00	22.800	–80.020	10	—	3.97	0.56	4.33	291
EPRIm	1953	3	26	0	0	00.00	28.600	–81.400	0	4	3.11	0.56	3.47	366
CUBA	1953	5	16	0	0	00.00	23.030	–82.130	10	—	4.48	0.56	4.84	320
EPRIm	1953	6	6	17	40	00.00	34.700	–96.700	0	4	3.11	0.56	3.47	>1609
CUBA	1954	0	0	0	0	00.00	22.500	–79.600	10	—	4.04	0.56	4.40	331
CUBA	1954	1	1	0	0	00.00	22.500	–79.600	10	—	4.04	0.56	4.40	331

Table 2.5.2-201 (Sheet 10 of 24)
Earthquake Catalog for the Phase 1 Investigation Region [22°N to 35°N, 100°W to 65°W] for which the Events are Rmb Magnitude Greater than or Equal to 3.0 or Intensity [Int] Greater than or Equal to IV(4)

Catalog Reference[a]	Year	Month	Day	Hour	Min	Sec	Lat	Lon	Depth (km)	Int	Emb	Smb	Rmb	Epicenter (km)[b]
EPRIm	1954	4	11	0	0	00.00	35.000	–96.400	0	4	3.11	0.56	3.47	>1609
EPRIm	1955	2	1	14	45	00.00	30.400	–89.100	0	5	4.30	0.30	4.40	1020
CUBA	1956	0	0	0	0	00.00	22.810	–80.080	10	—	3.75	0.56	4.11	289
EPRIm	1956	1	5	8	0	00.00	34.300	–82.400	0	4	3.11	0.56	3.47	1003
EPRIm	1956	1	8	0	35	00.00	29.300	–94.800	0	4	3.11	0.56	3.47	1487
EPRIm	1956	4	2	16	3	18.00	34.200	–95.600	0	5	3.70	0.30	3.80	>1609
EPRIm	1956	9	27	14	15	00.00	31.900	–88.400	0	4	3.11	0.56	3.47	1063
EPRIm	1957	3	19	16	37	38.00	32.600	–94.700	0	5	4.20	0.30	4.30	1604
EPRIm	1957	4	23	9	23	39.00	33.770	–86.720	5	6	4.11	0.20	4.16	1111
CUBA	1957	9	11	23	30	00.00	22.180	–83.650	10	—	4.63	0.56	4.99	491
EPRIm	1957	11	24	20	6	17.00	35.000	–83.500	0	6	3.90	0.30	4.00	1104
CUBA	1958	0	0	0	0	00.00	22.710	–83.060	15	—	4.12	0.56	4.48	407
EPRIm	1958	3	5	11	53	43.00	34.200	–77.800	0	5	3.70	0.56	4.06	1002
SEUSN	1958	4	8	17	0	00.00	31.500	–83.500	0	3	2.70	0.56	3.06	739
EPRIm	1958	10	20	6	16	00.00	34.500	–82.700	0	5	3.70	0.56	4.06	1031
EPRIm	1958	11	6	23	8	00.00	29.900	–90.100	0	4	3.11	0.56	3.47	1079
EPRIm	1958	11	19	18	15	00.00	30.500	–91.200	0	5	3.20	0.30	3.30	1203
EPRIm	1959	6	15	12	45	00.00	34.700	–96.700	0	5	3.90	0.30	4.00	>1609
FD02	1959	6	17	16	27	07.00	34.500	–98.500	0	—	4.70	0.10	4.71	>1609
EPRIm	1959	8	3	6	8	36.80	33.050	–80.130	1	6	4.31	0.20	4.36	844
EPRIm	1959	8	12	18	6	01.40	34.790	–86.560	5	6	3.71	0.20	3.76	1198
EPRIm	1959	10	15	15	45	00.00	29.800	–93.100	0	4	3.70	0.30	3.80	1344
EPRIm	1959	10	27	2	7	28.00	34.500	–80.200	0	6	4.30	0.55	4.65	1005
CUBA	1960	0	0	0	0	00.00	22.080	–78.340	10	—	3.97	0.56	4.33	420
EPRIm	1960	5	4	16	31	32.00	34.200	–92.000	0	4	3.11	0.56	3.47	1486
CUBA	1960	5	25	15	30	00.00	22.580	–79.480	15	—	4.63	0.56	4.99	325
CUBA	1960	7	0	0	0	00.00	22.480	–79.550	10	—	3.97	0.56	4.33	334
CUBA	1960	7	18	13	35	00.00	22.480	–79.550	10	—	3.75	0.56	4.11	334
USN	1960	7	28	3	37	30.00	32.800	–82.700	0	5	3.70	0.56	4.07	847
CUBA	1960	12	0	0	0	00.00	22.480	–79.550	10	—	3.97	0.56	4.33	334

Table 2.5.2-201 (Sheet 11 of 24)
Earthquake Catalog for the Phase 1 Investigation Region [22°N to 35°N, 100°W to 65°W] for which the Events are Rmb Magnitude Greater than or Equal to 3.0 or Intensity [Int] Greater than or Equal to IV(4)

Catalog Reference[a]	Year	Month	Day	Hour	Min	Sec	Lat	Lon	Depth (km)	Int	Emb	Smb	Rmb	Epicenter (km)[b]
CUBA	1961	0	0	0	0	00.00	22.330	–79.260	10	—	3.97	0.56	4.33	358
CUBA	1961	1	0	0	0	00.00	22.980	–80.590	10	—	3.97	0.56	4.33	270
EPRIm	1961	1	11	1	40	00.00	34.900	–95.500	0	5	3.70	0.30	3.80	>1609
EPRIm	1961	4	26	7	5	00.00	34.600	–95.000	0	3	3.70	0.30	3.80	>1609
EPRIm	1961	4	27	7	30	00.00	34.900	–95.300	0	5	4.00	0.30	4.10	>1609
STO	1962	8	10	20	47	19.00	34.800	–97.400	0	—	3.25	0.41	3.45	>1609
STO	1962	9	7	22	53	44.00	34.700	–98.400	0	—	3.25	0.41	3.45	>1609
STO	1962	10	23	17	55	58.00	35.000	–98.500	0	—	3.01	0.41	3.20	>1609
CUBA	1963	1	0	0	0	00.00	22.480	–79.550	10	—	3.97	0.56	4.33	334
STO	1963	2	2	16	57	39.00	34.700	–98.200	0	—	2.93	0.41	3.12	>1609
EPRIm	1963	2	7	21	18	36.00	34.400	–92.100	0	—	3.31	0.20	3.36	1507
EPRIm	1963	4	11	17	45	00.00	34.900	–82.400	0	4	3.11	0.56	3.47	1069
STO	1963	5	7	20	3	29.00	34.300	–96.400	0	—	3.09	0.41	3.28	>1609
CUBA	1963	8	26	0	0	00.00	22.480	–79.550	10	—	3.75	0.56	4.11	334
SEUSN	1963	10	8	6	1	43.40	33.900	–82.500	0	—	3.20	0.10	3.21	961
EPRIm	1963	11	5	22	45	03.40	27.490	–92.580	15	—	4.71	0.20	4.76	1236
EPRIm	1964	2	18	9	31	10.40	34.670	–85.390	1	5	4.18	0.10	4.19	1134
EPRIm	1964	3	13	1	20	17.50	33.190	–83.310	1	5	4.38	0.10	4.39	906
CUBA	1964	3	27	0	0	00.00	22.070	–81.040	10	—	4.41	0.56	4.77	377
EPRIm	1964	4	20	19	4	44.10	33.840	–81.100	3	5	3.48	0.10	3.49	935
EPRIm	1964	4	24	7	33	51.90	31.420	–93.810	5	4	3.58	0.10	3.59	1472
EPRIm	1964	6	3	9	37	00.00	31.000	–94.000	0	4	2.81	0.56	3.17	1470
PDEnp	1965	3	29	13	10	22.30	33.900	–65.000	10	—	4.20	0.10	4.21	>1609
EPRIm	1965	9	9	14	42	20.00	34.700	–81.200	0	—	3.82	0.41	4.01	1031
SEUSN	1965	11	8	12	58	01.00	33.200	–83.200	0	—	3.30	0.10	3.31	904
CUBA	1966	0	0	0	0	00.00	22.640	–80.280	10	—	3.90	0.56	4.26	307
CUBA	1966	1	1	0	0	00.00	22.640	–80.280	10	—	3.90	0.56	4.26	307
SEUSN	1966	2	13	6	29	43.00	33.600	–87.000	0	—	3.50	0.10	3.51	1111
CUBA	1966	7	29	0	0	00.00	22.310	–79.240	10	—	3.97	0.56	4.33	361
CUBA	1966	7	29	15	0	00.00	22.310	–79.240	10	—	3.75	0.56	4.11	361

Table 2.5.2-201 (Sheet 12 of 24)
Earthquake Catalog for the Phase 1 Investigation Region [22°N to 35°N, 100°W to 65°W] for which the Events are Rmb Magnitude Greater than or Equal to 3.0 or Intensity [Int] Greater than or Equal to IV(4)

Catalog Reference[a]	Year	Month	Day	Hour	Min	Sec	Lat	Lon	Depth (km)	Int	Emb	Smb	Rmb	Epicenter (km)[b]
ISC	1966	12	15	8	16	00.00	23.130	–69.010	32	—	5.70	0.10	5.71	1171
PEREZ	1967	2	4	14	8	50.00	24.000	–65.700	1	—	6.55	0.10	6.56	1480
ISC	1967	3	13	0	58	48.10	24.290	–65.390	280	—	4.60	0.10	4.61	1507
ISC	1967	3	21	20	41	27.00	24.000	–97.000	33	—	3.90	0.10	3.91	>1609
EPRIm	1967	6	4	16	14	12.60	33.550	–90.840	6	6	4.28	0.10	4.29	1356
ISC	1967	6	20	3	57	18.00	22.000	–96.000	33	—	4.00	0.10	4.01	>1609
ISC	1967	10	4	2	45	45.00	27.000	–94.000	33	—	3.20	0.10	3.21	1369
EPRIm	1967	10	23	9	4	02.50	32.800	–80.220	19	5	3.78	0.10	3.79	816
CUBA	1968	1	1	0	0	00.00	22.980	–80.590	10	—	3.97	0.56	4.33	270
EPRIm	1968	1	4	22	30	00.00	34.850	–95.550	0	4	3.11	0.56	3.47	>1609
EPRIm	1968	7	12	1	12	00.00	32.800	–79.700	0	4	3.11	0.56	3.47	818
EPRIm	1968	9	22	21	41	18.20	34.110	–81.480	1	4	3.68	0.10	3.69	968
EPRIm	1968	10	14	14	42	54.00	34.000	–96.800	0	6	3.48	0.10	3.49	>1609
EPRIm	1968	11	25	20	0	00.00	34.100	–77.900	0	4	3.11	0.56	3.47	989
EPRIm	1969	1	1	23	35	38.70	34.990	–92.690	7	6	4.38	0.10	4.39	1591
EPRIm	1969	4	13	6	27	51.00	34.200	–96.300	0	—	3.48	0.10	3.49	>1609
CUBA	1969	5	0	0	0	00.00	22.140	–78.980	10	—	3.97	0.56	4.33	387
EPRIm	1969	5	18	0	0	00.00	33.950	–82.580	0	—	3.50	0.41	3.69	968
CUBA	1969	6	0	0	0	00.00	22.180	–78.980	10	—	3.97	0.56	4.33	383
CUBA	1969	6	1	3	0	00.00	22.140	–78.980	10	—	3.97	0.56	4.33	387
CUBA	1969	12	0	0	0	00.00	22.180	–78.980	10	—	3.97	0.56	4.33	383
EPRIm	1970	2	3	0	0	00.00	31.000	–97.000	0	4	3.11	0.56	3.47	>1609
CUBA	1970	4	27	11	55	00.00	23.050	–81.580	10	—	3.97	0.56	4.33	290
CUBA	1970	7	24	0	0	00.00	22.900	–83.160	20	—	3.90	0.56	4.26	399
CUBA	1970	10	16	13	7	22.00	23.100	–82.900	10	—	4.34	0.56	4.70	364
EPRIm	1971	3	14	17	27	54.60	33.180	–87.840	12	3	3.88	0.10	3.89	1125
EPRIm	1971	3	15	14	53	22.00	32.800	–88.300	0	—	3.48	0.10	3.49	1124
EPRIm	1971	5	19	12	54	03.60	33.360	–80.660	1	4	4.08	0.10	4.09	879
EPRIm	1971	7	13	11	42	26.00	34.800	–83.000	0	5	3.78	0.10	3.79	1070
EPRIm	1972	8	14	15	5	19.00	33.200	–81.400	0	3	3.14	0.33	3.27	866

Table 2.5.2-201 (Sheet 13 of 24)
Earthquake Catalog for the Phase 1 Investigation Region [22°N to 35°N, 100°W to 65°W] for which the Events are Rmb Magnitude Greater than or Equal to 3.0 or Intensity [Int] Greater than or Equal to IV(4)

Catalog Reference[a]	Year	Month	Day	Hour	Min	Sec	Lat	Lon	Depth (km)	Int	Emb	Smb	Rmb	Epicenter (km)[b]
CUBA	1973	0	0	0	0	00.00	22.660	–83.580	20	—	3.75	0.56	4.11	448
CUBA	1973	1	1	0	0	00.00	22.660	–83.580	20	—	3.75	0.56	4.11	448
EPRIm	1973	1	8	9	11	37.00	33.800	–90.600	0	3	3.48	0.10	3.49	1357
CUBA	1973	8	11	0	38	35.00	22.600	–74.000	0	—	4.82	0.41	5.01	712
EPRIm	1973	10	27	6	21	02.00	28.480	–80.650	5	5	3.48	0.10	3.49	338
EPRIm	1973	12	25	2	46	00.00	29.000	–98.300	0	4	3.11	0.56	3.47	>1609
CUBA	1974	0	0	0	0	00.00	22.700	–81.200	18	—	4.19	0.56	4.55	313
EPRIm	1974	2	15	22	32	38.20	34.040	–92.980	17	3	3.48	0.10	3.49	1548
EPRIm	1974	8	2	8	52	11.10	33.910	–82.530	4	6	4.28	0.10	4.29	963
ISC c	1974	9	13	17	29	57.80	23.782	–96.428	0	—	3.60	0.10	3.61	>1609
EPRIm	1974	11	5	3	0	00.00	33.730	–82.220	0	3	3.68	0.10	3.69	937
EPRIm	1974	11	22	5	25	56.70	32.920	–80.160	6	6	4.28	0.10	4.29	829
SEUSN	1974	12	9	18	40	00.00	34.200	–77.200	0	3	2.70	0.56	3.06	1018
CUBA	1975	0	0	0	0	00.00	22.700	–79.690	10	—	3.97	0.56	4.33	307
EPRIm	1975	4	1	21	9	00.00	33.200	–83.200	0	—	3.82	0.41	4.01	904
EPRIm	1975	6	24	11	11	36.60	33.700	–87.840	4	4	3.78	0.10	3.79	1168
EPRIm	1975	8	29	4	22	52.10	33.660	–86.590	4	6	3.48	0.10	3.49	1094
PDE	1975	10	12	2	58	11.20	34.816	–97.406	20	—	3.20	0.10	3.21	>1609
EPRIm	1975	10	18	4	31	00.00	34.900	–83.000	0	4	3.11	0.56	3.47	1081
EPRIm	1975	11	7	23	39	31.70	33.310	–87.330	4	—	3.48	0.10	3.49	1104
EPRIm	1975	11	29	14	29	44.90	34.680	–97.420	14	4	3.48	0.10	3.49	>1609
EPRIm	1975	12	4	11	57	00.00	29.200	–81.000	0	4	3.29	0.33	3.42	422
CUBA	1976	0	0	0	0	00.00	22.550	–79.720	10	—	3.75	0.56	4.11	323
EPRIm	1976	2	4	19	53	53.00	34.970	–84.700	14	6	3.58	0.10	3.59	1138
CUBA	1976	3	9	16	5	00.00	22.650	–83.010	15	—	3.68	0.56	4.04	408
CUBA	1976	3	10	15	40	00.00	22.650	–83.010	15	—	3.68	0.56	4.04	408
CUBA	1976	3	15	18	50	00.00	22.650	–83.010	15	—	3.68	0.56	4.04	408
CUBA	1976	10	20	8	15	00.00	22.300	–79.450	10	—	3.97	0.56	4.33	356
CUBA	1976	11	0	0	0	00.00	22.000	–79.370	5	—	3.90	0.56	4.26	390
CUBA	1976	11	1	0	0	00.00	22.000	–79.370	5	—	3.90	0.56	4.26	390

Table 2.5.2-201 (Sheet 14 of 24)
Earthquake Catalog for the Phase 1 Investigation Region [22°N to 35°N, 100°W to 65°W] for which the Events are Rmb Magnitude Greater than or Equal to 3.0 or Intensity [Int] Greater than or Equal to IV(4)

Catalog Reference[a]	Year	Month	Day	Hour	Min	Sec	Lat	Lon	Depth (km)	Int	Emb	Smb	Rmb	Epicenter (km)[b]
EPRIm	1976	12	27	6	57	15.20	32.060	–82.500	14	5	3.68	0.10	3.69	763
CUBA	1977	0	0	0	0	00.00	22.680	–80.150	10	—	3.75	0.56	4.11	303
EPRIm	1977	3	30	8	27	47.80	32.950	–80.180	8	5	4.17	0.27	4.25	832
EPRIm	1977	5	4	2	0	24.30	31.960	–88.440	0	5	3.58	0.10	3.59	1070
EPRIm	1977	6	2	23	29	10.60	34.560	–94.170	10	6	3.58	0.10	3.59	>1609
ISC	1977	9	27	20	56	03.70	33.880	–97.480	5	—	3.00	0.10	3.01	>1609
CUBA	1977	10	7	5	36	55.00	22.350	–76.100	0	—	4.26	0.41	4.45	546
SLU	1977	11	4	11	21	06.80	34.010	–89.220	2	—	3.40	0.10	3.41	1280
CUBA	1978	0	0	0	0	00.00	23.050	–81.580	10	—	3.53	0.56	3.89	290
CUBA	1978	0	0	0	0	00.00	22.240	–83.580	10	—	3.97	0.56	4.33	481
CUBA	1978	1	1	0	0	00.00	23.050	–81.580	10	—	3.53	0.56	3.89	290
CUBA	1978	1	1	10	0	00.00	22.240	–83.580	10	—	3.97	0.56	4.33	481
SEUSN	1978	1	12	21	10	00.00	28.100	–81.600	0	4	3.30	0.56	3.66	321
EPRIm	1978	3	24	0	42	36.30	29.800	–67.400	20	—	6.08	0.10	6.09	1359
SLU	1978	4	11	8	51	02.43	34.693	–95.681	5	—	3.00	0.10	3.01	>1609
SLU	1978	4	20	8	13	04.00	34.586	–96.293	5	—	3.00	0.10	3.01	>1609
CUBA	1978	5	31	16	2	00.00	23.500	–82.100	0	—	3.77	0.41	3.96	277
PDE	1978	6	9	23	15	19.10	32.094	–88.580	10	—	3.30	0.10	3.31	1089
EPRIm	1978	7	24	8	6	16.90	26.380	–88.720	15	—	4.88	0.10	4.89	842
SEUSN	1978	11	6	23	0	00.00	30.200	–82.650	0	4	3.30	0.56	3.66	574
EPRIm	1978	12	11	2	6	50.10	31.910	–88.470	3	5	3.48	0.10	3.49	1068
CUBA	1979	0	0	0	0	00.00	22.640	–79.750	10	—	3.97	0.56	4.33	312
SEUSN	1979	2	27	8	25	00.00	34.200	–92.000	0	4	3.10	0.10	3.11	1486
SLU	1979	7	13	7	48	13.44	34.033	–95.087	5	—	3.00	0.10	3.01	>1609
DNA	1979	8	7	19	32	17.20	34.333	–81.358	3	—	3.00	0.10	3.01	992
SEUSN	1979	8	13	5	19	25.20	33.900	–82.540	23	—	3.97	0.30	4.08	962
DNA	1979	8	26	1	31	45.00	34.916	–82.956	1	—	3.70	0.10	3.71	1082
DNA	1979	10	8	23	20	11.00	34.306	–81.344	1	—	3.01	0.41	3.20	989
CUBA	1979	11	19	6	0	00.00	22.480	–79.550	10	—	3.97	0.56	4.33	334
EPRIm	1980	1	10	19	16	23.50	24.130	–85.710	15	—	3.88	0.10	3.89	559

Table 2.5.2-201 (Sheet 15 of 24)
Earthquake Catalog for the Phase 1 Investigation Region [22°N to 35°N, 100°W to 65°W] for which the Events are Rmb Magnitude Greater than or Equal to 3.0 or Intensity [Int] Greater than or Equal to IV(4)

Catalog Reference[a]	Year	Month	Day	Hour	Min	Sec	Lat	Lon	Depth (km)	Int	Emb	Smb	Rmb	Epicenter (km)[b]
DNA	1980	4	24	6	16	57.20	34.329	–81.324	3	—	2.97	0.30	3.08	991
ISC	1980	7	18	1	34	44.10	34.000	–97.350	5	—	3.00	0.10	3.01	>1609
STO	1980	7	25	15	30	12.50	33.940	–87.440	0	—	3.10	0.10	3.11	1166
DNA	1980	7	29	1	10	22.70	34.351	–81.364	1	—	3.16	0.30	3.26	994
EPRIm	1980	9	1	5	44	42.20	32.980	–80.190	7	4	3.29	0.33	3.42	836
SLU	1980	9	7	1	50	14.23	34.953	–97.258	5	—	3.48	0.10	3.49	>1609
CUBA	1980	10	18	0	0	00.00	22.600	–83.710	20	—	3.68	0.56	4.04	462
CUBA	1980	10	24	0	0	00.00	22.600	–83.710	20	—	3.68	0.56	4.04	462
SLU	1980	12	4	23	48	43.22	33.942	–97.352	5	1	3.60	0.10	3.61	>1609
CUBA	1981	0	0	0	0	00.00	22.900	–83.160	20	—	3.75	0.56	4.11	399
CUBA	1981	1	1	0	0	00.00	22.900	–83.160	20	—	3.75	0.56	4.11	399
SEUSN	1981	2	13	2	15	00.00	30.000	–91.800	0	4	3.10	0.56	3.46	1233
CUBA	1981	6	9	23	3	00.00	22.280	–83.840	15	—	3.90	0.56	4.26	496
CUBA	1981	6	11	18	35	00.00	22.200	–83.480	10	—	4.41	0.56	4.77	477
SLU	1981	7	9	22	47	11.09	34.955	–97.651	5	—	3.72	0.10	3.73	>1609
EPRIm	1981	7	11	21	9	21.84	34.850	–97.730	5	5	3.48	0.10	3.49	>1609
SLU	1981	9	17	19	31	00.45	34.481	–96.823	5	—	3.72	0.10	3.73	>1609
CUBA	1981	9	30	0	54	00.00	22.350	–83.570	10	—	3.97	0.56	4.33	471
SLU	1981	11	6	19	28	25.31	34.676	–96.682	5	—	3.54	0.10	3.55	>1609
CUBA	1981	11	11	20	30	00.00	22.160	–84.100	15	—	4.55	0.56	4.92	525
CUBA	1982	0	0	0	0	00.00	22.660	–83.960	20	—	4.26	0.56	4.62	477
SLU	1982	1	12	23	40	25.00	34.742	–97.406	5	—	3.00	0.10	3.01	>1609
SEUSN	1982	1	28	4	52	51.90	32.982	–81.393	7	—	3.40	0.10	3.41	842
CUBA	1982	2	22	17	4	20.00	22.300	–83.200	0	—	3.28	0.41	3.47	450
CUBA	1982	2	26	18	23	47.00	22.300	–83.400	0	—	3.28	0.41	3.47	464
SLU	1982	3	15	21	39	10.98	34.832	–97.608	5	—	3.72	0.10	3.73	>1609
SLU	1982	3	18	9	51	52.95	34.175	–97.608	5	—	3.48	0.10	3.49	>1609
TEIC	1982	4	13	9	25	09.30	34.251	–81.260	12	—	3.17	0.41	3.37	982
SLU	1982	7	9	3	38	11.35	34.963	–97.432	5	—	3.54	0.10	3.55	>1609
SEUSN	1982	7	16	14	16	02.90	34.320	–81.550	2	3	3.06	0.27	3.15	992

Table 2.5.2-201 (Sheet 16 of 24)
Earthquake Catalog for the Phase 1 Investigation Region [22°N to 35°N, 100°W to 65°W] for which the Events are Rmb Magnitude Greater than or Equal to 3.0 or Intensity [Int] Greater than or Equal to IV(4)

Catalog Reference[a]	Year	Month	Day	Hour	Min	Sec	Lat	Lon	Depth (km)	Int	Emb	Smb	Rmb	Epicenter (km)[b]
SLU	1982	8	22	1	1	02.42	34.840	–96.936	5	—	3.72	0.10	3.73	>1609
TEIC	1982	9	2	21	52	05.30	34.917	–82.891	8	—	3.09	0.41	3.28	1080
CUBA	1982	11	0	0	0	00.00	22.590	–81.240	20	—	3.75	0.56	4.11	326
CUBA	1982	11	16	20	20	17.00	22.610	–81.230	30	—	5.36	0.56	5.72	323
EPRIm	1983	1	26	14	7	44.70	32.850	–83.560	0	—	3.48	0.10	3.49	879
SLU	1983	3	28	9	32	24.86	34.635	–96.561	5	—	3.60	0.10	3.61	>1609
EPRIm	1983	10	16	19	40	50.80	30.240	–93.390	5	3	3.78	0.10	3.79	1386
CUBA	1983	11	1	17	9	20.00	23.300	–82.800	0	—	3.24	0.41	3.43	342
EPRIm	1983	11	6	9	2	19.80	32.940	–80.160	10	5	3.51	0.27	3.59	831
CUBA	1983	11	30	17	15	13.00	22.200	–77.830	5	—	3.64	0.30	3.74	437
SLU	1983	12	9	20	52	11.04	33.227	–92.739	4	—	3.00	0.10	3.01	1479
CUBA	1984	0	0	0	0	00.00	22.510	–79.470	0	—	3.61	0.56	3.97	333
CUBA	1984	1	1	0	0	00.00	22.600	–83.710	20	—	3.82	0.56	4.19	462
CUBA	1984	1	16	18	41	27.00	22.300	–83.800	0	—	3.49	0.41	3.68	492
CUBA	1984	1	17	20	55	00.00	23.400	–83.700	0	—	3.20	0.41	3.40	406
ANSS	1984	1	23	0	11	59.38	26.716	–87.339	5	—	2.85	0.41	3.04	712
TEIme	1984	1	23	1	15	09.40	26.716	–87.339	5	—	2.85	0.41	3.04	712
NAOme	1984	4	9	23	8	20.00	22.600	–80.300	33	—	4.50	0.10	4.51	311
CUBA	1984	4	17	20	23	04.00	23.200	–83.600	0	—	3.17	0.41	3.36	411
CUBA	1984	4	19	19	54	39.00	23.100	–82.400	0	—	3.20	0.41	3.40	330
CUBA	1984	5	16	2	50	37.00	22.930	–80.500	15	—	4.19	0.56	4.55	275
EPRIm	1984	8	9	2	42	35.81	34.620	–86.300	8	—	3.15	0.30	3.25	1169
CUBA	1984	8	20	18	37	26.00	22.500	–79.740	10	—	3.53	0.30	3.64	328
SLU	1984	9	25	1	53	26.26	34.018	–89.835	5	—	3.00	0.10	3.01	1321
EPRIm	1984	10	9	11	54	26.97	34.750	–85.200	12	6	4.18	0.10	4.19	1134
CUBA	1984	11	7	7	42	22.00	22.510	–79.470	0	—	3.61	0.56	3.97	333
SLU	1984	11	16	11	50	04.51	34.641	–97.487	5	—	3.60	0.10	3.61	>1609
CUBA	1984	11	16	13	34	11.00	23.010	–79.320	27	—	3.68	0.30	3.78	285
CUBA	1984	11	22	18	35	56.00	22.960	–79.640	20	—	3.97	0.30	4.07	280
CUBA	1985	1	21	10	45	33.00	22.390	–83.550	0	—	3.17	0.41	3.36	467

Table 2.5.2-201 (Sheet 17 of 24)
Earthquake Catalog for the Phase 1 Investigation Region [22°N to 35°N, 100°W to 65°W] for which the Events are Rmb Magnitude Greater than or Equal to 3.0 or Intensity [Int] Greater than or Equal to IV(4)

Catalog Reference[a]	Year	Month	Day	Hour	Min	Sec	Lat	Lon	Depth (km)	Int	Emb	Smb	Rmb	Epicenter (km)[b]
CUBA	1985	2	0	0	0	00.00	22.600	–83.710	20	—	4.12	0.56	4.48	462
CUBA	1985	2	21	20	22	25.00	23.250	–83.400	0	—	3.93	0.30	4.04	391
CUBA	1985	2	28	12	52	21.00	22.070	–83.760	0	—	3.49	0.41	3.68	507
ISC	1985	5	6	2	11	13.60	34.875	–97.572	5	5	2.30	0.10	2.31	>1609
CUBA	1985	5	17	11	50	26.00	22.310	–83.180	0	—	3.49	0.41	3.68	448
CUBA	1985	5	17	11	53	20.00	22.330	–83.360	0	—	3.49	0.41	3.68	459
CUBA	1985	9	13	10	2	49.00	24.070	–76.970	0	—	3.59	0.30	3.69	370
CUBA	1985	9	13	17	49	45.00	23.360	–82.830	0	—	3.31	0.41	3.51	339
FD02	1985	9	18	15	54	04.00	33.470	–97.040	0	5	3.30	0.10	3.31	>1609
CUBA	1985	9	21	18	34	20.00	22.560	–83.880	0	—	3.24	0.41	3.43	478
CUBA	1986	0	0	0	0	00.00	22.480	–84.240	20	—	4.26	0.56	4.62	512
TEIC	1986	2	13	1	35	00.00	34.793	–82.938	1	—	3.25	0.41	3.45	1068
SLU	1986	2	13	11	35	47.05	34.816	–82.944	4	—	3.00	0.10	3.01	1071
SEUSN	1986	3	13	2	29	31.40	33.229	–83.226	5	4	3.30	0.27	3.38	908
PDE	1986	5	7	2	27	00.46	33.233	–87.361	1	—	4.50	0.10	4.51	1100
SLU	1986	5	12	4	18	48.31	30.902	–89.159	10	—	3.60	0.10	3.61	1054
SEUSN	1986	7	11	14	26	14.80	34.937	–84.987	13	6	3.80	0.10	3.81	1145
SEUSN	1986	9	17	9	33	49.50	32.931	–80.159	6	4	3.30	0.27	3.38	830
CUBA	1986	10	8	4	51	46.00	22.220	–78.700	0	—	3.90	0.56	4.26	390
PDE	1986	11	7	13	53	18.50	34.671	–70.896	10	—	4.00	0.10	4.01	1369
TEIC	1986	12	11	14	5	50.00	34.889	–82.887	9	—	2.93	0.41	3.12	1077
TEIC	1986	12	11	14	7	11.00	34.898	–82.880	9	—	3.09	0.41	3.28	1078
CUBA	1986	12	25	6	13	20.00	22.230	–79.030	0	—	3.24	0.30	3.34	376
CUBA	1986	12	30	8	16	27.00	22.350	–79.330	0	—	3.39	0.30	3.49	354
CUBA	1987	2	2	0	0	00.00	22.600	–83.710	20	—	3.68	0.56	4.04	462
NENG	1987	2	8	18	25	37.09	29.697	–67.634	12	—	4.70	0.10	4.71	1334
ISCwy	1987	2	21	2	17	52.40	29.560	–66.960	18	—	4.20	0.10	4.21	1392
SEUSN	1987	3	16	13	9	26.80	34.560	–80.948	3	—	3.06	0.30	3.17	1014
CUBA	1987	3	29	22	24	12.00	22.170	–77.930	5	—	3.14	0.30	3.24	433
PDE	1987	6	1	17	44	33.20	34.615	–97.380	5	4	2.90	0.10	2.91	>1609

Table 2.5.2-201 (Sheet 18 of 24)
Earthquake Catalog for the Phase 1 Investigation Region [22°N to 35°N, 100°W to 65°W] for which the Events are Rmb Magnitude Greater than or Equal to 3.0 or Intensity [Int] Greater than or Equal to IV(4)

Catalog Reference[a]	Year	Month	Day	Hour	Min	Sec	Lat	Lon	Depth (km)	Int	Emb	Smb	Rmb	Epicenter (km)[b]
TEIC	1987	12	12	3	53	28.00	34.154	–82.714	9	—	3.33	0.41	3.53	994
TEIC	1987	12	24	22	46	44.20	34.154	–82.723	6	—	3.09	0.41	3.28	994
CUBA	1988	1	4	10	33	30.00	22.320	–78.940	20	—	3.99	0.30	4.09	370
SEUSN	1988	1	23	1	57	16.40	32.935	–80.157	7	5	3.50	0.27	3.58	831
PRSN	1988	3	3	13	52	05.64	22.280	–70.270	5	—	4.10	0.23	4.16	1077
PRSN	1988	4	28	6	46	27.22	22.030	–67.510	25	—	3.80	0.23	3.86	1353
PRSN	1988	5	5	17	39	20.20	29.420	–71.660	54	—	5.40	0.23	5.46	961
PRSN	1988	5	9	0	31	29.37	22.320	–69.600	25	—	4.10	0.23	4.16	1140
CUBA	1988	6	0	0	0	00.00	22.650	–83.010	15	—	3.68	0.56	4.04	408
CUBA	1988	6	1	0	0	00.00	22.650	–83.010	15	—	3.68	0.56	4.04	408
PRSN	1988	8	15	5	46	56.00	23.850	–69.250	104	—	4.10	0.23	4.16	1129
PRSN	1988	12	20	7	24	27.76	22.090	–70.710	25	—	4.10	0.23	4.16	1042
PRSN	1988	12	21	19	18	37.07	22.560	–69.460	25	—	4.50	0.23	4.56	1145
SLU	1988	12	25	15	57	57.53	34.197	–92.718	15	—	3.42	0.41	3.61	1539
TAC c	1989	1	29	4	57	40.50	22.780	–99.470	20	—	4.52	0.10	4.53	>1609
SLU	1989	2	28	17	31	50.68	33.399	–87.118	0	—	3.50	0.10	3.51	1100
PRSN	1989	5	25	23	12	09.08	22.690	–67.170	25	—	3.80	0.23	3.86	1365
SEUSN	1989	6	2	5	4	34.00	32.934	–80.166	5	4	3.30	0.27	3.38	831
PDE	1989	8	13	20	16	02.90	33.632	–87.086	0	—	3.40	0.10	3.41	1118
SEUSN	1989	8	20	0	3	18.30	34.803	–87.596	6	6	3.90	0.10	3.91	1252
SLU	1989	11	26	22	41	09.90	34.763	–91.086	5	—	3.00	0.10	3.01	1463
CUBA	1990	3	14	11	56	37.00	22.180	–70.500	70	—	5.21	0.10	5.22	1059
CUBA	1990	6	2	23	54	18.00	23.420	–79.480	17	—	4.09	0.30	4.19	237
SEUSN	1990	6	23	20	44	02.10	33.720	–87.946	6	—	3.06	0.30	3.17	1176
CUBA	1990	7	19	12	36	03.00	22.470	–78.470	5	—	3.19	0.30	3.29	376
TEIC	1990	7	28	7	53	33.00	34.600	–93.376	4	—	3.01	0.41	3.20	>1609
TEIC	1990	8	23	8	23	11.00	34.036	–82.503	14	—	2.93	0.41	3.12	976
SEUSN	1990	9	2	4	35	40.20	33.758	–87.928	0	—	3.16	0.30	3.26	1179
PDE	1990	9	16	21	13	32.40	34.800	–95.530	5	4	2.50	0.10	2.51	>1609
TEIC	1990	9	19	5	36	56.00	34.838	–83.002	5	—	3.09	0.41	3.28	1074

Table 2.5.2-201 (Sheet 19 of 24)
Earthquake Catalog for the Phase 1 Investigation Region [22°N to 35°N, 100°W to 65°W] for which the Events are Rmb Magnitude Greater than or Equal to 3.0 or Intensity [Int] Greater than or Equal to IV(4)

Catalog Reference[a]	Year	Month	Day	Hour	Min	Sec	Lat	Lon	Depth (km)	Int	Emb	Smb	Rmb	Epicenter (km)[b]
TEIC	1990	9	19	8	14	04.00	34.868	–83.016	16	—	2.85	0.41	3.04	1078
SEUSN	1990	11	13	15	22	13.00	32.947	–80.136	3	5	3.50	0.10	3.51	832
PDE	1990	11	15	11	44	41.40	34.760	–97.590	5	5	3.90	0.10	3.91	>1609
TEIC	1991	1	15	8	48	22.50	33.204	–83.205	12	—	3.25	0.41	3.45	904
TEIC	1991	1	16	15	26	39.40	33.171	–83.264	22	—	2.85	0.41	3.04	903
TEIC	1991	1	27	2	20	34.90	33.230	–83.247	20	—	3.17	0.41	3.37	908
TEIC	1991	2	7	4	3	14.30	33.195	–83.183	8	—	3.17	0.41	3.37	903
TEIC	1991	2	11	15	36	44.40	34.108	–90.599	12	—	2.85	0.41	3.04	1380
SEUSN	1991	6	2	6	5	34.90	32.980	–80.214	5	5	3.50	0.27	3.58	836
PRSN	1991	7	3	14	39	24.42	22.160	–65.580	20	—	5.70	0.23	5.76	1538
NENG	1991	7	9	6	53	36.00	23.217	–65.569	9	—	6.11	0.10	6.12	1509
CUBA	1991	9	26	8	27	35.00	22.500	–75.200	20	—	3.66	0.41	3.86	611
SEUSN	1991	10	30	14	54	12.60	34.904	–84.713	8	—	3.06	0.30	3.17	1132
TEIC	1991	11	17	21	11	31.70	34.987	–82.956	8	—	3.01	0.41	3.20	1089
SEUSN	1992	1	3	4	21	23.90	33.981	–82.421	3	5	3.50	0.27	3.58	969
ISC	1992	1	4	3	19	06.70	24.371	–65.279	10	—	4.20	0.10	4.21	1516
PDE	1992	2	22	4	21	34.65	26.356	–78.888	10	—	3.20	0.10	3.21	177
PDE	1992	3	31	14	59	39.64	26.019	–85.731	5	—	3.80	0.10	3.81	543
PDE	1992	7	30	14	40	55.87	24.705	–99.779	10	—	4.30	0.10	4.31	>1609
PDE	1992	8	10	20	3	04.20	34.982	–97.453	5	4	2.88	0.27	2.97	>1609
SEUSN	1992	8	21	16	31	56.10	32.985	–80.163	6	6	4.10	0.10	4.11	837
SEUSN	1992	9	11	16	34	11.70	33.171	–87.501	6	—	2.97	0.30	3.08	1103
CUBA	1992	9	25	0	51	43.00	22.650	–79.400	15	—	4.28	0.30	4.39	320
CUBA	1992	9	25	3	15	57.00	22.690	–79.300	15	—	3.54	0.30	3.64	319
TEIC	1992	9	27	17	2	25.70	27.225	–88.711	10	—	3.80	0.10	3.81	855
PDE	1992	11	30	8	33	01.48	23.251	–98.199	10	—	4.61	0.30	4.71	>1609
PDE	1992	12	6	5	39	22.15	31.442	–66.108	10	—	3.90	0.10	3.91	1538
PDE	1992	12	17	7	18	04.27	34.744	–97.581	5	4	3.60	0.10	3.61	>1609
PRSN	1993	1	3	6	8	10.98	22.150	–67.960	54	—	5.70	0.23	5.76	1305
PDE	1993	7	16	10	54	32.86	31.747	–88.341	5	6	3.70	0.10	3.71	1047

Table 2.5.2-201 (Sheet 20 of 24)
Earthquake Catalog for the Phase 1 Investigation Region [22°N to 35°N, 100°W to 65°W] for which the Events are Rmb Magnitude Greater than or Equal to 3.0 or Intensity [Int] Greater than or Equal to IV(4)

Catalog Reference[a]	Year	Month	Day	Hour	Min	Sec	Lat	Lon	Depth (km)	Int	Emb	Smb	Rmb	Epicenter (km)[b]
SEUSN	1993	8	8	9	24	32.40	33.597	–81.591	8	5	3.20	0.10	3.21	913
PDE	1993	8	23	12	5	43.40	22.405	–99.347	33	—	4.00	0.10	4.01	>1609
ISC	1993	10	20	8	37	14.10	22.137	–99.051	10	—	4.00	0.10	4.01	>1609
PDE	1994	3	26	21	33	35.25	28.913	–66.146	10	—	4.70	0.10	4.71	1451
SEUSN	1994	4	5	22	22	00.40	34.969	–85.491	24	5	3.20	0.10	3.21	1168
ISC	1994	4	16	7	20	20.00	34.660	–97.710	5	—	3.17	0.23	3.23	>1609
SEUSN	1994	5	4	9	12	03.40	34.222	–87.195	19	4	3.00	0.10	3.01	1178
PDE	1994	6	10	23	34	02.92	33.013	–92.671	5	3	3.20	0.10	3.21	1460
PDE	1994	6	30	1	8	24.22	27.911	–90.177	10	—	4.20	0.10	4.21	1013
PRSN	1994	10	14	22	26	23.54	22.980	–66.720	25	—	3.90	0.23	3.96	1401
PRSN	1994	11	4	6	0	41.77	22.610	–67.270	50	—	3.90	0.23	3.96	1357
PDE	1995	1	4	1	46	14.09	29.450	–96.950	5	4	2.70	0.10	2.71	>1609
PDE	1995	1	18	15	51	39.42	34.774	–97.596	5	5	4.20	0.10	4.21	>1609
CUBA	1995	1	18	20	45	07.00	22.320	–71.930	20	—	4.58	0.30	4.69	917
CUBA	1995	3	9	18	29	13.00	22.900	–82.210	3	—	3.24	0.30	3.34	337
SEUSN	1995	4	17	13	46	00.00	32.997	–80.171	8	6	3.90	0.10	3.91	838
PRSN	1995	5	1	7	30	46.77	22.230	–72.160	25	—	4.20	0.23	4.26	900
SEUSN	1995	5	28	15	28	37.00	33.191	–87.827	1	F(c)	3.40	0.10	3.41	1125
PDE	1995	6	1	4	49	29.32	34.287	–96.732	5	5	3.00	0.10	3.01	>1609
NENG	1995	7	2	3	35	11.33	30.974	–65.234	2	—	4.71	0.10	4.72	1598
SEUSN	1995	7	15	1	3	28.40	33.478	–87.665	1	—	3.30	0.10	3.31	1139
PRSN	1995	9	12	15	15	03.04	22.170	–66.140	25	—	3.80	0.23	3.86	1482
PRSN	1996	3	17	5	59	09.10	22.280	–66.820	25	—	3.60	0.23	3.66	1412
PDE	1996	3	25	14	15	50.55	32.131	–88.671	5	—	3.50	0.10	3.51	1099
PDE	1996	4	11	21	54	57.63	34.969	–91.162	5	5	3.30	0.10	3.31	1483
PDE	1996	8	8	22	25	11.03	22.110	–80.184	10	—	3.80	0.10	3.81	366
PDE	1996	8	11	18	17	49.88	33.577	–90.874	10	—	3.50	0.10	3.51	1361
PDE	1996	12	22	20	13	53.55	32.224	–65.447	10	—	4.40	0.10	4.41	>1609
PDE	1997	3	16	19	7	27.95	34.209	–93.435	5	4	3.40	0.10	3.41	1594
PDE	1997	4	18	14	57	35.39	25.782	–86.552	33	—	3.90	0.10	3.91	623

Table 2.5.2-201 (Sheet 21 of 24)
Earthquake Catalog for the Phase 1 Investigation Region [22°N to 35°N, 100°W to 65°W] for which the Events are Rmb Magnitude Greater than or Equal to 3.0 or Intensity [Int] Greater than or Equal to IV(4)

Catalog Reference[a]	Year	Month	Day	Hour	Min	Sec	Lat	Lon	Depth (km)	Int	Emb	Smb	Rmb	Epicenter (km)[b]
SEUSN	1997	5	4	3	39	12.80	30.934	–87.494	0	4	3.10	0.10	3.11	928
SEUSN	1997	5	19	19	45	35.80	34.622	–85.353	2	4	2.90	0.10	2.91	1128
FD02	1997	5	31	3	26	41.00	33.200	–96.100	0	4	3.40	0.10	3.41	>1609
PDE	1997	7	1	21	12	20.59	33.136	–67.854	10	—	3.60	0.10	3.61	1479
SEUSN	1997	7	19	17	6	34.40	34.953	–84.811	2	4	3.50	0.10	3.51	1140
PDE	1997	9	6	23	38	00.91	34.660	–96.435	5	5	4.50	0.10	4.51	>1609
NENG	1997	10	24	8	35	18.75	31.123	–87.272	2	—	4.96	0.10	4.97	925
ISC	1997	12	6	11	11	23.60	34.895	–95.968	5	—	3.01	0.10	3.02	>1609
PDE	1997	12	12	8	42	20.25	33.466	–87.306	1	—	4.00	0.10	4.01	1116
PRSN	1998	3	30	7	15	36.26	22.960	–66.360	25	—	3.90	0.23	3.96	1437
SEUSN	1998	4	13	9	56	15.60	34.471	–80.603	6	5	3.90	0.10	3.91	1002
FD02	1998	4	28	14	13	02.00	34.780	–98.420	0	—	4.20	0.10	4.21	>1609
SEUSN	1998	6	24	15	20	04.70	32.760	–87.759	2	—	3.40	0.10	3.41	1085
NENG	1998	6	30	20	19	15.68	22.351	–69.892	14	—	4.80	0.10	4.81	1110
PDE	1998	7	6	6	54	03.79	25.016	–93.633	10	—	3.40	0.10	3.41	1333
PDE	1998	7	7	18	44	44.46	34.719	–97.589	5	—	3.20	0.10	3.21	>1609
ISC	1998	8	14	17	5	11.80	27.744	–99.864	0	—	3.90	0.10	3.91	>1609
PRSN	1998	12	14	3	10	38.19	22.650	–70.240	25	—	3.90	0.23	3.96	1066
PDE	1999	1	18	7	0	53.47	33.405	–87.255	1	—	4.80	0.10	4.81	1108
SEUSN	1999	3	29	14	49	37.80	33.064	–80.140	10	3	2.97	0.27	3.06	845
ISC	1999	5	28	11	36	48.90	22.117	–75.228	33	—	4.63	0.10	4.64	633
MIDAS	1999	9	10	17	16	28.68	29.906	–70.976	56	—	4.96	0.10	4.97	1043
PDE	1999	11	28	11	0	09.30	33.416	–87.253	1	—	3.80	0.10	3.81	1109
ISC	2000	1	14	10	39	34.90	34.674	–95.095	18	—	3.09	0.23	3.15	>1609
SEUSN	2000	1	18	22	19	32.20	32.920	–83.465	19	5	3.50	0.10	3.51	883
SEUSN	2000	5	28	11	32	06.30	33.708	–87.811	0	3	3.00	0.10	3.01	1167
PDE	2000	9	20	6	24	59.00	24.622	–99.933	33	—	4.24	0.30	4.35	>1609
PDE	2000	12	9	6	46	09.12	28.027	–90.171	10	—	4.96	0.10	4.97	1015
PDE	2001	3	3	10	46	13.00	33.190	–92.660	5	—	3.00	0.10	3.01	1470
PDE	2001	3	16	4	39	07.68	28.361	–89.029	10	—	3.60	0.10	3.61	918

Table 2.5.2-201 (Sheet 22 of 24)
Earthquake Catalog for the Phase 1 Investigation Region [22°N to 35°N, 100°W to 65°W] for which the Events are Rmb Magnitude Greater than or Equal to 3.0 or Intensity [Int] Greater than or Equal to IV(4)

Catalog Reference[a]	Year	Month	Day	Hour	Min	Sec	Lat	Lon	Depth (km)	Int	Emb	Smb	Rmb	Epicenter (km)[b]
SEUSN	2001	3	21	23	35	34.90	34.847	–85.438	0	3	3.16	0.27	3.24	1154
ISC	2001	6	3	14	58	12.30	29.890	–79.480	0	—	3.30	0.10	3.31	500
PDE	2001	6	11	18	27	54.25	30.226	–79.885	10	—	3.30	0.10	3.31	532
PDE	2001	8	4	1	13	25.38	34.292	–93.213	5	3	3.10	0.10	3.11	1582
SEUSN	2001	12	8	1	8	22.40	34.710	–86.231	0	5	3.90	0.10	3.91	1175
NENG	2002	1	12	8	26	53.23	28.126	–69.615	5	—	5.60	0.10	5.61	1101
PDE	2002	2	8	16	7	13.60	34.727	–98.361	5	5	3.80	0.10	3.81	>1609
SEUSN	2002	5	21	20	35	31.90	32.456	–88.221	27	3	2.97	0.27	3.06	1092
PDE	2002	5	27	0	28	16.99	27.117	–94.442	10	—	3.80	0.10	3.81	1414
PDE	2002	5	31	9	57	10.02	34.025	–97.619	5	3	3.30	0.10	3.31	>1609
SEUSN	2002	7	26	21	7	03.00	33.060	–80.195	10	—	2.97	0.30	3.08	845
PDE	2002	9	19	14	44	36.15	27.822	–89.135	10	—	3.70	0.10	3.71	911
PDE	2002	10	20	2	18	13.00	34.274	–96.079	5	5	3.40	0.10	3.41	>1609
PDE	2002	10	26	20	5	55.93	34.029	–90.683	5	—	3.10	0.10	3.11	1380
PDE	2002	11	8	13	29	03.19	32.422	–79.950	3	—	3.50	0.10	3.51	775
NENG	2002	11	11	23	39	29.62	32.456	–79.927	6	—	4.20	0.10	4.21	778
PDE	2002	11	21	11	17	22.61	22.947	–70.252	10	—	3.90	0.10	3.91	1055
PDE	2003	3	18	6	4	24.21	33.689	–82.888	5	4	3.50	0.10	3.51	948
PDE	2003	4	13	4	52	53.92	26.087	–86.085	10	—	3.20	0.10	3.21	579
SEUSN	2003	4	29	8	59	38.10	34.445	–85.620	9	6	4.60	0.10	4.61	1121
SEUSN	2003	5	5	10	53	49.90	33.055	–80.190	11	—	3.06	0.30	3.17	844
ISC	2003	6	22	20	47	40.90	23.016	–65.416	10	—	3.70	0.10	3.71	1530
PDE	2003	7	13	20	15	16.96	32.335	–82.144	5	3	3.60	0.10	3.61	784
SEUSN	2003	9	30	2	28	04.50	31.022	–87.462	12	—	2.97	0.30	3.08	931
NENG	2003	10	10	14	48	17.25	23.142	–84.932	15	—	4.30	0.10	4.31	528
SEUSN	2003	12	22	23	50	26.00	32.924	–80.157	5	—	2.97	0.30	3.08	830
SEUSN	2004	3	20	10	40	34.80	33.267	–86.955	0	3	2.97	0.27	3.06	1079
PDE	2004	4	6	19	1	02.70	25.172	–99.532	37	—	4.33	0.30	4.44	>1609
SEUSN	2004	5	9	8	56	10.40	33.231	–86.960	5	3	3.30	0.10	3.31	1076
PDE	2004	6	8	0	15	09.99	34.233	–97.254	5	4	3.50	0.10	3.51	>1609

Table 2.5.2-201 (Sheet 23 of 24)
Earthquake Catalog for the Phase 1 Investigation Region [22°N to 35°N, 100°W to 65°W] for which the Events are Rmb Magnitude Greater than or Equal to 3.0 or Intensity [Int] Greater than or Equal to IV(4)

Catalog Reference[a]	Year	Month	Day	Hour	Min	Sec	Lat	Lon	Depth (km)	Int	Emb	Smb	Rmb	Epicenter (km)[b]
ISC	2004	6	18	19	20	56.40	27.027	–86.997	10	—	3.50	0.10	3.51	685
SEUSN	2004	7	20	9	13	14.40	32.972	–80.248	10	—	3.06	0.30	3.17	835
ISC	2004	8	7	18	13	42.10	23.001	–70.239	0	—	3.68	0.10	3.69	1054
SEUSN	2004	8	19	23	51	49.40	33.203	–86.968	5	3	3.50	0.10	3.51	1074
NENG	2004	9	18	7	7	47.57	23.119	–67.594	5	—	5.70	0.10	5.71	1311
NENG	2004	11	7	11	20	22.19	32.700	–87.888	8	—	4.59	0.10	4.60	1088
PDE	2004	11	22	23	42	13.45	34.864	–97.672	5	—	3.00	0.10	3.01	>1609
PRSN	2005	1	11	8	9	38.09	22.803	–66.947	25	—	4.20	0.23	4.26	1384
PDE	2005	3	22	8	11	50.51	31.836	–88.060	5	4	3.30	0.10	3.31	1034
ISC	2005	3	30	2	22	57.70	22.572	–94.790	0	—	4.00	0.10	4.01	1496
PDE	2005	4	22	5	17	04.09	34.179	–95.192	5	5	3.00	0.10	3.01	>1609
ISC	2005	8	10	1	18	35.70	22.119	–98.731	25	—	4.10	0.10	4.11	>1609
PRSN	2005	9	2	21	12	00.87	22.833	–70.272	25	—	4.60	0.23	4.66	1056
PDE	2005	9	19	2	29	52.54	23.950	–66.442	15	—	4.52	0.30	4.62	1407
PDE	2005	12	20	0	52	20.51	30.258	–90.708	5	4	3.00	0.10	3.01	1149
PDE	2006	2	10	4	14	22.20	27.828	–90.210	5	3	5.58	0.10	5.59	1014
ISC	2006	2	18	15	59	56.70	22.426	–80.966	0	—	3.00	0.10	3.01	336
ISC	2006	4	3	2	30	13.00	22.455	–99.889	16	—	4.10	0.10	4.11	>1609
PDE	2006	4	5	18	46	23.14	34.069	–97.314	5	—	3.00	0.10	3.01	>1609
PRSN	2006	5	7	20	46	45.01	22.334	–66.804	126	—	4.20	0.23	4.26	1412
ISC	2006	6	19	5	31	54.10	23.111	–75.594	25	—	3.40	0.10	3.41	542
ISC	2006	9	8	12	24	06.80	23.605	–71.845	25	—	3.60	0.10	3.61	879
NENG	2006	9	10	14	56	07.75	26.258	–86.630	14	—	5.90	0.10	5.91	635
ISC	2006	9	15	8	39	33.20	22.196	–79.886	0	—	3.20	0.10	3.21	359
ISC	2006	9	20	20	53	33.20	22.966	–75.623	0	—	3.90	0.10	3.91	548
PDE	2006	9	22	11	22	00.28	34.551	–79.583	5	—	3.40	0.10	3.41	1014
PDE	2006	9	25	5	44	25.09	34.746	–79.876	5	4	3.70	0.10	3.71	1034
PDE	2006	10	6	22	13	16.78	34.122	–97.625	5	4	3.50	0.10	3.51	>1609
ISC	2006	11	5	14	1	41.60	22.628	–67.065	126	—	4.80	0.10	4.81	1377
ISC	2006	12	17	17	24	54.20	22.434	–76.982	0	—	3.10	0.10	3.11	473

Table 2.5.2-201 (Sheet 24 of 24)
Earthquake Catalog for the Phase 1 Investigation Region [22°N to 35°N, 100°W to 65°W] for which the Events are Rmb Magnitude Greater than or Equal to 3.0 or Intensity [Int] Greater than or Equal to IV(4)

Catalog Reference[a]	Year	Month	Day	Hour	Min	Sec	Lat	Lon	Depth (km)	Int	Emb	Smb	Rmb	Epicenter (km)[b]
ISC	2007	3	6	7	3	06.70	22.028	–71.023	20	—	4.20	0.10	4.21	1016
ISC	2007	4	26	22	13	50.10	22.692	–75.015	25	—	3.00	0.10	3.01	616
PDE	2007	5	4	16	16	28.18	33.797	–87.299	5	—	3.00	0.10	3.01	1145
PDE	2007	5	16	13	22	21.42	33.300	–92.587	5	4	3.00	0.10	3.01	1471
ISC	2007	5	23	19	9	14.40	22.049	–96.387	10	—	5.40	0.10	5.41	>1609
ISC	2007	6	1	4	49	19.10	22.738	–71.141	0	—	4.00	0.10	4.01	976
ISC	2007	8	22	6	19	23.00	22.236	–71.628	25	—	4.90	0.23	4.96	949
PDE-W	2007	12	27	20	51	57.49	27.679	–71.076	10	—	4.60	0.10	4.61	951

(a) "EPRIm" are the "MAIN" events from the EPRI catalog.
"***c" are constituent catalogs from IPGH catalog
"***wy" are constituent catalogs from Wysession et al. catalog (Reference 338)
"***me" are constituent catalogs from the Mexico Composite Catalog
"***np" are constituent catalogs from National Geophysical Data Center USGS "PDE" catalog

(b) Distance to epicenter ">1609" is greater than 1000 miles.

(c) "X" indicates modified Mercalli Intensity of {Roman numeral} 10; "F" indicates the earthquake was felt.

Table 2.5.2-202
Conversion between Body-Wave (m_b) and Moment (M_w) Magnitudes[(a)]

Convert	To	Convert	To
m_b	M_w	M_w	m_b
4.00	3.77	4.00	4.28
4.10	3.84	4.10	4.41
4.20	3.92	4.20	4.54
4.30	4.00	4.30	4.66
4.40	4.08	4.40	4.78
4.50	4.16	4.50	4.90
4.60	4.24	4.60	5.01
4.70	4.33	4.70	5.12
4.80	4.42	4.80	5.23
4.90	4.50	4.90	5.33
5.00	4.59	5.00	5.43
5.10	4.69	5.10	5.52
5.20	4.78	5.20	5.61
5.30	4.88	5.30	5.70
5.40	4.97	5.40	5.78
5.50	5.08	5.50	5.87
5.60	5.19	5.60	5.95
5.70	5.31	5.70	6.03
5.80	5.42	5.80	6.11
5.90	5.54	5.90	6.18
6.00	5.66	6.00	6.26
6.10	5.79	6.10	6.33
6.20	5.92	6.20	6.40
6.30	6.06	6.30	6.47
6.40	6.20	6.40	6.53
6.50	6.34	6.50	6.60
6.60	6.49	6.60	6.66
6.70	6.65	6.70	6.73
6.80	6.82	6.80	6.79
6.90	6.98	6.90	6.85
7.00	7.16	7.00	6.91
7.10	7.33	7.10	6.97
7.20	7.51	7.20	7.03
7.30	7.69	7.30	7.09
7.40	7.87	7.40	7.15
7.50	8.04	7.50	7.20
—	—	7.60	7.26
—	—	7.70	7.32
—	—	7.80	7.37
—	—	7.90	7.43
—	—	8.00	7.49

(a) Average of relations given by References 210, 244, and 252

Table 2.5.2-203 (Sheet 1 of 10)
Earthquake Catalog for the Phase 2 Investigation Region [15°N to 24°N, 100°W to 65°W] for which the Events are M_w Magnitude Greater than or Equal to 6.0

Catalog Reference[a]	Year	Month	Day	Hr	Min	Sec	Lat	Lon	Depth (km)	Int	M_w	Epicenter (km)[b]
CUBA	1502	0	0	0	0	0.00	18.400	–69.900	30	—	6.21	1324
FELD	1539	11	24	0	0	0.00	16.750	–86.750	5	X[c]	7.69	1166
CUBA	1562	12	3	1	0	0.00	19.600	–70.800	30	—	7.23	1168
CUBA	1578	8	0	0	0	0.00	19.900	–76.000	30	—	6.78	753
PM c	1591	3	14	0	0	0.00	16.000	–92.500	0	8	7.00	>1609
CUBA	1667	0	0	0	0	0.00	17.800	–77.000	30	—	6.78	909
CUBA	1673	5	9	11	30	0.00	18.400	–70.300	30	—	7.53	1291
CUBA	1678	2	11	14	59	0.00	19.900	–76.000	30	8[d]	6.78	753
CUBA	1684	0	0	0	0	0.00	18.400	–70.300	30	—	7.53	1291
NOAA	1691	0	0	0	0	0.00	18.300	–70.400	33	—	7.73	1289
CUBA	1692	6[e]	7[e]	0	0	0.00	18.200	–77.000	33	X[c],[e]	7.78	868
NOAA	1697	2	25	0	0	0.00	16.700	–99.200	0	—	7.83	>1609
CUBA	1701	11	9	0	0	0.00	18.700	–72.800	30	—	6.21	1072
SUARc	1711	8	15	0	0	0.00	19.000	–98.000	0	9	6.80	>1609
WHE c	1714	5	5	0	0	0.00	15.450	–92.200	10	7	6.23	>1609
WHE c	1728	0	0	0	0	0.00	15.755	–90.400	5	7	6.23	1496
WHE c	1741	2	15	0	0	0.00	15.750	–90.420	10	8	7.00	1497
W&C c	1743	5	30	0	0	0.00	16.750	–92.750	33	8	8.19	1603
WHE c	1750	3	8	0	0	0.00	15.450	–91.480	10	7	6.57	1600
CUBA	1751	9	16	3	29	0.00	18.600	–72.300	30	—	6.83	1117
CUBA	1751	10	18	20	0	0.00	18.400	–70.600	30	—	7.28	1266
NOAA	1754	9	1	0	0	0.00	16.700	–99.200	0	—	7.83	>1609
SAL c	1757	12	14	0	0	0.00	20.000	–75.833	10	—	6.23	755
CUBA	1760	7	11	0	0	0.00	19.900	–76.000	30	—	6.78	753
CUBA	1761	10	28	20	29	0.00	18.400	–69.900	30	—	6.21	1324
CUBA	1761	11	21	13	0	0.00	18.400	–70.800	30	—	6.64	1250
W&C c	1765	10	24	0	0	0.00	15.000	–91.916	0	8	7.59	>1609

Table 2.5.2-203 (Sheet 2 of 10)
Earthquake Catalog for the Phase 2 Investigation Region [15°N to 24°N, 100°W to 65°W] for which the Events are M_w Magnitude Greater than or Equal to 6.0

Catalog Reference[a]	Year	Month	Day	Hr	Min	Sec	Lat	Lon	Depth (km)	Int	M_w	Epicenter (km)[b]
CUBA	1766	6	12	5	14	0.00	19.900	–76.100	30	9[f]	7.53	747
CUBA	1770	6	4	0	15	0.00	18.600	–72.600	70	—	7.53	1095
SUARc	1776	4	21	0	0	0.00	16.800	100.000	0	9	7.70	>1609
CUBA	1783	2	11	0	0	0.00	19.700	–70.800	30	—	6.13	1162
SAL c	1784	7	29	0	0	0.00	19.780	–72.280	33	8	6.75	1033
NOAA	1785	0	0	0	0	0.00	16.700	–99.200	0	—	7.83	>1609
WHE c	1785	1	6	0	0	0.00	15.500	–89.700	5	9	7.40	1468
NOAA	1787	0	0	0	0	0.00	19.000	–66.000	33	—	8.03	>1609
SUARc	1787	3	28	0	0	0.00	16.000	–97.000	0	X[c]	8.40	>1609
CUBA	1793	4	0	0	0	0.00	18.400	–69.900	30	—	6.21	1324
WHE c	1795	12	29	0	0	0.00	15.375	–91.450	5	7	6.23	1604
SAL c	1798	5	28	0	0	0.00	18.800	–72.300	33	6	6.23	1102
WHE c	1798	7	2	0	0	0.00	15.080	–90.070	10	7	6.23	1529
W&C c	1804	0	0	0	0	0.00	16.500	–92.666	0	7	6.80	>1609
CUBA	1812	11	11	10	0	0.00	17.800	–77.000	20	—	6.13	909
NOAA	1816	7	22	0	0	0.00	15.500	–91.500	33	—	7.63	1598
SUARc	1820	5	4	0	0	0.00	16.500	–99.000	0	9	7.80	>1609
WHE c	1820	6	6	0	0	0.00	15.065	–90.320	5	7	6.23	1548
KSS c	1820	10	19	0	0	0.00	15.600	–88.050	10	8	6.44	1351
WHE c	1821	5	6	0	0	0.00	15.005	–91.165	15	8	6.37	>1609
SAL c	1826	9	18	9	8	0.00	19.500	–76.000	33	8	7.00	790
SAL c	1830	4	14	11	30	0.00	18.500	–72.300	10	7	6.57	1125
SUARc	1837	11	23	0	0	0.00	16.000	–98.000	0	—	7.70	>1609
CUBA	1842	5	7	22	15	0.00	19.800	–72.200	60	9[d]	8.23	1038
CUBA	1842	7	7	0	0	0.00	19.900	–76.000	30	—	6.13	753
CARIB	1844	4	16	13	20	0.00	18.300	–66.800	0	8	6.40	1599
SUARc	1845	8	7	0	0	0.00	16.800	100.000	0	X[c]	8.30	>1609

Table 2.5.2-203 (Sheet 3 of 10)
Earthquake Catalog for the Phase 2 Investigation Region [15°N to 24°N, 100°W to 65°W] for which the Events are M_w Magnitude Greater than or Equal to 6.0

Catalog Reference[a]	Year	Month	Day	Hr	Min	Sec	Lat	Lon	Depth (km)	Int	M_w	Epicenter (km)[b]
PM c	1851	5	17	0	0	0.00	15.083	–91.830	0	8	6.40	>1609
CUBA	1852	7	7	12	25	0.00	19.700	–79.700	30	9[f]	7.53	635
CUBA	1852	8	20	14	5	0.00	19.750	–75.320	30	—	7.33	809
CUBA	1852	11	26	8	44	0.00	19.900	–76.200	30	—	6.55	741
KSS c	1853	8	26	0	0	0.00	15.860	–86.265	0	7	6.03	1224
ROJ c	1856	5	5	0	0	0.00	16.400	–88.100	10	5	6.10	1282
KSS c	1856	8	4	22	47	0.00	16.750	–86.750	5	X[c]	7.69	1166
SAL c	1856	8	28	18	0	0.00	18.500	–65.000	33	6	6.40	>1609
CUBA	1858	1	28	10	14	0.00	19.900	–76.000	30	—	6.55	753
CUBA	1860	4	9	3	30	0.00	18.600	–73.200	50	—	6.73	1051
SAL c	1860	10	23	0	0	0.00	18.500	–67.500	33	7	6.57	1525
SUARc	1864	10	3	0	0	0.00	19.000	–97.000	0	9	7.40	>1609
SAL c	1865	8	30	0	0	0.00	18.000	–66.500	33	6	6.07	>1609
SAL c	1867	11	12	5	0	0.00	19.000	–76.250	10	6	6.40	823
SAL c	1867	11	18	20	0	0.00	18.500	–65.000	33	8	7.50	>1609
SAL c	1870	9	11	0	0	0.00	19.000	–77.000	10	6	6.23	787
SAL c	1874	8	26	11	15	0.00	19.000	–66.000	50	6	6.40	>1609
SAL c	1875	12	9	0	0	0.00	19.000	–67.000	50	7	6.40	1541
CUBA	1880	1	23	4	39	0.00	22.700	–83.000	15	8[f]	6.13	404
SAL c	1880	12	30	0	0	0.00	18.250	–76.500	10	6	6.07	885
KSS c	1881	4	23	0	0	0.00	16.550	–87.500	10	8	6.44	1230
SAL c	1882	0	0	0	0	0.00	18.500	–70.000	33	6	6.23	1309
SUARc	1882	7	19	0	0	0.00	18.000	–98.000	0	9	6.70	>1609
CUBA	1887	9	23	11	55	0.00	19.400	–73.400	60	9[d]	7.93	973
NOAA	1897	6	5	0	0	0.00	17.000	–96.300	0	—	7.03	>1609
CUBA	1897	12	29	11	32	0.00	20.100	–71.200	50	—	7.03	1102
NOAA	1899	1	24	23	43	0.00	17.000	–98.000	60	—	8.42	>1609

Table 2.5.2-203 (Sheet 4 of 10)
Earthquake Catalog for the Phase 2 Investigation Region [15°N to 24°N, 100°W to 65°W] for which the Events are M_w Magnitude Greater than or Equal to 6.0

Catalog Reference[a]	Year	Month	Day	Hr	Min	Sec	Lat	Lon	Depth (km)	Int	M_w	Epicenter (km)[b]
AMB c	1899	3	25	14	27	0.00	16.800	–92.800	35	—	6.26	1604
GUT c	1899	6	14	0	0	0.00	18.000	–77.000	0	—	7.80	888
CHA c	1902	1	16	0	0	0.00	17.620	–99.720	0	—	7.00	>1609
EV02	1902	2	17	0	31	0.00	20.000	–70.000	0	—	6.93	1214
EV02	1902	9	23	20	18	0.00	16.000	–93.000	0	—	7.80	>1609
EV02	1903	1	14	1	47	0.00	15.000	–98.000	0	—	7.40	>1609
GUT c	1903	8	16	0	0	0.00	20.000	–72.000	0	—	6.44	1041
MACRc	1906	6	22	0	0	0.00	19.500	–76.000	10	7	6.57	790
CUBA	1907	1	14	20	29	0.00	18.400	–76.800	20	—	6.64	856
EV02	1907	4	15	6	8	6.00	17.000	100.000	0	—	7.90	>1609
EV02	1908	3	26	23	3	30.00	18.000	–99.000	80	—	7.73	>1609
EV02	1910	1	1	11	2	0.00	16.500	–84.000	60	—	7.10	1057
CHA c	1911	2	3	0	0	0.00	18.200	–96.360	80	—	7.19	>1609
EV02	1911	10	6	10	16	12.00	19.000	–70.500	0	—	6.83	1233
CUBA	1912	4	9	8	32	29.00	19.000	–85.000	0	—	7.69	855
EV02	1912	6	12	12	43	42.00	17.000	–89.000	0	—	6.83	1292
EV02	1912	11	19	13	55	0.00	19.000	100.000	80	—	6.93	>1609
EV02	1912	12	9	8	32	24.00	15.500	–93.000	0	—	7.10	>1609
CUBA	1914	2	28	5	19	0.00	21.300	–76.200	50	—	6.29	619
ISSv	1914	3	30	0	41	11.00	19.000	–96.000	0	—	7.23	>1609
ISC	1914	8	3	11	25	30.00	18.500	–76.500	35	—	6.13	1136
CUBA	1914	8	25	5	19	0.00	19.530	–76.370	30	—	6.73	766
ISSv	1915	10	11	19	32	50.00	18.000	–69.500	0	—	6.83	1385
EV02	1916	6	2	13	59	24.00	17.500	–95.000	150	—	7.03	>1609
ISSv	1916	11	21	6	25	24.00	18.000	100.000	0	—	6.80	>1609
ISSv	1916	11	30	3	17	50.00	19.000	–70.000	0	—	7.00	1275
ISSv	1917	2	20	19	29	32.00	19.000	–80.000	0	6[d]	7.20	710

Table 2.5.2-203 (Sheet 5 of 10)
Earthquake Catalog for the Phase 2 Investigation Region [15°N to 24°N, 100°W to 65°W] for which the Events are M_w Magnitude Greater than or Equal to 6.0

Catalog Reference[a]	Year	Month	Day	Hr	Min	Sec	Lat	Lon	Depth (km)	Int	M_w	Epicenter (km)[b]
ISSv	1918	10	11	14	14	25.00	18.500	–68.000	0	—	7.30	1480
AMB c	1918	10	19	3	22	45.00	15.000	–91.000	35	—	6.24	1602
ISSv	1920	1	4	4	21	58.00	18.200	–97.500	0	—	7.83	>1609
ISSv	1920	4	19	21	6	25.00	18.400	–94.300	0	—	6.83	>1609
ISSv	1921	2	4	8	22	35.00	16.500	–89.500	0	—	7.43	1369
ISSv	1922	12	18	12	34	48.00	18.500	–68.000	0	—	6.29	1480
ISSv	1923	11	3	8	37	40.00	19.000	–74.000	95	—	6.13	962
ISSv	1925	6	14	22	28	6.00	17.500	–83.000	0	—	6.55	917
ISSv	1925	12	10	14	14	42.00	15.500	–92.500	0	—	7.00	>1609
ISSv	1928	3	22	4	16	50.00	16.000	–96.000	0	—	7.50	>1609
ISSv	1928	4	17	3	25	12.00	17.500	–94.500	0	—	7.73	>1609
ISSv	1928	6	17	3	19	19.00	16.200	–97.200	0	—	7.70	>1609
ISSv	1929	8	17	23	40	36.00	16.300	–99.000	0	—	6.17	>1609
ISSv	1931	1	15	1	50	49.00	16.400	–96.300	0	—	7.80	>1609
ISSv	1931	7	17	9	13	50.00	16.200	–97.200	0	—	6.29	>1609
ISSv	1931	9	26	19	50	33.00	15.000	–91.500	0	—	6.13	>1609
ISSv	1932	2	3	6	16	3.00	19.700	–75.500	0	—	6.83	802
ISSv	1932	6	6	11	50	0.00	19.600	–76.500	0	—	6.13	753
ISSv	1934	1	28	19	10	10.00	16.900	–99.600	0	—	6.83	>1609
ISC	1934	7	27	2	25	45.00	16.000	–92.500	50	—	6.29	>1609
ISC	1934	12	3	2	38	29.00	15.000	–88.750	35	—	6.29	1449
ISSv	1937	5	28	15	35	51.00	17.100	–93.400	95	—	6.55	>1609
ISSv	1937	7	26	3	47	3.00	18.500	–95.700	0	—	7.23	>1609
ISSv	1937	12	23	13	17	54.00	16.300	–98.600	0	—	7.40	>1609
ISC	1938	6	28	19	17	42.00	18.000	100.000	110	—	6.55	>1609
ISSv	1939	6	12	4	5	9.00	20.500	–66.000	0	—	6.29	1559
ISC	1939	9	28	14	58	27.00	15.500	–91.500	110	—	6.29	1598

Table 2.5.2-203 (Sheet 6 of 10)
Earthquake Catalog for the Phase 2 Investigation Region [15°N to 24°N, 100°W to 65°W] for which the Events are M_w Magnitude Greater than or Equal to 6.0

Catalog Reference[a]	Year	Month	Day	Hr	Min	Sec	Lat	Lon	Depth (km)	Int	M_w	Epicenter (km)[b]
ISSv	1941	4	7	23	29	17.00	17.500	–78.400	0	—	7.03	897
ISSv	1941	6	27	17	11	37.00	17.100	–93.400	160	—	6.29	>1609
ISSv	1942	10	28	10	44	39.00	15.000	–96.100	0	—	6.29	>1609
ISSv	1942	11	12	4	55	25.00	16.500	–94.400	0	—	6.83	>1609
ISSv	1943	7	29	3	2	14.00	19.100	–67.100	0	—	7.60	1526
EV02	1943	9	23	15	0	44.00	15.000	–91.500	110	—	6.83	>1609
EV02	1944	6	28	7	58	54.00	15.000	–92.500	0	—	7.13	>1609
ISSv	1945	10	11	16	53	2.00	18.300	–97.600	95	—	6.55	>1609
ISSv	1946	3	25	8	47	39.00	19.700	–74.700	0	—	6.13	855
ISSv	1946	5	15	22	10	34.00	15.500	–96.700	0	—	6.17	>1609
ISSv	1946	6	7	4	13	22.00	16.900	–94.200	95	—	6.93	>1609
ISSv	1946	8	4	17	51	4.00	18.900	–68.900	0	—	7.90	1377
ISSv	1946	8	8	13	28	28.00	19.600	–69.400	0	—	7.50	1290
ISSv	1947	8	7	0	40	20.00	19.900	–75.300	0	—	6.83	798
ISSv	1948	1	6	17	25	48.00	16.000	–98.400	0	—	7.03	>1609
ISSv	1948	8	11	10	36	18.00	17.700	–95.200	65	—	6.83	>1609
ISSv	1949	12	22	9	30	47.00	15.900	–93.000	65	—	6.57	>1609
ISSv	1950	8	3	6	14	55.00	18.100	–99.900	95	—	6.18	>1609
PDEnp	1950	10	23	17	5	25.00	15.000	–91.500	0	—	7.53	>1609
ISSv	1950	12	14	14	15	43.00	16.300	–98.600	0	—	7.30	>1609
ISSv	1951	12	12	1	37	40.00	16.500	–96.900	160	—	7.03	>1609
ISSv	1952	1	31	20	16	49.00	15.000	–93.800	95	—	6.34	>1609
ISSv	1952	5	14	21	11	35.00	16.500	–86.500	0	—	6.10	1175
ISSv	1952	10	28	4	29	52.00	18.300	–73.300	0	—	7.03	1069
ISSv	1953	5	31	19	58	39.00	19.400	–70.400	33	—	6.93	1215
PEREZ	1953	12	1	15	18	33.00	16.400	–98.850	0	—	6.70	>1609
ISC	1954	1	28	22	14	52.00	16.530	–99.720	0	—	6.04	>1609

Table 2.5.2-203 (Sheet 7 of 10)
Earthquake Catalog for the Phase 2 Investigation Region [15°N to 24°N, 100°W to 65°W] for which the Events are M_w Magnitude Greater than or Equal to 6.0

Catalog Reference[a]	Year	Month	Day	Hr	Min	Sec	Lat	Lon	Depth (km)	Int	M_w	Epicenter (km)[b]
ISSv	1954	5	13	14	46	39.00	16.900	–95.900	65	—	6.60	>1609
ISSv	1954	12	10	13	0	27.00	17.800	–81.800	0	—	6.37	855
ISSv	1955	9	26	8	28	31.00	15.900	–92.200	225	—	6.93	>1609
ISSv	1956	7	9	9	56	12.00	20.000	–72.950	40	—	6.93	963
ISSv	1956	11	9	13	6	15.00	17.450	–94.080	130	—	6.48	>1609
ISSv	1957	3	2	0	27	36.00	18.300	–78.150	0	—	6.61	818
ISSv	1957	4	10	5	12	7.00	15.530	–98.040	0	—	6.70	>1609
ISSv	1957	5	15	2	11	9.00	16.750	–93.510	125	—	6.03	>1609
ISSv	1957	7	28	8	40	7.00	17.070	–99.150	0	—	7.80	>1609
ISSv	1957	9	12	0	28	3.00	16.990	–85.600	0	—	6.04	1079
ISSv	1959	1	27	0	20	24.00	18.080	–68.660	90	—	6.04	1450
ISSv	1959	2	20	18	16	20.00	15.940	–90.590	48	7	6.57	1494
ISSv	1959	4	12	9	54	56.00	17.070	–95.040	124	—	6.40	>1609
PEREZ	1959	4	28	11	9	46.00	15.830	–92.830	0	—	6.34	>1609
ISSv	1959	5	24	19	17	40.00	17.610	–97.170	63	—	6.37	>1609
ISSv	1959	8	26	8	25	31.00	18.260	–94.430	0	—	6.93	>1609
ISC	1961	10	12	13	53	28.00	18.800	–65.000	50	—	6.37	>1609
ISSv	1961	11	16	8	19	49.00	18.500	–69.260	78	—	6.13	1371
PEREZ	1961	12	4	7	36	22.00	18.200	–69.100	0	—	6.34	1404
ISSv	1962	1	8	1	0	19.00	18.480	–70.400	0	—	6.73	1277
ISSv	1962	4	20	5	47	52.00	20.500	–72.140	0	—	6.73	997
ISSv	1962	4	22	4	45	26.00	15.470	–93.080	113	—	6.13	>1609
ISSv	1962	5	11	14	11	55.00	17.260	–99.630	37	—	7.30	>1609
ISSv	1962	5	20	15	1	15.00	20.630	–65.800	0	—	6.52	1573
ISSv	1962	7	24	21	8	22.00	15.420	–92.490	134	—	6.06	>1609
ISSv	1962	7	25	4	37	42.00	18.900	–81.410	0	—	6.29	728
EV02	1965	4	3	11	29	12.66	16.024	–97.861	30	—	6.29	>1609

Table 2.5.2-203 (Sheet 8 of 10)
Earthquake Catalog for the Phase 2 Investigation Region [15°N to 24°N, 100°W to 65°W] for which the Events are M_w Magnitude Greater than or Equal to 6.0

Catalog Reference[a]	Year	Month	Day	Hr	Min	Sec	Lat	Lon	Depth (km)	Int	M_w	Epicenter (km)[b]
NENG	1965	8	23	19	46	1.63	16.176	–95.847	10	—	6.73	>1609
CUBA	1965	10	16	9	30	0.00	18.500	–77.900	10	—	6.13	804
PDEnp	1965	12	9	6	7	47.70	17.300	100.000	54	—	6.04	>1609
PEREZ	1967	2	4	14	8	50.00	24.000	–65.700	1	—	6.43	1480
NENG	1968	8	2	14	6	46.18	16.493	–97.771	49	—	6.37	>1609
W&C c	1970	4	29	0	0	0.00	15.000	–92.333	56	—	7.09	>1609
NENG	1971	6	11	12	56	6.75	17.983	–69.809	59	—	6.04	1360
NENG	1972	9	16	9	14	35.88	15.187	–96.263	32	—	6.04	>1609
NENG	1973	8	28	9	50	41.02	18.233	–96.608	80	—	6.73	>1609
NENG	1976	2	4	9	1	46.20	15.296	–89.145	12	—	7.50	1448
NENG	1977	8	20	3	51	56.50	16.720	–86.638	31	—	6.40	1162
NENG	1978	3	19	1	39	11.37	16.932	–99.782	11	—	6.60	>1609
NENG	1978	11	29	19	52	50.15	16.011	–96.603	24	—	7.80	>1609
NENG	1979	3	23	19	32	32.73	17.963	–69.077	81	—	6.70	1422
NENG	1979	6	22	6	30	56.37	17.008	–94.623	113	—	6.90	>1609
NENG	1979	10	1	14	14	12.04	15.762	–92.198	164	—	6.20	>1609
NENG	1980	8	9	5	45	10.49	15.912	–88.490	16	—	6.50	1350
NENG	1980	10	24	14	53	35.55	18.175	–98.235	64	—	7.20	>1609
NENG	1981	9	14	12	44	31.00	18.260	–68.919	169	—	6.10	1416
NENG	1982	4	10	16	25	37.53	17.502	–83.427	19	—	6.30	931
NENG	1982	6	7	6	52	33.45	16.407	–98.294	8	—	6.90	>1609
NENG	1983	1	24	8	17	40.21	16.131	–95.238	48	—	6.80	>1609
NENG	1983	9	15	10	39	4.02	16.088	–93.179	118	—	6.30	>1609
NENG	1984	6	24	11	17	16.32	17.981	–69.371	45	—	6.70	1397
NENG	1984	7	2	4	50	44.25	16.753	–98.493	34	—	6.20	>1609
NENG	1985	9	15	7	57	55.31	17.940	–97.185	68	—	6.00	>1609
NENG	1986	7	5	22	9	34.27	15.488	–92.523	72	—	6.00	>1609

Table 2.5.2-203 (Sheet 9 of 10)
Earthquake Catalog for the Phase 2 Investigation Region [15°N to 24°N, 100°W to 65°W] for which the Events are M_w Magnitude Greater than or Equal to 6.0

Catalog Reference[a]	Year	Month	Day	Hr	Min	Sec	Lat	Lon	Depth (km)	Int	M_w	Epicenter (km)[b]
NENG	1987	3	12	12	18	13.86	15.545	–94.618	45	—	6.10	>1609
NENG	1987	7	15	7	16	14.62	17.508	–97.153	64	—	6.20	>1609
NENG	1988	11	3	19	42	20.70	19.000	–67.329	40	—	6.00	1511
NENG	1989	4	25	14	29	2.07	16.779	–99.275	19	—	6.90	>1609
NENG	1989	9	16	23	20	54.80	16.463	–93.661	113	—	6.10	>1609
NENG	1992	5	25	16	55	5.82	19.618	–77.883	23	7[f]	6.80	688
PRSN	1992	11	20	22	13	21.00	19.060	–71.660	47	—	6.37	1134
NENG	1993	5	15	3	12	35.09	16.725	–98.325	25	—	6.10	>1609
NENG	1993	9	30	18	27	50.98	15.176	–94.851	19	—	6.50	>1609
NENG	1993	10	24	7	52	17.07	16.753	–98.758	21	—	6.60	>1609
NENG	1994	3	14	20	51	25.80	15.943	–92.403	164	—	6.90	>1609
NENG	1995	6	27	10	10	0.41	18.794	–81.767	15	—	6.00	746
NENG	1995	9	14	14	4	33.23	16.849	–98.608	23	—	7.40	>1609
NENG	1995	10	21	2	38	58.25	16.836	–93.465	159	—	7.20	>1609
NENG	1997	7	19	14	22	7.07	16.203	–98.154	15	—	6.70	>1609
NENG	1998	2	3	3	2	0.63	15.900	–96.245	24	—	6.30	>1609
NENG	1998	6	7	23	20	14.04	15.966	–93.741	75	—	6.30	>1609
NENG	1999	6	15	20	42	6.60	18.381	–97.445	63	—	7.00	>1609
NENG	1999	7	11	14	14	18.97	15.791	–88.285	15	—	6.70	1348
NENG	1999	9	30	16	31	14.81	16.055	–96.905	40	—	7.50	>1609
NENG	1999	12	1	19	23	8.62	17.667	–82.370	15	—	6.30	882
NENG	2000	3	12	22	21	31.62	15.141	–92.411	53	—	6.30	>1609
ISC	2000	12	4	4	42	15.40	15.014	–93.833	36	—	6.13	>1609
NENG	2001	11	28	14	32	34.62	15.683	–93.118	84	—	6.40	>1609
NENG	2003	9	22	4	45	38.67	19.766	–70.693	14	—	6.40	1167
NENG	2004	12	14	23	20	13.77	18.939	–81.384	13	—	6.80	724
NENG	2005	3	17	13	37	36.93	15.183	–91.360	194	—	6.20	>1609

Table 2.5.2-203 (Sheet 10 of 10)
Earthquake Catalog for the Phase 2 Investigation Region [15°N to 24°N, 100°W to 65°W] for which the Events are M_w Magnitude Greater than or Equal to 6.0

Catalog Reference[(a)]	Year	Month	Day	Hr	Min	Sec	Lat	Lon	Depth (km)	Int	M_w	Epicenter (km)[(b)]
NENG	2007	2	4	20	56	58.82	19.326	–78.521	10	—	6.20	698
NENG	2007	7	6	1	9	18.50	16.493	–93.638	113	—	6.10	>1609
PDE-W	2008	2	12	12	50	18.49	16.360	–94.300	83	—	6.40	>1609

(a) "***c" are constituent catalogs from IPGH catalog
"***np" are constituent catalogs from National Geophysical Data Center USGS "PDE" catalog
(b) Distance to epicenter ">1609" is greater than 1000 miles.
(c) "X" indicates modified Mercalli Intensity of {Roman numeral} 10.
(d) McCann (Reference 282).
(e) DeMets and Wiggins-Grandison (Reference 229).
(f) Garcia et al. (Reference 254).

Table 2.5.2-204
Seismicity Events Recommended for Recurrence Analysis within the Gulf of Mexico

Earthquakes in the Gulf of Mexico: MAIN [or equivalent] Events, Rmb ≥ 3.0 or Int ≥ IV(4)													
Source Catalog[a]	Year	Month	Day	Hour	Minute	Second	Lat	Lon	Depth (km)	Int	Emb	Smb	Rmb
EPRIm	1927	12	15	4	30	0.00	28.900	–89.400	0	4	3.80	0.30	3.90
EPRIm	1929	7	28	17	0	0.00	28.900	–89.400	0	4	3.80	0.30	3.90
EPRIm	1958	11	6	23	8	0.00	29.900	–90.100	0	4	3.11	0.56	3.47
EPRIm	1963	11	5	22	45	3.40	27.490	–92.580	15	—	4.71	0.20	4.76
ISC	1967	3	21	20	41	27.00	24.000	–97.000	33	—	3.90	0.10	3.91
ISC	1967	10	4	2	45	45.00	27.000	–94.000	33	—	3.20	0.10	3.21
ISC c	1974	9	13	17	29	57.80	23.782	–96.428	0	—	3.60	0.10	3.61
EPRIm	1978	7	24	8	6	16.90	26.380	–88.720	15	—	4.88	0.10	4.89
EPRIm	1980	1	10	19	16	23.50	24.130	–85.710	15	—	3.88	0.10	3.89
ANSS	1984	1	23	0	11	59.38	26.716	–87.339	5	—	2.85	0.41	3.04
TEIme	1984	1	23	1	15	9.40	26.716	–87.339	5	—	2.85	0.41	3.04
PDE	1992	3	31	14	59	39.64	26.019	–85.731	5	—	3.80	0.10	3.81
TEIC	1992	9	27	17	2	25.70	27.225	–88.711	10	—	3.80	0.10	3.81
PDE	1992	11	30	8	33	1.48	23.251	–98.199	10	—	4.61	0.30	4.71
PDE	1994	6	30	1	8	24.22	27.911	–90.177	10	—	4.20	0.10	4.21
PDE	1997	4	18	14	57	35.39	25.782	–86.552	33	—	3.90	0.10	3.91
PDE	1998	7	6	6	54	3.79	25.016	–93.633	10	—	3.40	0.10	3.41
PDE	2000	12	9	6	46	9.12	28.027	–90.171	10	—	4.96	0.10	4.97
PDE	2001	3	16	4	39	7.68	28.361	–89.029	10	—	3.60	0.10	3.61
PDE	2002	5	27	0	28	16.99	27.117	–94.442	10	—	3.80	0.10	3.81
PDE	2002	9	19	14	44	36.15	27.822	–89.135	10	—	3.70	0.10	3.71
PDE	2003	4	13	4	52	53.92	26.087	–86.085	10	—	3.20	0.10	3.21
NENG	2003	10	10	14	48	17.25	23.142	–84.932	15	—	4.30	0.10	4.31
ISC	2004	6	18	19	20	56.40	27.027	–86.997	10	—	3.50	0.10	3.51
PDE	2006	2	10	4	14	22.20	27.828	–90.210	5	3	5.58	0.10	5.59
NENG	2006	9	10	14	56	7.75	26.258	–86.630	14	—	5.90	0.10	5.91

(a) "EPRIm" are the "MAIN" events from the EPRI catalog.
"***c" are constituent catalogs from IPGH catalog.
"***me" are constituent catalogs from the Mexico Composite Catalog.

Table 2.5.2-205 (Sheet 1 of 2)
Region 2 Matrix of Detection Probabilities; Modified to Extend the Matrix to Year 2007

Detection Probability Matrix: EPRI (Reference 243) Incompleteness Region 2 [Modified]								
	Year Intervals							
	1625–1779	1780–1859	1860–1909	1910–1949	1950–1974	1975–1084	1985–2007	
Magnitude Intervals	**155 years**	**80 years**	**50 years**	**40 years**	**25 years**	**10 years**	**23 years**	**Total Years**
3.3–3.89	0.00	0.00	0.10	0.51	0.63	1.00	1.00	74.2
3.9–4.49	0.00	0.00	0.15	0.90	1.00	1.00	1.00	101.5
4.5–5.09	0.00	0.00	0.24	0.98	1.00	1.00	1.00	109.2
5.1–5.69	0.00	0.00	0.24	0.98	1.00	1.00	1.00	109.2
5.7–6.29	0.00	0.00	0.70	1.00	1.00	1.00	1.00	133.0
6.3–7.5	0.00	0.01	1.00	1.00	1.00	1.00	1.00	148.8

Detection Probability Matrix: EPRI (Reference 243) Incompleteness Region 2 [Modified]												
	Year Intervals											
	1625–1779	1780–1859	1860–1899	1900–1924	1925–1949	1950–1959	1960–1964	1965–1969	1970–1974	1975–1979	1980–2007	
Magnitude Intervals	**155 years**	**80 years**	**40 years**	**25 years**	**25 years**	**10 years**	**5 years**	**5 years**	**5 years**	**5 years**	**28 years**	**Total Years**
3.3–3.89	0.00	0.00	0.10	0.31	0.51	0.55	0.60	0.65	0.80	1.00	1.00	73.1
3.9–4.49	0.00	0.00	0.15	0.53	0.90	0.99	1.00	1.00	1.00	1.00	1.00	99.5
4.5–5.09	0.00	0.00	0.24	0.61	0.98	0.99	1.00	1.00	1.00	1.00	1.00	107.3
5.1–5.69	0.00	0.00	0.24	0.61	0.98	0.99	1.00	1.00	1.00	1.00	1.00	107.3
5.7–6.29	0.00	0.00	0.70	0.85	1.00	1.00	1.00	1.00	1.00	1.00	1.00	132.3
6.3–7.5	0.00	0.01	1.00	1.00	1.00	1.00	1.00	1.00	1.00	1.00	1.00	148.8

Table 2.5.2-205 (Sheet 2 of 2)
Region 2 Matrix of Detection Probabilities; Modified to Extend the Matrix to Year 2007

Detection Probability Matrix: EPRI (Reference 243) Incompleteness Region 13 [Modified]												
	Year Intervals											
	1625–1779	1780–1859	1860–1899	1900–1924	1925–1949	1950–1959	1960–1964	1965–1969	1970–1974	1975–1979	1980–2007	
Magnitude Intervals	**155 years**	**80 years**	**40 years**	**25 years**	**25 years**	**10 years**	**5 years**	**5 years**	**5 years**	**5 years**	**28 years**	**Total Years**
3.3–3.89	0.00	0.00	0.24	0.48	0.71	0.80	0.88	0.93	0.98	1.00	1.00	94.2
3.9–4.49	0.00	0.00	0.24	0.51	0.77	0.90	0.97	0.98	0.99	1.00	1.00	98.2
4.5–5.09	0.00	0.00	0.30	0.61	0.92	0.97	0.99	1.00	1.00	1.00	1.00	107.9
5.1–5.69	0.00	0.03	0.69	0.84	0.99	0.99	1.00	1.00	1.00	1.00	1.00	133.7
5.7–6.29	0.11	0.54	0.98	0.99	1.00	1.00	1.00	1.00	1.00	1.00	1.00	207.2
6.3–7.5	0.51	0.90	1.00	1.00	1.00	1.00	1.00	1.00	1.00	1.00	1.00	299.1

Table 2.5.2-206
Matrix of Detection Probabilities for the Gulf of Mexico

Detection Probability Matrix: Gulf of Mexico and Near Atlantic												
	Year Intervals											
	1625–1779	1780–1859	1860–1899	1900–1924	1925–1949	1950–1959	1960–1964	1965–1969	1970–1974	1975–1979	1980–2007	
Magnitude Intervals	**155 years**	**80 years**	**40 years**	**25 years**	**25 years**	**10 years**	**5 years**	**5 years**	**5 years**	**5 years**	**28 years**	**Total Years**
3.3–3.89	0.00	0.00	0.00	0.00	0.00	0.00	0.00	0.00	0.00	0.00	0.30	8.4
3.9–4.49	0.00	0.00	0.00	0.00	0.00	0.00	0.00	0.00	0.00	0.50	0.60	19.3
4.5–5.09	0.00	0.00	0.00	0.00	0.00	0.00	0.00	0.50	0.70	0.70	0.90	34.7
5.1–5.69	0.00	0.00	0.00	0.00	0.00	0.00	0.70	0.90	1.00	1.00	1.00	46.0
5.7–6.29	0.00	0.00	0.00	0.00	0.70	0.90	1.00	1.00	1.00	1.00	1.00	74.5
6.3–7.5	0.00	0.00	0.00	0.30	0.90	1.00	1.00	1.00	1.00	1.00	1.00	88.0

Detection Probability Matrix: Near Florida												
	Year Intervals											
	1625–1779	1780–1859	1860–1899	1900–1924	1925–1949	1950–1959	1960–1964	1965–1969	1970–1974	1975–1979	1980–2007	
Magnitude Intervals	**155 years**	**80 years**	**40 years**	**25 years**	**25 years**	**10 years**	**5 years**	**5 years**	**5 years**	**5 years**	**28 years**	**Total Years**
3.3–3.89	0.00	0.00	0.12	0.24	0.36	0.40	0.44	0.47	0.49	0.50	0.65	51.3
3.9–4.49	0.00	0.00	0.12	0.25	0.39	0.45	0.49	0.49	0.50	0.75	0.80	58.7
4.5–5.09	0.00	0.00	0.15	0.31	0.46	0.49	0.50	0.75	0.85	0.85	0.95	71.3
5.1–5.69	0.00	0.02	0.35	0.42	0.50	0.50	0.85	0.95	1.00	1.00	1.00	89.8
5.7–6.29	0.06	0.27	0.49	0.50	0.85	0.95	1.00	1.00	1.00	1.00	1.00	140.9
6.3–7.5	0.26	0.45	0.50	0.65	0.95	1.00	1.00	1.00	1.00	1.00	1.00	193.5

Table 2.5.2-207 (Sheet 1 of 2)
Summary of EPRI Seismic Sources within the Site Region

Source	Description	Pa[a]	Mmax (m_b) and Weights[b]	Smoothing Options and Weights[c]	Interdependencies [d]	Largest Earthquake in Catalog (Emb)		New Data to Suggest Change in Source?			Updated Mmax (m_b) and Weights
						EPRI catalog (1627–1984)	Phase 1 Updated Catalog (1698–2007)	Geom.[e]	Mmax[f]	RI[g]	
Bechtel Group											
BZ1	Gulf Coast	1.00	5.4 [0.10] 5.7 [0.40] 6.0 [0.40] 6.6 [0.10]	1 [0.33] 2 [0.34] 3 [0.33]	Background P_B=1.00	4.9	5.9	No	Yes	No	6.1 [0.10] 6.4 [0.40] 6.6 [0.10] 6.7 [0.40]
Dames & Moore											
20	So. Coastal Marg.	1.00	5.3 [0.80] 7.2 [0.20]	1 [0.75] 2 [0.25]	None	4.6	5.6	No	Yes	No	5.6 [0.80] 7.2 [0.20]
Law Engineering											
126	South Coastal Block	1.00	4.6 [0.90] 4.9 [0.10]	1a [1.00]	Background P_B=0.49	4.4	5.0	No	Yes	No	5.6 [0.90] 5.7 [0.10]
Rondout Associates											
49-05	Appalachian Basement	1.00	4.8 [0.20] 5.5 [0.60] 5.8 [0.20]	2 [1.00]	Background P_B=1.00	4.4	5.0	No	Yes	No	5.0 [0.20] 5.5 [0.60] 5.8 [0.20]
51	Gulf Coast to Bahamas Fract. Zone	1.00	4.8 [0.20] 5.5 [0.60] 5.8 [0.20]	3 [1.00]	Background P_B=1.00	4.9	5.9	No	Yes	No	6.1 [0.30] 6.3 [0.55] 6.5 [0.15]
Weston Geophysical											
107	Gulf Coast	1.00	5.4 [0.71] 6.0 [0.29]	1a [0.20] 2a [0.80]	Background P_B=1.00	4.9	5.9	No	Yes	No	6.6 [0.89] 7.2 [0.11]
Woodward-Clyde Consultants											
BG-35	Turkey Point Background	N/A	5.8 [0.33] 6.2 [0.34] 6.6 [0.33]	1 [0.25] 6 [0.25] 7 [0.25] 8 [0.25]	N/A	3.7	6.1	Yes	No	No	5.8 [0.33] 6.2 [0.34] 6.6 [0.33]

Table 2.5.2-207 (Sheet 2 of 2)
Summary of EPRI Seismic Sources within the Site Region

Notes:

(a) Pa = Probability of activity (**Reference 243**)
(b) Maximum Magnitude (Mmax) and weights (**Reference 243**)
(c) Smoothing options are defined as follows (**Reference 243**):
Bechtel
1 = constant a, constant b (no prior); 2 = low smoothing on a, high smoothing on b (no prior); 3 = low smoothing on a, low smoothing on b (no prior)
Weights on magnitude intervals are all 1.0
Dames & Moore
1 = no smoothing on a, no smoothing on b (strong prior of 1.04); 2 = no smoothing on a, no smoothing on b (weak prior of 1.04)
Weights on magnitude units are [0.1, 0.2, 0.4, 1.0, 1.0, 1.0, 1.0]
Law Engineering
1a = high smoothing on a, constant b (strong prior of 1.05)
Weights on magnitude units are [0.0, 1.0, 1.0, 1.0, 1.0, 1.0, 1.0]
Rondout Associates
3 = low smoothing on a, constant b (strong prior of 1.0)
Weston Geophysical
1a = constant a, constant b (medium prior of 1.04); 2a = medium smoothing on a, medium smoothing on b (medium prior of 1.0)
Woodward-Clyde Consultants
1 = low smoothing on a, high smoothing on b (no prior); 6 = low smoothing on a, high smoothing on b (moderate prior of 1.0);
7 = low smoothing on a, high smoothing on b (moderate prior of 0.9); 8 = low smoothing on a, high smoothing on b (moderate prior of 0.8)
Weights on magnitude intervals are all 1.0
(d) P_B = the fraction of area of the background that is active (**Reference 243**)
(e) No, unless (1) new geometry proposed in literature or (2) new seismicity pattern.
(f) No, unless (1) new data suggest Mmax exceeds or differs significantly from the EPRI Mmax distribution or (2) exceeded by historical seismicity
(g) RI = recurrence interval; assumed no change if no new paleoseismic data or rate of seismicity has not significantly changed
N/A = Not Applicable

Table 2.5.2-208 (Sheet 1 of 2)
Mean and Fractile Seismic Hazard Data for Crystal River Site from EPRI-SOG Study and Units 6 & 7 Study

PGA		Bechtel			Dames & More			Law Engineering		
Ampl. cm/s^2	Hazard	EPRI-SOG	Units 6 & 7 Study	% diff	EPRI-SOG	Units 6 & 7 Study	% diff	EPRI-SOG	Units 6 & 7 Study	% diff
100	mean	1.47E-05	1.48E-05	0%	1.57E-05	1.58E-05	1%	2.23E-07	8.72E-08	–61%
	0.15	6.70E-06	6.46E-06	–4%	3.93E-06	3.98E-06	1%	1.49E-10	3.39E-29	–100%
	0.5	1.25E-05	1.29E-05	3%	8.84E-06	9.12E-06	3%	1.53E-07	3.89E-29	–100%
	0.85	2.25E-05	2.24E-05	0%	1.74E-05	2.48E-05	43%	2.38E-07	5.25E-09	–98%
250	mean	1.83E-06	1.86E-06	1%	2.08E-06	2.11E-06	1%	1.08E-08	9.18E-10	–92%
	0.15	7.77E-07	8.13E-07	5%	3.11E-07	3.09E-07	–1%	1.49E-10	3.39E-29	–100%
	0.5	1.50E-06	1.62E-06	8%	8.35E-07	8.71E-07	4%	1.18E-08	3.89E-29	–100%
	0.85	2.93E-06	3.02E-06	3%	6.06E-06	4.27E-06	–30%	1.61E-08	6.46E-12	–100%
500	mean	1.82E-07	1.90E-07	4%	2.99E-07	3.06E-07	2%	3.80E-10	7.52E-12	–98%
	0.15	4.64E-08	5.13E-08	11%	1.24E-08	1.29E-08	4%	1.49E-10	3.39E-29	–100%
	0.5	1.20E-07	1.45E-07	20%	4.52E-08	5.13E-08	13%	5.74E-10	3.89E-29	–100%
	0.85	3.67E-07	3.55E-07	–3%	1.08E-06	7.85E-07	–27%	6.74E-10	6.46E-15	–100%

Table 2.5.2-208 (Sheet 2 of 2)
Mean and Fractile Seismic Hazard Data for Crystal River Site from EPRI-SOG Study and Units 6 & 7 Study

PGA		Rondout			Weston			Woodward-Clyde			Total		
Ampl. cm/s^2	Hazard	EPRI-SOG	Units 6 & 7 Study	% diff	EPRI-SOG	Units 6 & 7 Study	% diff	EPRI-SOG	Units 6 & 7 Study	% diff	EPRI-SOG	Units 6 & 7 Study	% diff
100	mean	1.48E-05	1.48E-05	0%	2.47E-05	2.48E-05	0%	2.59E-05	2.60E-05	0%	1.60E-05	1.60E-05	0%
	0.15	5.27E-07	1.05E-08	–98%	7.94E-06	7.94E-06	0%	6.78E-07	4.96E-08	–93%	5.37E-06	5.37E-10	–100%
	0.5	1.55E-05	1.59E-05	3%	1.78E-05	1.82E-05	2%	1.65E-05	1.70E-05	3%	1.52E-05	1.20E-05	–21%
	0.85	2.71E-05	2.75E-05	1%	3.79E-05	3.89E-05	3%	4.97E-05	5.13E-05	3%	3.06E-05	3.06E-05	0%
250	mean	1.61E-06	1.63E-06	1%	2.79E-06	2.83E-06	1%	3.58E-06	3.62E-06	1%	1.98E-06	2.01E-06	2%
	0.15	2.60E-08	1.12E-11	–100%	6.72E-07	6.61E-07	–2%	4.44E-08	2.09E-11	–100%	5.40E-07	8.32E-14	–100%
	0.5	1.67E-06	1.74E-06	4%	1.79E-06	1.86E-06	4%	1.89E-06	2.00E-06	6%	1.67E-06	1.23E-06	–26%
	0.85	2.69E-06	2.82E-06	5%	5.17E-06	5.25E-06	2%	6.98E-06	6.92E-06	–1%	3.76E-06	3.35E-06	–11%
500	mean	1.19E-07	1.24E-07	4%	2.36E-07	2.46E-07	4%	4.52E-07	4.65E-07	3%	2.15E-07	2.22E-07	3%
	0.15	1.24E-09	9.12E-15	–100%	2.98E-08	2.95E-08	–1%	1.79E-09	4.42E-15	–100%	2.78E-08	1.64E-23	–100%
	0.5	1.11E-07	1.26E-07	14%	1.06E-07	1.18E-07	11%	1.40E-07	1.55E-07	11%	1.06E-07	7.76E-08	–27%
	0.85	1.81E-07	2.27E-07	25%	5.37E-07	5.75E-07	7%	8.74E-07	8.71E-07	0%	4.69E-07	3.67E-07	–22%

PGA = Peak ground acceleration
% diff = Percent difference between the 1989 calculations and the current hazard calculations at the Crystal River site

Table 2.5.2-209
Mean Hard Rock UHRS Accelerations (g)

Frequency, Hz	Mean 1E-04	Mean 1E-05	Mean 1E-06
PGA	0.0399	0.147	0.542
25	0.104	0.414	1.50
10	0.0822	0.278	0.932
5	0.0661	0.184	0.561
2.5	0.0499	0.110	0.275
1	0.0343	0.0663	0.131
0.5	0.0267	0.0519	0.104

UHRS = Uniform hazard response spectra
PGA = Peak ground acceleration

Table 2.5.2-210 (Sheet 1 of 2)
HF and LF Horizontal 1E-04 Rock Spectra, Amplification Factors, Site Spectra, and Raw and Smoothed Envelope Spectra

Horizontal 1E-04 Rock and Site Spectra UHRS (g)								
Freq,	Rock UHRS		Transfer Function		Surface UHRS		Raw Envelope	Smooth Spectrum
Hz	LF SA(g)	HF SA(g)	LF Amp	HF Amp	LF SA(g)	HF SA(g)	SA(g)	SA(g)
100	3.99E-02	3.99E-02	1.302	0.870	5.20E-02	3.47E-02	5.20E-02	5.20E-02
90	4.39E-02	4.40E-02	1.186	0.793	5.21E-02	3.49E-02	5.21E-02	5.21E-02
80	5.05E-02	5.07E-02	1.035	0.693	5.23E-02	3.52E-02	5.23E-02	5.23E-02
70	6.06E-02	6.10E-02	0.871	0.587	5.28E-02	3.58E-02	5.28E-02	5.28E-02
60	7.36E-02	7.43E-02	0.730	0.500	5.37E-02	3.71E-02	5.37E-02	5.37E-02
50	8.66E-02	8.76E-02	0.636	0.445	5.51E-02	3.90E-02	5.51E-02	5.51E-02
45	9.20E-02	9.31E-02	0.612	0.440	5.64E-02	4.09E-02	5.64E-02	5.65E-02
40	9.65E-02	9.77E-02	0.607	0.455	5.85E-02	4.44E-02	5.85E-02	5.86E-02
35	9.98E-02	1.01E-01	0.619	0.491	6.18E-02	4.96E-02	6.18E-02	6.18E-02
30	1.02E-01	1.03E-01	0.642	0.540	6.57E-02	5.57E-02	6.57E-02	6.55E-02
25	1.04E-01	1.04E-01	0.642	0.542	6.67E-02	5.64E-02	6.67E-02	6.65E-02
20	1.00E-01	1.02E-01	0.644	0.523	6.44E-02	5.33E-02	6.44E-02	6.43E-02
15	9.34E-02	9.58E-02	0.677	0.544	6.32E-02	5.21E-02	6.32E-02	6.29E-02
12.5	8.86E-02	9.02E-02	0.710	0.575	6.29E-02	5.19E-02	6.29E-02	6.28E-02
10	8.22E-02	8.22E-02	0.821	0.701	6.74E-02	5.76E-02	6.74E-02	6.71E-02
9	8.01E-02	8.05E-02	0.869	0.755	6.96E-02	6.07E-02	6.96E-02	6.99E-02
8	7.75E-02	7.81E-02	0.950	0.847	7.37E-02	6.62E-02	7.37E-02	7.32E-02
7	7.45E-02	7.50E-02	1.010	0.897	7.52E-02	6.73E-02	7.52E-02	7.52E-02
6	7.07E-02	7.11E-02	1.100	0.994	7.78E-02	7.07E-02	7.78E-02	7.84E-02
5	6.61E-02	6.61E-02	1.310	1.216	8.65E-02	8.03E-02	8.65E-02	8.63E-02
4	5.96E-02	5.60E-02	1.437	1.302	8.57E-02	7.29E-02	8.57E-02	8.69E-02
3	5.29E-02	4.40E-02	2.147	2.047	1.14E-01	9.01E-02	1.14E-01	1.11E-01
2.5	4.99E-02	3.69E-02	2.060	1.888	1.03E-01	6.97E-02	1.03E-01	1.02E-01
2	4.54E-02	2.88E-02	1.787	1.625	8.11E-02	4.69E-02	8.11E-02	8.07E-02
1.5	4.05E-02	2.00E-02	1.988	1.828	8.06E-02	3.65E-02	8.06E-02	8.02E-02
1.25	3.71E-02	1.55E-02	2.376	2.213	8.82E-02	3.43E-02	8.82E-02	8.84E-02
1	3.43E-02	1.12E-02	3.022	2.859	1.04E-01	3.21E-02	1.04E-01	1.05E-01
0.9	3.41E-02	9.61E-03	3.461	3.325	1.18E-01	3.20E-02	1.18E-01	1.15E-01
0.8	3.32E-02	8.06E-03	3.401	3.247	1.13E-01	2.62E-02	1.13E-01	1.12E-01
0.7	3.18E-02	6.59E-03	3.019	2.867	9.59E-02	1.89E-02	9.59E-02	9.72E-02
0.6	2.96E-02	5.21E-03	3.014	2.877	8.92E-02	1.50E-02	8.92E-02	8.86E-02
0.5	2.67E-02	3.92E-03	2.752	2.653	7.34E-02	1.04E-02	7.34E-02	7.17E-02
0.4	2.14E-02	3.14E-03	2.057	1.967	4.39E-02	6.17E-03	4.39E-02	4.46E-02
0.3	1.60E-02	2.35E-03	1.864	1.784	2.99E-02	4.20E-03	2.99E-02	3.00E-02
0.2	1.07E-02	1.57E-03	1.888	1.771	2.02E-02	2.78E-03	2.02E-02	2.01E-02
0.15	8.01E-03	1.18E-03	1.599	1.519	1.28E-02	1.79E-03	1.28E-02	1.29E-02

Table 2.5.2-210 (Sheet 2 of 2)
HF and LF Horizontal 1E-04 Rock Spectra, Amplification Factors, Site Spectra, and Raw and Smoothed Envelope Spectra

Horizontal 1E-04 Rock and Site Spectra UHRS (g)								
Freq,	Rock UHRS		Transfer Function		Surface UHRS		Raw Envelope	Smooth Spectrum
Hz	LF SA(g)	HF SA(g)	LF Amp	HF Amp	LF SA(g)	HF SA(g)	SA(g)	SA(g)
0.125	6.64E-03	9.75E-04	1.421	1.377	9.44E-03	1.34E-03	9.44E-03	9.37E-03
0.1	4.27E-03	6.27E-04	1.323	1.268	5.65E-03	7.95E-04	5.65E-03	5.65E-03

UHRS = Uniform hazard response spectra
LF = Low frequencies
HF = High frequencies
SA = Spectral acceleration
Amp = Amplitude

Table 2.5.2-211
Summary of Supplemental Sources and Truncated Woodward-Clyde Source

EPRI EST	New Source Area (km^2)[a]	New Source Total Earthquakes[b]	New Source Max Recorded Event (Emb)[b]	Mmax (m_b) and Weights
Bechtel	136,769	1	4.09	6.1 [0.10] 6.4 [0.40] 6.6 [0.10] 6.7 [0.40]
Dames & Moore	139,208	2	4.09	5.6 [0.80] 7.2 [0.20]
Law Engineering	97,273	1	4.09	5.6 [0.90] 5.7 [0.10]
Rondout Associates	103.436	1	4.09	6.1 [0.30] 6.3 [0.55] 6.5 [0.15]
Weston Geophysical	171,264	2	4.09	6.6 [0.89] 7.2 [0.11]
Woodward-Clyde[c] (truncated)	349,569	8	4.09	5.8 [0.33] 6.2 [0.34] 6.6 [0.33]

(a) Area calculated using North America Albers equal area conic projection.
(b) From updated earthquake catalog.
(c) Not a “supplemental” zone; Woodward-Clyde source BG-35 geometry is truncated by the northern boundary of the Cuba area and Northern Caribbean seismic source model.

EST = Earth Science Team

Table 2.5.2-212 (Sheet 1 of 2)
Geographic Coordinates of Supplemental Sources and Truncated Woodward-Clyde Source

Bechtel Group		Dames & Moore		Law Engineering		Rondout Associates		Weston Geophysical		Woodward-Clyde Consultants[a]	
Latitude	Longitude	Latitude	Longitude	Latitude	Longitude	Latitude	Longitude	Latitude	Longitude	Latitude	Longitude
27.512	–78.336	25.440	–83.228	25.026	–77.0478	26.630	–77.711	28.317	–80.311	26.006	–77.500
27.033	–77.927	26.133	–83.129	24.853	–77.495	26.531	–77.659	28.263	–79.768	25.420	–77.439
26.531	–77.659	25.030	–82.570	24.309	–77.662	25.986	–77.494	28.098	–79.223	24.840	–77.500
25.986	–77.494	25.000	–80.000	23.811	–77.930	25.420	–77.439	27.829	–78.721	22.400	–77.499
25.420	–77.439	25.020	–79.290	23.372	–78.292	24.853	–77.495	27.470	–78.285	22.400	–77.613
24.853	–77.495	25.620	–78.940	23.012	–78.733	24.309	–77.662	27.033	–77.927	22.760	–78.456
24.309	–77.662	27.100	–78.870	22.911	–78.923	23.811	–77.930	26.531	–77.659	22.911	–78.923
23.811	–77.930	28.032	–79.101	23.421	–80.497	23.372	–78.292	25.986	–77.494	23.421	–80.497
23.372	–78.292	27.829	–78.721	23.505	–81.043	23.012	–78.733	25.420	–77.439	23.505	–81.043
23.012	–78.733	27.470	–78.285	23.506	–82.095	22.911	–78.923	24.853	–77.495	23.506	–82.095
22.911	–78.923	27.033	–77.927	23.456	–82.445	23.421	–80.497	24.309	–77.662	23.456	–82.445
23.421	–80.497	26.531	–77.659	23.828	–82.748	23.505	–81.043	23.811	–77.930	23.304	–83.500
23.505	–81.043	25.986	–77.494	24.332	–83.014	23.506	–82.095	23.372	–78.292	28.400	–83.500
23.506	–82.095	25.420	–77.439	24.873	–83.175	23.456	–82.445	23.012	–78.733	28.400	–77.500
23.456	–82.445	24.853	–77.495	25.008	–83.188	23.828	–82.748	22.911	–78.923	26.006	–77.500
23.828	–82.748	24.309	–77.662	25.000	–79.999	24.332	–83.014	23.421	–80.497	—	—
24.332	–83.014	23.811	–77.930	25.026	–77.478	24.873	–83.175	23.505	–81.043	—	—
24.873	–83.175	23.372	–78.292	25.026	–77.478	25.000	–83.187	23.506	–82.095	—	—
25.182	–83.204	23.012	–78.733	—	—	25.000	–80.000	23.456	–82.445	—	—
25.150	–81.710	22.911	–78.923	—	—	25.030	–78.230	23.828	–82.748	—	—
25.070	–80.210	23.421	–80.497	—	—	25.160	–78.110	24.332	–83.014	—	—
25.440	–79.470	23.505	–81.043	—	—	25.520	–77.900	24.873	–83.175	—	—
26.240	–78.780	23.506	–82.095	—	—	25.980	–77.770	25.003	–83.187	—	—
27.150	–78.410	23.456	–82.445	—	—	26.630	–77.711	25.000	–80.000	—	—
27.512	–78.336	23.828	–82.748	—	—	—	—	26.620	–79.900	—	—
—	—	24.332	–83.014	—	—	—	—	28.317	–80.311	—	—
—	—	24.873	–83.175	—	—	—	—	—	—	—	—

Table 2.5.2-212 (Sheet 2 of 2)
Geographic Coordinates of Supplemental Sources and Truncated Woodward-Clyde Source

Bechtel Group		Dames & Moore		Law Engineering		Rondout Associates		Weston Geophysical		Woodward-Clyde Consultants[(a)]	
Latitude	Longitude	Latitude	Longitude	Latitude	Longitude	Latitude	Longitude	Latitude	Longitude	Latitude	Longitude
—	—	25.440	–83.228	—	—	—	—	—	—	—	—

(a) Not a “supplemental” zone; Woodward-Clyde source BG-35 geometry is truncated by the northern boundary of the Cuba area and Northern Caribbean seismic source model.
Note: Coordinates in decimal degrees.

Table 2.5.2-213
Geographic Coordinates of Updated Charleston Seismic Source (UCSS) Model Sources

UCSS Source	Longitude	Latitude
A	–80.707	32.811
A	–79.840	33.354
A	–79.527	32.997
A	–80.392	32.455
B	–81.216	32.485
B	–78.965	33.891
B	–78.3432	33.168
B	–80.587	31.775
B'	–78.965	33.891
B'	–78.654	33.531
B'	–80.900	32.131
B'	–81.216	32.485
C	–80.397	32.687
C	–79.776	34.425
C	–79.483	34.351
C	–80.109	32.614

Note: Coordinates in decimal degrees.

Table 2.5.2-214
Comparison of Post-EPRI Magnitude Estimates for the 1886 Charleston Earthquake

Study	Magnitude Estimation Method	Reported Magnitude Estimate	Assigned Weights	Mean Magnitude (M_w)
Johnston et al. (Reference 268)	Worldwide survey of passive-margin, extended-crust earthquakes	M_w 7.56 ± 0.35[(a)]	—	7.56
Martin and Clough (Reference 279)	Geotechnical assessment of 1886 liquefaction data	M_w 7–7.5	—	7.25
Johnston (Reference 267)	Isoseismal area regression, accounting for eastern North America anelastic attenuation	M_w 7.3 ± 0.26	—	7.3
Chapman and Talwani (Reference 223) (SCDOT)	Consideration of available magnitude estimates	M_w 7.1 M_w 7.3 M_w 7.5	0.2 0.6 0.2	7.3
Bakun and Hopper (Reference 211)	Isoseismal area regression, including empirical site corrections	M_I 6.4–7.2[(b)]	—	6.9[(c)]
Petersen et al. (Reference 300) (USGS)	Consideration of available magnitude estimates	M_w 6.8 M_w 7.1 M_w 7.3 M_w 7.5	0.20 0.20 0.45 0.15	7.2

(a) Estimate from Johnston et al. (Reference 268), Chapter 3.
(b) 95 percent confidence interval estimate; M_I (intensity magnitude) is considered equivalent to M_w (moment magnitude) (Reference 211).
(c) Bakun and Hopper's preferred estimate (Reference 211).

Table 2.5.2-215
Comparison of Talwani and Schaeffer and UCSS Age Constraints on Charleston-Area Paleoliquefaction Events

Liquefaction Event	Event Age (YBP)[b]	Talwani and Schaeffer (Reference 223)[a]				This Study
		Scenario 1		Scenario 2		
		Source	M[c]	Source	M[c]	Event Age (YBP)[b][d]
1886 A.D.	64	Charleston	7.3	Charleston	7.3	64
A	546 ± 17	Charleston	7+	Charleston	7+	600 ± 70
B	1,021 ± 30	Charleston	7+	Charleston	7+	1,025 ± 25
C	1,648 ± 74	Northern (Georgetown)	6+	—	—	—
C'	1,683 ± 70	—	—	Charleston	7+	1,695 ± 175
D	1,966 ± 212	Southern (Bluffton)	6+	—	—	—
E	3,548 ± 66	Charleston	7+	Charleston	7+	3,585 ± 115
F	5,038 ± 166	Northern (Georgetown)	6+	Charleston	7+	—
F'	—	—	—	—	—	5,075 ± 215
G	5,800 ± 500	Charleston	7+	Charleston	7+	—

(a) YBP = years before present, relative to 1950 A.D.
(b) Modified after Talwani and Schaeffer's (Reference 323) Table 2.
(c) Unspecified magnitude type.
(d) Event ages based upon our recalibration of radiocarbon ages to 2-sigma using OxCal 3.8, from data presented in Talwani and Schaeffer's (Reference 323) Table 2.

Table 2.5.2-216
List of Experts Contacted as part of Cuba and Northern Caribbean Source Model SSHAC Level 2 Process

Name	Affiliation	Response
Prof. Gail Atkinson	Carleton University, Ottawa, Canada	*[declined, lack of expertise]*
Prof. Eric Calais	Purdue University	Detailed response; email and telephone
Prof. Charles DeMets	University Wisconsin	Detailed response; email and telephone
Prof. James Dolan	University of Southern California	Detailed response; email and in-person
Dr. Art Frankel	U.S. Geological Survey	*[declined, conflict]*
Dr. Julio Garcia	National Institute of Oceanography and Experimental Geophysics (OGS), Trieste, Italy	Detailed response; email
Prof. Paul Mann	University of Texas	Detailed response; email
Dr. William McCann	Earth Scientific Consultants; TAG member	Detailed response; email, telephone, and in-person
Dr. James Pindell	Tectonic Analysis, Ltd.; Rice U.	*[declined, lack of expertise]*
Dr. Uri ten Brink	U.S. Geological Survey	*[declined, conflict]*
Dr. Marticia Tuttle	M. Tuttle & Associates	*[declined, conflict]*
Prof. Margaret Wiggins-Grandison	University of West Indies, Mona, Jamaica	Detailed response; email

SSHAC = Senior Seismic Hazard Analysis Committee

Table 2.5.2-217
Summary of Cuba and Northern Caribbean Seismic Source Parameters

Area Source	Closest Distance to Units 6 & 7 (mi)	Annual Number of Earthquakes of M_w 5.0 and Greater	*b*-value	Mmax (M_w)
1. Cuba areal source zone	140	0.0592	0.839	7.0 [0.5] 7.25 [0.5][(a)]

(a) For the PSHA calculation, this value was rounded up to M_w 7.3.

Fault Source	Closest Distance to Units 6 & 7 (mi)	Fault Type/ Dip	Slip Rate (mm/yr)	Seismic Coupling	Mmax (M_w)
2. Oriente – Western	420	Strike-slip/ 90°	8 [0.1] 11 [0.7] 13 [0.2]	0.6 [0.2] 0.8 [0.2] 1.0 [0.6]	7.5 [0.3] 7.7 [0.4] 8.0 [0.3]
3. Oriente – Eastern	445	Strike-slip/ 90°	8 [0.1] 11 [0.7] 13 [0.2]	1.0 [1.0]	7.5 [0.2] 7.7 [0.6] 7.9 [0.2]
4. Septentrional	545	Strike-slip/ 90°	6 [0.2] 9 [0.6] 12 [0.2]	1.0 [1.0]	8.0 [0.5] 8.25 [0.5]
5. Northern Hispaniola — Western	550	Thrust/ 20-25° south	4 [0.2] 6 [0.7] 8 [0.1]	1.0 [1.0]	7.8 [0.2] 8.0 [0.6] 8.3 [0.2]
6. Northern Hispaniola — Eastern	760	Thrust/ 20-25° south	4 [0.2] 6 [0.7] 8 [0.1]	1.0 [1.0]	8.0 [0.2] 8.3 [0.6] 8.6 [0.2]
7. Swan Islands — Western	620	Strike-slip/ 90°	18 [0.2] 19 [0.6] 20 [0.2]	1.0 [1.0]	7.8 [0.2] 8.0 [0.7] 8.3 [0.1]
8. Swan Islands — Eastern	540	Strike-slip/ 90°	18 [0.2] 19 [0.6] 20 [0.2]	0.6 [0.2] 0.8 [0.2] 1.0 [0.6]	7.2 [0.4] 7.5 [0.5] 7.7 [0.1]
9. Walton — Duanvale	490	Strike-slip/ 90°	6 [0.2] 8 [0.6] 10 [0.2]	0.8 [0.3] 1.0 [0.7]	7.3 [0.3] 7.6 [0.6] 7.8 [0.1]
10. Enriquillo-Plantain Garden	560	Strike-slip/ 90°	6 [0.2] 8 [0.6] 10 [0.2]	1.0 [1.0]	7.5 [0.2] 7.7 [0.6] 7.9 [0.2]

Table 2.5.2-218
Geographic Coordinates of Cuba Areal Source Zone

Latitude	Longitude
21.207	–74.814
20.377	–73.219
19.834	–77.659
19.995	–77.919
20.506	–78.637
20.892	–79.345
21.259	–80.143
21.385	–80.609
21.429	–81.290
21.358	–82.724
21.295	–83.549
21.331	–84.024
21.483	–84.643
21.609	–84.975
21.686	–85.518
22.087	–85.457
22.251	–85.347
22.963	–84.450
23.179	–83.983
23.285	–83.634
23.506	–82.095
23.505	–81.043
23.421	–80.497
22.760	–78.456
21.207	–74.814

Note: Coordinates in decimal degrees.

Table 2.5.2-219
Geographic Coordinates of Cuba and Northern Caribbean Model Fault Sources

Source No.:	2		3		4	
Source Name	Oriente-Western		Oriente-Eastern		Septentrional	
	Latitude	Longitude	Latitude	Longitude	Latitude	Longitude
	18.951	–81.483	19.663	–77.134	19.990	–74.120
	19.247	–79.991	19.674	–77.037	20.005	–72.979
	19.563	–77.138	19.733	–76.518	19.936	–72.606
	—	—	19.819	–75.012	19.718	–71.775
	—	—	19.959	–74.472	19.562	–70.998
	—	—	19.982	–74.205	19.151	–69.689
	—	—	—	—	19.081	–68.741

Source No.:	5		6		7	
Source Name	Northern Hispaniola-Western		Northern Hispaniola-Eastern		Swan Islands-Western	
	Latitude	Longitude	Latitude	Longitude	Latitude	Longitude
	20.415	–73.267	19.843	–70.026	15.905	–88.280
	20.400	–72.755	19.555	–68.531	17.346	–84.602
	20.165	–71.530	19.759	–66.270	—	—
	19.907	–70.025	—	—	—	—

Source No.:	8		9		10	
Source Name	Swan Islands-Eastern		Walton-Duanvale		Enriquillo-Plantain Garden fault	
	Latitude	Longitude	Latitude	Longitude	Latitude	Longitude
	17.190	–84.572	17.740	–81.480	17.990	–76.672
	17.758	–81.940	18.335	–79.295	17.927	–76.188
	—	—	18.467	–78.244	18.174	–75.026
	—	—	18.351	–77.429	18.296	–74.420
	—	—	—	—	18.438	–71.807
	—	—	—	—	18.347	–71.104

Note: Coordinates in decimal degrees.

Table 2.5.2-220
Empirical Relations between Rupture Area (A) and Moment Magnitude (M_w) and Rupture Length (L) and M_w Used to Determine Mmax for Cuba and Northern Caribbean Sources

Source	Equation (A and M_w)	Use
Wells and Coppersmith (Reference 334), all slip types	M_w = 0.98 Log A + 4.07	All faults
Wyss (Reference 339)(a)	M_w = Log A + 4.15	All faults
Hanks and Bakun (Reference 262)(b)	M_w = 4/3 Log A + 3.07	Strike-slip faults
WGCEP (Reference 337), equation 4.5b	M_w = Log A + 4.2	Strike-slip faults
Abe (References 201 and 202)	M_w = Log A + 3.99	Subduction zones
Geomatrix (Reference 257)	M_w = 0.81 Log A + 4.7	Subduction zones

Source	Equation (L and M_w)	Use
Wells and Coppersmith (Reference 334), all slip types	M_w = 1.49 Log L + 4.38	All faults
Geomatrix (Reference 257)	M_w = 1.39 Log L + 4.94	Subduction zones

(a) Valid for $M_w > 5.6$
(b) Valid for A > 537 km^2

Table 2.5.2-221 (Sheet 1 of 2)
Significant Earthquakes in the Cuba and Northern Caribbean Region, 1500 to 2010

Date	Location	Seismic Source	MMI	M, high	M, low	M_w
November 1539	Western Caribbean Sea	Swan Islands fault — Western	X	~8[a]		7.69
1551	SE Cuba	Cuba	VIII[b]			5.98
August 1578	Cuba	Cuba		6.75[b]		6.78
February 1678	SE Cuba	Oriente fault — Eastern	VIII[a]	7.0[a]		6.78
June 1692	S Jamaica	Enriquillo-Plantain Garden fault	X[c]	7.5[a]		7.78
October 1751	SW of Dominican Republic	Enriquillo-Plantain Garden fault		8.0[a]		7.28
September 1751	Haiti, near Port-au-Prince	Enriquillo-Plantain Garden fault		7.5[a]		6.83
June 1766	SE Cuba	Oriente fault — Eastern	IX[b]	7.5[b]	7.0[a]	7.53
June 1770	Haiti, west of Port-au-Prince	Enriquillo-Plantain Garden fault		7.5[a]		7.53
November 1812	SE Jamaica	Enriquillo-Plantain Garden fault		6.8[b]		6.13
May 1842	Offshore Haiti to Dominican Republic	Septentrional fault	IX[a]	8.2[d]	8.0[a]	8.23
July 1852	North-Central Cayman Trough	Oriente fault — Western		6.6[a]		7.53
August 1852	Offshore Santiago de Cuba	Oriente fault — Eastern	IX[a]	7.5[a]	7.3[b]	7.33
August 1856	Offshore N Honduras	Swan Islands fault — Western		8.3[a]		7.69
April 1860	Haiti, near Port-au-Prince	Enriquillo-Plantain Garden fault				6.73
January 1880	North Cuba	Cuba	VIII[b]	6.6[a]	6.0[b]	6.13
September 1887	W offshore Haiti	Septentrional fault	IX[a]	7.9[d]	7.75[a]	7.93
January 1907	N Jamaica	Walton-Duanvale fault		7[a]	6.5[c]	6.64
January 1910	Caribbean Sea	Swan Islands — Western		7.0[a]		7.10
February 1914	East-Central Cuba	Cuba		6.2[d]		6.29
February 1917	Offshore S Cuba	Oriente fault — Eastern	VI[a]	7.1[a]	7.0[e]	7.20
February 1932	Offshore Santiago de Cuba	Oriente fault — Eastern		6.8[a]	6.75[b]	6.83
April 1941	Offshore SW Jamaica	Enriquillo-Plantain Garden fault		7[a]	6.9[e]	7.03
August 1946	Offshore Hispaniola	Northern Hispaniola — Eastern		8.1[f]	7.8[a]	7.90
August 1947	Offshore Santiago de Cuba	Oriente fault — Eastern		6.8[a]	6.6[e]	6.83
May 1953	Offshore Hispaniola	Northern Hispaniola — Western		7.0[e]	6.9[a]	6.93
March 1957	W Jamaica	Walton-Duanvale fault		6.9[e]	6.6[a]	6.61
May 1992	Cabo Cruz	Oriente fault — Western	VII[b]	7.0[e]	6.8[b]	6.80

Table 2.5.2-221 (Sheet 2 of 2)
Significant Earthquakes in the Cuba and Northern Caribbean Region, 1500 to 2010

Date	Location	Seismic Source	MMI	M, high	M, low	M_w
January 2010	Haiti, near Port-au-Prince	Enriquillo-Plantain Garden fault	>IX[(h)]			7.0[(g)]

(a) McCann (Reference 282).
(b) Garcia et al. (Reference 254).
(c) DeMets and Wiggins-Grandison (Reference 229).
(d) Cotilla et al. (Reference 226).
(e) van Dusen and Doser (Reference 331).
(f) Dolan and Wald (Reference 236).
(g) U.S. Geological Survey (Reference 238).
(h) Pacific Disaster Center (Reference 260).

Notes:
MMI = Modified Mercalli Intensity
M, high = Upper estimate from literature (magnitude scale unspecified)
M, low = Lower estimate from literature (magnitude scale unspecified)
M_w = Estimate of moment magnitude from Phase 2 earthquake catalog.

Table 2.5.2-222
Comparison of Seismic Source Parameters with USGS Initial Seismic Hazard Maps for Haiti Region

Fault Source[a]	Slip Rate (mm/yr)	M_{char} or Mmax (M_w)[b]
Enriquillo [Enriquillo-Plantain Garden fault]	7 [6–10]	7.7 [7.5–7.9]
Septentrional [Septentrional fault]	12 [6–12]	7.8 [8.0–8.25]
Eastern and central portions of northern subduction zone [Northern Hispaniola fault - eastern]	11 [4–8]	8.0 [8.0–8.6]
Western portion of northern subduction zone [Northern Hispaniola fault - western]	2.5 [4–8]	8.0 [7.0–8.3]
Matheux Neiba [NA]	1 [NA]	7.7 [NA]
Muertos Trough subduction zone, Neiba segment [NA]	7 [NA]	8.0 [NA]
Muertos Trough subduction zone, central segment [NA]	7 [NA]	8.0 [NA]

(a) Reference 235 source listed, with equivalent Turkey Point Units 6 & 7 source shown in [square brackets].
(b) Reference 235 M_{char} (characteristic magnitude), with Turkey Point Units 6 &7 Mmax values shown in [square brackets].

NA Equivalent source not included in Turkey Point Units 6 & 7 source characterization.

Table 2.5.2-223 (Sheet 1 of 5)
Mean and Fractile Rock Seismic Hazard Curves

Ampl. (g)	MEAN (a.f.e.)	0.05 (a.f.e)	0.16 (a.f.e)	0.50 (a.f.e)	0.84 (a.f.e)	0.95 (a.f.e)
PGA Hazard Curves						
0.001	4.39E-02	1.38E-02	2.24E-02	4.17E-02	6.31E-02	7.24E-02
0.0015	3.14E-02	7.94E-03	1.38E-02	2.95E-02	4.79E-02	5.89E-02
0.002	2.34E-02	5.62E-03	9.77E-03	2.24E-02	3.89E-02	4.47E-02
0.003	1.42E-02	3.02E-03	5.25E-03	1.38E-02	2.40E-02	2.95E-02
0.005	6.45E-03	1.27E-03	2.14E-03	6.03E-03	1.12E-02	1.48E-02
0.007	3.51E-03	6.84E-04	1.15E-03	3.24E-03	5.62E-03	7.94E-03
0.01	1.73E-03	3.67E-04	6.17E-04	1.51E-03	2.82E-03	3.72E-03
0.015	7.42E-04	1.72E-04	2.69E-04	6.17E-04	1.15E-03	1.62E-03
0.02	4.04E-04	9.89E-05	1.45E-04	3.31E-04	6.17E-04	8.71E-04
0.03	1.75E-04	4.62E-05	6.31E-05	1.26E-04	2.51E-04	3.94E-04
0.05	6.44E-05	1.82E-05	2.40E-05	4.47E-05	8.91E-05	1.45E-04
0.07	3.49E-05	1.05E-05	1.48E-05	2.48E-05	5.13E-05	8.04E-05
0.1	1.89E-05	5.43E-06	7.94E-06	1.43E-05	2.75E-05	4.47E-05
0.15	9.67E-06	2.54E-06	3.98E-06	7.41E-06	1.48E-05	2.32E-05
0.2	6.02E-06	1.37E-06	2.46E-06	4.57E-06	9.12E-06	1.48E-05
0.3	3.02E-06	5.19E-07	1.00E-06	2.21E-06	4.57E-06	7.67E-06
0.5	1.18E-06	1.18E-07	2.51E-07	7.85E-07	2.14E-06	3.47E-06
0.7	5.92E-07	3.63E-08	8.32E-08	3.31E-07	1.15E-06	1.93E-06
1	2.65E-07	8.51E-09	2.40E-08	1.35E-07	5.37E-07	9.33E-07
1.5	9.39E-08	1.32E-09	4.90E-09	3.27E-08	1.66E-07	3.67E-07
2	4.10E-08	2.99E-10	1.23E-09	1.12E-08	6.31E-08	1.78E-07
3	1.09E-08	2.66E-11	1.35E-10	1.86E-09	1.59E-08	5.50E-08
5	1.49E-09	7.85E-13	6.03E-12	1.45E-10	2.00E-09	8.22E-09
7	3.26E-10	6.31E-14	6.61E-13	2.09E-11	3.55E-10	1.74E-09
10	5.30E-11	2.63E-15	4.79E-14	2.00E-12	5.13E-11	2.69E-10
25 Hz Hazard Curves						
0.001	5.06E-02	1.70E-02	2.75E-02	5.13E-02	7.24E-02	8.32E-02
0.0015	3.85E-02	1.05E-02	1.82E-02	3.89E-02	5.89E-02	7.24E-02
0.002	3.05E-02	7.41E-03	1.29E-02	3.16E-02	4.79E-02	5.89E-02
0.003	2.05E-02	4.57E-03	7.41E-03	2.09E-02	3.16E-02	4.17E-02
0.005	1.11E-02	2.29E-03	3.72E-03	1.12E-02	1.70E-02	2.24E-02
0.007	6.93E-03	1.41E-03	2.46E-03	6.92E-03	1.12E-02	1.38E-02
0.01	4.03E-03	9.02E-04	1.51E-03	3.72E-03	6.46E-03	7.94E-03
0.015	2.12E-03	5.19E-04	8.13E-04	1.74E-03	3.47E-03	4.42E-03
0.02	1.34E-03	3.43E-04	4.68E-04	1.07E-03	2.14E-03	2.82E-03
0.03	7.08E-04	1.66E-04	2.34E-04	5.37E-04	1.07E-03	1.57E-03
0.05	3.20E-04	7.24E-05	9.55E-05	2.19E-04	4.68E-04	7.08E-04
0.07	1.89E-04	4.17E-05	5.50E-05	1.18E-04	2.51E-04	4.37E-04

Table 2.5.2-223 (Sheet 2 of 5)
Mean and Fractile Rock Seismic Hazard Curves

Ampl. (g)	MEAN (a.f.e.)	0.05 (a.f.e)	0.16 (a.f.e)	0.50 (a.f.e)	0.84 (a.f.e)	0.95 (a.f.e)
25 Hz Hazard Curves (cont.)						
0.1	1.07E-04	2.40E-05	3.16E-05	6.31E-05	1.35E-04	2.34E-04
0.15	5.49E-05	1.25E-05	1.70E-05	3.16E-05	7.76E-05	1.18E-04
0.2	3.40E-05	7.67E-06	1.12E-05	2.02E-05	4.79E-05	7.24E-05
0.3	1.73E-05	3.72E-06	6.03E-06	1.12E-05	2.40E-05	3.89E-05
0.5	7.26E-06	1.37E-06	2.29E-06	4.90E-06	1.20E-05	1.82E-05
0.7	4.06E-06	6.38E-07	1.15E-06	2.82E-06	6.92E-06	1.08E-05
1	2.14E-06	2.43E-07	4.68E-07	1.41E-06	3.72E-06	6.03E-06
1.5	9.98E-07	7.50E-08	1.55E-07	5.96E-07	2.00E-06	3.13E-06
2	5.60E-07	2.75E-08	6.31E-08	2.88E-07	1.15E-06	2.00E-06
3	2.33E-07	5.82E-09	1.59E-08	9.55E-08	4.37E-07	8.71E-07
5	6.73E-08	5.56E-10	1.86E-09	1.76E-08	1.02E-07	3.31E-07
7	2.68E-08	9.89E-11	3.80E-10	4.90E-09	3.16E-08	1.55E-07
10	8.99E-09	1.38E-11	5.13E-11	1.15E-09	8.51E-09	5.50E-08
10 Hz Hazard Curves						
0.001	5.99E-02	2.09E-02	3.63E-02	5.89E-02	8.32E-02	9.55E-02
0.0015	4.80E-02	1.38E-02	2.57E-02	4.79E-02	6.76E-02	8.32E-02
0.002	3.96E-02	1.05E-02	1.95E-02	3.89E-02	5.89E-02	7.24E-02
0.003	2.84E-02	6.46E-03	1.12E-02	2.75E-02	4.47E-02	5.50E-02
0.005	1.65E-02	3.47E-03	5.25E-03	1.59E-02	2.57E-02	3.63E-02
0.007	1.06E-02	2.00E-03	3.24E-03	1.05E-02	1.70E-02	2.24E-02
0.01	6.21E-03	1.19E-03	1.86E-03	6.03E-03	9.77E-03	1.38E-02
0.015	3.09E-03	6.17E-04	1.00E-03	2.82E-03	5.25E-03	6.46E-03
0.02	1.80E-03	3.80E-04	6.17E-04	1.51E-03	3.02E-03	3.72E-03
0.03	8.03E-04	1.97E-04	2.88E-04	6.61E-04	1.41E-03	1.74E-03
0.05	2.79E-04	7.24E-05	1.10E-04	2.04E-04	4.68E-04	5.96E-04
0.07	1.39E-04	3.76E-05	5.13E-05	1.10E-04	2.04E-04	2.99E-04
0.1	6.71E-05	1.88E-05	2.75E-05	5.13E-05	9.55E-05	1.45E-04
0.15	3.06E-05	9.77E-06	1.38E-05	2.40E-05	4.47E-05	7.00E-05
0.2	1.80E-05	5.62E-06	7.94E-06	1.48E-05	2.75E-05	4.17E-05
0.3	8.70E-06	2.63E-06	3.72E-06	6.92E-06	1.38E-05	2.09E-05
0.5	3.46E-06	8.41E-07	1.41E-06	2.72E-06	5.62E-06	8.51E-06
0.7	1.81E-06	3.67E-07	6.61E-07	1.37E-06	3.02E-06	4.42E-06
1	8.64E-07	1.40E-07	2.69E-07	6.17E-07	1.51E-06	2.21E-06
1.5	3.39E-07	3.63E-08	7.76E-08	2.19E-07	5.75E-07	9.33E-07
2	1.63E-07	1.25E-08	2.95E-08	9.55E-08	2.88E-07	4.68E-07
3	5.16E-08	2.29E-09	6.03E-09	2.57E-08	8.91E-08	1.72E-07
5	9.83E-09	1.97E-10	6.61E-10	3.98E-09	1.70E-08	3.76E-08
7	2.87E-09	3.06E-11	1.26E-10	1.00E-09	4.90E-09	1.29E-08
10	6.86E-10	3.72E-12	1.95E-11	1.78E-10	1.07E-09	3.24E-09

Table 2.5.2-223 (Sheet 3 of 5)
Mean and Fractile Rock Seismic Hazard Curves

Ampl. (g)	MEAN (a.f.e.)	0.05 (a.f.e)	0.16 (a.f.e)	0.50 (a.f.e)	0.84 (a.f.e)	0.95 (a.f.e)
5 Hz Hazard Curves						
0.001	6.55E-02	2.75E-02	4.47E-02	6.31E-02	8.91E-02	9.55E-02
0.0015	5.32E-02	1.70E-02	3.16E-02	5.13E-02	7.76E-02	8.91E-02
0.002	4.43E-02	1.29E-02	2.40E-02	4.47E-02	6.31E-02	7.76E-02
0.003	3.21E-02	7.67E-03	1.48E-02	3.16E-02	5.13E-02	6.31E-02
0.005	1.88E-02	3.72E-03	6.92E-03	1.82E-02	3.16E-02	3.89E-02
0.007	1.20E-02	2.29E-03	3.98E-03	1.12E-02	2.09E-02	2.66E-02
0.01	6.86E-03	1.23E-03	2.00E-03	6.46E-03	1.20E-02	1.59E-02
0.015	3.24E-03	5.37E-04	8.71E-04	3.02E-03	5.62E-03	7.41E-03
0.02	1.77E-03	2.99E-04	5.01E-04	1.62E-03	2.82E-03	3.98E-03
0.03	6.98E-04	1.30E-04	2.19E-04	6.17E-04	1.15E-03	1.51E-03
0.05	1.99E-04	4.17E-05	7.24E-05	1.66E-04	3.09E-04	4.22E-04
0.07	8.67E-05	2.09E-05	3.39E-05	6.76E-05	1.35E-04	1.78E-04
0.1	3.72E-05	9.77E-06	1.38E-05	2.95E-05	5.50E-05	8.04E-05
0.15	1.52E-05	4.27E-06	6.03E-06	1.16E-05	2.24E-05	3.39E-05
0.2	8.39E-06	2.29E-06	3.24E-06	6.24E-06	1.20E-05	1.95E-05
0.3	3.71E-06	9.02E-07	1.32E-06	2.82E-06	5.62E-06	9.12E-06
0.5	1.29E-06	2.43E-07	3.80E-07	9.33E-07	2.14E-06	3.35E-06
0.7	6.11E-07	8.61E-08	1.55E-07	4.22E-07	1.07E-06	1.74E-06
1	2.59E-07	2.57E-08	5.13E-08	1.66E-07	4.37E-07	7.59E-07
1.5	8.87E-08	5.43E-09	1.20E-08	4.79E-08	1.55E-07	2.79E-07
2	3.87E-08	1.51E-09	4.27E-09	1.70E-08	7.76E-08	1.40E-07
3	1.09E-08	2.11E-10	6.61E-10	3.98E-09	2.09E-08	4.47E-08
5	1.80E-09	1.29E-11	4.79E-11	4.22E-10	2.82E-09	8.51E-09
7	4.86E-10	1.51E-12	7.41E-12	7.50E-11	7.08E-10	2.29E-09
10	1.08E-10	1.18E-13	7.59E-13	1.12E-11	1.35E-10	4.68E-10
2.5 Hz Hazard Curves						
0.001	6.52E-02	3.16E-02	4.47E-02	6.31E-02	8.32E-02	9.55E-02
0.0015	5.20E-02	1.95E-02	3.16E-02	5.13E-02	7.24E-02	8.32E-02
0.002	4.26E-02	1.29E-02	2.24E-02	4.17E-02	6.31E-02	7.24E-02
0.003	3.02E-02	7.41E-03	1.38E-02	2.75E-02	4.79E-02	5.50E-02
0.005	1.71E-02	3.24E-03	6.03E-03	1.38E-02	3.16E-02	3.63E-02
0.007	1.06E-02	1.74E-03	3.47E-03	7.94E-03	2.09E-02	2.40E-02
0.01	5.82E-03	8.41E-04	1.62E-03	4.27E-03	1.20E-02	1.48E-02
0.015	2.56E-03	3.31E-04	6.61E-04	1.86E-03	5.25E-03	6.46E-03
0.02	1.30E-03	1.72E-04	3.09E-04	1.00E-03	2.63E-03	3.47E-03
0.03	4.46E-04	6.10E-05	1.02E-04	3.55E-04	8.71E-04	1.15E-03
0.05	9.94E-05	1.53E-05	2.57E-05	7.76E-05	1.55E-04	2.19E-04
0.07	3.60E-05	6.03E-06	1.12E-05	2.75E-05	5.13E-05	7.00E-05
0.1	1.28E-05	2.37E-06	3.98E-06	9.12E-06	1.70E-05	2.57E-05

Table 2.5.2-223 (Sheet 4 of 5)
Mean and Fractile Rock Seismic Hazard Curves

Ampl. (g)	MEAN (a.f.e.)	0.05 (a.f.e)	0.16 (a.f.e)	0.50 (a.f.e)	0.84 (a.f.e)	0.95 (a.f.e)
25 Hz Hazard Curves (cont.)						
0.15	4.37E-06	7.33E-07	1.32E-06	2.82E-06	6.46E-06	1.05E-05
0.2	2.15E-06	2.88E-07	5.37E-07	1.37E-06	3.24E-06	5.82E-06
0.3	8.15E-07	7.50E-08	1.55E-07	4.84E-07	1.41E-06	2.46E-06
0.5	2.38E-07	1.12E-08	2.75E-08	1.26E-07	4.68E-07	8.41E-07
0.7	1.01E-07	2.72E-09	8.51E-09	4.47E-08	2.04E-07	4.07E-07
1	3.87E-08	5.01E-10	1.74E-09	1.38E-08	7.24E-08	1.78E-07
1.5	1.18E-08	5.69E-11	2.34E-10	2.92E-09	1.82E-08	5.89E-08
2	4.77E-09	1.05E-11	4.79E-11	9.02E-10	6.92E-09	2.24E-08
3	1.19E-09	7.85E-13	4.27E-12	1.45E-10	1.62E-09	5.25E-09
5	1.68E-10	1.88E-14	1.55E-13	1.12E-11	1.91E-10	6.84E-10
7	4.03E-11	1.04E-15	1.38E-14	1.51E-12	3.63E-11	1.45E-10
10	7.81E-12	4.47E-23	6.61E-16	1.55E-13	4.90E-12	2.40E-11
1 Hz Hazard Curves						
0.0001	1.04E-01	8.91E-02	9.55E-02	1.02E-01	1.10E-01	1.18E-01
0.0003	8.45E-02	6.31E-02	7.24E-02	8.32E-02	9.55E-02	1.02E-01
0.0005	7.06E-02	4.79E-02	5.50E-02	7.24E-02	8.32E-02	8.91E-02
0.0006	6.53E-02	4.17E-02	5.13E-02	6.76E-02	7.76E-02	8.91E-02
0.0007	6.07E-02	3.63E-02	4.47E-02	6.31E-02	7.76E-02	8.32E-02
0.0008	5.67E-02	3.16E-02	3.89E-02	5.89E-02	7.24E-02	7.76E-02
0.001	5.01E-02	2.40E-02	3.16E-02	5.13E-02	6.31E-02	7.24E-02
0.0015	3.85E-02	1.38E-02	1.95E-02	3.89E-02	5.50E-02	6.31E-02
0.002	3.08E-02	8.51E-03	1.29E-02	2.95E-02	4.79E-02	5.50E-02
0.003	2.09E-02	4.27E-03	6.46E-03	1.82E-02	3.63E-02	4.17E-02
0.005	1.10E-02	1.41E-03	2.63E-03	7.41E-03	1.95E-02	2.95E-02
0.007	6.39E-03	6.61E-04	1.32E-03	3.72E-03	1.12E-02	2.09E-02
0.01	3.19E-03	2.60E-04	5.37E-04	1.74E-03	5.62E-03	1.20E-02
0.015	1.23E-03	7.76E-05	1.55E-04	7.08E-04	2.00E-03	5.62E-03
0.02	5.58E-04	3.16E-05	6.31E-05	3.31E-04	8.71E-04	2.63E-03
0.03	1.59E-04	7.67E-06	1.48E-05	8.32E-05	2.19E-04	8.13E-04
0.05	2.73E-05	1.11E-06	2.29E-06	1.12E-05	3.89E-05	1.26E-04
0.07	8.24E-06	2.79E-07	7.59E-07	2.82E-06	1.12E-05	2.75E-05
0.1	2.41E-06	6.10E-08	1.91E-07	7.08E-07	3.24E-06	5.43E-06
0.15	6.38E-07	7.94E-09	2.24E-08	1.91E-07	8.13E-07	1.74E-06
0.2	2.61E-07	1.68E-09	7.41E-09	6.31E-08	3.55E-07	9.33E-07
0.3	7.85E-08	1.50E-10	1.00E-09	1.48E-08	1.26E-07	3.80E-07
0.5	1.86E-08	5.62E-12	5.89E-11	2.00E-09	3.16E-08	9.23E-08
0.7	7.21E-09	5.56E-13	7.94E-12	5.01E-10	1.12E-08	3.16E-08
1	2.53E-09	3.63E-14	7.08E-13	8.91E-11	2.82E-09	1.01E-08

Table 2.5.2-223 (Sheet 5 of 5)
Mean and Fractile Rock Seismic Hazard Curves

Ampl. (g)	MEAN (a.f.e.)	0.05 (a.f.e)	0.16 (a.f.e)	0.50 (a.f.e)	0.84 (a.f.e)	0.95 (a.f.e)
0.5 Hz Hazard Curves						
0.0001	8.85E-02	7.24E-02	7.76E-02	8.91E-02	9.55E-02	1.02E-01
0.0003	6.30E-02	4.47E-02	5.13E-02	6.31E-02	7.24E-02	7.76E-02
0.0005	5.14E-02	2.75E-02	3.89E-02	5.13E-02	6.31E-02	6.76E-02
0.0006	4.73E-02	2.24E-02	3.16E-02	4.79E-02	5.89E-02	6.31E-02
0.0007	4.39E-02	1.82E-02	2.75E-02	4.47E-02	5.89E-02	6.31E-02
0.0008	4.09E-02	1.48E-02	2.40E-02	4.17E-02	5.50E-02	5.89E-02
0.001	3.58E-02	1.05E-02	1.82E-02	3.63E-02	5.13E-02	5.50E-02
0.0015	2.69E-02	5.25E-03	1.05E-02	2.75E-02	4.47E-02	5.13E-02
0.002	2.09E-02	2.92E-03	6.92E-03	1.95E-02	3.89E-02	4.47E-02
0.003	1.35E-02	1.23E-03	3.24E-03	1.05E-02	2.95E-02	3.63E-02
0.005	6.60E-03	3.31E-04	9.33E-04	3.47E-03	1.48E-02	2.40E-02
0.007	3.64E-03	1.26E-04	3.55E-04	1.41E-03	7.94E-03	1.59E-02
0.01	1.71E-03	3.76E-05	1.02E-04	5.37E-04	3.72E-03	9.12E-03
0.015	6.07E-04	7.94E-06	2.40E-05	1.45E-04	1.15E-03	3.47E-03
0.02	2.60E-04	2.29E-06	8.51E-06	5.50E-05	4.37E-04	1.62E-03
0.03	6.84E-05	4.37E-07	1.74E-06	1.16E-05	8.32E-05	4.37E-04
0.05	1.13E-05	4.03E-08	1.78E-07	1.46E-06	1.12E-05	5.13E-05
0.07	3.62E-06	6.68E-09	3.89E-08	4.68E-07	2.82E-06	9.77E-06
0.1	1.13E-06	9.33E-10	7.94E-09	8.91E-08	8.13E-07	1.57E-06
0.15	2.91E-07	6.76E-11	9.33E-10	1.29E-08	1.35E-07	3.94E-07
0.2	1.06E-07	8.81E-12	1.26E-10	3.98E-09	4.79E-08	1.66E-07
0.3	2.42E-08	3.55E-13	1.20E-11	5.37E-10	1.38E-08	5.50E-08
0.5	4.02E-09	2.29E-15	1.66E-13	3.16E-11	2.14E-09	1.20E-08
0.7	1.36E-09	3.16E-17	8.51E-15	3.72E-12	5.75E-10	3.85E-09
1	4.46E-10	1.02E-28	1.91E-16	4.37E-13	1.26E-10	9.33E-10

a.f.e. = annual frequency of exceedance

Table 2.5.2-224 (Sheet 1 of 3)
Percent Contribution to Deaggregation

Percent Contribution to Low-Frequency Deaggregation for 1E-04								
	Percent Contribution By Moment Magnitude [M] — Distance [R, km] Bin							
R \ M	5.25	5.75	6.25	6.75	7.25	7.75	8.25	8.75
0–20	3.358	0.6060	0.2397	0.02748	8.323E-3	9.539E-4	1.104E-20	1.104E-20
20–40	2.196	0.8873	0.4379	0.05555	0.01653	1.935E-3	1.682E-20	1.682E-20
40–60	0.8486	0.6860	0.4743	0.06720	0.02084	2.372E-3	2.673E-20	2.673E-20
60–80	0.3818	0.4289	0.4089	0.07140	0.02415	2.839E-3	2.672E-20	2.672E-20
80–100	0.2062	0.3388	0.3626	0.07307	0.02675	3.208E-3	2.553E-20	2.553E-20
100–210	0.3826	0.8812	1.295	0.3402	0.1589	0.02034	6.516E-20	6.516E-20
210–330	0.07032	0.6397	3.239	8.021	3.472	0.01310	3.978E-20	3.978E-20
>330	4.096E-3	0.08651	0.9054	6.256	27.78	32.16	1.977	0.03270

Percent Contribution to High-Frequency Deaggregation for 1E-04								
	Percent Contribution By Moment Magnitude [M] — Distance [R, km] Bin							
R \ M	5.25	5.75	6.25	6.75	7.25	7.75	8.25	8.75
0–20	9.682	0.8214	0.2675	0.02847	8.420E-3	9.426E-4	5.424E-21	5.424E-21
20–40	12.53	1.835	0.6223	0.06477	0.01742	1.948E-3	1.236E-20	1.236E-20
40–60	7.102	1.940	0.8323	0.08947	0.02330	2.589E-3	2.163E-20	2.163E-20
60–80	3.856	1.452	0.8217	0.1040	0.02850	3.106E-3	2.235E-20	2.235E-20
80–100	2.539	1.306	0.7968	0.1130	0.03231	3.550E-3	2.268E-20	2.268E-20
100–210	5.533	3.894	3.092	0.5538	0.1957	0.02274	6.059E-20	6.059E-20
210–330	0.7292	2.440	6.396	9.927	3.393	0.01361	3.864E-20	3.864E-20
>330	0.02732	0.1954	1.027	3.831	8.740	3.003	0.06259	1.947E-4

Table 2.5.2-224 (Sheet 2 of 3)
Percent Contribution to Deaggregation

Percent Contribution to Low-Frequency Deaggregation for 1E-05								
	Percent Contribution By Moment Magnitude [M] — Distance [R, km] Bin							
R \ M	5.25	5.75	6.25	6.75	7.25	7.75	8.25	8.75
0–20	12.15	3.879	1.943	0.2549	0.08261	9.658E-3	1.464E-19	1.464E-19
20–40	3.472	3.102	2.368	0.4021	0.1452	0.01803	1.866E-19	1.866E-19
40–60	0.7056	1.364	1.664	0.3581	0.1528	0.01961	2.652E-19	2.652E-19
60–80	0.2055	0.5543	0.9977	0.2854	0.1481	0.02069	2.418E-19	2.418E-19
80–100	0.08325	0.3335	0.6990	0.2373	0.1433	0.02116	2.153E-19	2.153E-19
100–210	0.1133	0.6144	1.742	0.7683	0.6158	0.1023	4.922E-19	4.922E-19
210–330	6.898E-3	0.1182	1.198	5.745	4.268	0.04352	2.548E-19	2.548E-19
>330	1.738E-4	7.247E-3	0.1672	3.428	28.87	15.48	0.8831	8.244E-3

Percent Contribution to High-Frequency Deaggregation for 1E-05								
	Percent Contribution By Moment Magnitude [M] — Distance [R, km] Bin							
R \ M	5.25	5.75	6.25	6.75	7.25	7.75	8.25	8.75
0–20	40.80	6.066	2.324	0.2676	0.08196	9.276E-3	1.094E-19	1.094E-19
20–40	15.35	5.979	3.210	0.4532	0.1469	0.01742	1.475E-19	1.475E-19
40–60	3.048	2.545	2.122	0.3819	0.1490	0.01923	2.246E-19	2.246E-19
60–80	0.8306	0.9665	1.146	0.2708	0.1341	0.01861	2.141E-19	2.141E-19
80–100	0.3785	0.6072	0.8052	0.2195	0.1229	0.01816	1.993E-19	1.993E-19
100–210	0.5505	1.159	1.927	0.6413	0.4498	0.07458	4.284E-19	4.284E-19
210–330	0.01752	0.1130	0.6067	1.879	1.253	0.02071	1.728E-19	1.728E-19
>330	2.546E-4	3.359E-3	0.03420	0.3020	2.390	0.09811	8.617E-4	6.446E-7

Table 2.5.2-224 (Sheet 3 of 3)
Percent Contribution to Deaggregation

Percent Contribution to Low-Frequency Deaggregation for 1E-06								
	Percent Contribution By Moment Magnitude [M] — Distance [R, km] Bin							
R \ M	5.25	5.75	6.25	6.75	7.25	7.75	8.25	8.75
0–20	19.29	13.59	10.37	1.814	0.7091	0.08862	1.680E-18	1.680E-18
20–40	1.613	4.002	6.005	1.678	0.9085	0.1309	1.744E-18	1.744E-18
40–60	0.1375	0.8059	2.227	0.8867	0.6630	0.1078	2.006E-18	2.006E-18
60–80	0.02297	0.1897	0.8379	0.4697	0.4684	0.08811	1.618E-18	1.618E-18
80–100	6.569E-3	0.08325	0.4397	0.2939	0.3611	0.07376	1.354E-18	1.354E-18
100–210	6.415E-3	0.1091	0.7689	0.6570	1.050	0.2427	2.846E-18	2.846E-18
210–330	1.432E-4	7.221E-3	0.1538	1.234	1.759	0.06449	1.203E-18	1.203E-18
>330	1.425E-6	2.598E-4	0.01353	0.9716	21.14	3.306	0.1628	7.440E-4

Percent Contribution to High-Frequency Deaggregation for 1E-06								
	Percent Contribution By Moment Magnitude [M] — Distance [R, km] Bin							
R \ M	5.25	5.75	6.25	6.75	7.25	7.75	8.25	8.75
0–20	53.64	17.36	9.988	1.553	0.5884	0.07252	1.248E-18	1.248E-18
20–40	3.143	3.754	4.109	1.060	0.5958	0.08899	1.408E-18	1.408E-18
40–60	0.1753	0.4668	0.9073	0.3421	0.3022	0.05753	1.586E-18	1.586E-18
60–80	0.02240	0.07983	0.2270	0.1166	0.1499	0.03383	1.176E-18	1.176E-18
80–100	6.819E-3	0.03427	0.1105	0.06464	0.09602	0.02359	9.290E-19	9.290E-19
100–210	6.744E-3	0.04374	0.1743	0.1210	0.2085	0.05592	1.688E-18	1.688E-18
210–330	5.549E-5	9.710E-4	9.667E-3	0.03550	0.05705	6.170E-3	4.768E-19	4.768E-19
>330	1.102E-7	1.140E-5	2.378E-4	2.641E-3	0.1054	8.841E-4	3.100E-19	3.100E-19

Table 2.5.2-225
Controlling Magnitudes and Distances from Deaggregation

Struct. Frequency	Annual Freq. Exceed.	Overall Hazard		Hazard from R > 100 km	
		M	R, km	M	R, km
1 & 2.5 Hz	1E-04	7.1	400	7.3	570
5 & 10 Hz	1E-04	5.9	110	6.5	290
1 & 2.5 Hz	1E-05	6.7	190	7.2	560
5 & 10 Hz	1E-05	5.5	31	6.7	250
1 & 2.5 Hz	1E-06	6.3	61	7.2	600
5 & 10 Hz	1E-06	5.5	17	6.9	180

Notes:
Shaded cells indicate values used to construct UHRS
“M” is moment magnitude; “R” is epicentral distance

Table 2.5.2-226
Assigned Strong Motion Durations in P-SHAKE

Set of Runs	Description	Recurrence	Input Rock Spectra	
			Moment Magnitude	Duration [sec]
LF4	Low Freq.	1E-04	7.3	13
HF4	High Freq.	1E-04	5.9	6
LF5	Low Freq.	1E-05	7.2	13
HF5	High Freq.	1E-05	5.5	6

Table 2.5.2-227 (Sheet 1 of 2)
HF and LF horizontal 1E-05 Rock Spectra, Amplification Factors, Site Spectra, and Raw and Smoothed Envelope Spectra

Horizontal 1E-05 Rock and Site Spectra UHRS (g)								
Freq, Hz	Rock UHRS		Transfer Function		Surface UHRS		Raw Envelope	Smooth Spectrum
	LF SA(g)	HF SA(g)	LF Amp	HF Amp	LF SA(g)	HF SA(g)	SA(g)	SA(g)
100	1.47E-01	1.47E-01	0.767	0.646	1.13E-01	9.49E-02	1.13E-01	1.13E-01
90	1.63E-01	1.63E-01	0.694	0.584	1.13E-01	9.55E-02	1.13E-01	1.13E-01
80	1.89E-01	1.90E-01	0.601	0.507	1.13E-01	9.65E-02	1.13E-01	1.14E-01
70	2.29E-01	2.31E-01	0.501	0.427	1.14E-01	9.85E-02	1.14E-01	1.15E-01
60	2.80E-01	2.84E-01	0.415	0.361	1.16E-01	1.02E-01	1.16E-01	1.16E-01
50	3.33E-01	3.39E-01	0.360	0.323	1.20E-01	1.09E-01	1.20E-01	1.20E-01
45	3.56E-01	3.62E-01	0.347	0.322	1.23E-01	1.17E-01	1.23E-01	1.24E-01
40	3.75E-01	3.82E-01	0.346	0.338	1.30E-01	1.29E-01	1.30E-01	1.32E-01
35	3.91E-01	3.98E-01	0.359	0.376	1.40E-01	1.50E-01	1.50E-01	1.50E-01
30	4.04E-01	4.09E-01	0.384	0.426	1.55E-01	1.74E-01	1.74E-01	1.73E-01
25	4.14E-01	4.14E-01	0.394	0.436	1.63E-01	1.80E-01	1.80E-01	1.79E-01
20	3.85E-01	3.93E-01	0.407	0.426	1.57E-01	1.68E-01	1.68E-01	1.67E-01
15	3.42E-01	3.52E-01	0.448	0.453	1.53E-01	1.59E-01	1.59E-01	1.58E-01
12.5	3.14E-01	3.20E-01	0.481	0.483	1.51E-01	1.54E-01	1.54E-01	1.54E-01
10	2.78E-01	2.78E-01	0.588	0.606	1.64E-01	1.68E-01	1.68E-01	1.67E-01
9	2.63E-01	2.64E-01	0.647	0.665	1.70E-01	1.75E-01	1.75E-01	1.76E-01
8	2.47E-01	2.47E-01	0.732	0.757	1.81E-01	1.87E-01	1.87E-01	1.86E-01
7	2.29E-01	2.29E-01	0.813	0.822	1.86E-01	1.88E-01	1.88E-01	1.88E-01
6	2.08E-01	2.08E-01	0.903	0.908	1.88E-01	1.89E-01	1.89E-01	1.91E-01
5	1.84E-01	1.84E-01	1.118	1.131	2.06E-01	2.08E-01	2.08E-01	2.07E-01
4	1.60E-01	1.51E-01	1.271	1.228	2.03E-01	1.86E-01	2.03E-01	2.05E-01
3	1.29E-01	1.14E-01	1.919	1.925	2.48E-01	2.20E-01	2.48E-01	2.42E-01
2.5	1.10E-01	9.37E-02	2.005	1.855	2.21E-01	1.74E-01	2.21E-01	2.19E-01
2	9.82E-02	7.11E-02	1.734	1.588	1.70E-01	1.13E-01	1.70E-01	1.69E-01
1.5	8.51E-02	4.77E-02	1.852	1.744	1.58E-01	8.33E-02	1.58E-01	1.57E-01
1.25	7.66E-02	3.64E-02	2.221	2.119	1.70E-01	7.72E-02	1.70E-01	1.70E-01
1	6.63E-02	2.58E-02	2.844	2.742	1.89E-01	7.09E-02	1.89E-01	1.91E-01
0.9	6.60E-02	2.19E-02	3.292	3.230	2.17E-01	7.07E-02	2.17E-01	2.13E-01
0.8	6.45E-02	1.81E-02	3.360	3.223	2.17E-01	5.84E-02	2.17E-01	2.13E-01
0.7	6.17E-02	1.46E-02	3.041	2.859	1.88E-01	4.17E-02	1.88E-01	1.90E-01
0.6	5.76E-02	1.13E-02	3.036	2.862	1.75E-01	3.23E-02	1.75E-01	1.74E-01
0.5	5.19E-02	8.26E-03	2.784	2.645	1.44E-01	2.19E-02	1.44E-01	1.41E-01
0.4	4.15E-02	6.61E-03	2.073	1.948	8.61E-02	1.29E-02	8.61E-02	8.74E-02
0.3	3.11E-02	4.96E-03	1.866	1.753	5.81E-02	8.69E-03	5.81E-02	5.83E-02
0.2	2.08E-02	3.30E-03	1.882	1.767	3.91E-02	5.84E-03	3.91E-02	3.90E-02
0.15	1.56E-02	2.48E-03	1.602	1.523	2.49E-02	3.78E-03	2.49E-02	2.51E-02

Table 2.5.2-227 (Sheet 2 of 2)
HF and LF horizontal 1E-05 Rock Spectra, Amplification Factors, Site Spectra, and Raw and Smoothed Envelope Spectra

Horizontal 1E-05 Rock and Site Spectra UHRS (g)								
Freq, Hz	Rock UHRS		Transfer Function		Surface UHRS		Raw Envelope	Smooth Spectrum
	LF SA(g)	HF SA(g)	LF Amp	HF Amp	LF SA(g)	HF SA(g)	SA(g)	SA(g)
0.125	1.29E-02	2.06E-03	1.423	1.377	1.84E-02	2.83E-03	1.84E-02	1.82E-02
0.1	8.30E-03	1.32E-03	1.324	1.268	1.10E-02	1.68E-03	1.10E-02	1.10E-02

UHRS = Uniform hazard response spectra
LF = Low frequencies
HF = High frequencies
SA = Spectral acceleration
Amp = Amplitude

Table 2.5.2-228
Horizontal 1E-04 and 1E-05 Site Spectra, Values of AR and DF, and GMRS

Freq. Hz	Horizontal 1E-04 (g)	Horizontal 1E-05 (g)	AR	DF	Horizontal GMRS (g)
100	5.20E-02	1.13E-01	2.17	1.11	5.79E-02
90	5.21E-02	1.13E-01	2.17	1.11	5.81E-02
80	5.23E-02	1.14E-01	2.17	1.11	5.83E-02
70	5.28E-02	1.15E-01	2.17	1.11	5.89E-02
60	5.37E-02	1.16E-01	2.17	1.11	5.98E-02
50	5.51E-02	1.20E-01	2.18	1.12	6.16E-02
45	5.65E-02	1.24E-01	2.19	1.12	6.35E-02
40	5.86E-02	1.32E-01	2.25	1.15	6.72E-02
35	6.18E-02	1.50E-01	2.43	1.22	7.53E-02
30	6.55E-02	1.73E-01	2.64	1.30	8.54E-02
25	6.65E-02	1.79E-01	2.69	1.33	8.82E-02
20	6.43E-02	1.67E-01	2.60	1.29	8.28E-02
15	6.29E-02	1.58E-01	2.51	1.25	7.88E-02
12.5	6.28E-02	1.54E-01	2.45	1.23	7.72E-02
10	6.71E-02	1.67E-01	2.49	1.24	8.35E-02
9	6.99E-02	1.76E-01	2.52	1.26	8.78E-02
8	7.32E-02	1.86E-01	2.53	1.26	9.25E-02
7	7.52E-02	1.88E-01	2.50	1.25	9.38E-02
6	7.84E-02	1.91E-01	2.44	1.22	9.59E-02
5	8.63E-02	2.07E-01	2.40	1.21	1.04E-01
4	8.69E-02	2.05E-01	2.36	1.19	1.04E-01
3	1.11E-01	2.42E-01	2.18	1.12	1.24E-01
2.5	1.02E-01	2.19E-01	2.15	1.11	1.13E-01
2	8.07E-02	1.69E-01	2.10	1.08	8.75E-02
1.5	8.02E-02	1.57E-01	1.96	1.03	8.24E-02
1.25	8.84E-02	1.70E-01	1.92	1.01	8.94E-02
1	1.05E-01	1.91E-01	1.83	1.00	1.05E-01
0.9	1.15E-01	2.13E-01	1.85	1.00	1.15E-01
0.8	1.12E-01	2.13E-01	1.91	1.01	1.12E-01
0.7	9.72E-02	1.90E-01	1.95	1.03	9.96E-02
0.6	8.86E-02	1.74E-01	1.96	1.03	9.11E-02
0.5	7.17E-02	1.41E-01	1.97	1.03	7.39E-02
0.4	4.46E-02	8.74E-02	1.96	1.03	4.59E-02
0.3	3.00E-02	5.83E-02	1.95	1.02	3.06E-02
0.2	2.01E-02	3.90E-02	1.94	1.02	2.05E-02
0.15	1.29E-02	2.51E-02	1.95	1.02	1.32E-02
0.125	9.37E-03	1.82E-02	1.95	1.02	9.58E-03
0.1	5.65E-03	1.10E-02	1.95	1.02	5.78E-03

Notes:
A_R and DF are defined in Equations 2.5.2-14 and 2.5.2-15, respectively.
GMRS = Ground motion response spectrum

Table 2.5.2-229
Smooth 1E-04, 1E-05, and 1E-06 Spectra at GMRS Elevation

Freq, Hz	Smooth Spectra (g)		
	1E-04	1E-05	1E-06
100	5.20E-02	1.13E-01	2.50E-01
90	5.21E-02	1.13E-01	2.51E-01
80	5.23E-02	1.14E-01	2.53E-01
70	5.28E-02	1.15E-01	2.56E-01
60	5.37E-02	1.16E-01	2.63E-01
50	5.51E-02	1.20E-01	2.77E-01
45	5.65E-02	1.24E-01	2.92E-01
40	5.86E-02	1.32E-01	3.18E-01
35	6.18E-02	1.50E-01	3.61E-01
30	6.55E-02	1.73E-01	4.19E-01
25	6.65E-02	1.79E-01	4.51E-01
20	6.43E-02	1.67E-01	4.35E-01
15	6.29E-02	1.58E-01	4.19E-01
12.5	6.28E-02	1.54E-01	4.06E-01
10	6.71E-02	1.67E-01	4.36E-01
9	6.99E-02	1.76E-01	4.63E-01
8	7.32E-02	1.86E-01	4.91E-01
7	7.52E-02	1.88E-01	5.06E-01
6	7.84E-02	1.91E-01	5.09E-01
5	8.63E-02	2.07E-01	5.45E-01
4	8.69E-02	2.05E-01	5.20E-01
3	1.11E-01	2.42E-01	5.73E-01
2.5	1.02E-01	2.19E-01	5.12E-01
2	8.07E-02	1.69E-01	3.82E-01
1.5	8.02E-02	1.57E-01	3.02E-01
1.25	8.84E-02	1.70E-01	3.11E-01
1	1.05E-01	1.91E-01	3.34E-01
0.9	1.15E-01	2.13E-01	3.77E-01
0.8	1.12E-01	2.13E-01	4.01E-01
0.7	9.72E-02	1.90E-01	3.78E-01
0.6	8.86E-02	1.74E-01	3.52E-01
0.5	7.17E-02	1.41E-01	2.93E-01
0.4	4.46E-02	8.74E-02	1.79E-01
0.3	3.00E-02	5.83E-02	1.17E-01
0.2	2.01E-02	3.90E-02	7.78E-02
0.15	1.29E-02	2.51E-02	5.05E-02
0.125	9.37E-03	1.82E-02	3.67E-02
0.1	5.65E-03	1.10E-02	2.21E-02

GMRS = Ground motion response spectrum

Table 2.5.2-230
V/H Ratios, Vertical 1E-04 and 1E-05 Site Spectra, Values of A_R and DF, and GMRS

Freq. Hz	V/H	Vertical 1E-04 (g)	Vertical 1E-05 (g)	AR	DF	Vertical GMRS (g)
100	1.000	5.20E-02	1.13E-01	2.17	1.11	5.79E-02
90	1.000	5.21E-02	1.13E-01	2.17	1.11	5.81E-02
80	1.000	5.23E-02	1.14E-01	2.17	1.11	5.83E-02
70	1.000	5.28E-02	1.15E-01	2.17	1.11	5.89E-02
60	1.000	5.37E-02	1.16E-01	2.17	1.11	5.98E-02
50	1.000	5.51E-02	1.20E-01	2.18	1.12	6.16E-02
45	1.000	5.65E-02	1.24E-01	2.19	1.12	6.35E-02
40	1.000	5.86E-02	1.32E-01	2.25	1.15	6.72E-02
35	1.000	6.18E-02	1.50E-01	2.43	1.22	7.53E-02
30	1.000	6.55E-02	1.73E-01	2.64	1.30	8.54E-02
25	1.000	6.65E-02	1.79E-01	2.69	1.33	8.82E-02
20	1.000	6.43E-02	1.67E-01	2.60	1.29	8.28E-02
15	1.000	6.29E-02	1.58E-01	2.51	1.25	7.88E-02
12.5	1.000	6.28E-02	1.54E-01	2.45	1.23	7.72E-02
10	1.000	6.71E-02	1.67E-01	2.49	1.24	8.35E-02
9	1.000	6.99E-02	1.76E-01	2.52	1.26	8.78E-02
8	1.000	7.32E-02	1.86E-01	2.53	1.26	9.24E-02
7	1.000	7.52E-02	1.88E-01	2.50	1.25	9.38E-02
6	0.999	7.84E-02	1.91E-01	2.44	1.22	9.59E-02
5	0.999	8.62E-02	2.07E-01	2.40	1.21	1.04E-01
4	0.999	8.68E-02	2.05E-01	2.36	1.19	1.04E-01
3	0.857	9.53E-02	2.08E-01	2.18	1.12	1.07E-01
2.5	0.715	7.28E-02	1.57E-01	2.15	1.11	8.07E-02
2	0.710	5.73E-02	1.20E-01	2.10	1.08	6.22E-02
1.5	0.704	5.65E-02	1.11E-01	1.96	1.03	5.81E-02
1.25	0.701	6.19E-02	1.19E-01	1.92	1.01	6.27E-02
1	0.696	7.27E-02	1.33E-01	1.83	1.00	7.27E-02
0.9	0.694	7.97E-02	1.47E-01	1.85	1.00	7.97E-02
0.8	0.691	7.72E-02	1.47E-01	1.91	1.01	7.77E-02
0.7	0.689	6.69E-02	1.31E-01	1.95	1.03	6.86E-02
0.6	0.686	6.08E-02	1.19E-01	1.96	1.03	6.25E-02
0.5	0.682	4.89E-02	9.61E-02	1.97	1.03	5.04E-02
0.4	0.678	3.02E-02	5.92E-02	1.96	1.03	3.11E-02
0.3	0.672	2.01E-02	3.92E-02	1.95	1.02	2.06E-02
0.2	0.668	1.34E-02	2.61E-02	1.94	1.02	1.37E-02
0.15	0.668	8.60E-03	1.68E-02	1.95	1.02	8.80E-03
0.125	0.668	6.26E-03	1.22E-02	1.95	1.02	6.40E-03
0.1	0.668	3.78E-03	7.35E-03	1.95	1.02	3.86E-03

Notes:
A_R and DF are defined in Equations 2.5.2-14 and 2.5.2-15, respectively.
GMRS = Ground motion response spectrum

Table 2.5.2-231
Regional Attenuation and Source Parameters Estimated in the Motazedian and Atkinson Study and Used in the Simulation of Ground Motions for the Cuba and Caribbean Region

Parameter	Motazedian and Atkinson (Reference 287) Values	Simulation Values
Stress Parameter	130 bars	65 bars (Low Case) 130 bars (Base Case) 260 bars (High Case)
Geometrical Spreading	1/R for R<75km 1.0 for 75<R<100km 1/SQRT(R) for R>100km	1/R for R<75km 1.0 for 75<R<100km 1/SQRT(R) for R>100km
Anelastic Attenuation Factor (Q) Model	$359\ f^{0.59}$	$241\ f^{0.59}$ (Low Case) $359\ f^{0.59}$ (Base Case) $536\ f^{0.59}$ (High Case)
Path Duration	Atkinson and Boore (Reference 210) Model with hinge points at 75 and 100 km	Atkinson and Boore (Reference 210) Model with hinge points at 75 and 100 km
Site Amplification	Puerto Rico specific for soft rock site (NEHRP C) conditions based on H/V ratio	Chen and Atkinson (Reference 343) CEUS Hard Rock
Kappa	0.03 sec	0.006 sec (Reference 244)
Shear Wave Velocity (Vs) at the Source	3.6 km/sec	3.6 km/sec
Density	$2.8\ g/cm^3$	$2.8\ g/cm^3$

Table 2.5.2-232
Experts Contacted for the SSHAC Level 2 Study in Support of Cuba Hazard Sensitivity Calculations

Expert	Affiliation	Expertise	Response
Coppersmith, Kevin	Coppersmith Consulting	Seismic hazard modeling, seismic source characterization	Email response
Cotilla-Rodríguez, Mario Octavio	Departmento de Fisca de la Tierra y Astrofisica, Facultad de Ciencias Fisicas, Universidad Complutense de Madrid (Madrid, Spain)	Cuba faults and neotectonics	Detailed email response
Garcia, Julio	Centro Nacional de Investigaciones Sismológicas (CENAIS) (Havana, Cuba)	Seismic hazard modeling in Cuba	No response
Hanson, Kathryn	AMEC	Seismic hazard modeling, seismic source characterization	Declined to participate
Ituralde-Vinent, Manuel	Museo Nacional de Historia Natural (Havana, Cuba) and Departamento de Geociencias, Instituto Superior Politécnico J.A. Echeverria (Havana, Cuba)	Geology of Cuba	No response
Moreno, Toiran Bladimir	Inst. of Solid Earth Physics, University of Bergen (Norway) and Centro Nacional de Investigaciones Sismologicas (CENAIS) (Santiago de Cuba, Cuba)	Seismology and geophysics of Cuba	Email response
Slejko, Dario	Istituto Nazionale di Oceanografia e di Geofisica Sperimetale (OGS) (Trieste, Italy)	Seismic hazard modeling in Cuba	Detailed email response
Toscano, Marguerite	Department of Paleobiology, Smithsonian Institute	Marine terrace mapping and dating in northern Cuba	Email response and telephone conversation regarding marine terraces in northern Cuba
Wong, Ivan	URS Corporation	Seismic hazard modeling, seismic source characterization	Detailed email responses
Youngs, Robert	AMEC	Seismic hazard modeling	Declined to participate
Zapata Balanque, Jose Alejandro	Universidad de Oriente (Santiago de Cuba, Cuba)	Cuba faults and neotectonics	Email response regarding plans for future paleoseismic studies in Cuba

Table 2.5.2-233
Cuba Seismic Source Alternatives for Hazard Sensitivity Calculations

		Source Zone Scenarios Increasing Hazard ➔			
		No Areal Sources	**Z6 Six Areal Sources**	**Z1 Single Areal Source**	**Z11% Elevated Rate Areal Source (+11% Increase in Rate)**
Fault Source Scenarios ➔ Increasing	No fault sources	N/A	Z6	Z1	Z11%
	SF Scaled Fault Sources	SF	Z6+SF[a]	Z1+SF[a]	Z11%+SF[b]
	FF Full Fault Sources	FF[c]	Z6+FF[c]	Z1+FF[c]	Z11%+FF[c]

(a) Z1+SF was evaluated as a reasonable combination scenario in the hazard sensitivity calculations. As discussed in the text, area source scenario Z6 was found to result in lower hazard than area source scenario Z1. Thus, it is unnecessary to further investigate the combination scenario Z6+SF.

(b) As discussed in the text, source area scenario Z11% is considered a conservative assessment of the seismic hazard derived from the cataloged seismicity. Therefore, the combination scenario Z11%+SF is considered overly conservative for consideration in the hazard sensitivity calculations.

(c) As discussed in the text, fault source scenario FF was determined to be technically indefensible compared to the cataloged seismicity. Therefore, any combination scenarios with FF were similarly eliminated as technically indefensible.

Shaded source scenarios not quantitatively evaluated.

Table 2.5.2-234
Cuba Areal Source Zone and Northern Cuba Subzone Recurrence Parameters

Zone	Zone Area (km^2)	# Events Events[a]	a-value[b]	b-value	Rate of M_w 5 to 7.3 events per year/km^2
Cuba areal source zone	250,286	152	-2.430	0.839	2.341E-7
Northern Cuba subzone	80,770	46	-2.383[c]	0.839[d]	2.609E-7

(a) Events ≥ M_w 3.0, filtered for completeness periods
(b) Normalized to events per year/km^2
(c) Value represents the 11 percent increase discussed in text
(d) Fixed to Cuba areal source zone b-value

Table 2.5.2-235
Completeness Periods and Earthquake Counts in Each Bin from the Phase 2 Earthquake Catalog

Magnitude Range (M_w)	Start Date	End Date	Number of Earthquakes from Phase 2 Earthquake Catalog
3.0–4.0	1/1960	3/2008	119
4.0–5.0	1/1940	3/2008	17
5.0–6.0	1/1850	3/2008	14
6.0–7.0	1/1500	3/2008	2

Source: Reference 255

Table 2.5.2-236
Summary of Seismic Source Parameters for Intraplate Cuba Fault Sources for Hazard Sensitivity Calculation

Sensitivity Fault Source	Dip	Rupture Depth Range (km)	Length (km)	Magnitude (M_w) [and weight]	Slip Rate (mm/yr) [and weight]
Baconao SE	90°	0–15	101	7.0 [0.5] 7.3 [0.5]	0.01 [0.1] 0.1 [0.5] 1.0 [0.4]
Baconao NW	90°	0–15	191	7.0 [0.5] 7.3 [0.5]	0.001 [0.33] 0.01 [0.34] 0.1 [0.33]
Camaguey	90°	0–15	131	7.0 [0.5] 7.3 [0.5]	0.001 [0.33] 0.01 [0.34] 0.1 [0.33]
Cochinos	90°	0–15	68	7.0 [0.5] 7.3 [0.5]	0.001 [0.33] 0.01 [0.34] 0.1 [0.33]
Cubitas	90°	0–15	283	7.0 [0.5] 7.3 [0.5]	0.001 [0.33] 0.01 [0.34] 0.1 [0.33]
Guane	90°	0–15	292	7.0 [0.5] 7.3 [0.5]	0.001 [0.33] 0.01 [0.34] 0.1 [0.33]
Habana-Cienfuegos	90°	0–15	269	7.0 [0.5] 7.3 [0.5]	0.001 [0.33] 0.01 [0.34] 0.1 [0.33]
Hicacos	90°	0–15	114	7.0 [0.5] 7.3 [0.5]	0.001 [0.33] 0.01 [0.34] 0.1 [0.33]
La Trocha	90°	0–15	257	7.0 [0.5] 7.3 [0.5]	0.001 [0.33] 0.01 [0.34] 0.1 [0.33]
Las Villas	90°	0–15	197	7.0 [0.5] 7.3 [0.5]	0.001 [0.33] 0.01 [0.34] 0.1 [0.33]
Nipe	90°	0–15	292	7.0 [0.5] 7.3 [0.5]	0.01[0.1] 0.1 [0.5] 1.0 [0.4]
Nortecubana West	30°S	0–15	595	7.0 [0.5] 7.3 [0.5]	0.001 [0.33] 0.01 [0.34] 0.1 [0.33]
Nortecubana Central	30°S	0–15	441	7.0 [0.5] 7.3 [0.5]	0.001 [0.33] 0.01 [0.34] 0.1 [0.33]
Nortecubana East	30°S	0–15	340	7.0 [0.5] 7.3 [0.5]	0.01[0.1] 0.1 [0.5] 1.0 [0.4]
Pinar	90°	0–15	215	7.0 [0.5] 7.3 [0.5]	0.001 [0.33] 0.01 [0.34] 0.1 [0.33]

Table 2.5.2-237
Moment Rates, Ratio of Fault-Based Moment Rate to Seismicity-Based Moment Rates, and Return Periods for M_w 6.5 and 7.0 from Cuba Sensitivity Options

Moment Rate Options	Moment Rate (dyne-cm/yr)	Ratio, Fault-based/Seismicity-based	Return Period for M_w 6.5 (years)	Return Period for M_w 7 (years)
Historical Seismicity[a]	7.7844E+23	Not applicable	81	456
Low Slip Rate Option[b]	6.6686E+22	0.0857	946	5321
Middle Slip Rate Option[b]	6.6686E+23	0.8567	95	532
High Slip Rate Option[b]	6.6686E+24	8.5666	9.5	53
Weighted Mean Slip Rate[c]	2.8535E+24	3.6657	22	124

(a) Moment rate obtained from seismicity catalog and used for Cuba areal source (Z1) and for scaled fault scenario (SF).
(b) Moment rates obtained from low, middle, and high slip rate values presented in Table 2.5.2-236.
(c) Moment rate obtained from weighted mean of slip rate values presented in Table 2.5.2-236 and used for full fault scenario (FF).

Table 2.5.2-238
Summary of Hazard Sensitivity Study Results: Comparison of MAFE

	Base Case Z1		Scenario Z6		Scenario SF		Scenario Z11%		Scenario Z1+SF	
10^{-4} mean annual frequency of exceedance (MAFE)										
Freq	MAFE	Amp[(a)]	MAFE	% Diff	MAFE	% Diff	MAFE	% Diff	MAFE	% Diff
1 Hz	1.00E-04	0.0343	9.499E-05	-5.0%	9.676E-05	-3.2%	1.018E-04	1.8%	1.114E-04	11.4%
10 Hz	1.00E-04	0.0822	9.122E-05	-8.8%	8.798E-05	-12.0%	1.025E-04	2.5%	1.094E-04	9.4%
10^{-5} mean annual frequency of exceedance (MAFE)										
Freq	MAFE	Amp[(a)]	MAFE	% Diff	MAFE	% Diff	MAFE	% Diff	MAFE	% Diff
1 Hz	1.00E-05	0.0663	9.539E-06	-4.6%	1.010E-05	1.0%	1.013E-05	1.3%	1.131E-05	13.1%
10 Hz	1.00E-05	0.278	9.891E-06	-1.1%	9.969E-06	-0.3%	9.992E-06	-0.1%	1.014E-05	1.4%

(a) Rock motion (g)

Table 2.5.2-239
Summary of Hazard Sensitivity Results: Comparison of Rock Motion Amplitudes

	Base Case Z1	Scenario Z6			Scenario SF			Scenario Z11%			Scenario Z1+SF		
Rock motions (g) at 10^{-4} mean annual frequency of exceedance (MAFE)													
Freq	Amp	Amp	Amp Diff	% Diff	Amp	Amp Diff	% Diff	Amp	Amp Diff	% Diff	Amp	Amp Diff	% Diff
1 Hz	0.0343	0.0338	-0.0005	-1.5%	0.0340	-0.0003	-0.9%	0.0345	0.0002	0.6%	0.0354	0.0011	3.2%
10 Hz	0.0822	0.0784	-0.0038	-4.6%	0.0765	-0.0057	-6.9%	0.0832	0.0010	1.2%	0.0858	0.0036	4.4%
Rock motions (g) at 10^{-5} mean annual frequency of exceedance (MAFE)													
Freq	Amp	Amp	Amp Diff	% Diff	Amp	Amp Diff	% Diff	Amp	Amp Diff	% Diff	Amp	Amp Diff	% Diff
1 Hz	0.0663	0.0654	-0.0009	-1.4%	0.0665	0.0002	0.3%	0.0665	0.0002	0.3%	0.0686	0.0023	3.5%
10 Hz	0.278	0.276	-0.0020	-0.7%	0.278	0.0000	0.0%	0.278	0.0000	0.0%	0.280	0.0020	0.7%

Table 2.5.2-240
Santaren Anticline Fault Source Parameters

Length (km)	Nearest Distance to Site (km)	Farthest Distance to Site (km)	Uplift Rate (mm/yr)	Fault Dip (degrees)	Slip Rate (mm/yr)
70.5	267.7	333.4	0.05	45	0.071

Table 2.5.2-241
Summary of Rock Hazard Sensitivity to Santaren Anticline Fault Source: Comparison of Exceedance (MAFE) at FSAR Amplitudes

	FSAR		FSAR + Santaren Anticline Fault Source	
	10^{-4} mean annual frequency of exceedance			
Freq	MAFE	Amp.	MAFE	MAFE % Diff
1 Hz	1.00E-04	0.0343	1.0605E-04	6.05%
10 Hz	1.00E-04	0.0822	1.0726E-04	7.26%
	10^{-5} mean annual frequency of exceedance			
Freq	MAFE	Amp.	MAFE	MAFE % Diff
1 Hz	1.00E-05	0.0663	1.0880E-05	8.80%
10 Hz	1.00E-05	0.278	1.0142E-05	1.42%

Table 2.5.2-242
Summary of Rock Motion Sensitivity to Santaren Anticline Fault Source: Ground Motion Amplitudes in Comparison to FSAR Ground Motion Amplitudes

	FSAR	FSAR + Santaren Anticline Fault Source		
	Rock motions (g) at 10^{-4} mean annual frequency of exceedance			
Freq	Amp.	Amp.	Amp. Diff	Amp. % Diff
1 Hz	0.0343	0.034899	0.000599	1.75%
10 Hz	0.0822	0.085058	0.002858	3.48%
	Rock motions (g) at 10^{-5} mean annual frequency of exceedance			
Freq	Amp.	Amp.	Amp. Diff	Amp. % Diff
1 Hz	0.0663	0.067900	0.001600	2.41%
10 Hz	0.278	0.280139	0.002139	0.77%

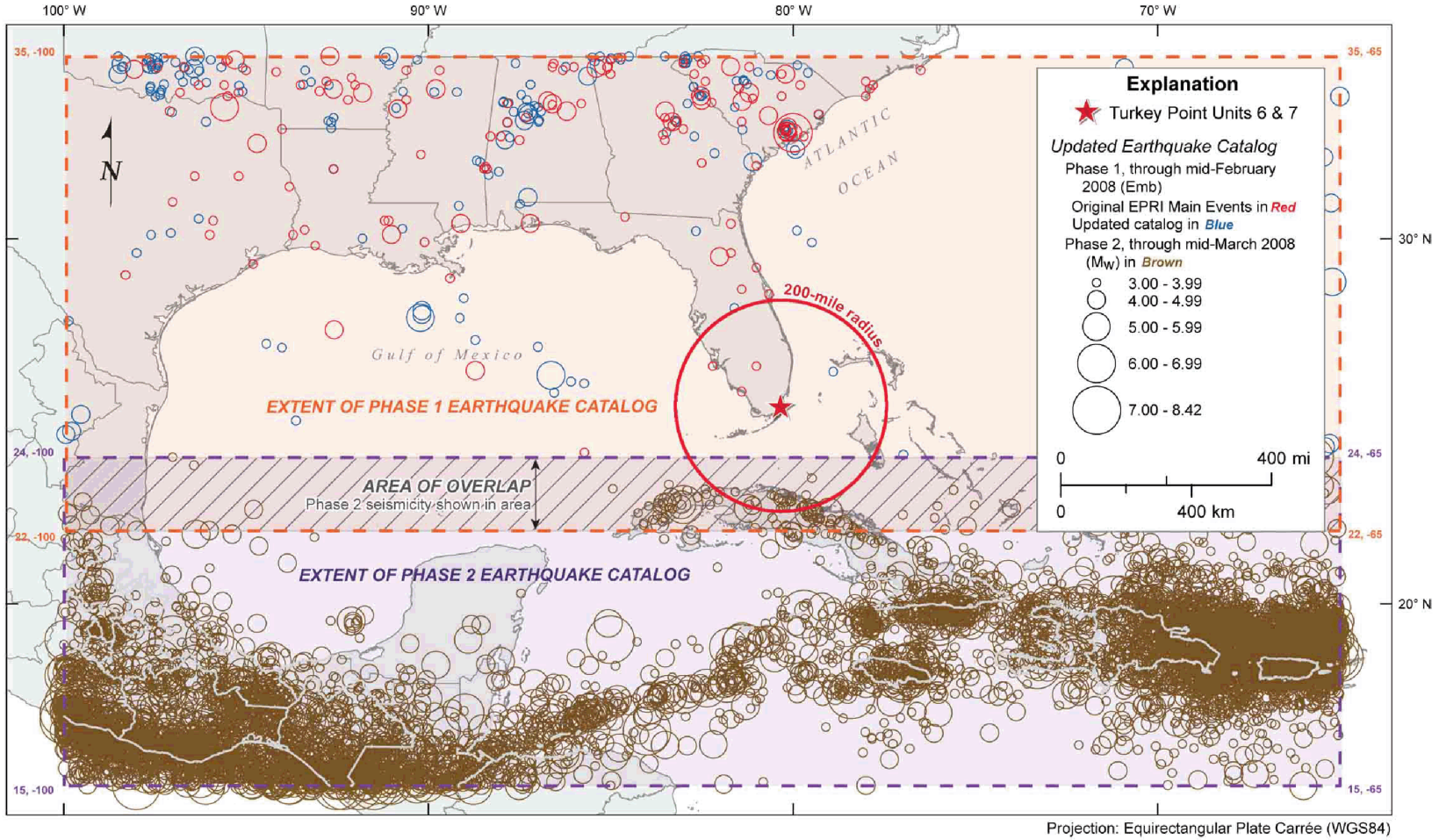

Figure 2.5.2-201 Seismicity in the Study Region, Phase 1 and Phase 2

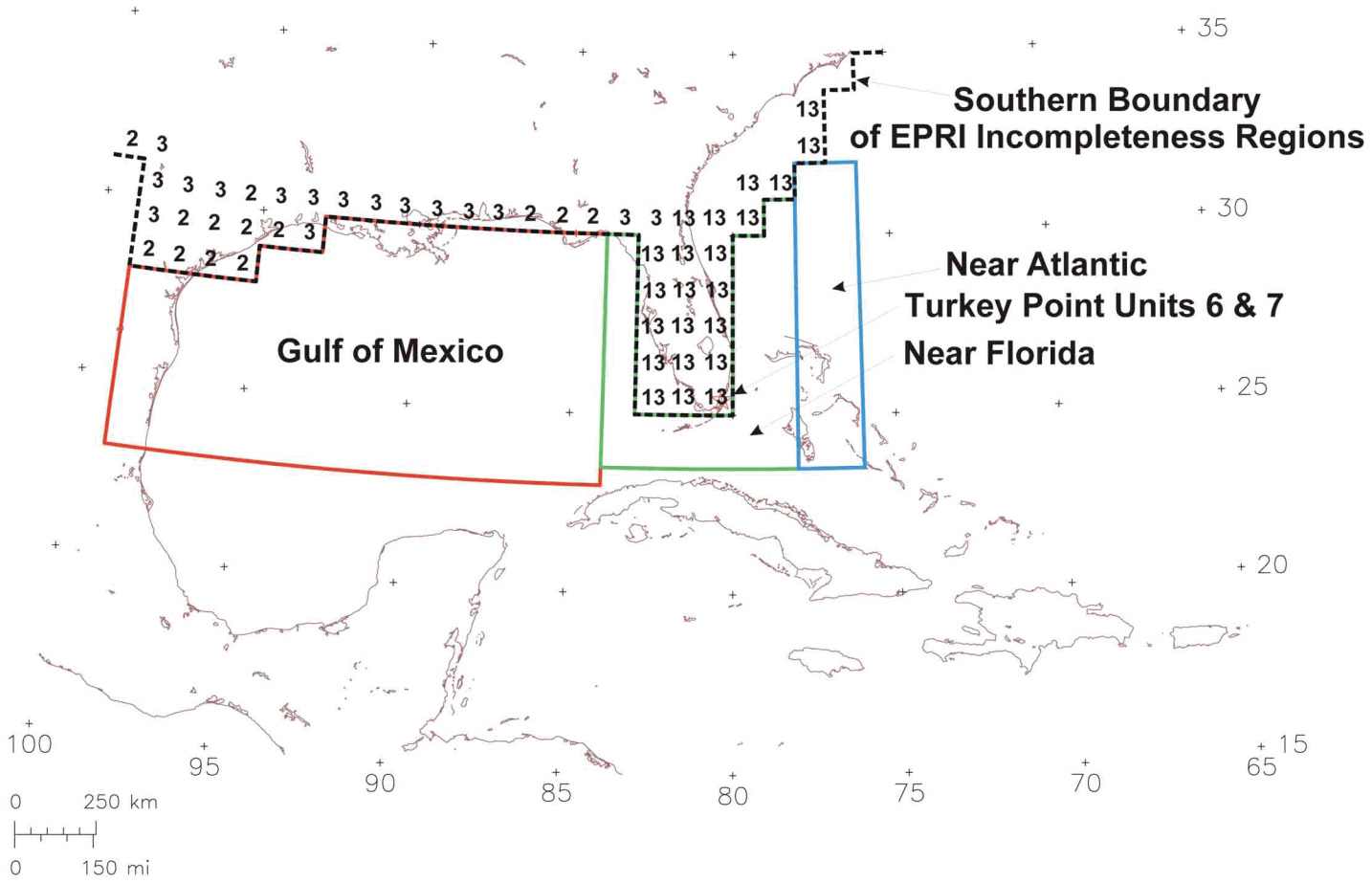

Notes:
See Table 5-1 of EPRI (Reference 243) for EPRI Incompleteness Regions.
Numbers indicate the EPRI 1 degree x 1 degree regions of incompleteness along the southern border of 1989 EPRI-SOG coverage.

Figure 2.5.2-202 Supplemental Areas of Incompleteness Regions, Gulf of Mexico, Near Florida, and Near Atlantic, South of the Boundary of EPRI Incompleteness Regions

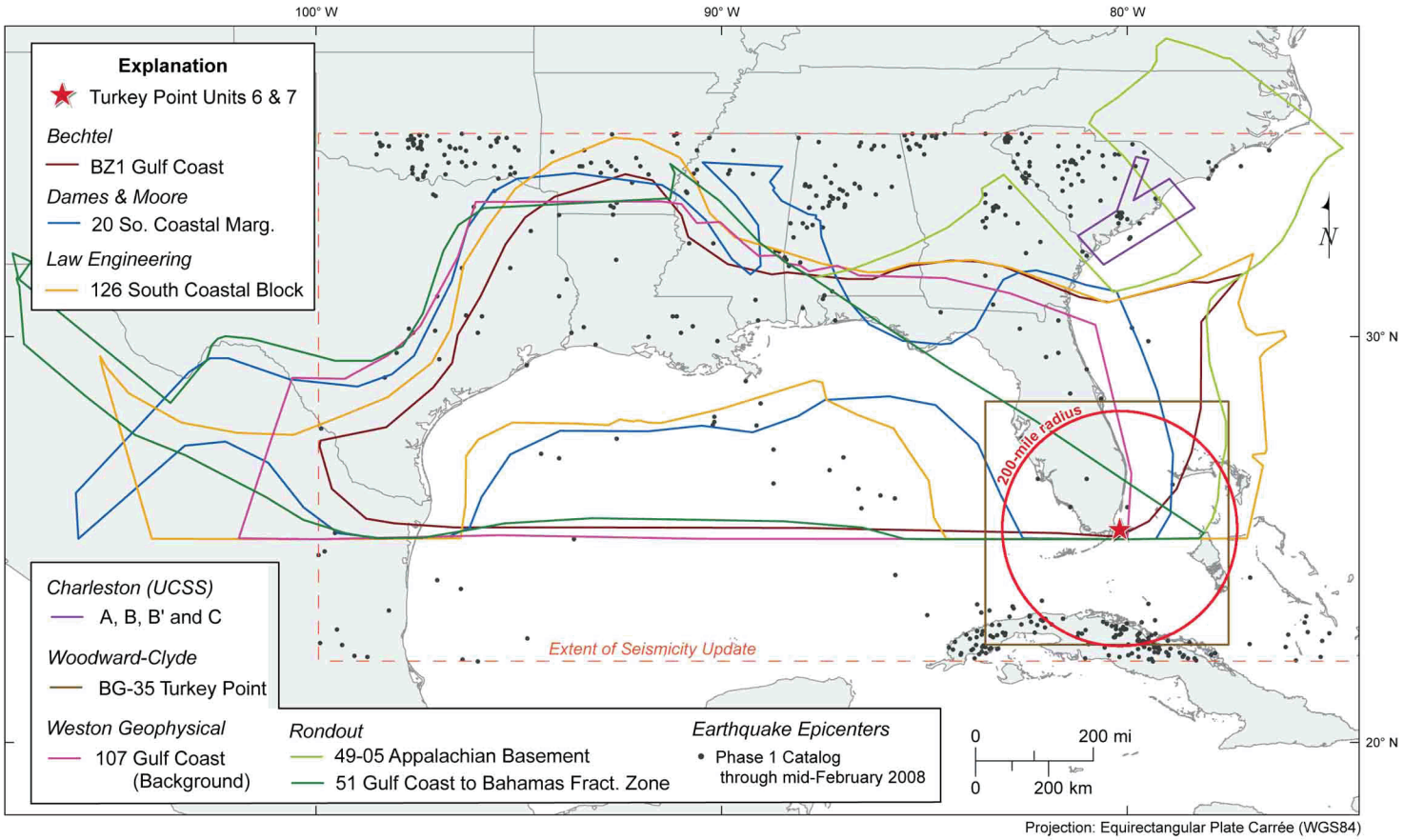

Figure 2.5.2-203 EPRI Seismic Source Zones and Updated Charleston Seismic Source (UCSS) Model Sources

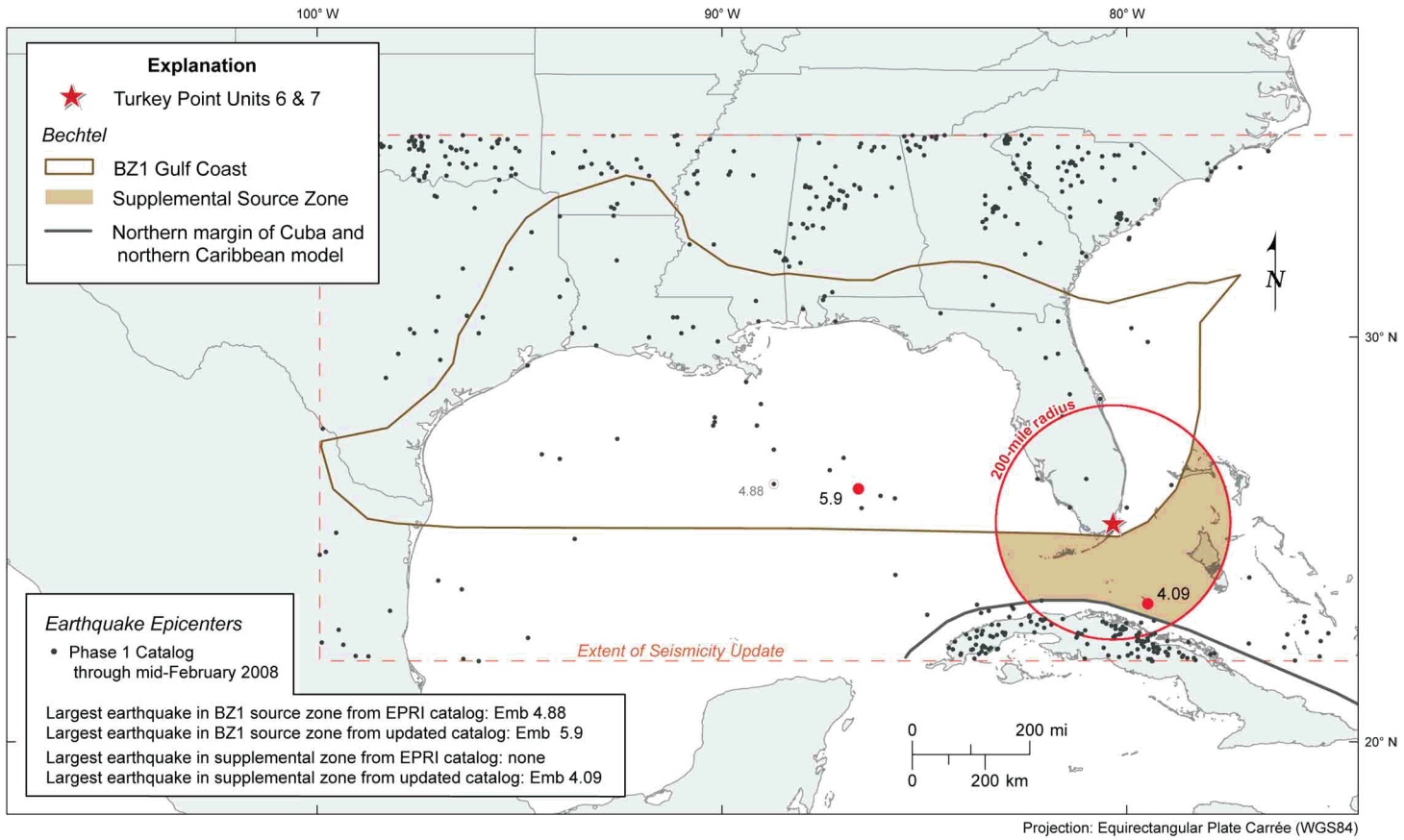

Note: Epicenters of the largest magnitude events in the seismic source zones are highlighted as red dots.

Figure 2.5.2-204 EPRI and Supplemental Source Zones — Bechtel

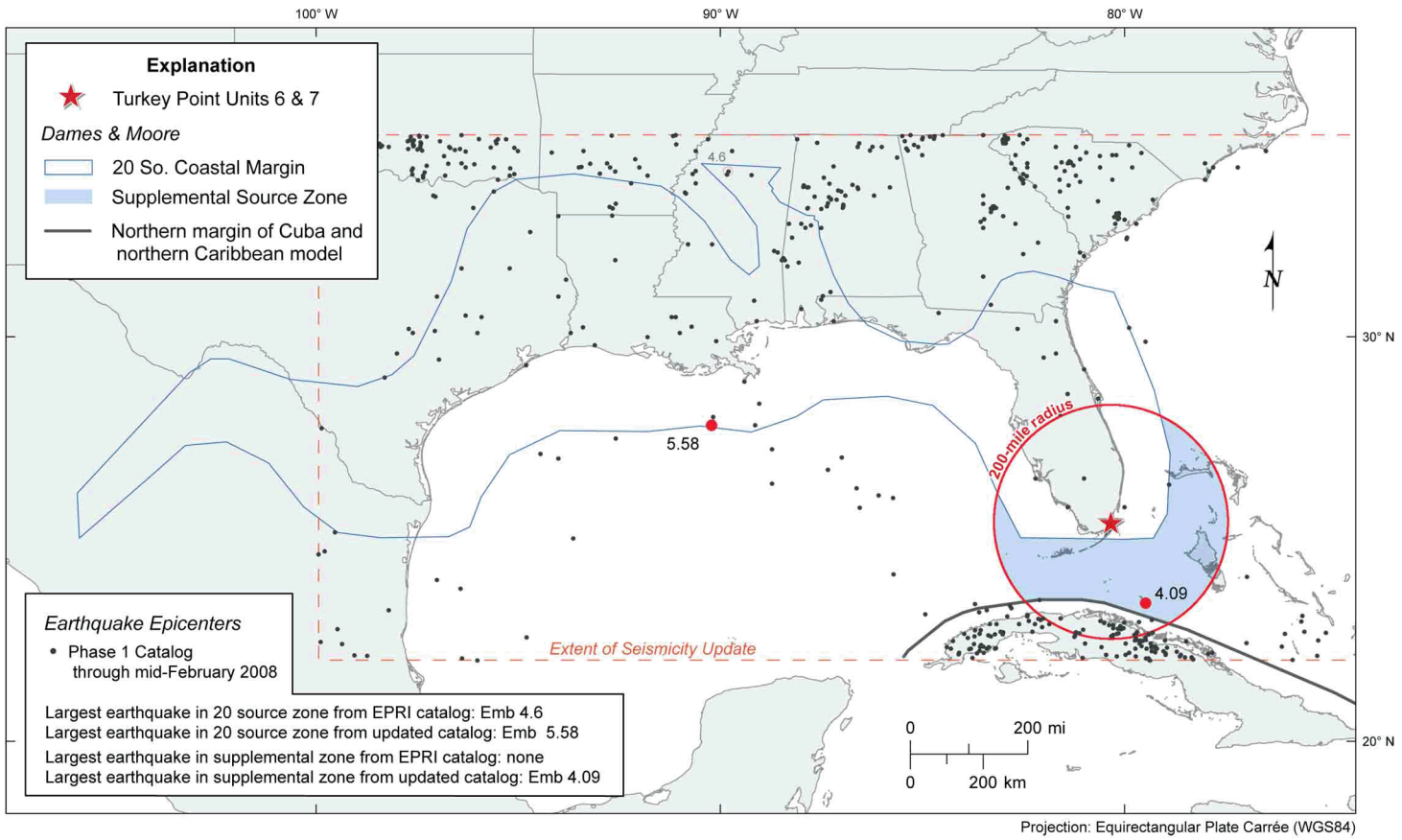

Note: Epicenters of the largest magnitude events in the seismic source zones are highlighted as red dots.

Figure 2.5.2-205 EPRI and Supplemental Source Zones — Dames & Moore

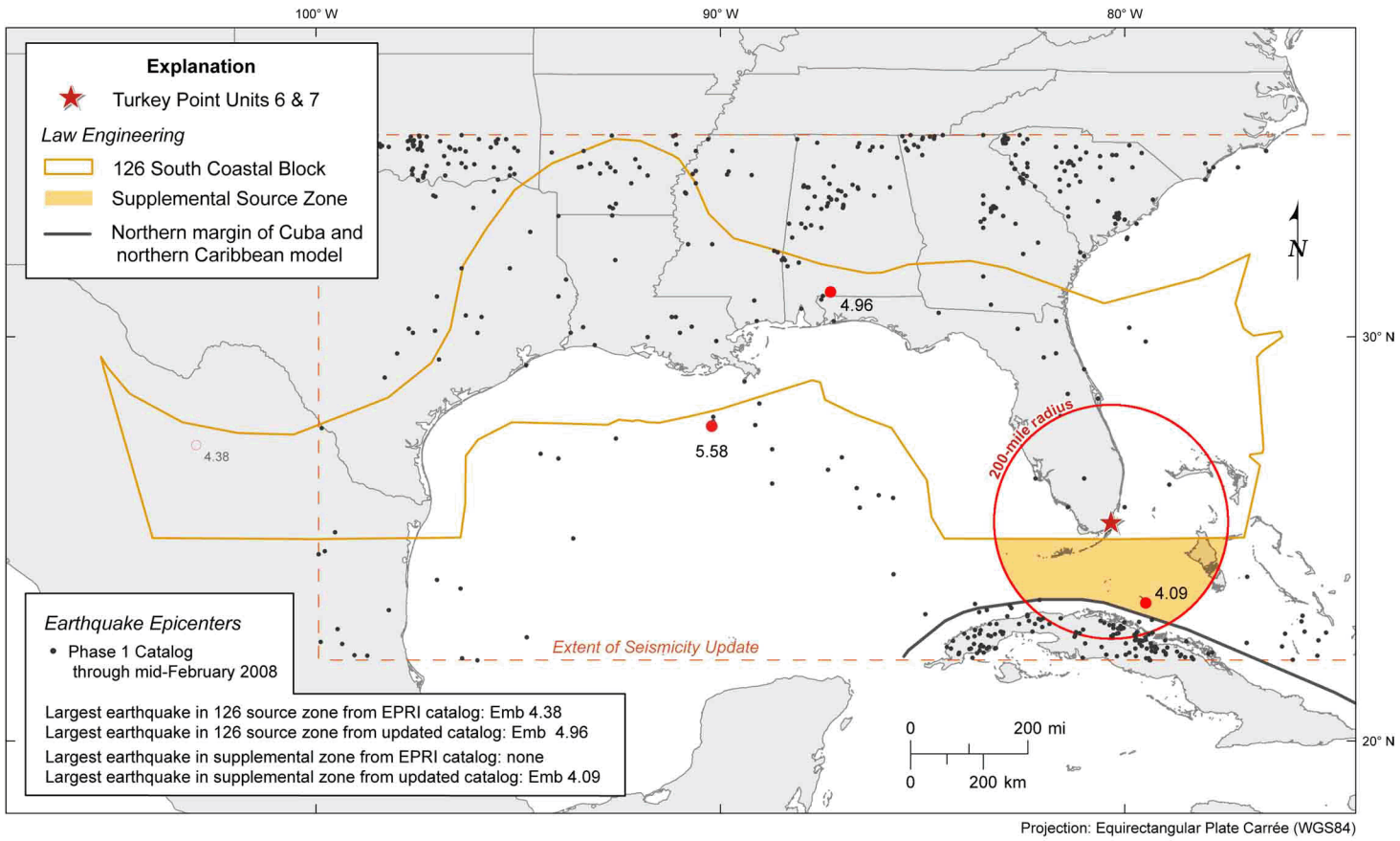

Note: Epicenters of the largest magnitude events in the seismic source zones are highlighted as red dots.

Figure 2.5.2-206 EPRI and Supplemental Source Zones — Law Engineering

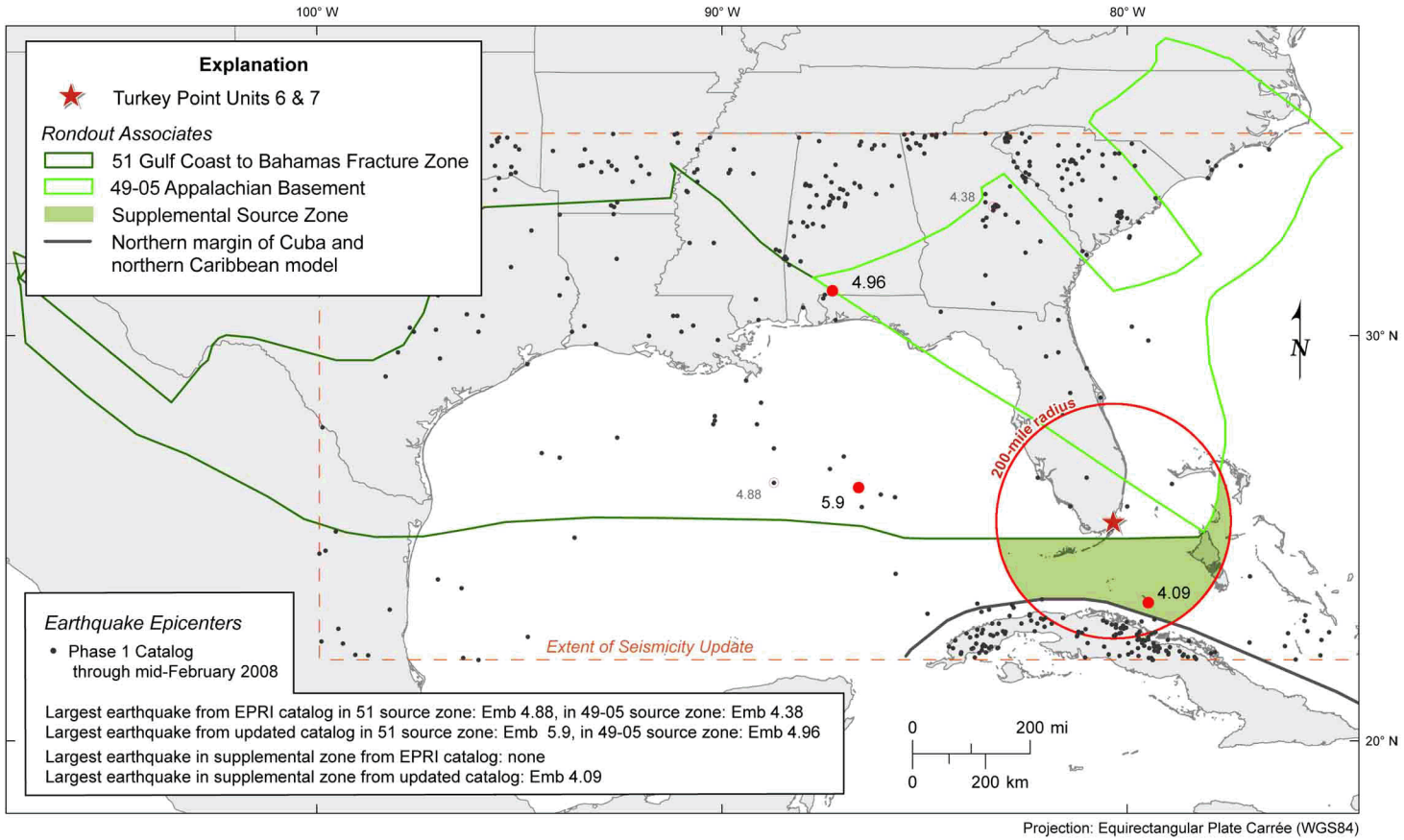

Note: Epicenters of the largest magnitude events in the seismic source zones are highlighted as red dots.

Figure 2.5.2-207 EPRI and Supplemental Source Zones — Rondout Associates

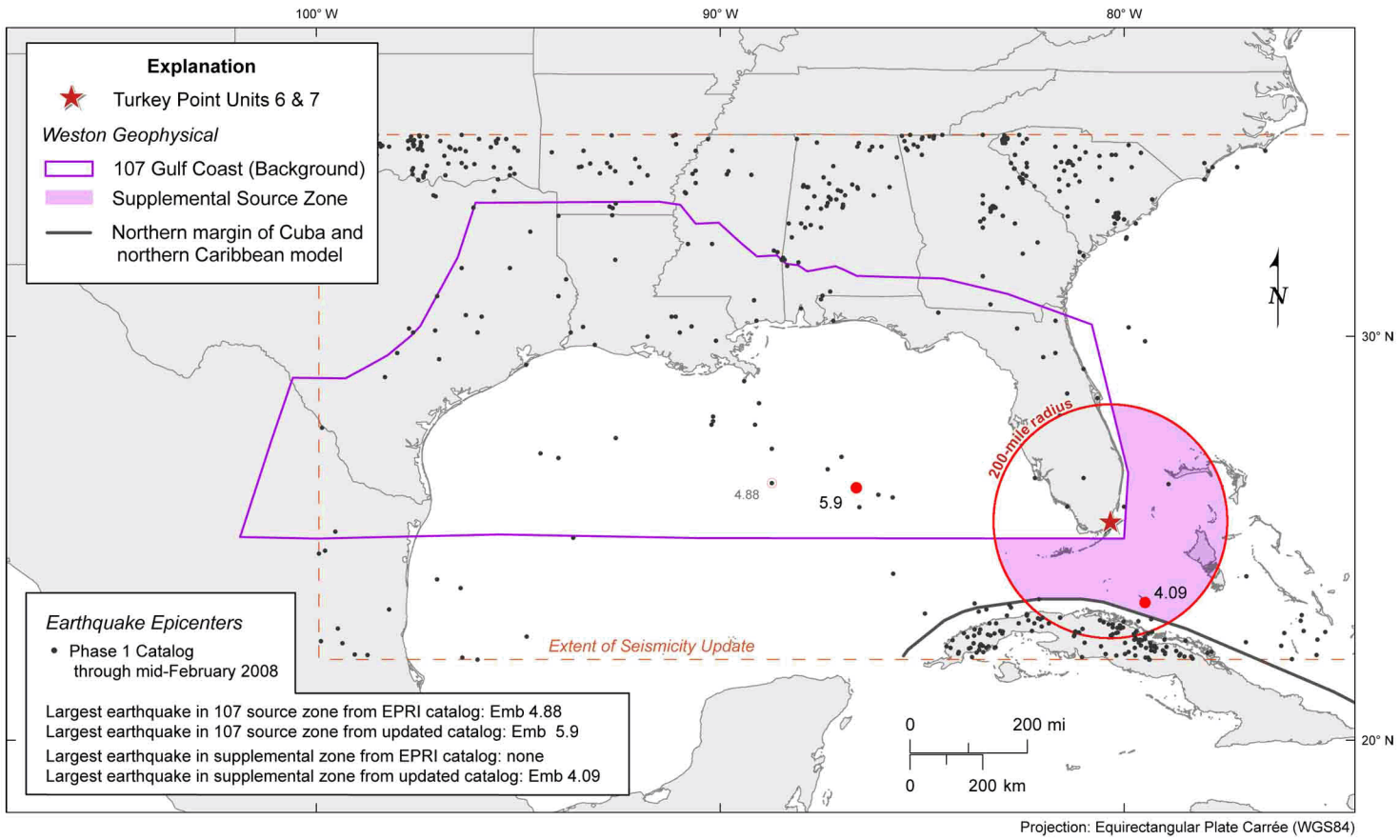

Note: Epicenters of the largest magnitude events in the seismic source zones are highlighted as red dots.

Figure 2.5.2-208 EPRI and Supplemental Source Zones — Weston Geophysical

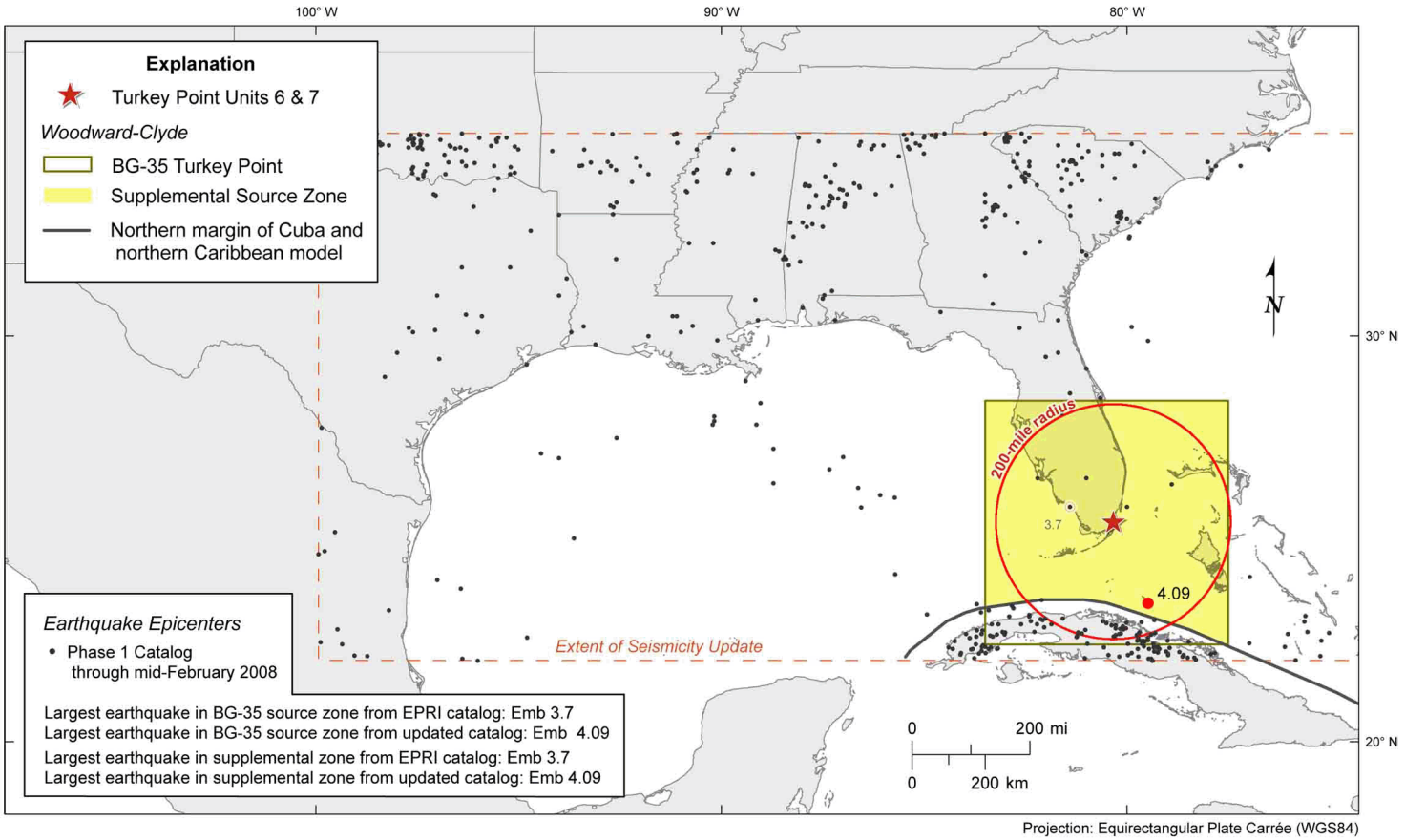

Note: Epicenters of the largest magnitude events in the seismic source zones are highlighted as red dots.

Figure 2.5.2-209 EPRI and Supplemental Source Zones — Woodward-Clyde

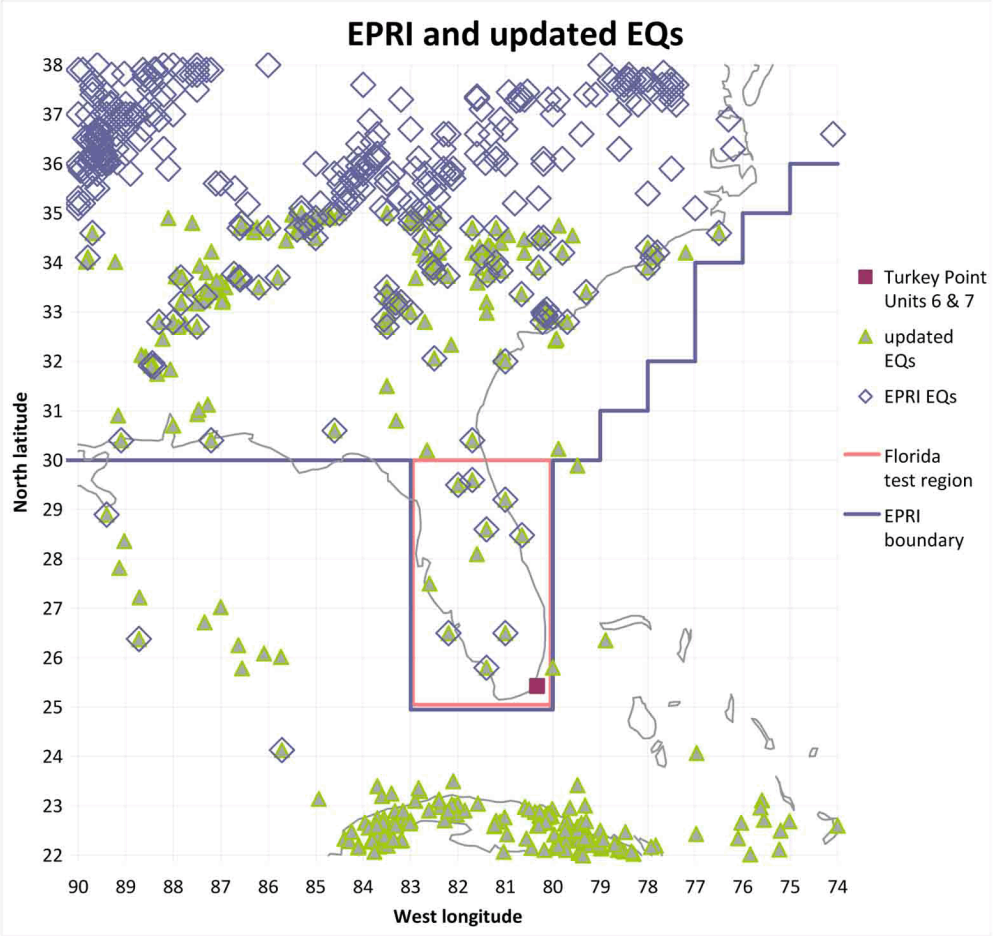

Note: The boundary of the EPRI study region is shown in blue, and the Florida test region used to compare seismicity rates is shown in orange.

Figure 2.5.2-210 Historical Seismicity from EPRI Earthquake Catalog and from Updated Catalog (Through 2007) in Southeastern United States

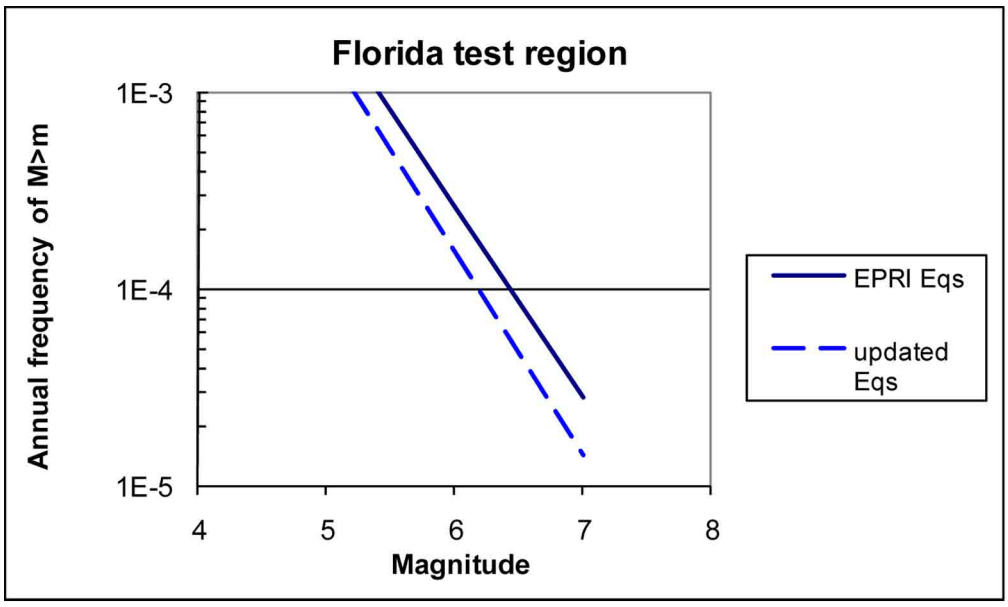

Sources: References 245 and 246

Figure 2.5.2-211 Earthquake Occurrence Rates for EPRI Catalog and for Updated Catalog Extended Through 2007 for Florida Test Region

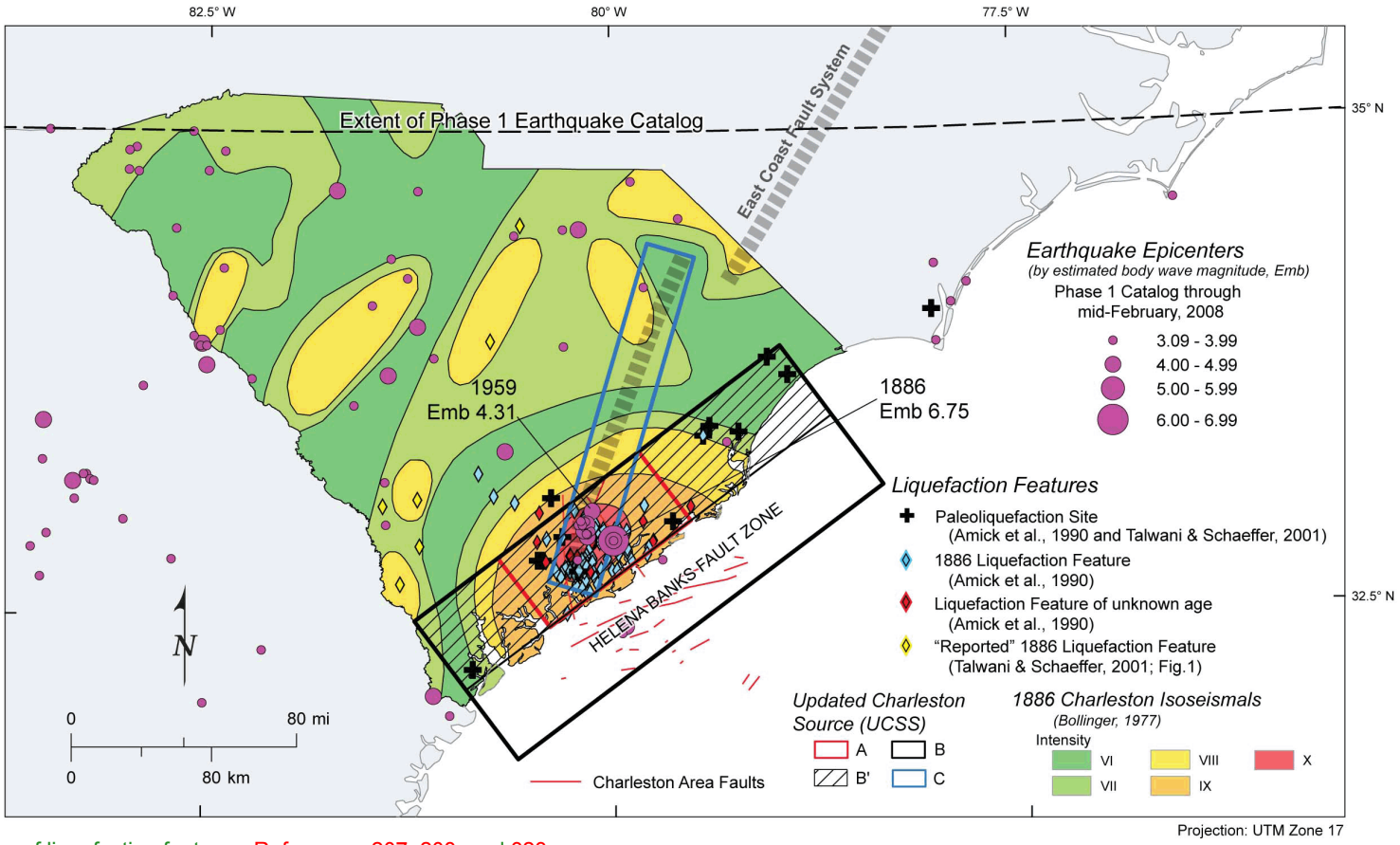

Sources of liquefaction features: References 207, 208, and 323
Source of the 1886 Charleston isoseismals: Reference 216

Figure 2.5.2-212 Updated Charleston Seismic Source (UCSS) Model Sources

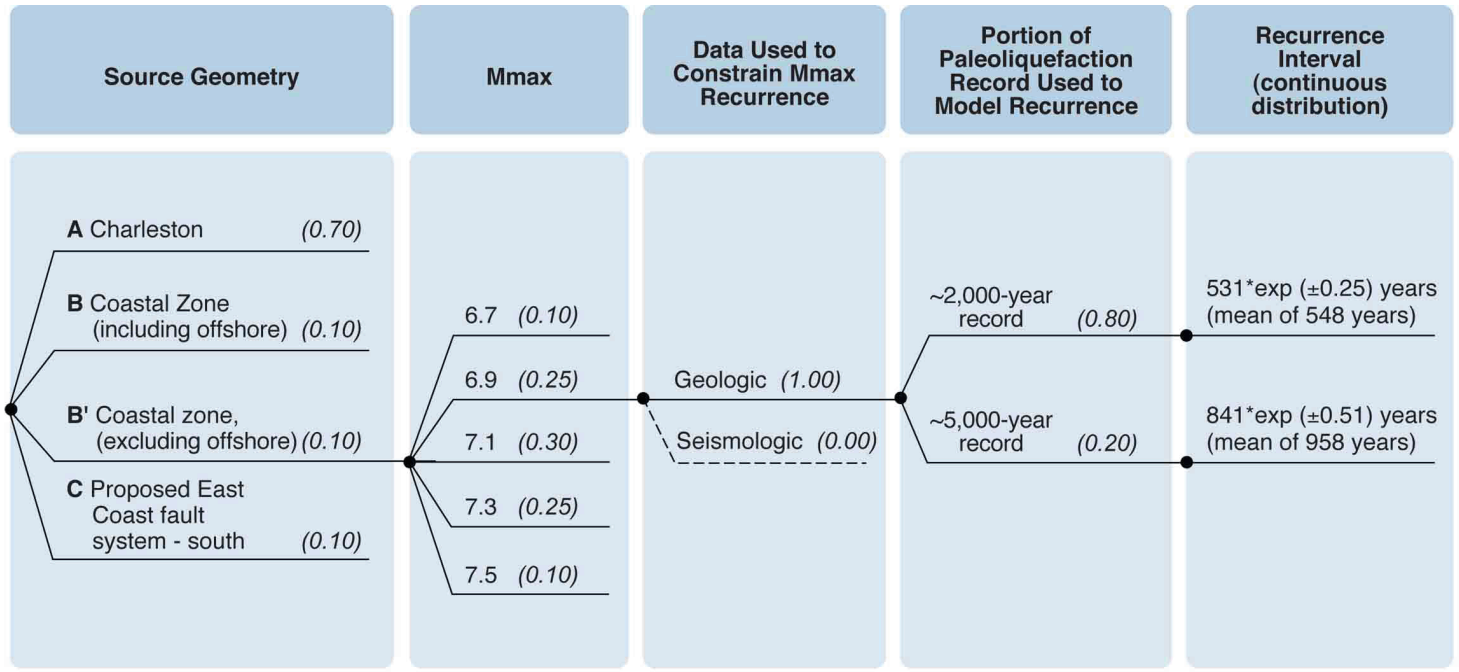

Figure 2.5.2-213 Updated Charleston Seismic Source (UCSS) Logic Tree with Weights for Each Branch

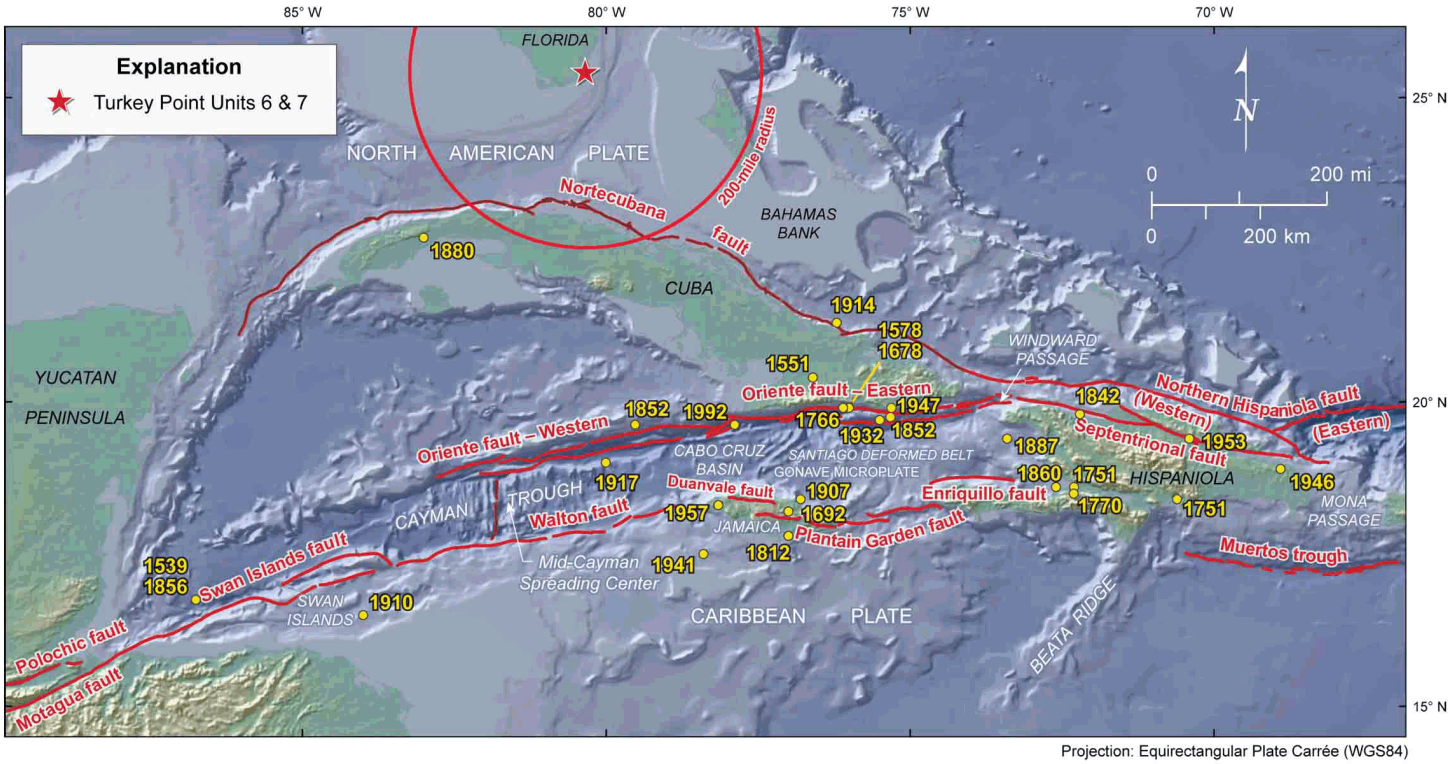

Figure 2.5.2-214 Tectonic Features and Significant Earthquakes of Cuba Area and the North America-Caribbean Plate Boundary Region

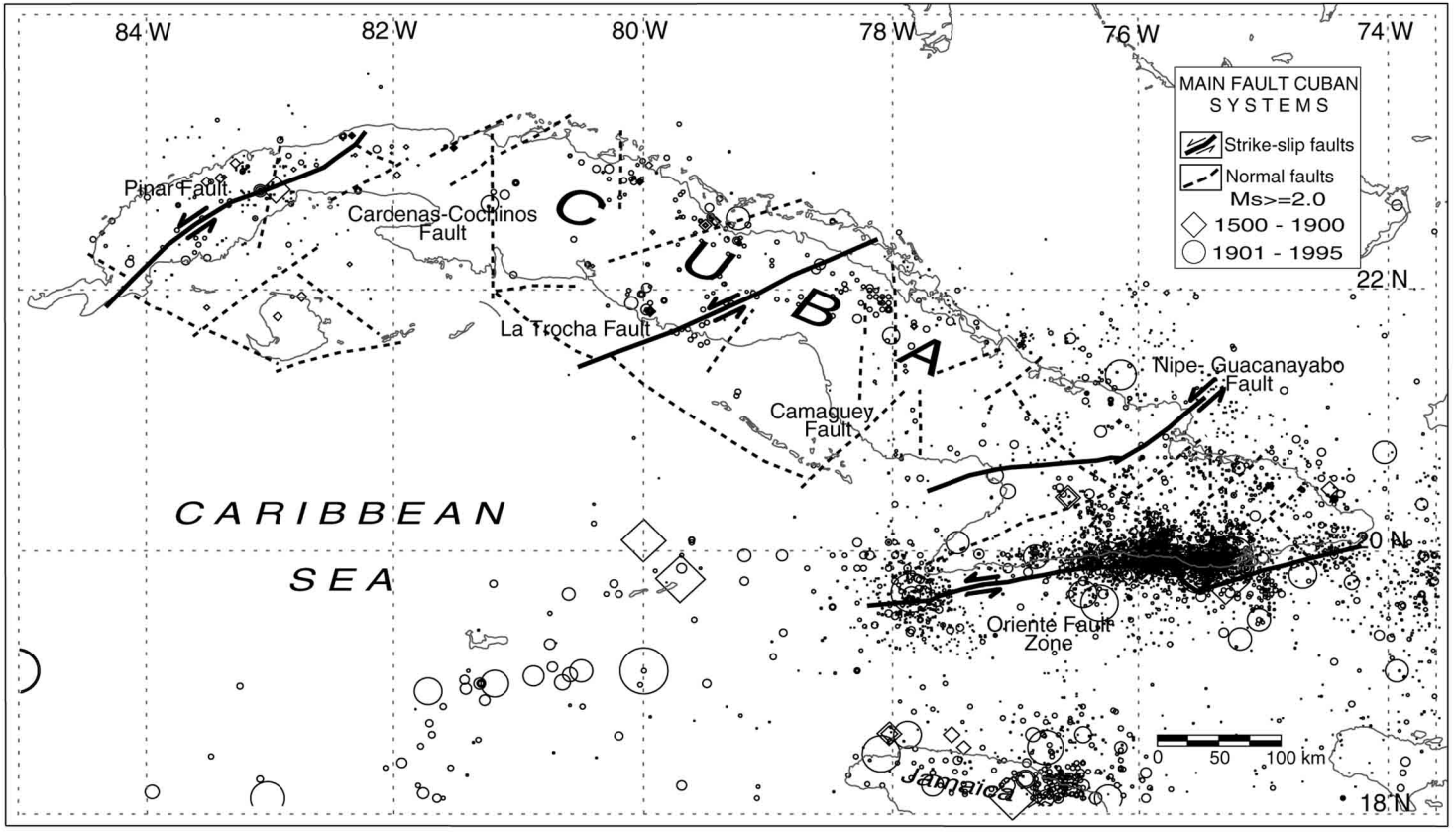

Figure 5. Map of the principal faults in Cuba (modified from Iturralde-Vinent, 1996). Solid lines show strike-slip faults; dashed lines represent normal faults. The epicenters of earthquakes (diamond, pre-1900; circles, during the twentieth century) with magnitude larger than, or equal to, 2 are reported.

Source: Reference 254

Figure 2.5.2-215 Fault Map of Cuba from Garcia et al.

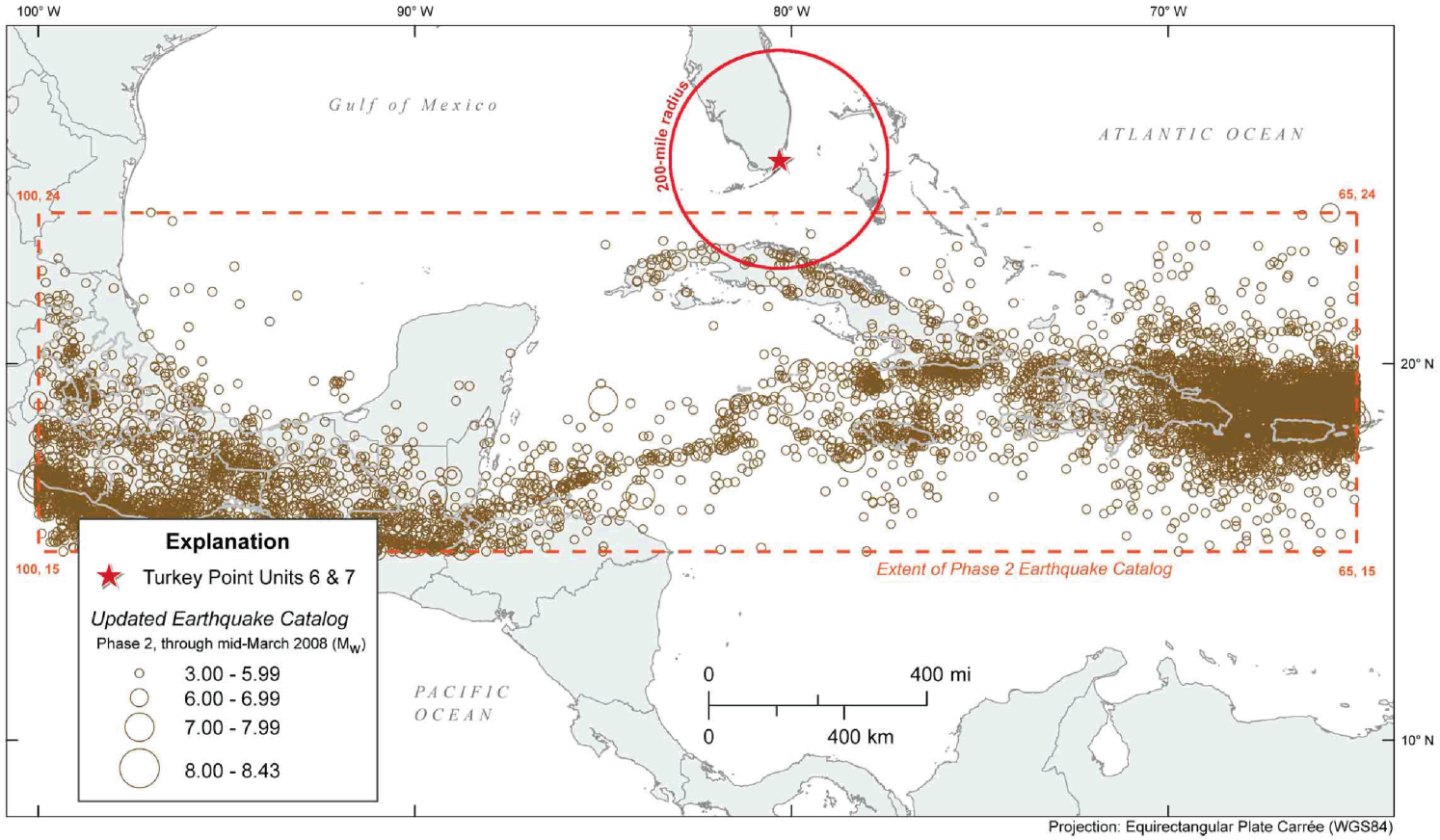

Figure 2.5.2-216 Seismicity in the Cuba Area and the North America-Caribbean Plate Boundary Region, 1500–2008

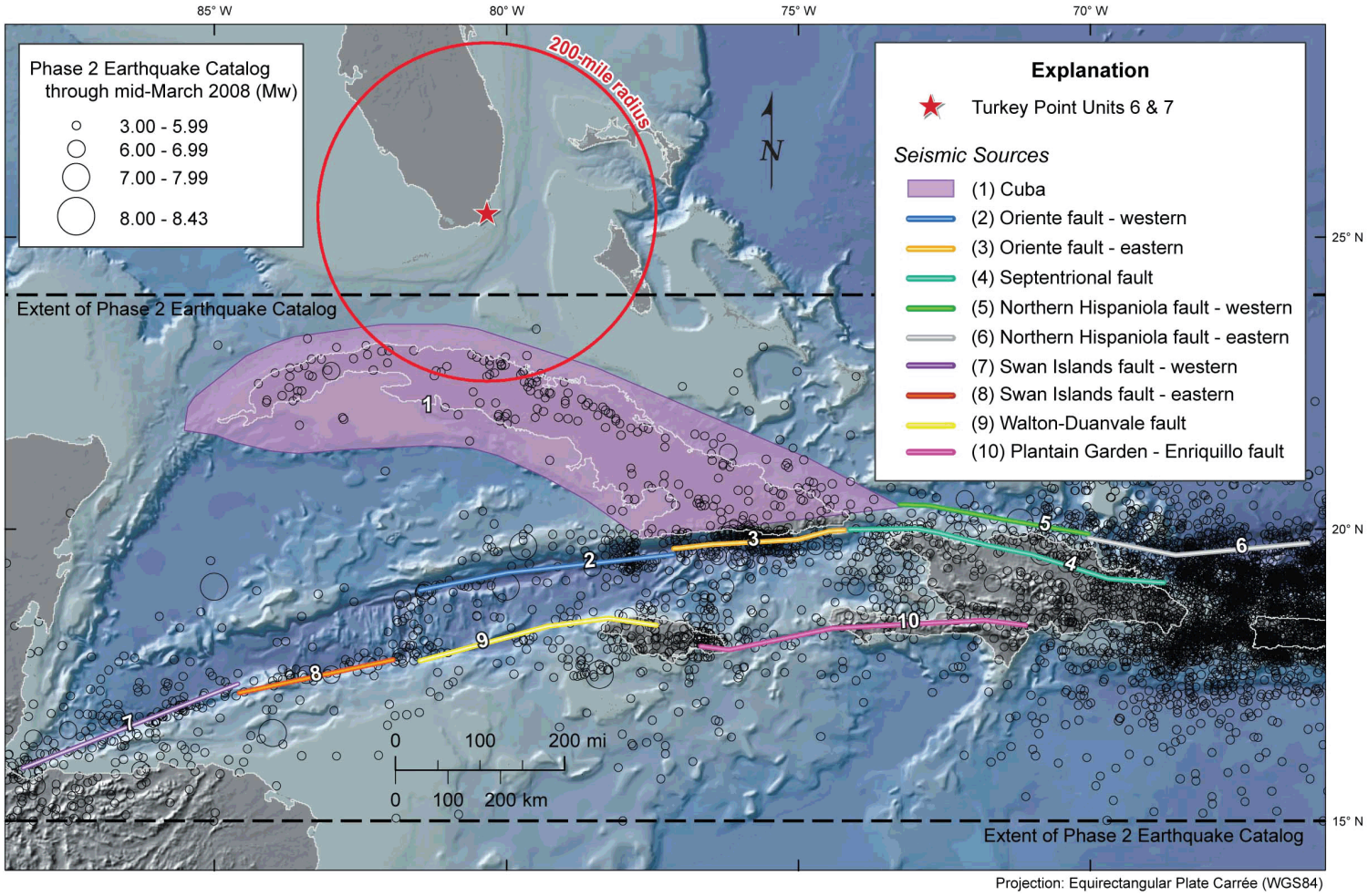

Figure 2.5.2-217 Cuba and Northern Caribbean Seismic Source Model Sources

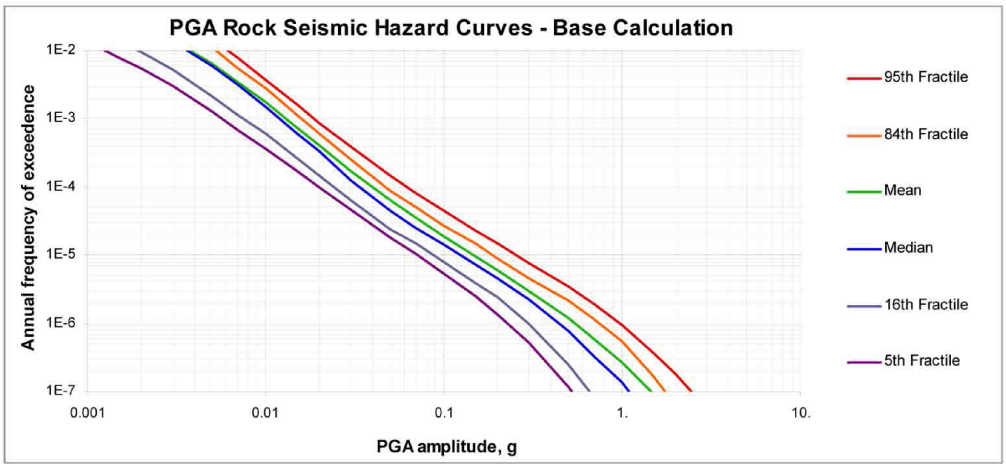

Figure 2.5.2-218 Mean and Fractile Rock PGA Seismic Hazard Curves

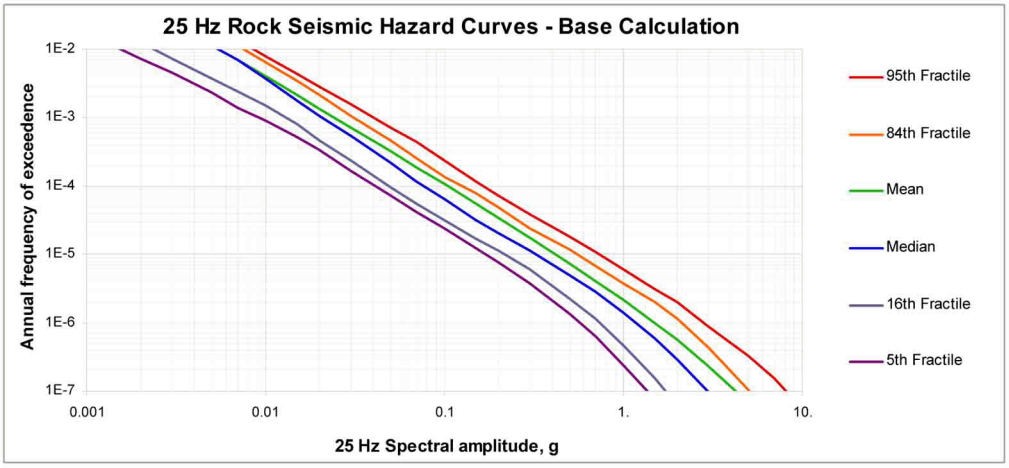

Figure 2.5.2-219 Mean and Fractile Rock 25 Hz Seismic Hazard Curves, Rock

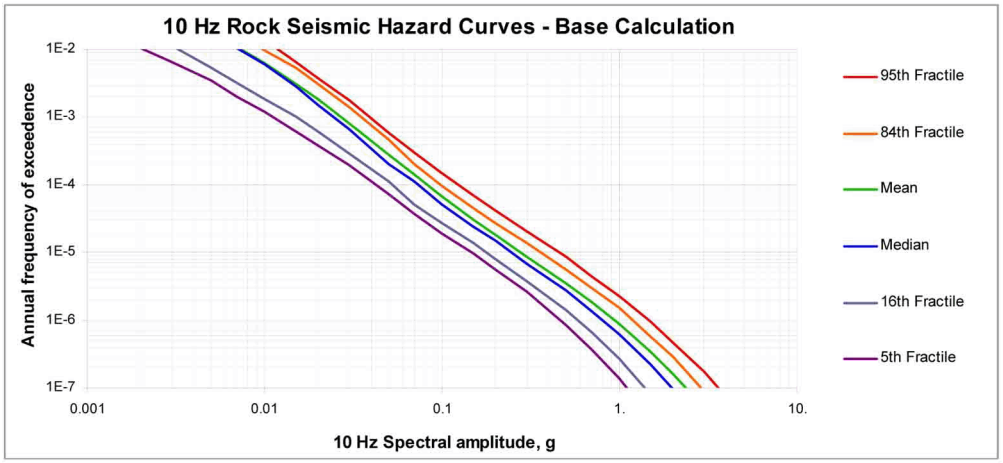

Figure 2.5.2-220 Mean and Fractile Rock 10 Hz Seismic Hazard Curves, Rock

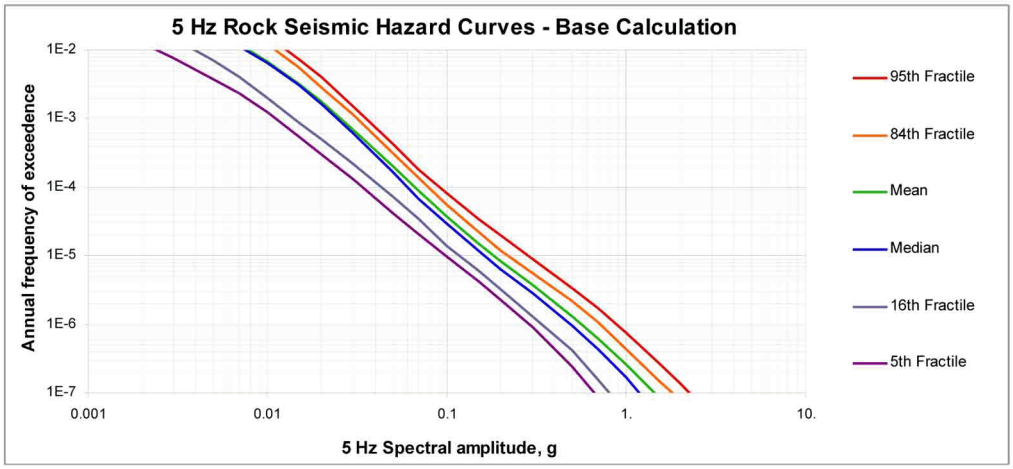

Figure 2.5.2-221 Mean and Fractile Rock 5 Hz Seismic Hazard Curves, Rock

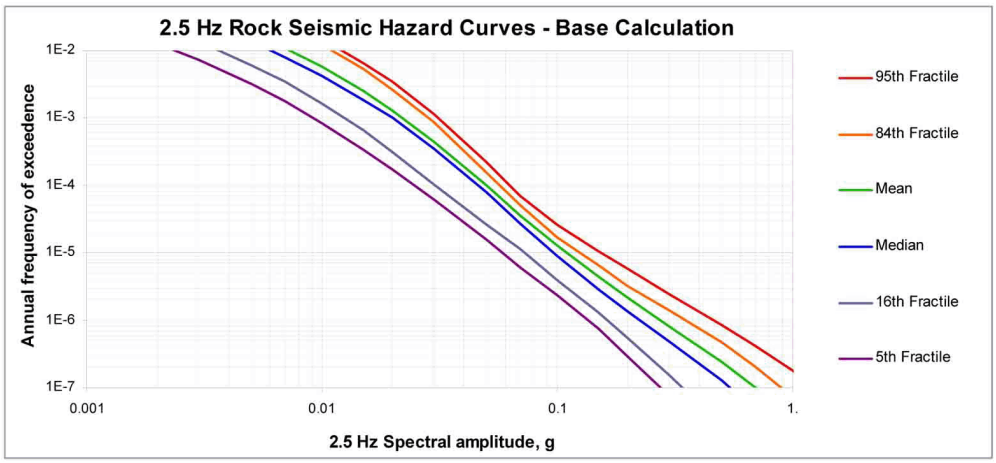

Figure 2.5.2-222 Mean and Fractile Rock 2.5 Hz Seismic Hazard Curves, Rock

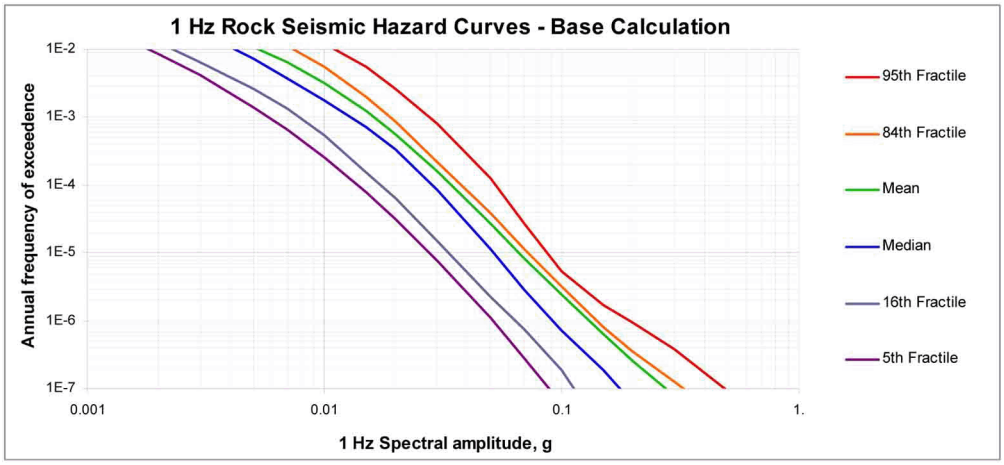

Figure 2.5.2-223 Mean and Fractile Rock 1 Hz Seismic Hazard Curves, Rock

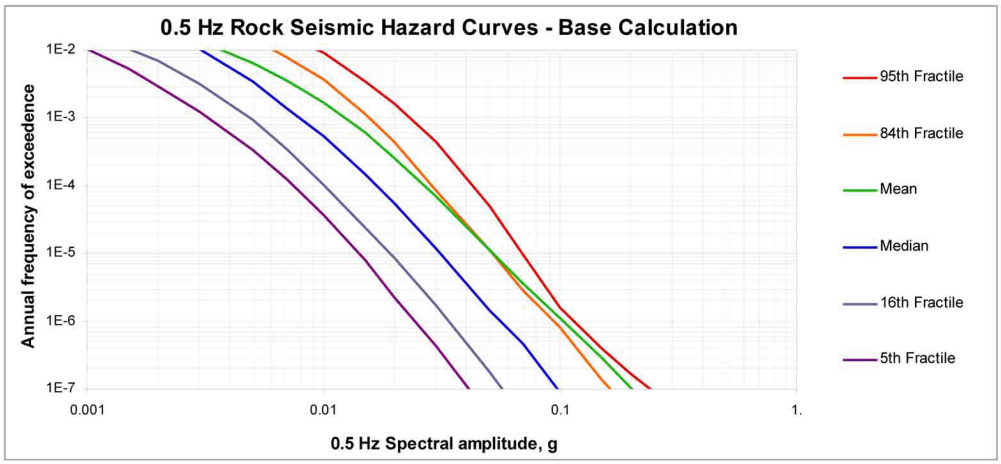

Figure 2.5.2-224 Mean and Fractile Rock 0.5 Hz Seismic Hazard Curves, Rock

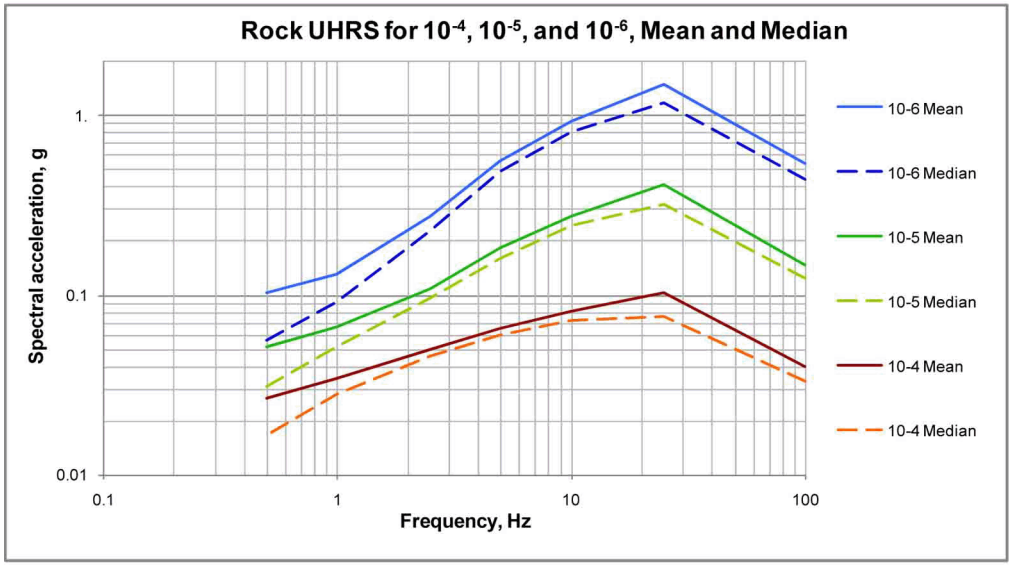

Figure 2.5.2-225 Mean and Median Rock UHRS for 1E-04, 1E-05, and 1E-06

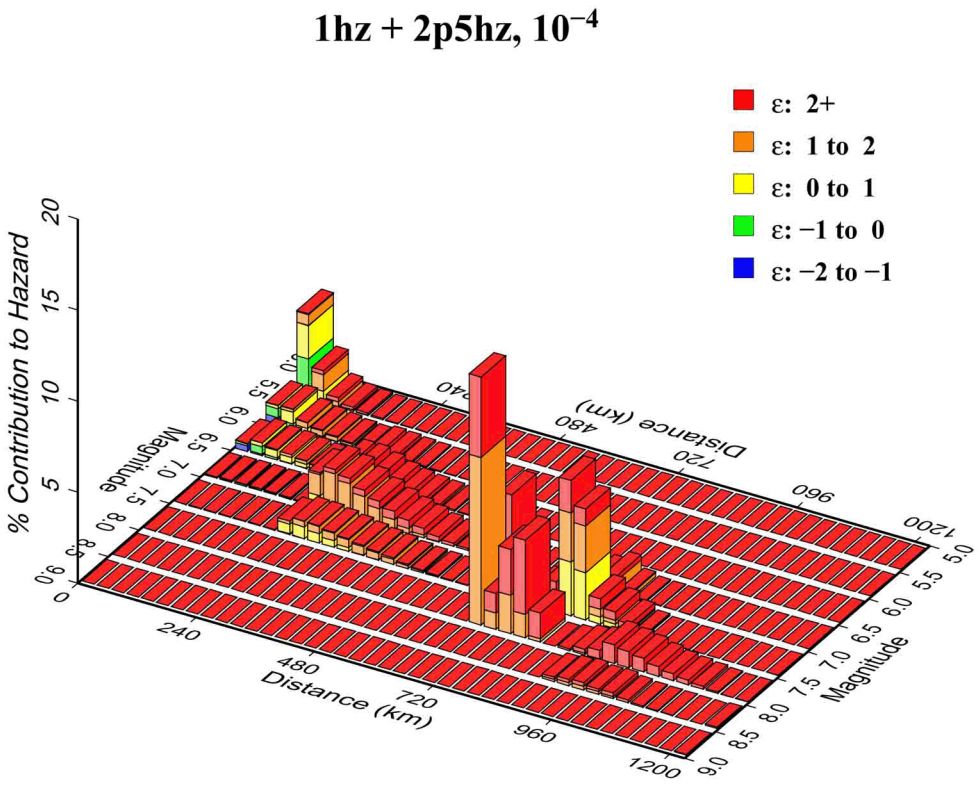

Figure 2.5.2-226 M and R Deaggregation for 1 and 2.5 Hz at 1E-04 Annual Frequency of Exceedence

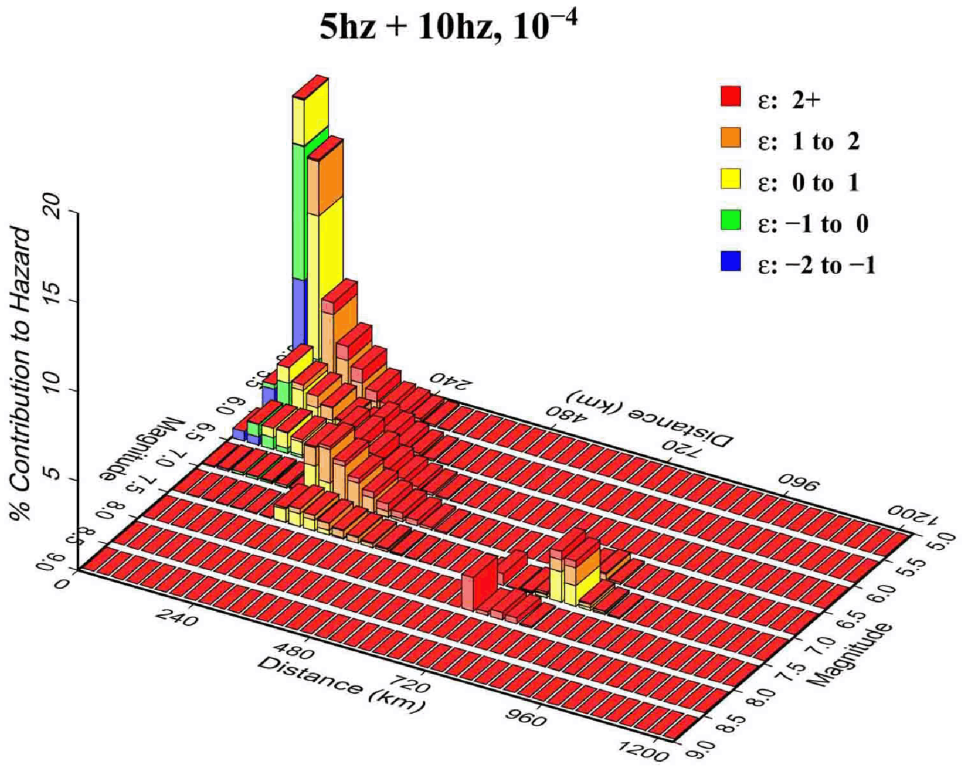

Figure 2.5.2-227 M and R Deaggregation for 5 and 10 Hz at 1E-04 Annual Frequency of Exceedence

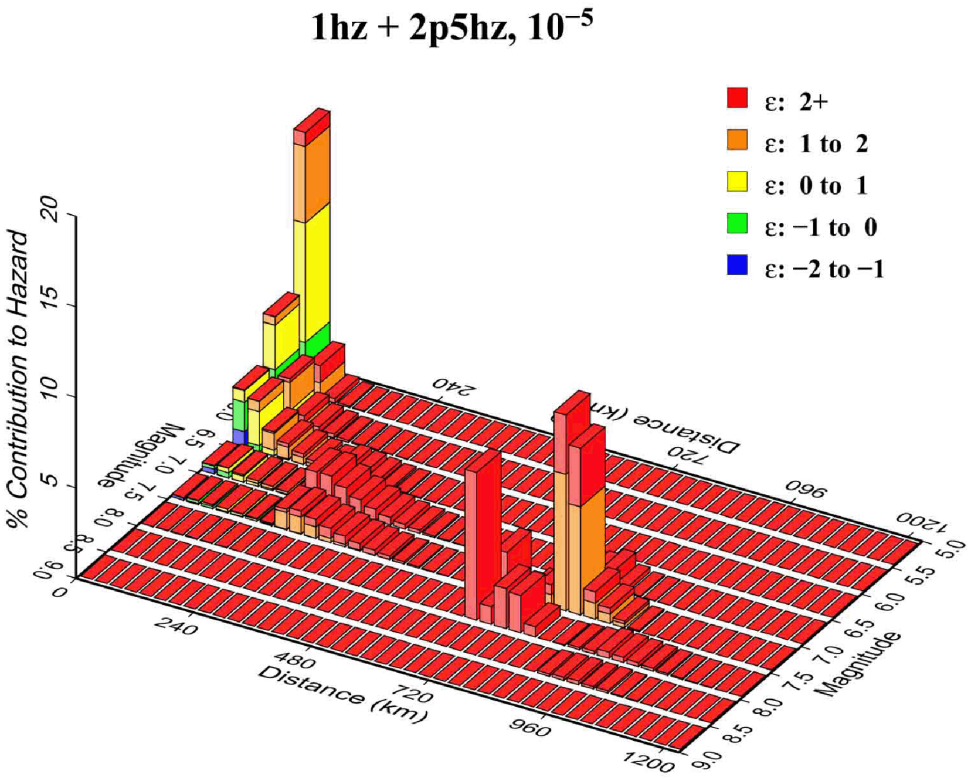

Figure 2.5.2-228 M and R Deaggregation for 1 and 2.5 Hz at 1E-05 Annual Frequency of Exceedence

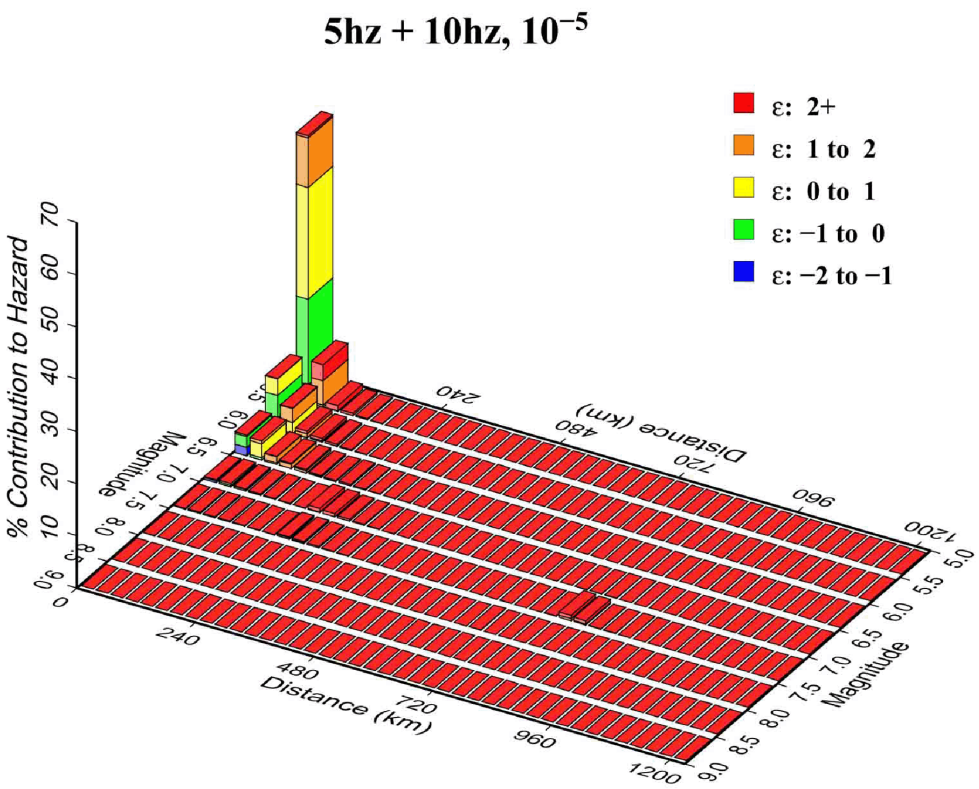

Figure 2.5.2-229 M and R Deaggregation for 5 and 10 Hz at 1E-05 Annual Frequency of Exceedence

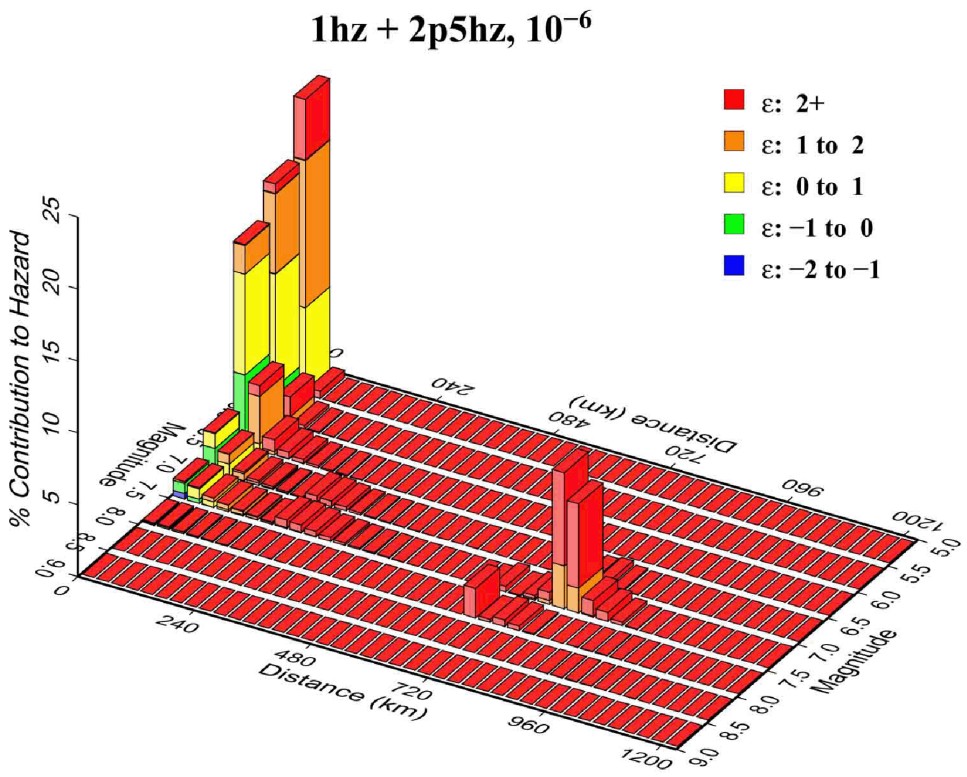

Figure 2.5.2-230 M and R Deaggregation for 1 and 2.5 Hz at 1E-06 Annual Frequency of Exceedence

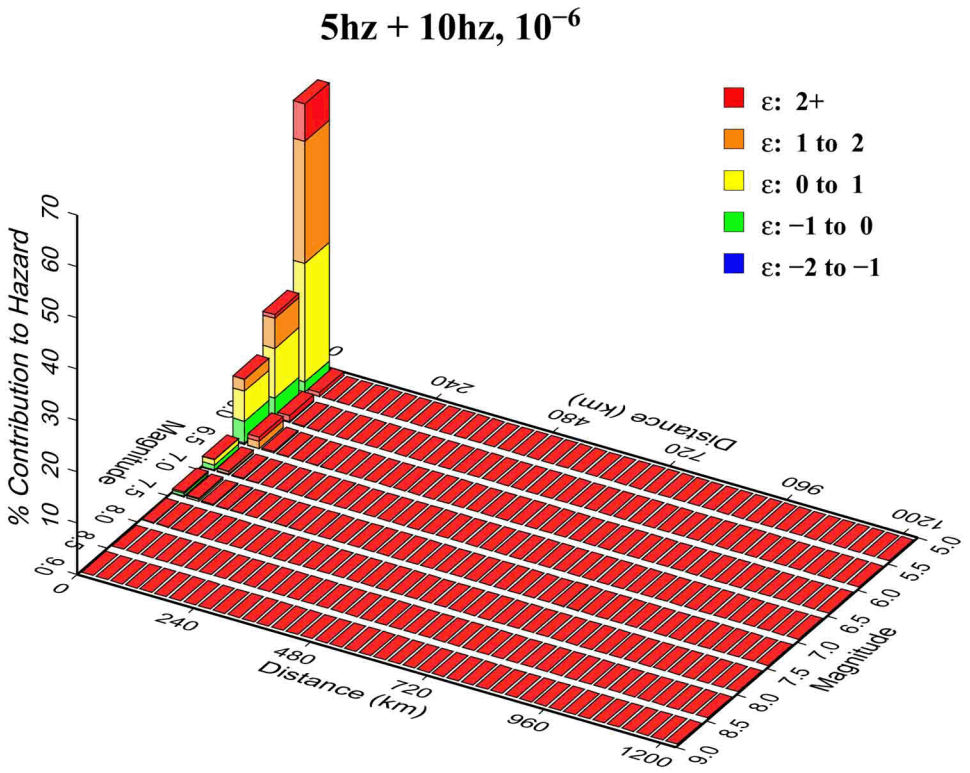

Figure 2.5.2-231 M and R Deaggregation for 5 and 10 Hz at 1E-06 Annual Frequency of Exceedence

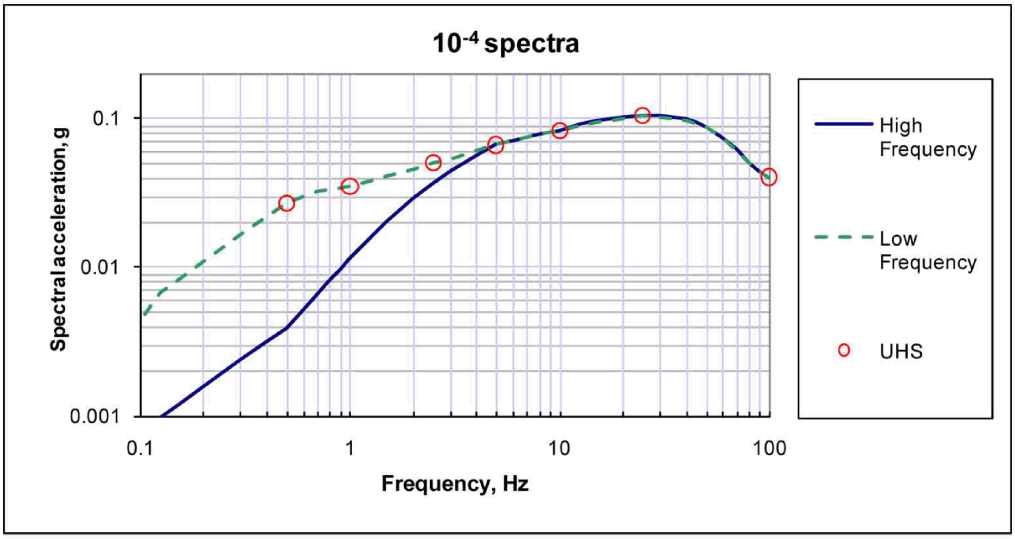

Figure 2.5.2-232 HF and LF Rock Spectra Anchored to Mean UHRS Values from Hazard Calculation for 1E-04 Spectra

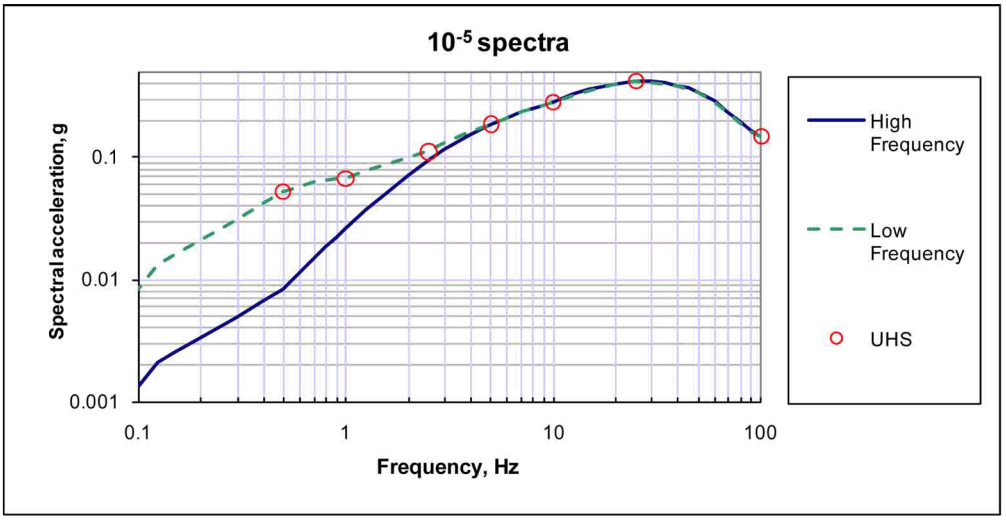

Figure 2.5.2-233 HF and LF Rock Spectra Anchored to Mean UHRS Values from Hazard Calculation for 1E-05 Spectra

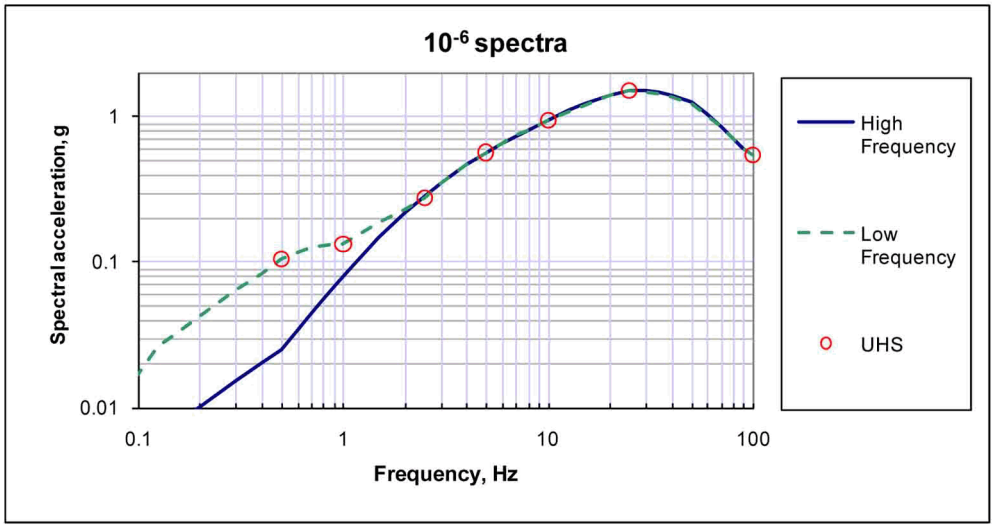

Figure 2.5.2-234 HF and LF Rock Spectra Anchored to Mean UHRS Values from Hazard Calculation for 1E-06 Spectra

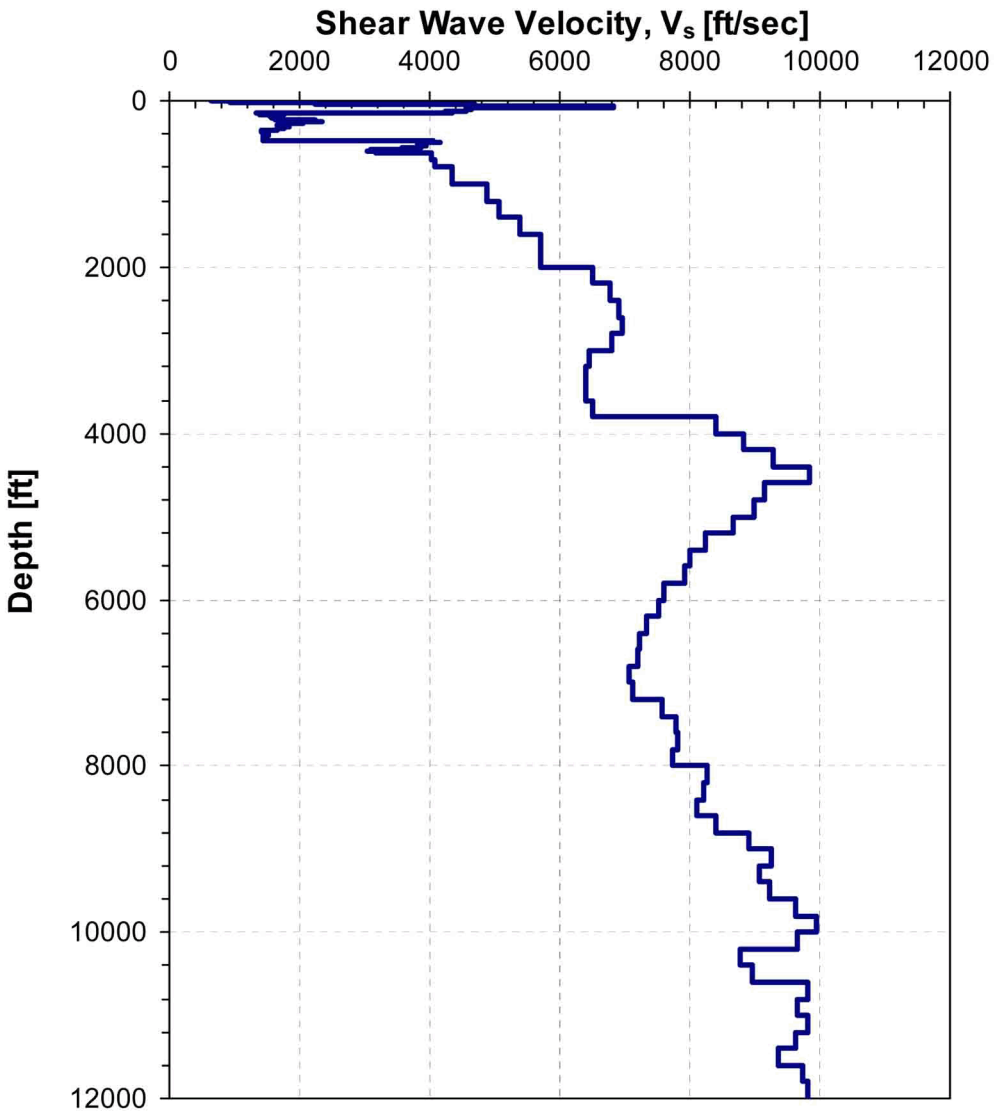

Figure 2.5.2-235 Input Base Case Shear Wave Velocity Profile

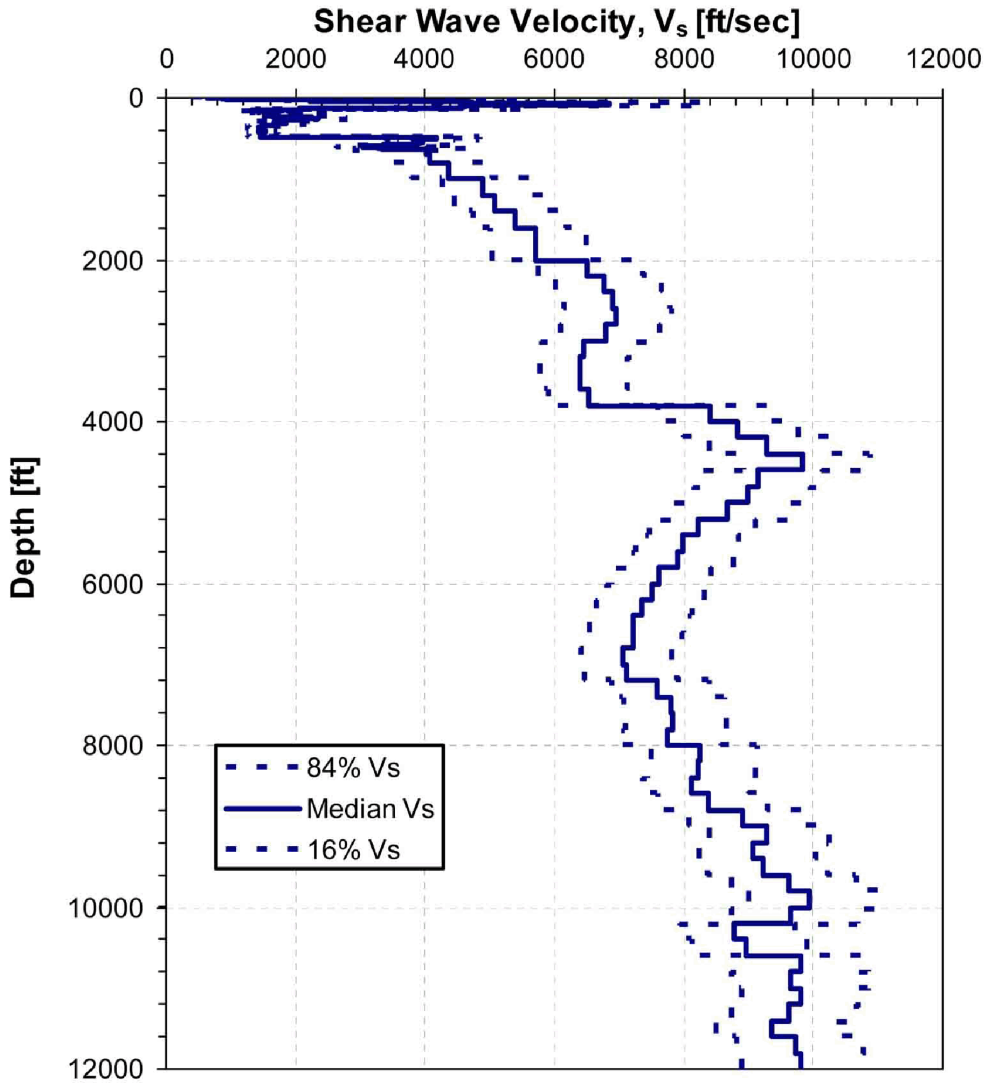

Figure 2.5.2-236 Input Median Shear Wave Velocity Profile (+/- One Standard Deviation) for Randomization Process

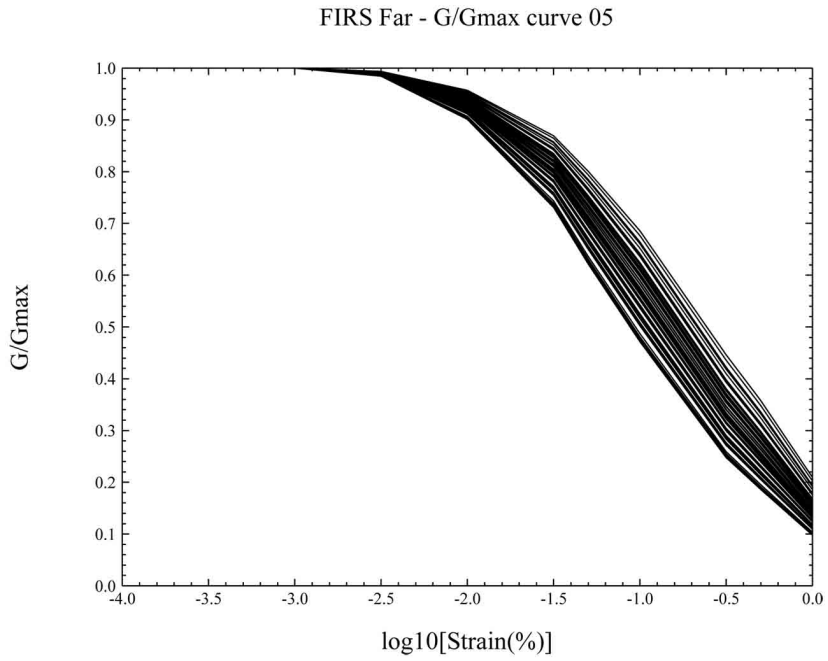

Figure 2.5.2-237 Strain Dependent Degradation Curves for Natural Soils (<150 feet)

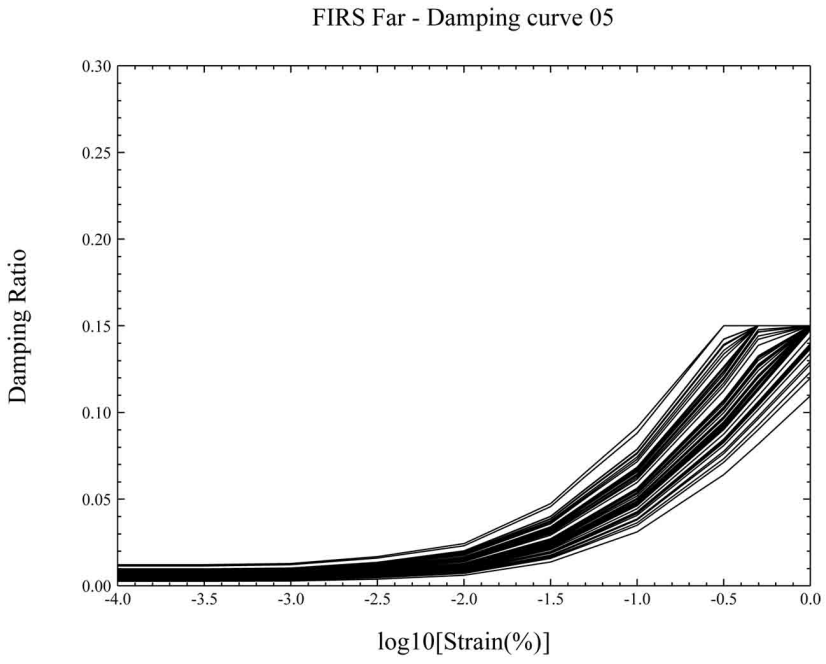

Figure 2.5.2-238 Strain Dependent Damping Ratio Properties for Natural Soils (<150 feet)

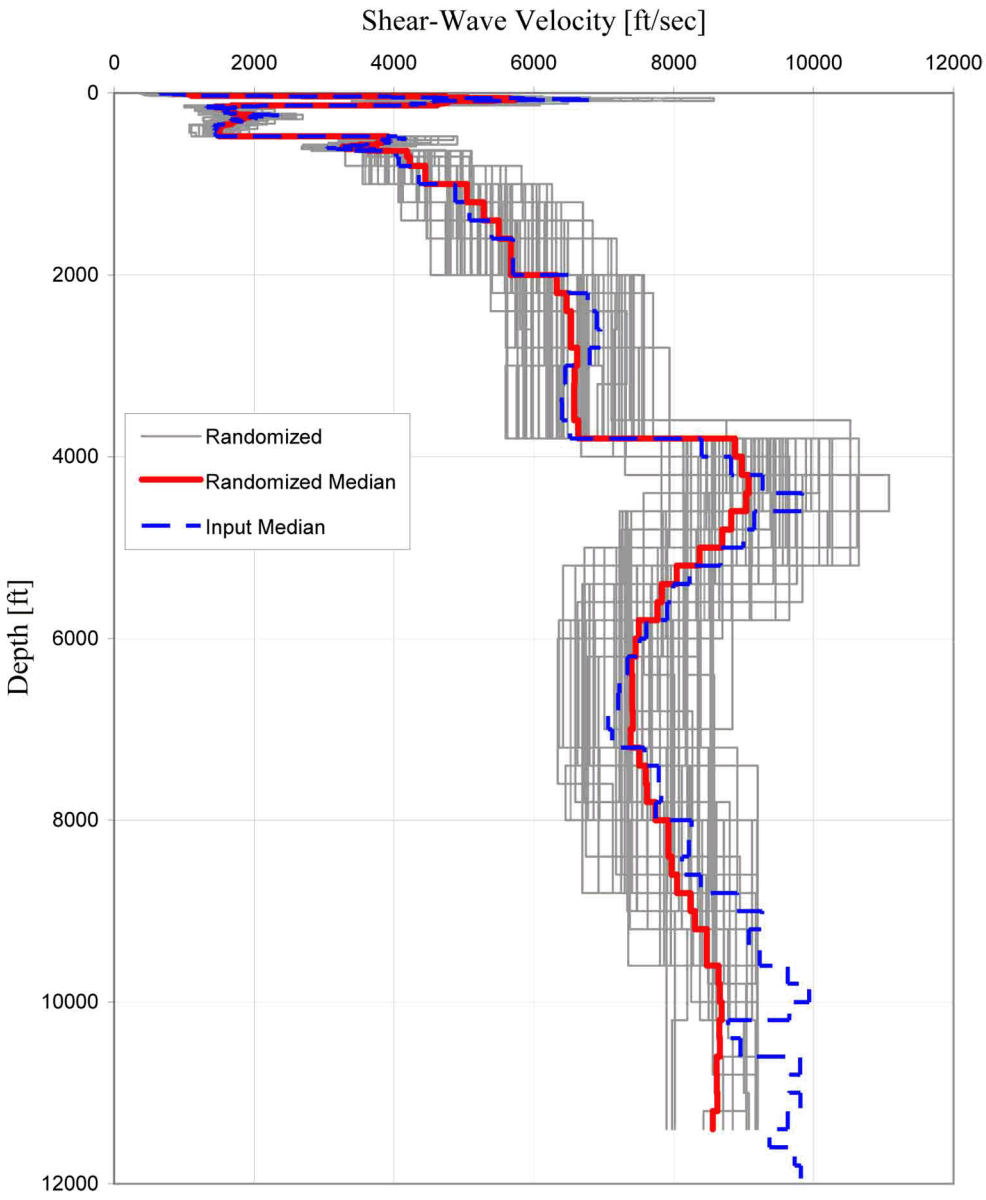

Figure 2.5.2-239 Randomized Shear Wave Velocity Profiles, Median Shear Wave Velocity Profile and the Input Median Profile Used For Randomization

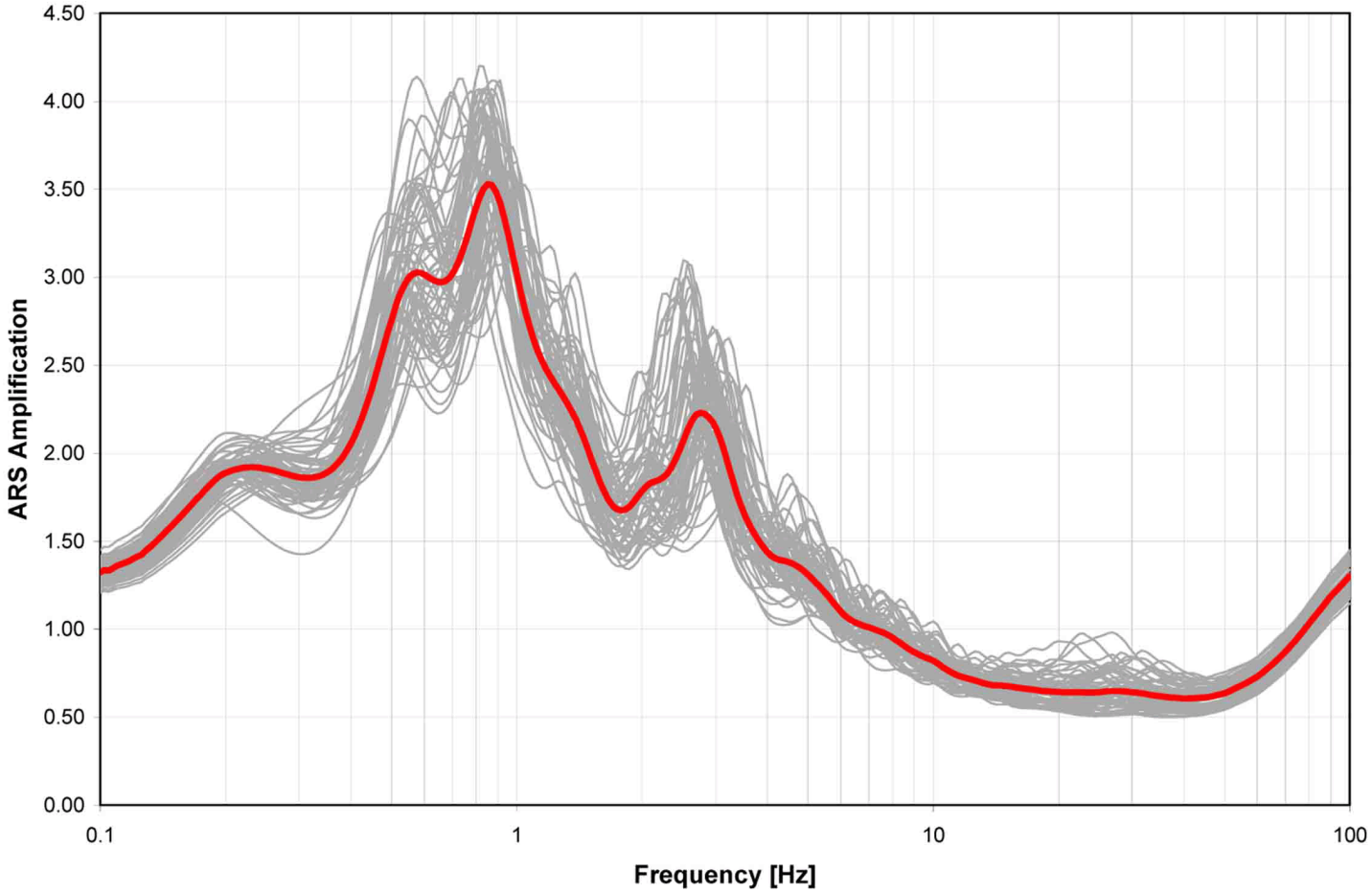

Figure 2.5.2-240 Median of Site Amplification Factors at GMRS Horizon (El. –35 feet) from Analyses of the 60 Random Profiles with the 1E-04 LF Input Motion

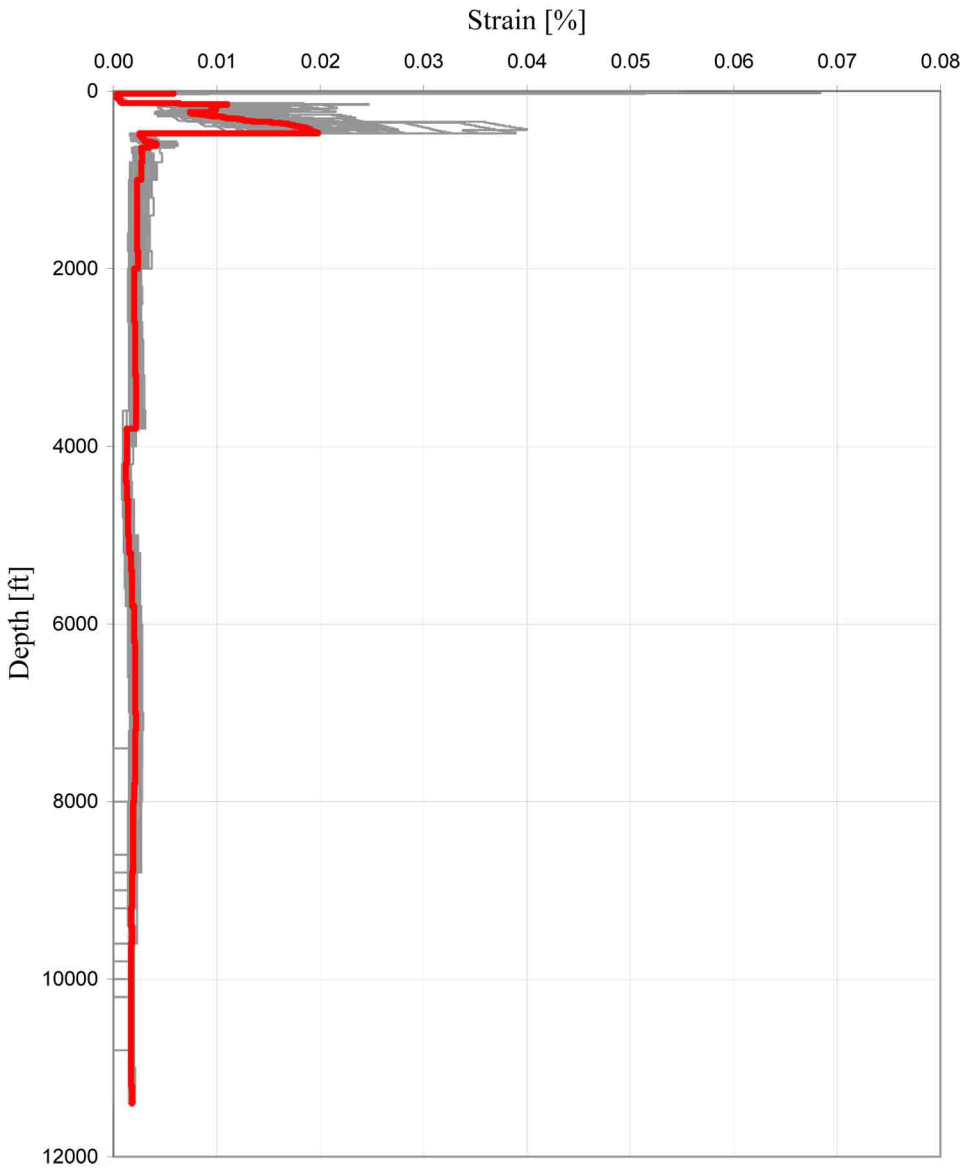

Figure 2.5.2-241 Maximum Strains Versus Depth that are Calculated for the 60 Profiles and their Median (Thick Red Line) with the 1E-04 LF Input Motion

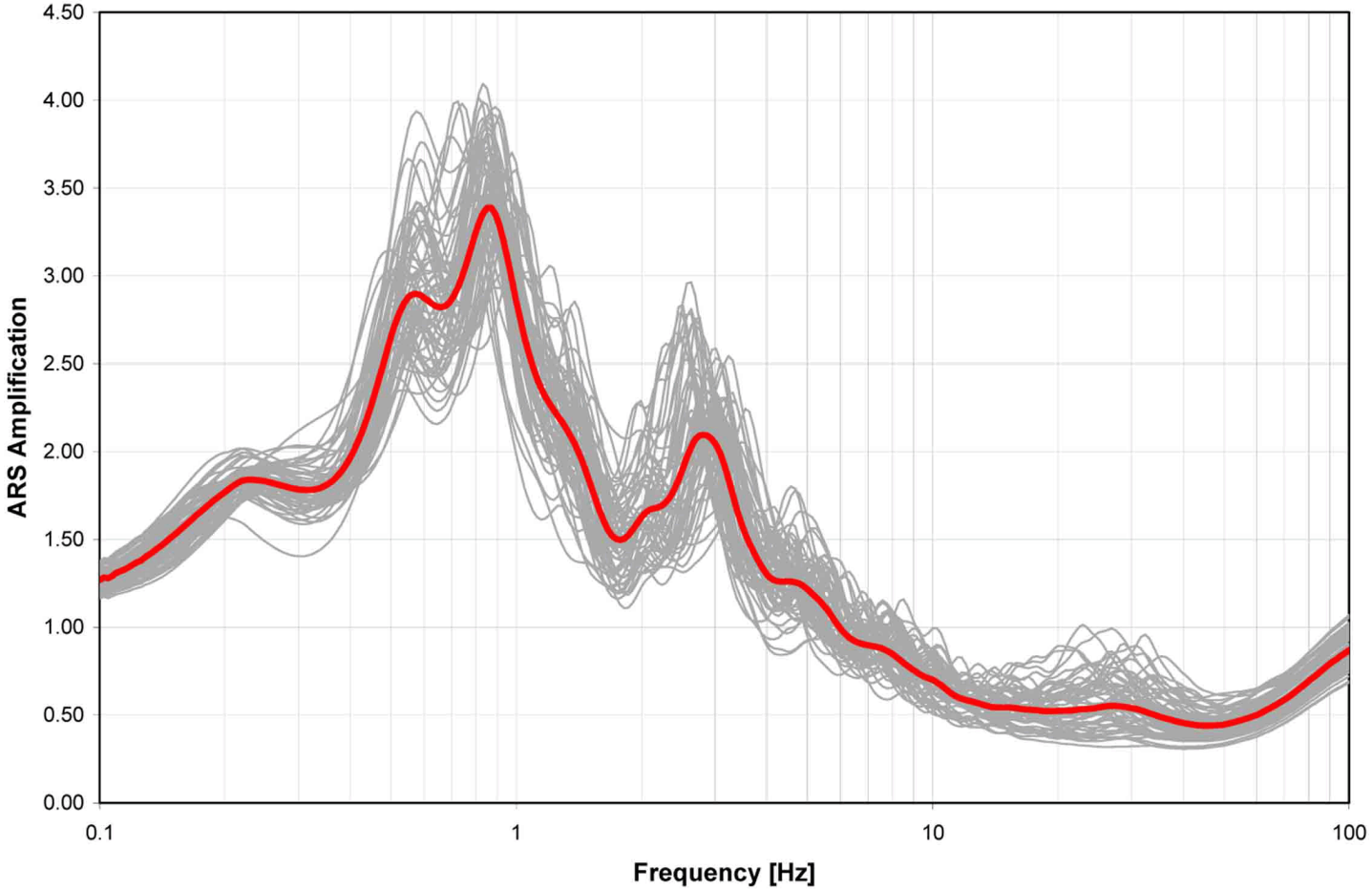

Figure 2.5.2-242 Median of Site Amplification Factors at GMRS Horizon (El. –35 feet) from Analyses of the 60 Random Profiles with the 1E-04 HF Input Motion

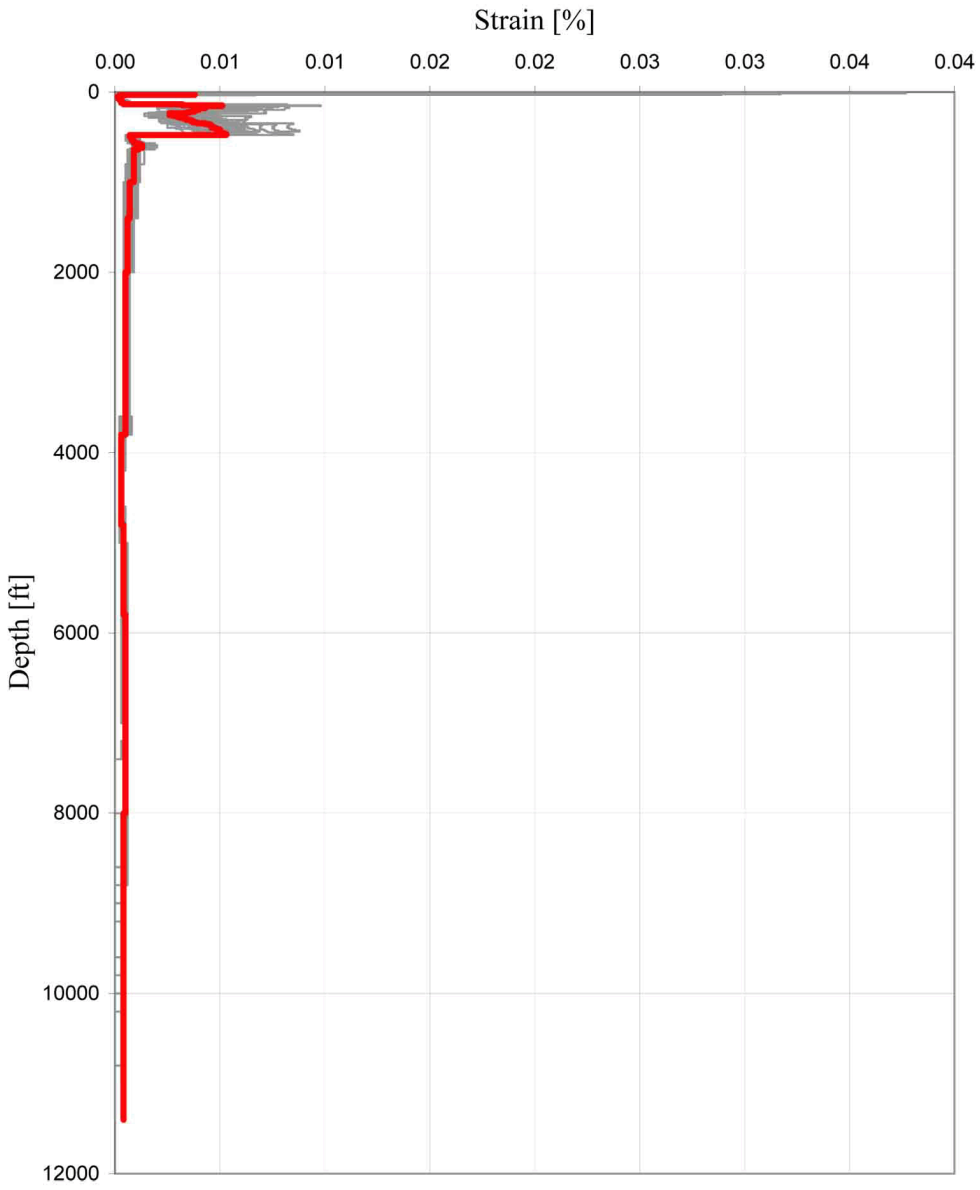

Figure 2.5.2-243 Maximum Strains Versus Depth that are Calculated for the 60 Profiles and their Median (Thick Red Line) with the 1E-04 HF Input Motion

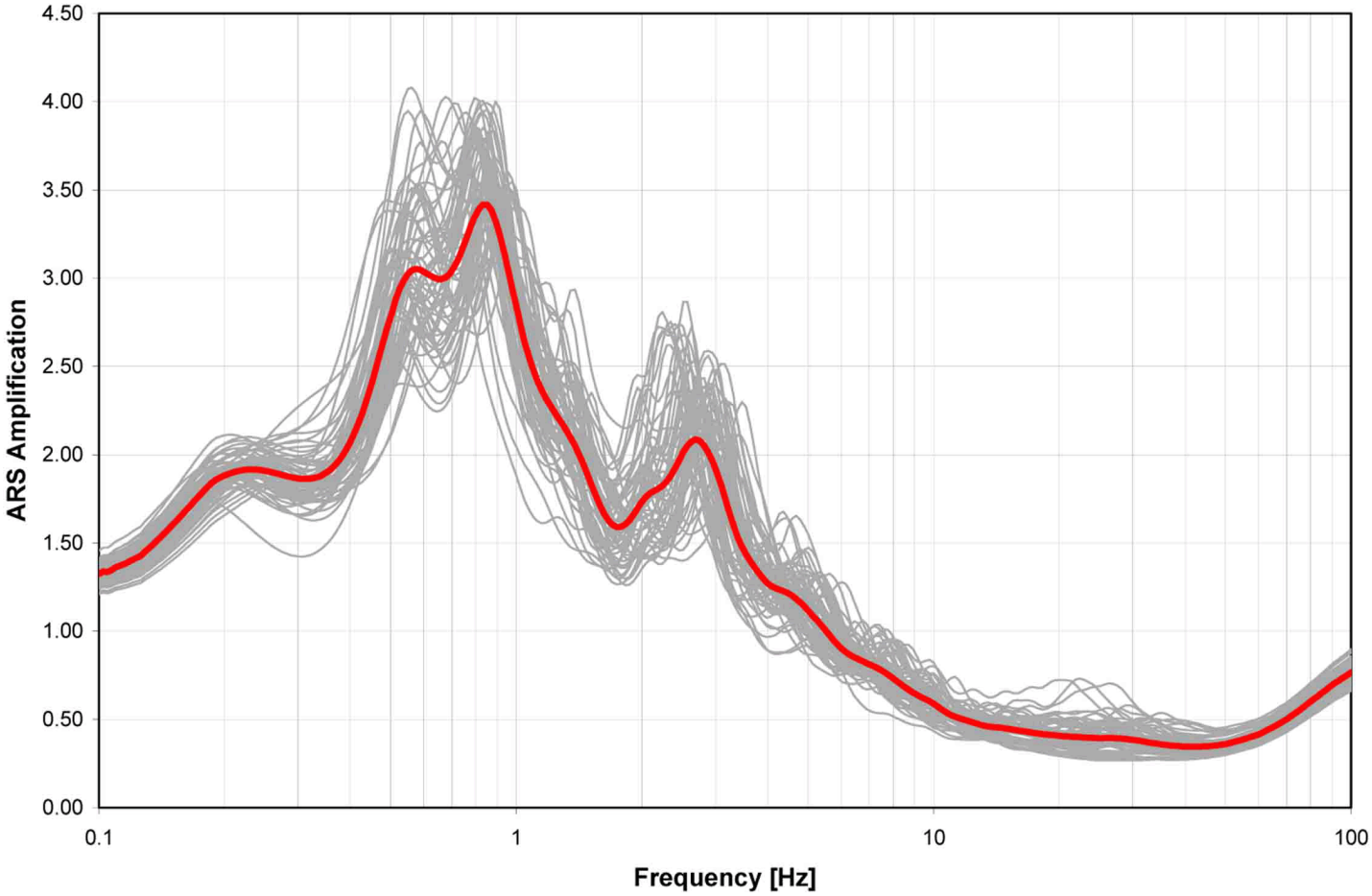

Figure 2.5.2-244 Median of Site Amplification Factors at GMRS Horizon (El. –35 feet) from Analyses of the 60 Random Profiles with the 1E-05 LF Input Motion

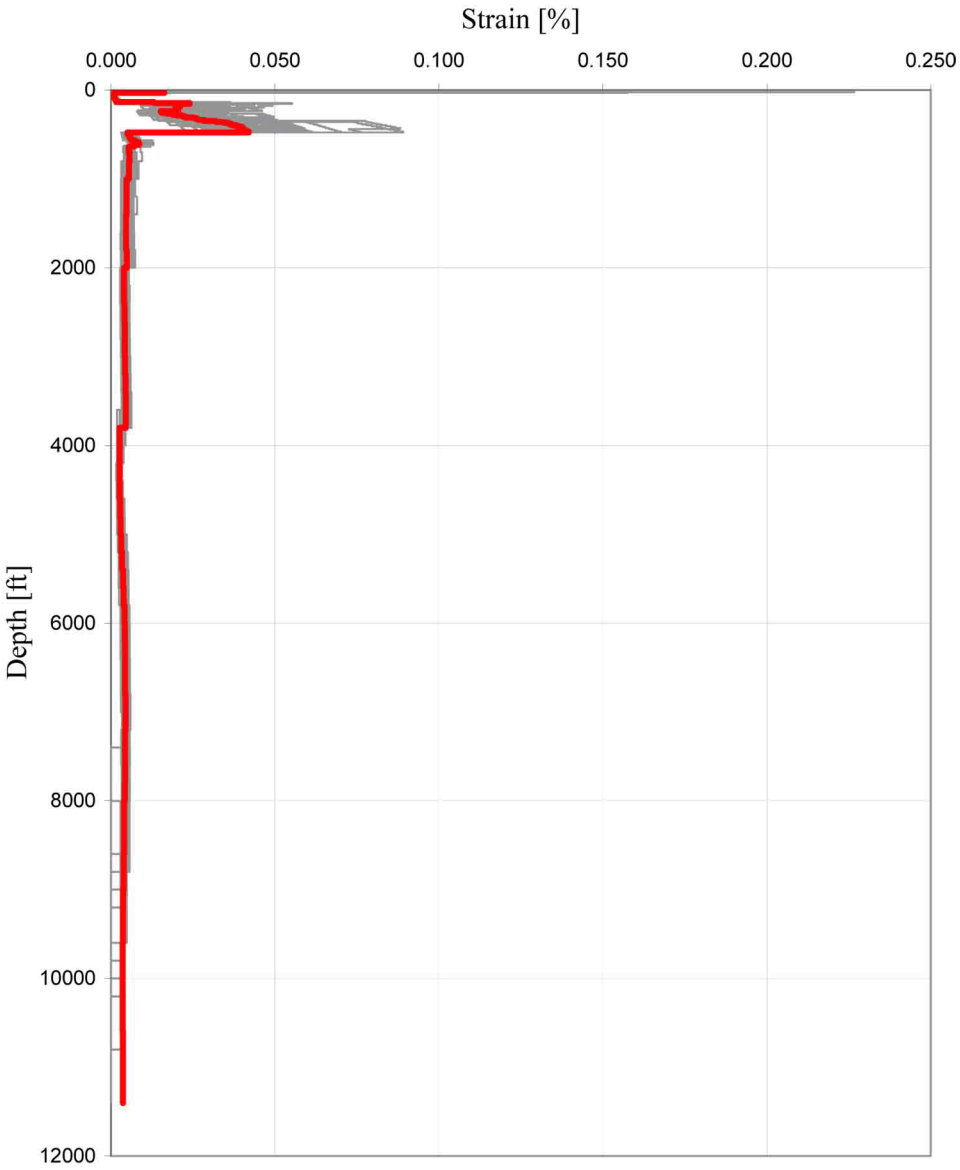

Figure 2.5.2-245 Maximum Strains Versus Depth that are Calculated for the 60 Profiles and their Median (Thick Red Line) with the 1E-05 LF Input Motion

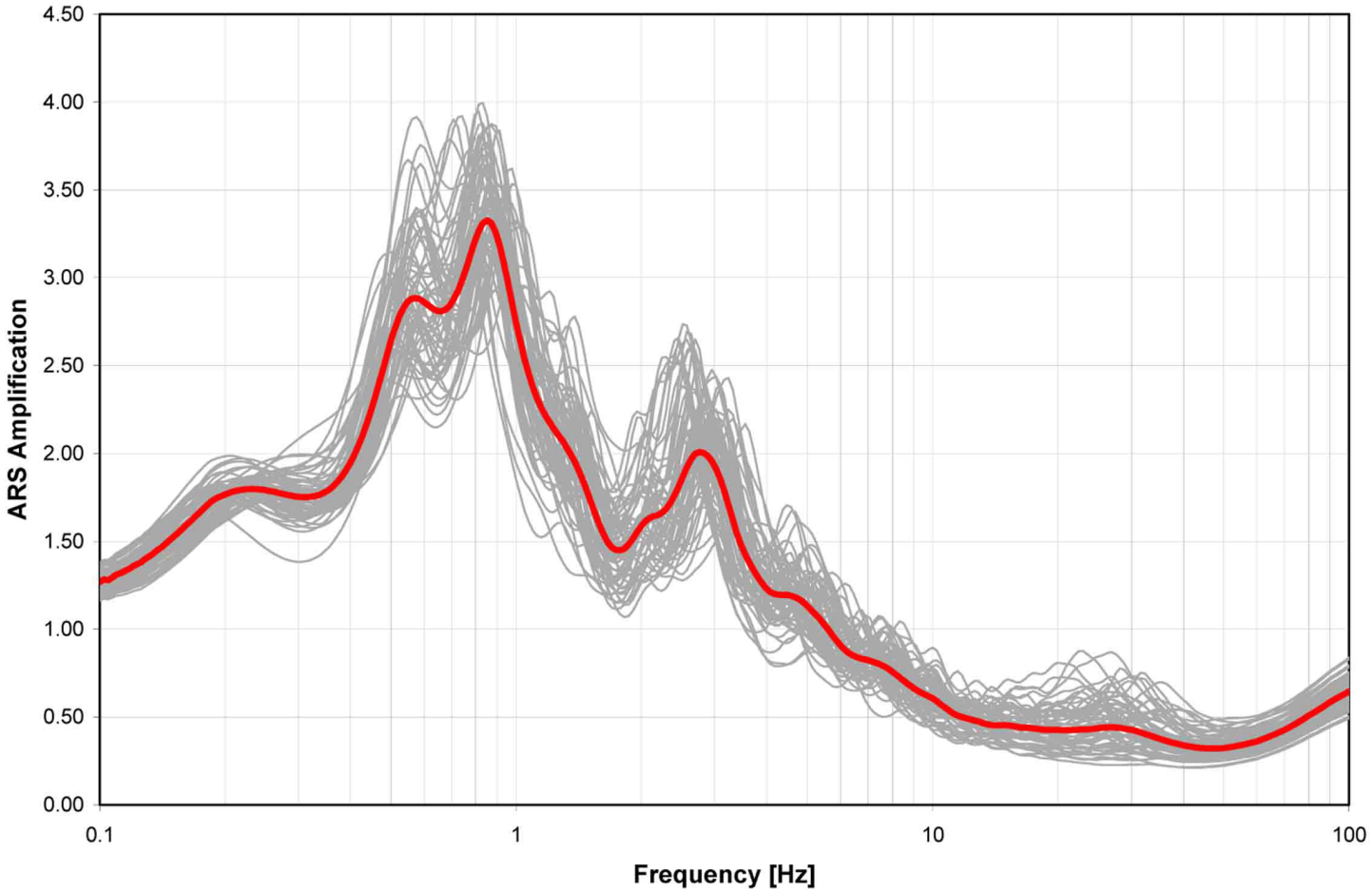

Figure 2.5.2-246 Median of Site Amplification Factors at GMRS Horizon (El. –35 feet) from Analyses of the 60 Random Profiles with the 1E-05 HF Input Motion

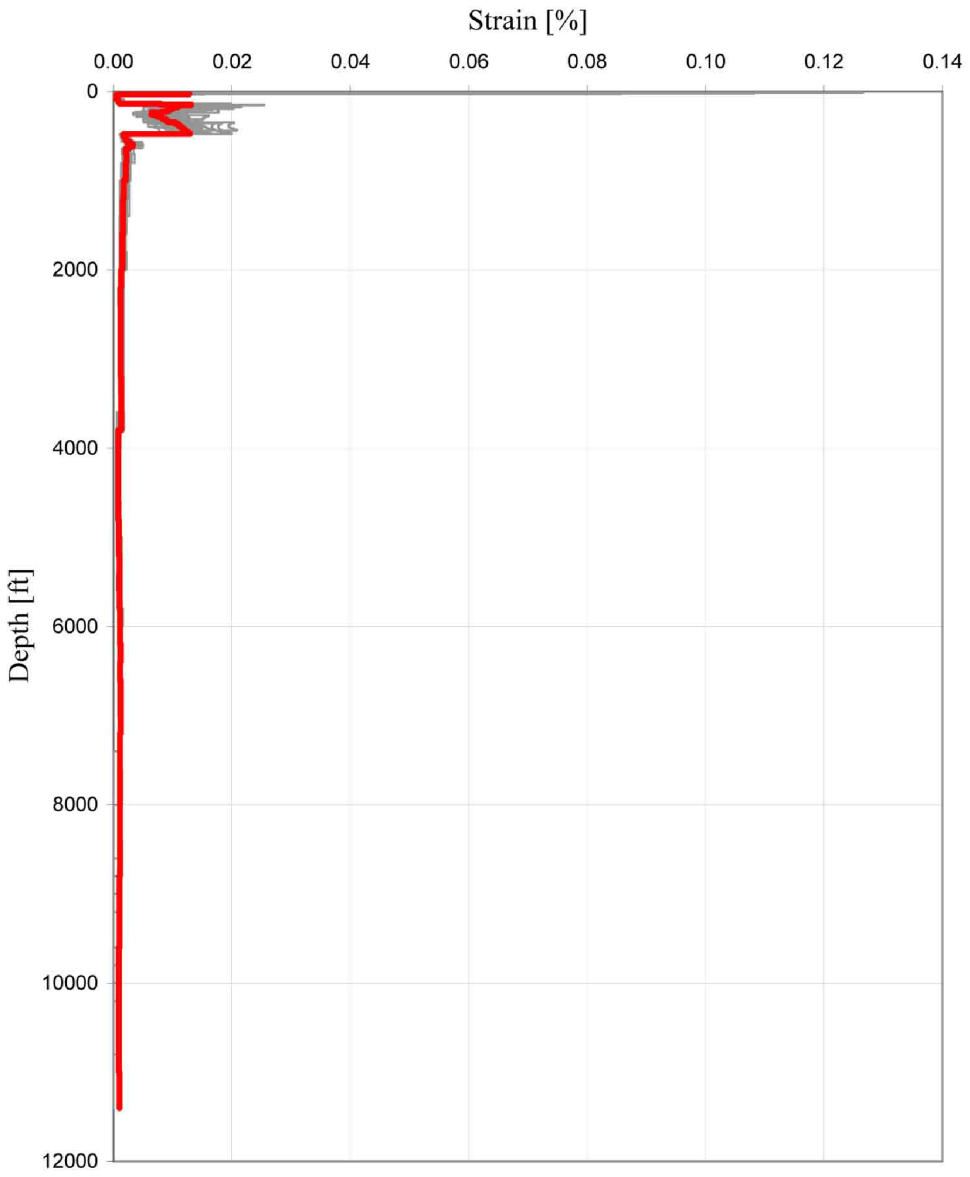

Figure 2.5.2-247 Maximum Strains Versus Depth that are Calculated for the 60 Profiles and their Median (Thick Red Line) with the 1E-05 HF Input Motion

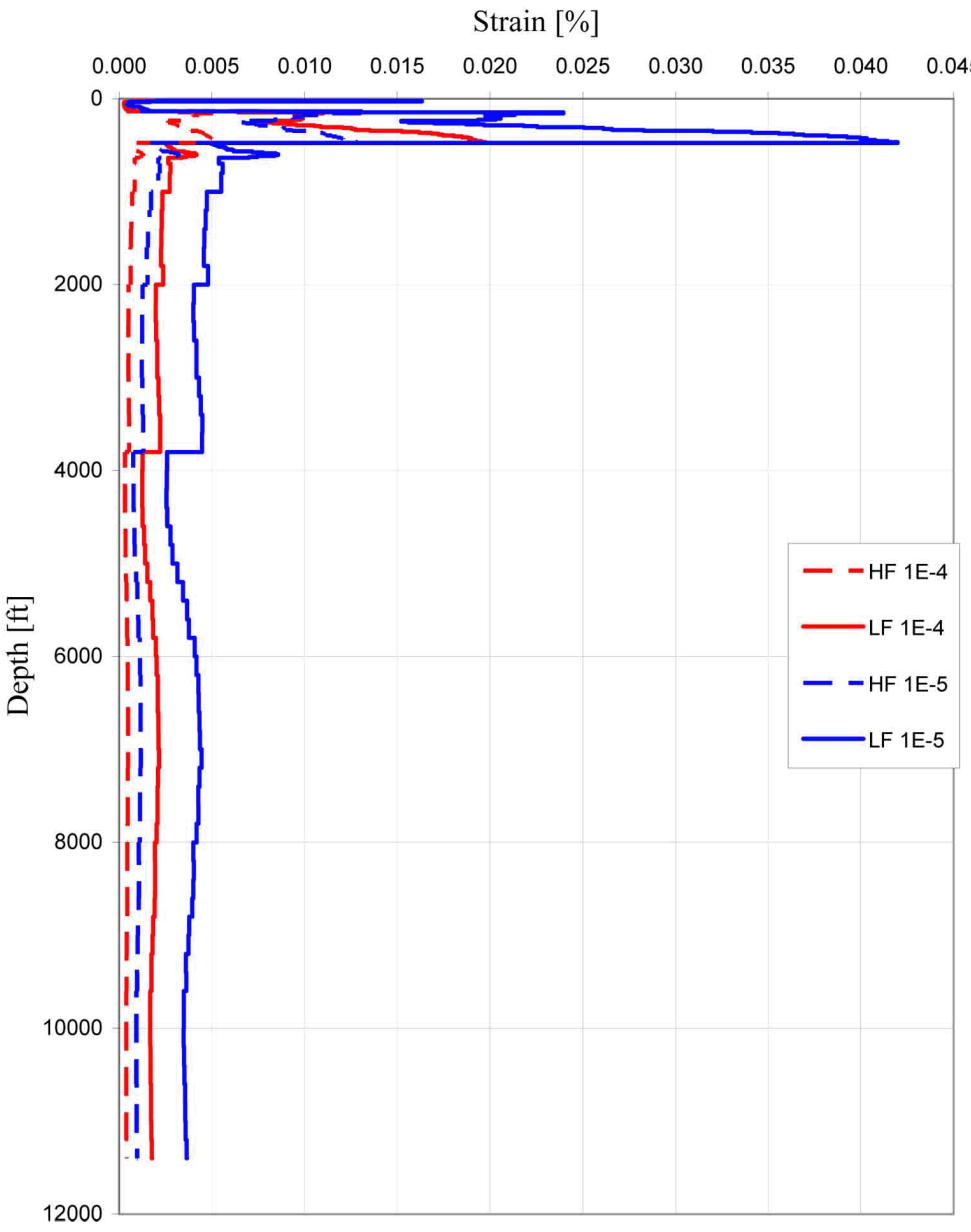

Figure 2.5.2-248 Median Maximum Strain Profiles (Full Soil Column) (Sheet 1 of 2)

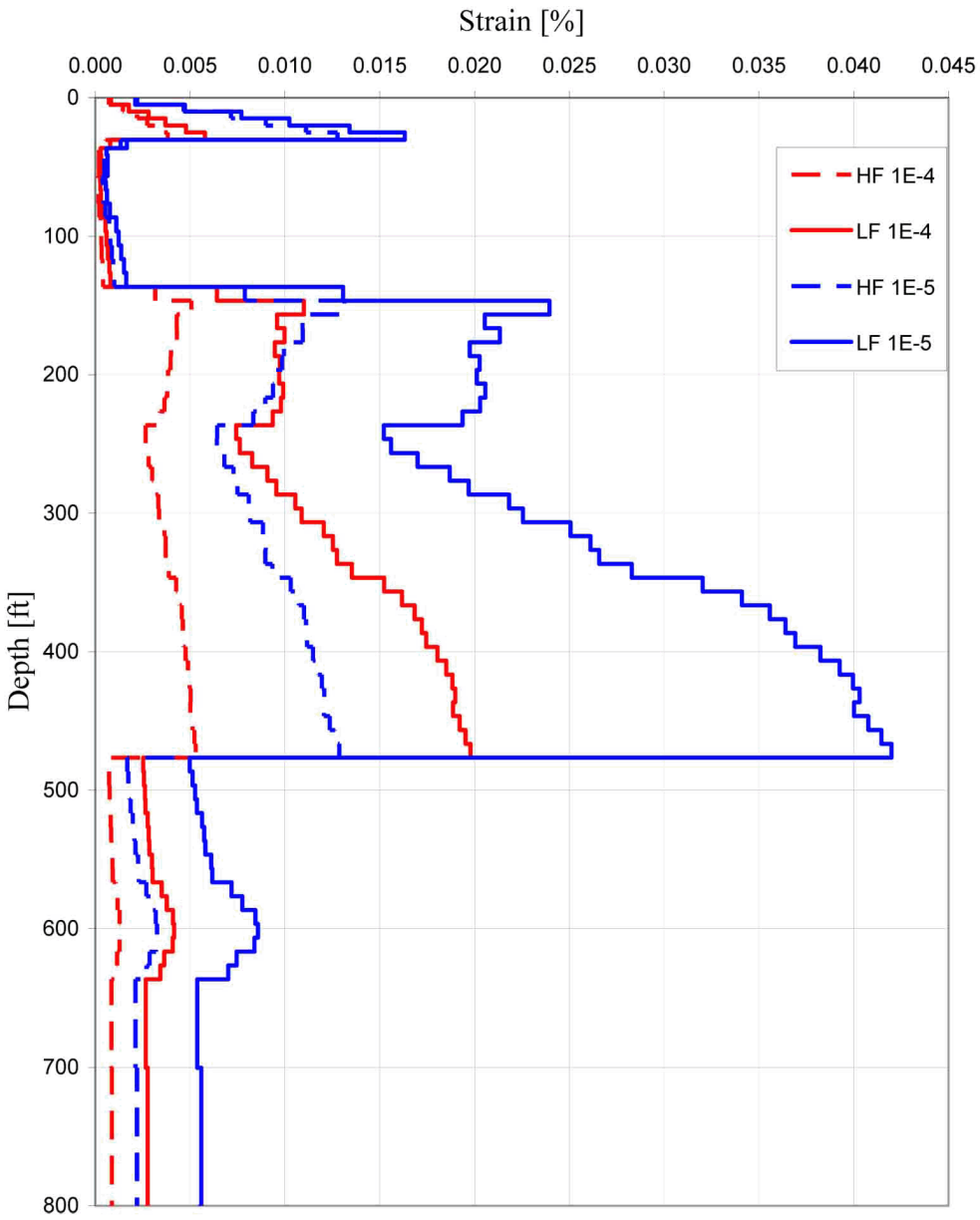

Figure 2.5.2-248 Median Maximum Strain Profiles (Upper 800 feet) (Sheet 2 of 2)

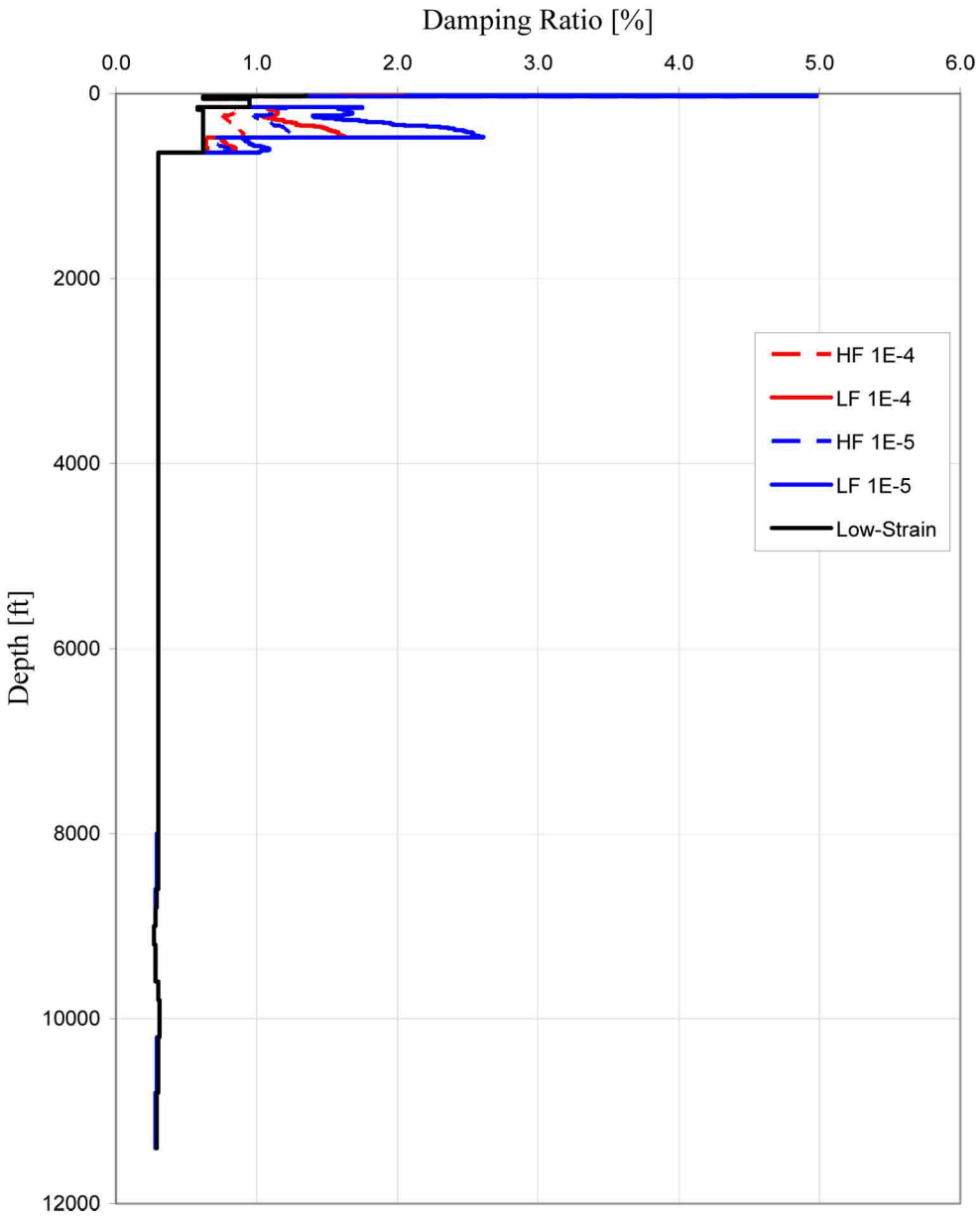

Figure 2.5.2-249 Median Profiles of Strain-Compatible Soil Damping (Full Soil Column) (Sheet 1 of 2)

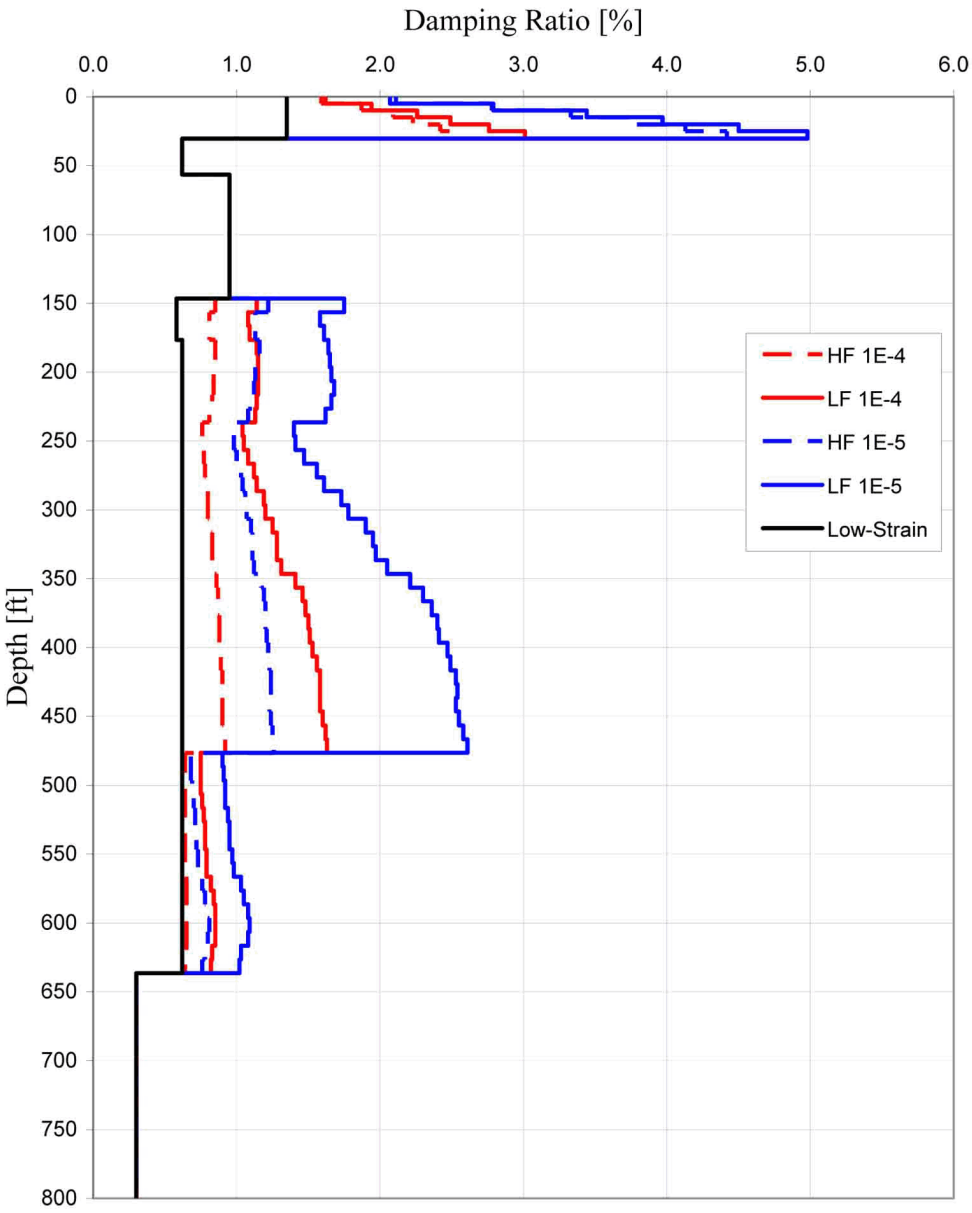

Figure 2.5.2-249 Median Profiles of Strain-Compatible Soil Damping (Upper 800 feet) (Sheet 2 of 2)

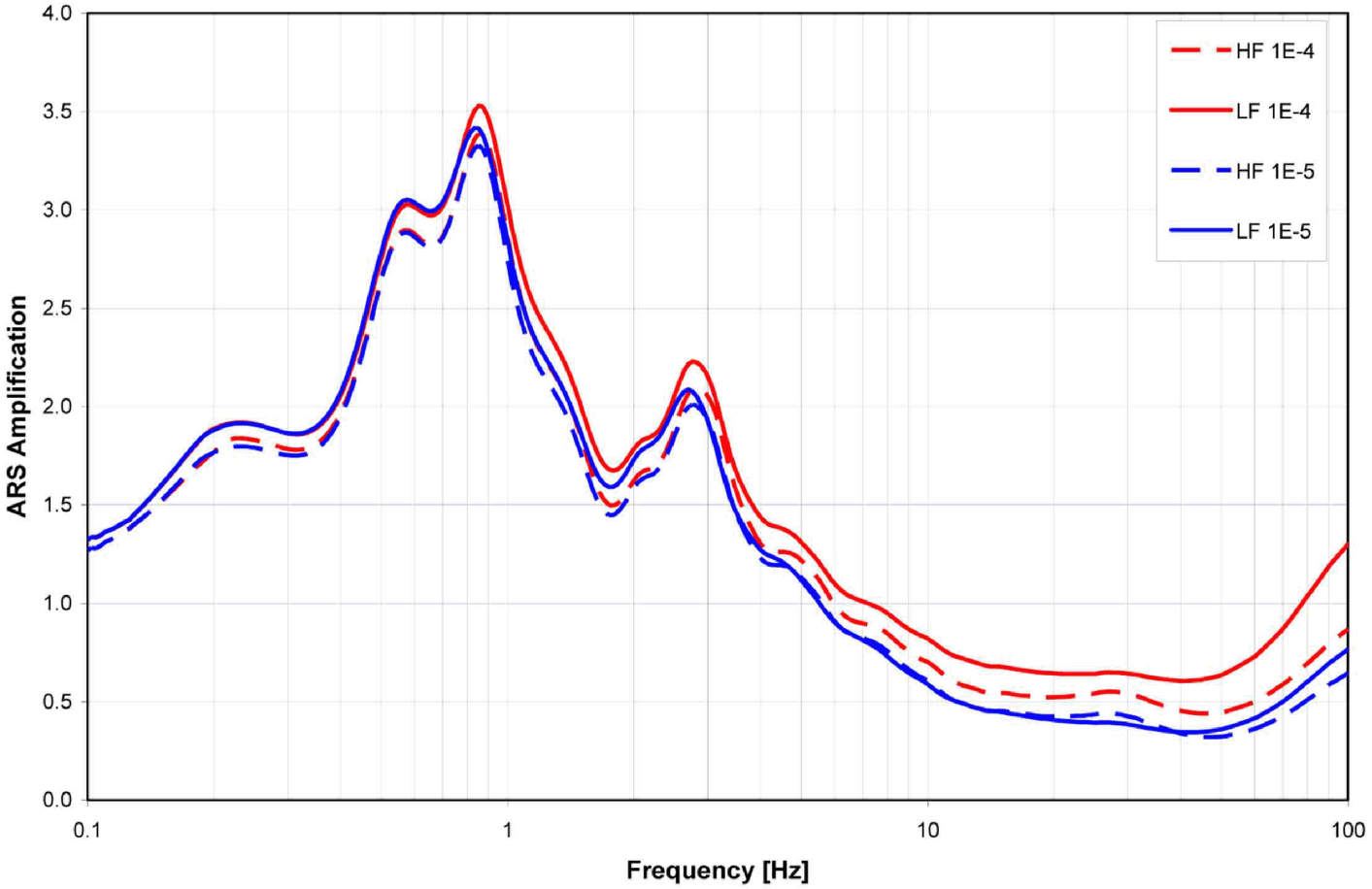

Figure 2.5.2-250 Comparison of Median Soil Amplification Factors at GMRS Horizon for LF and HF 1E-04 and 1E-05 Input Motions

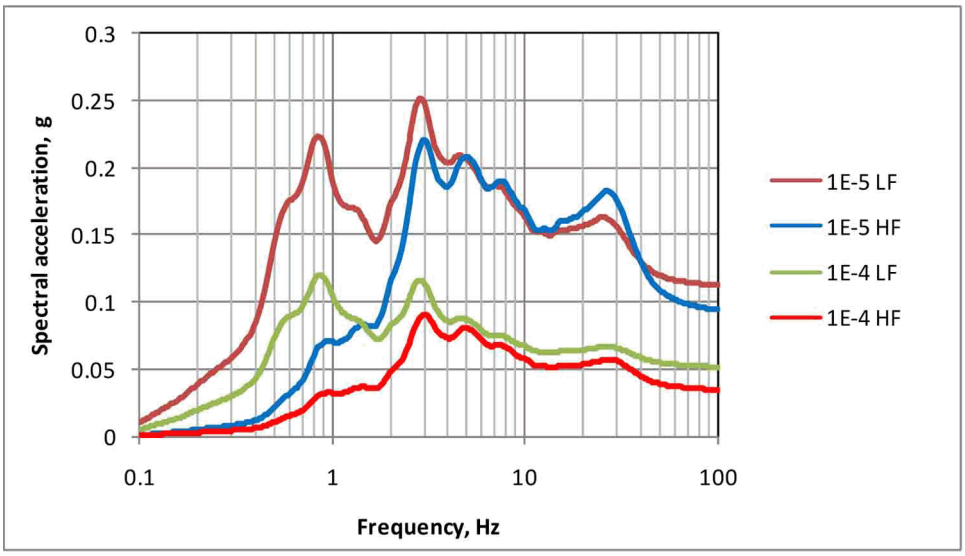

Figure 2.5.2-251 HF and LF Horizontal 1E-04 and 1E-05 Site Spectra

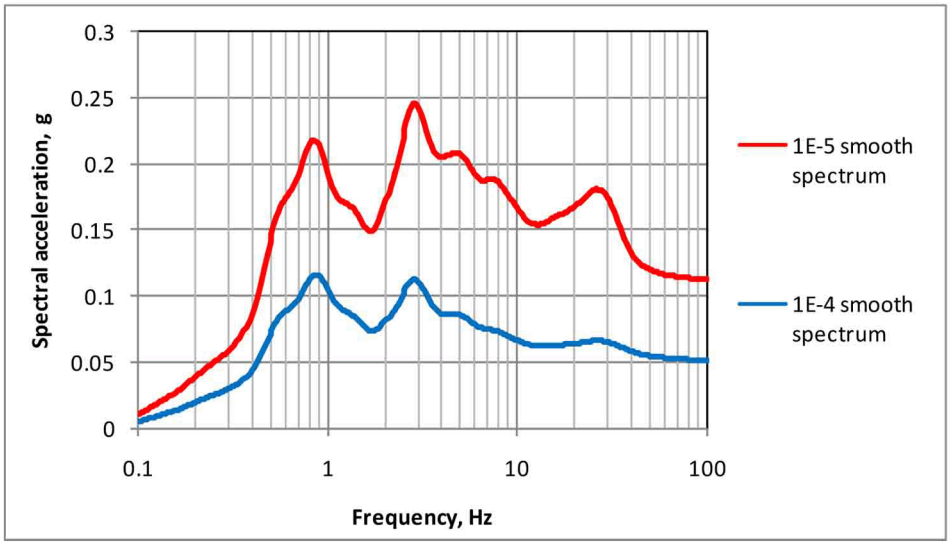

Figure 2.5.2-252 Smoothed Horizontal 1E-04 and 1E-05 Site Spectra

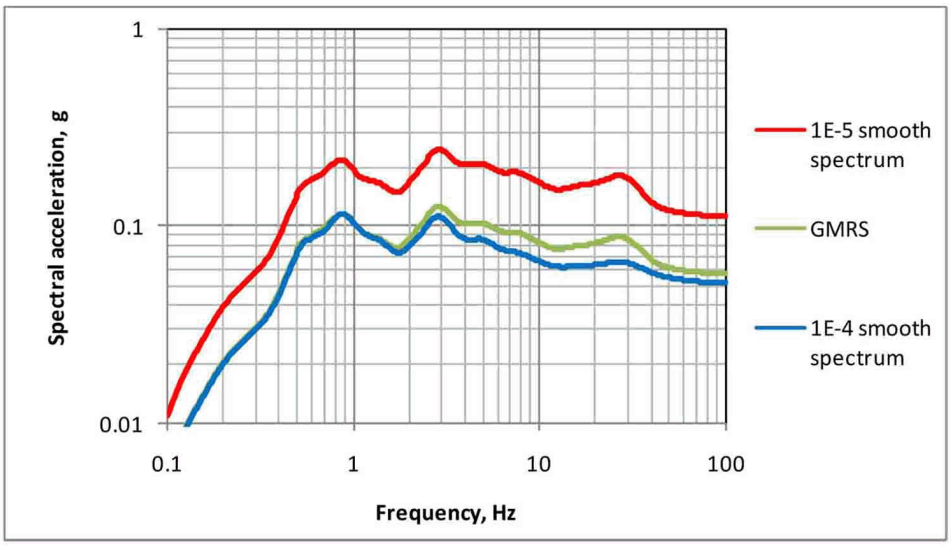

Figure 2.5.2-253 Smoothed Horizontal 1E-04 and 1E-05 Site Spectra and GMRS

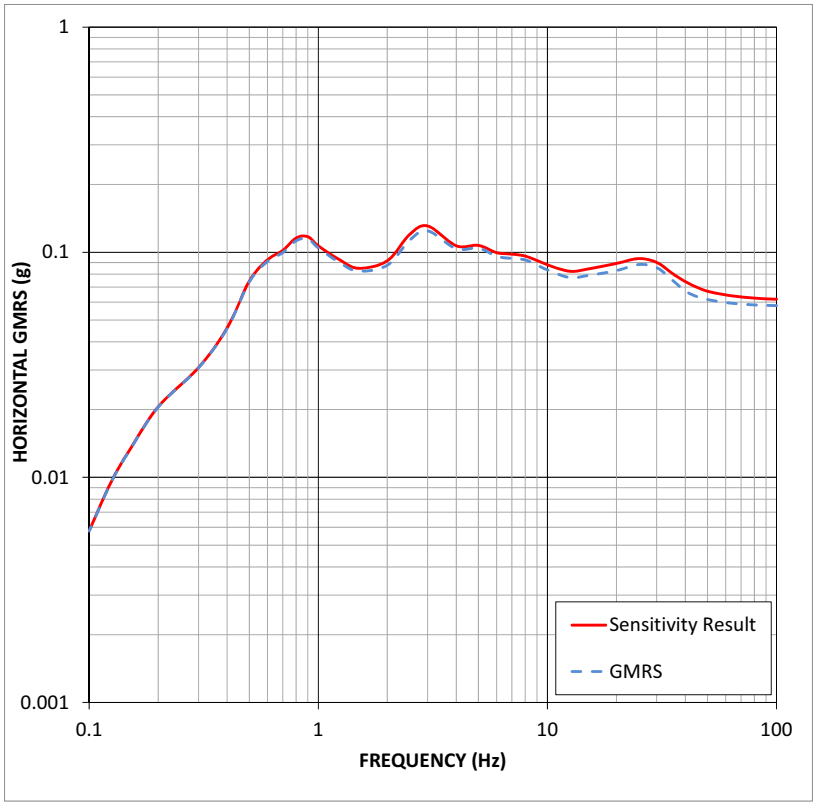

Figure 2.5.2-253a Sensitivity Result Showing the Effect on the 5% Damped Horizontal GMRS of an Updated Soil Column

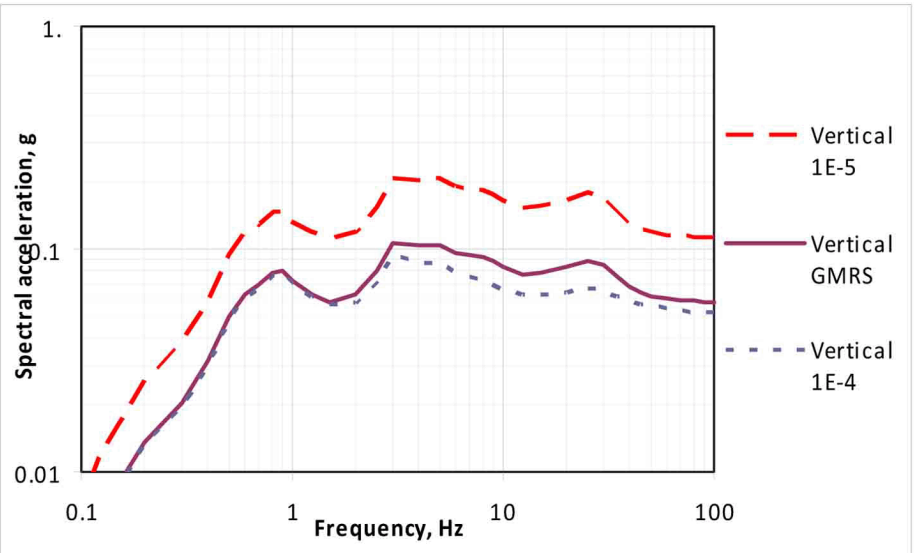

Figure 2.5.2-254 Smoothed Vertical 1E-04 and 1E-05 Site Spectra and GMRS

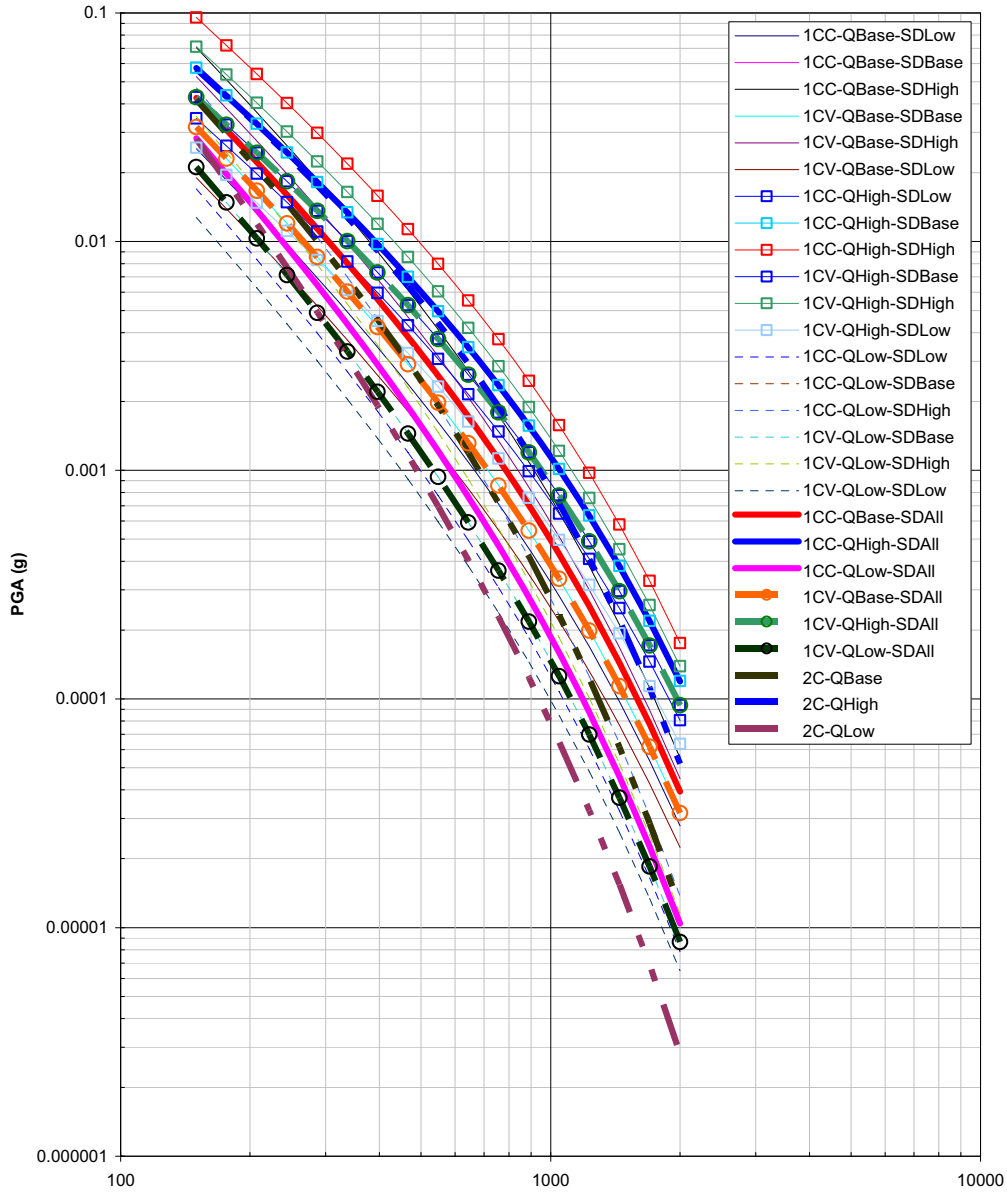

Note: Adopted nine ground motion attenuation models are indicated with thicker lines. Seismic source models are differentiated as 1CC=single corner constant stress parameter, 1CV=single corner variable stress parameter, and 2C=double corner. Stress parameter is indicated in the legend by SD.

Figure 2.5.2-255 Comparison of PGA Attenuation Curves for the Cuba and Caribbean Region for a Magnitude M_w 7 Earthquake

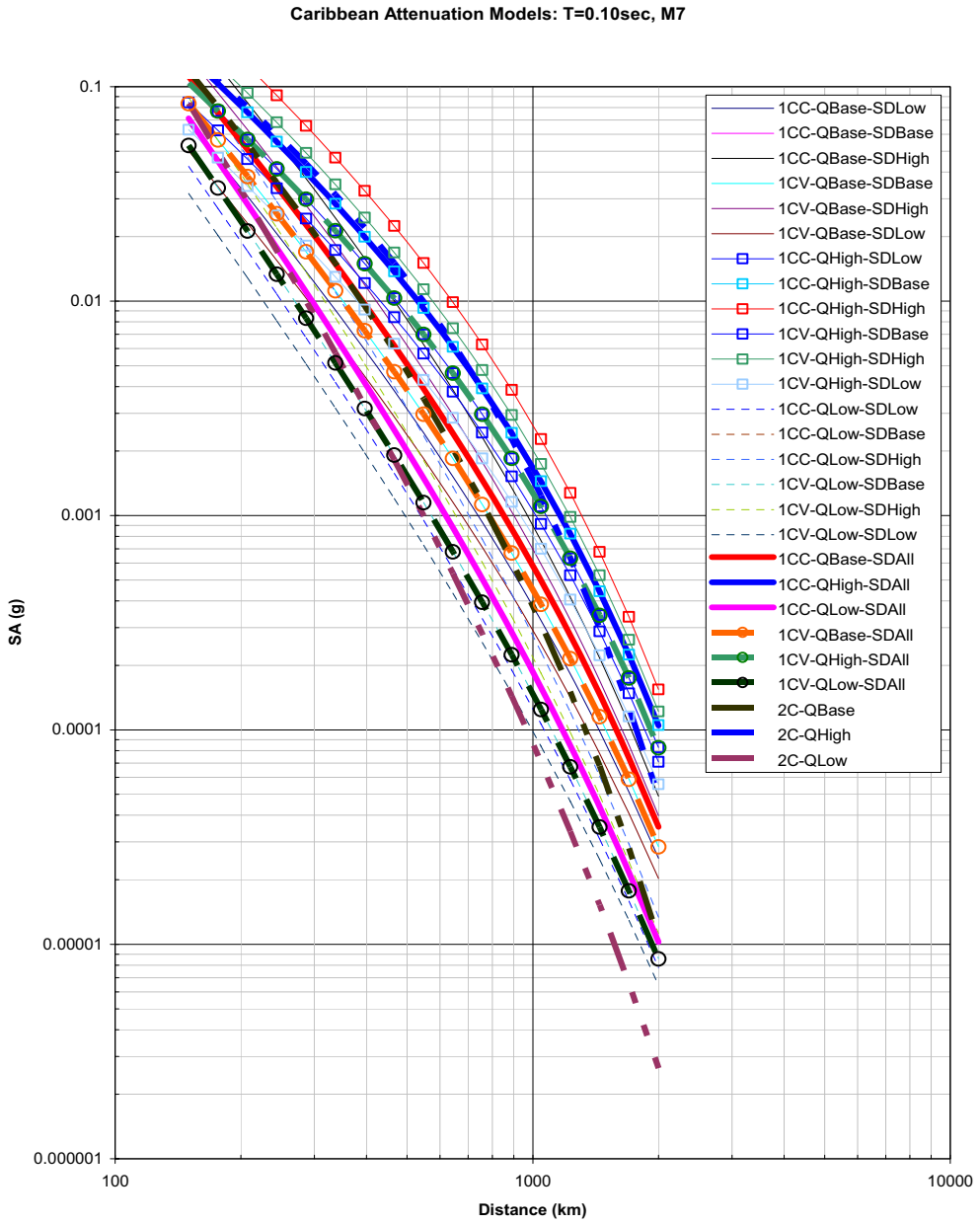

Note: Adopted nine ground motion attenuation models are indicated with thicker lines. Seismic source models are differentiated as 1CC=single corner constant stress parameter, 1CV=single corner variable stress parameter, and 2C=double corner. Stress parameter is indicated in the legend by SD.

Figure 2.5.2-256 Comparison of 10 Hz (T=0.1sec) Attenuation Curves for the Cuba and Caribbean Region for a Magnitude M_W 7 Earthquake

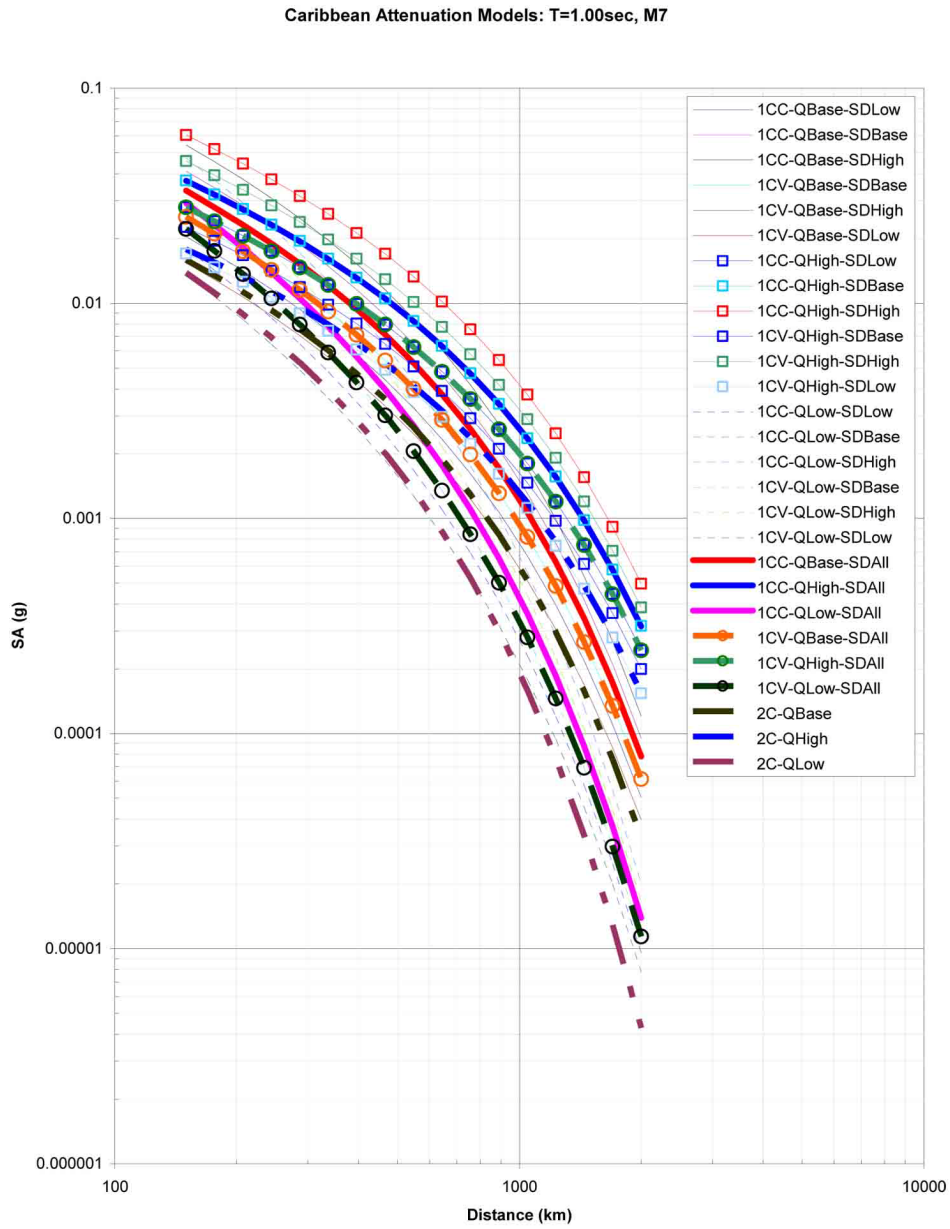

Note: Adopted nine ground motion attenuation models are indicated with thicker lines. Seismic source models are differentiated as 1CC=single corner constant stress parameter, 1CV=single corner variable stress parameter, and 2C=double corner. Stress parameter is indicated in the legend by SD.

Figure 2.5.2-257 Comparison of 1 Hz (T=1.0sec) Attenuation Curves for the Cuba and Caribbean Region for a Magnitude M_w 7 Earthquake

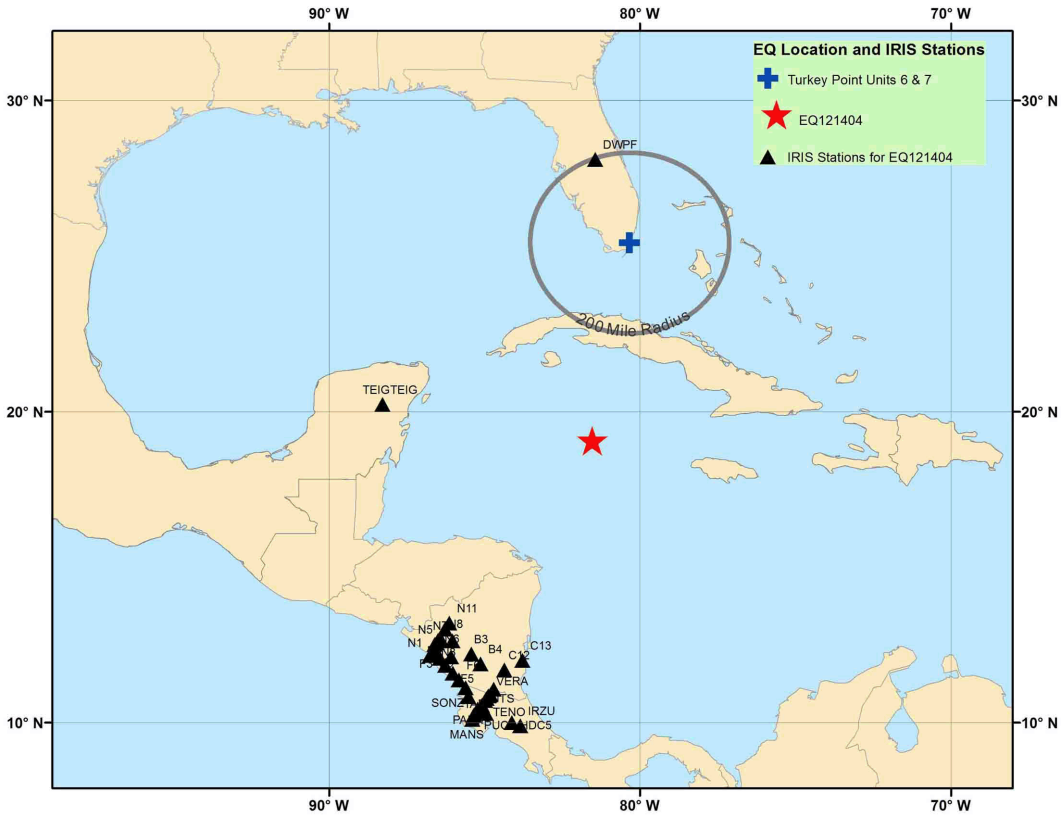

Figure 2.5.2-258a Map Showing the Earthquake Location for the 12/14/2004 Caribbean Sea Region Earthquake (M_w 6.8), the IRIS Station Locations Used in the Analysis (Shown as Black Triangles in this and Similar Subsequent Figures), and Turkey Point Units 6 & 7 Site Location

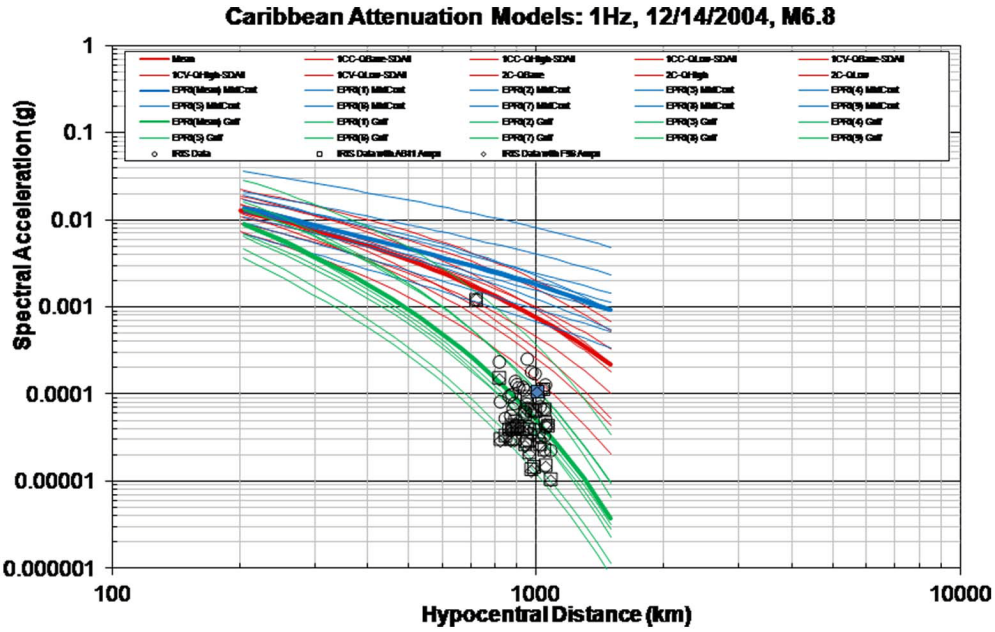

Figure 2.5.2-258b Comparison of Caribbean (Red), EPRI (2004) (Reference 242), Mid-Continent (Blue), and Gulf Coast Region (Green) GMPEs with Raw Empirical IRIS Data (Open Circle), IRIS Data with Atkinson and Boore (2011) (Reference 359) Amplification Factor Corrections (Open Squares) and IRIS Data with Frankel et al. (1996) (Reference 252) Amplification Factor Corrections (Open Diamonds) for a Spectral Frequency of 1 Hz

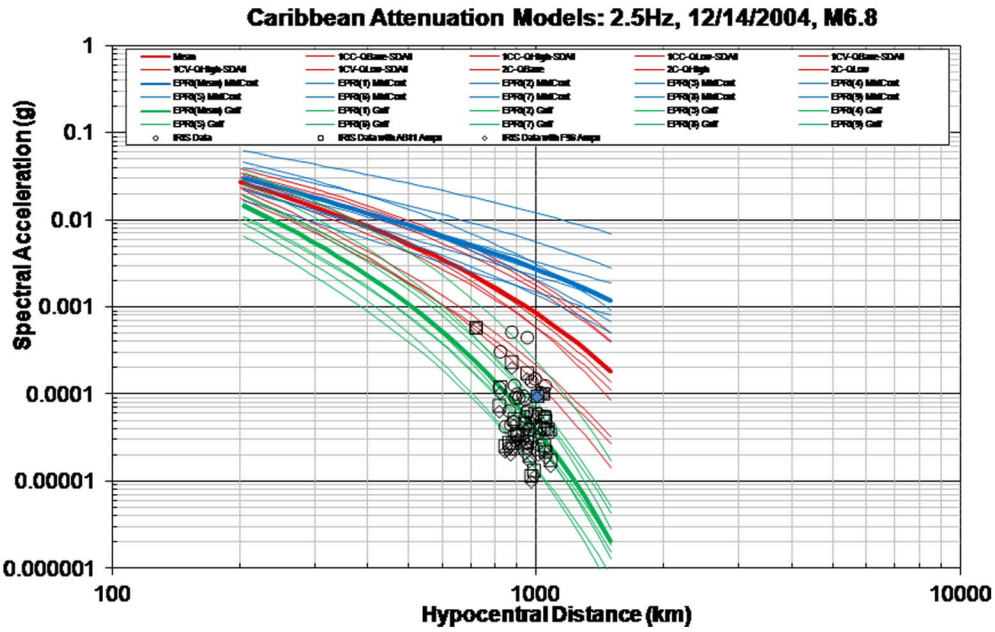

Figure 2.5.2-258c Comparison of Caribbean (Red), EPRI (2004) (Reference 242), Mid-Continent (Blue), and Gulf Coast Region (Green) GMPEs with Raw Empirical IRIS Data (Open Circle), IRIS Data with Atkinson and Boore (2011) (Reference 359) Amplification Factor Corrections (Open Squares) and IRIS Data with Frankel et al. (1996) (Reference 252) Amplification Factor Corrections (Open Diamonds) for a Spectral Frequency of 2.5 Hz

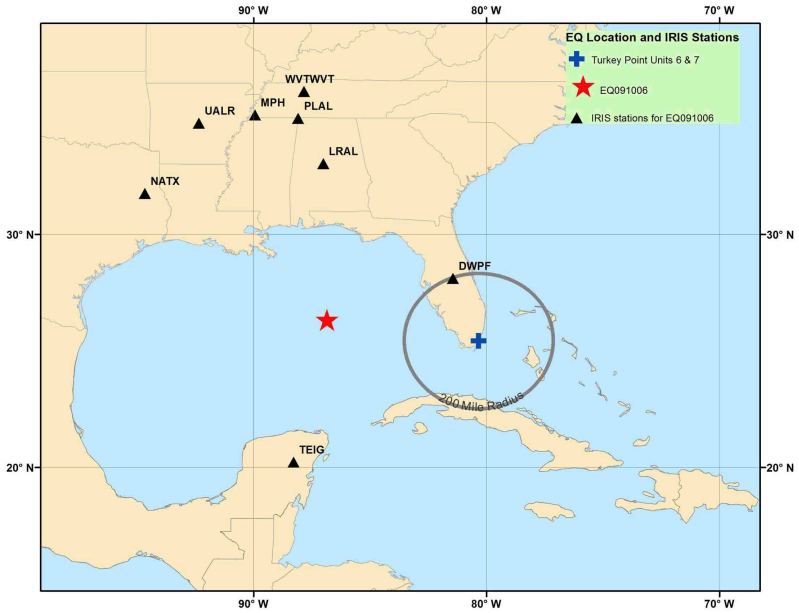

Figure 2.5.2-259a Map Showing the Earthquake Location for the 09/10/2006 Gulf Of Mexico Earthquake (M_W5.9), the IRIS Station Locations Used in the Analysis, and Turkey Point Units 6 & 7 Site Location

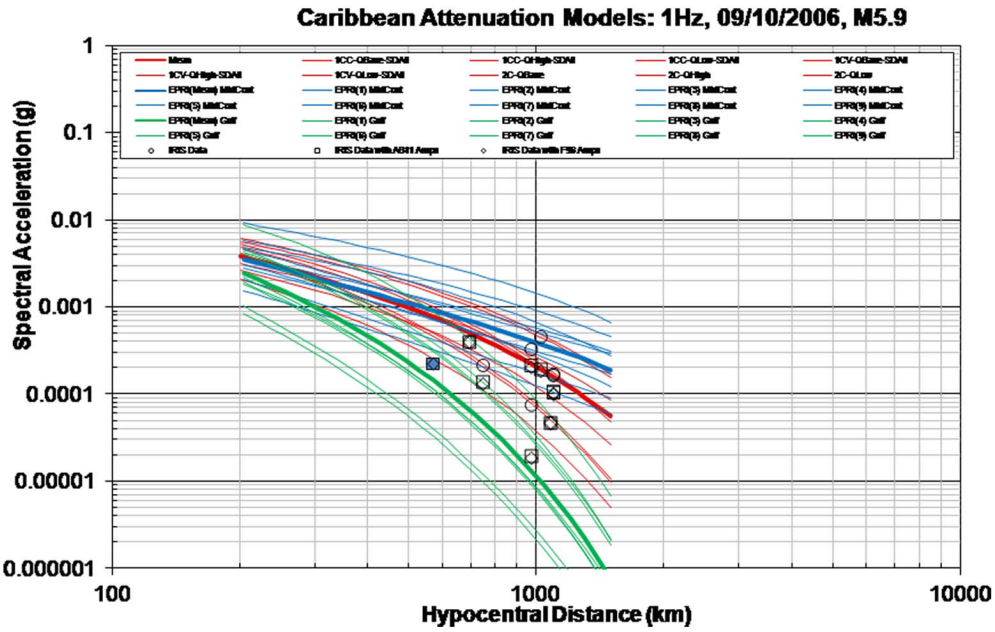

Figure 2.5.2-259b Comparison of Caribbean (Red) EPRI (2004) (Reference 242), Mid-Continent (Blue) and Gulf Coast Region (Green) GMPEs with Raw Empirical IRIS Data (Open Circle), IRIS Data with Atkinson and Boore (2011) (Reference 359) Amplification Factor Corrections (Open Squares) and IRIS Data with Frankel et al. (1996) (Reference 252) Amplification Factor Corrections (Open Diamonds) for a Spectral Frequency of 1 Hz

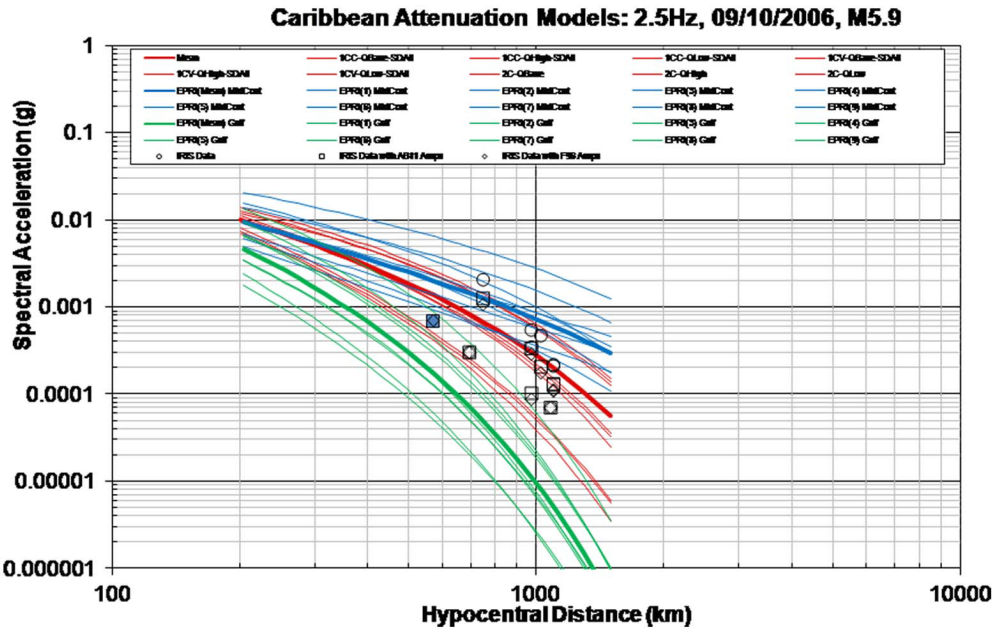

Figure 2.5.2-259c Comparison of Caribbean (Red), EPRI (2004) (Reference 242), Mid-Continent (Blue), and Gulf Coast Region (Green) GMPEs with Raw Empirical IRIS Data (Open Circle), IRIS Data with Atkinson and Boore (2011) (Reference 359) Amplification Factor Corrections (Open Squares) and IRIS Data with Frankel et al. (1996) (Reference 252) Amplification Factor Corrections (Open Diamonds) for a Spectral Frequency of 2.5 Hz

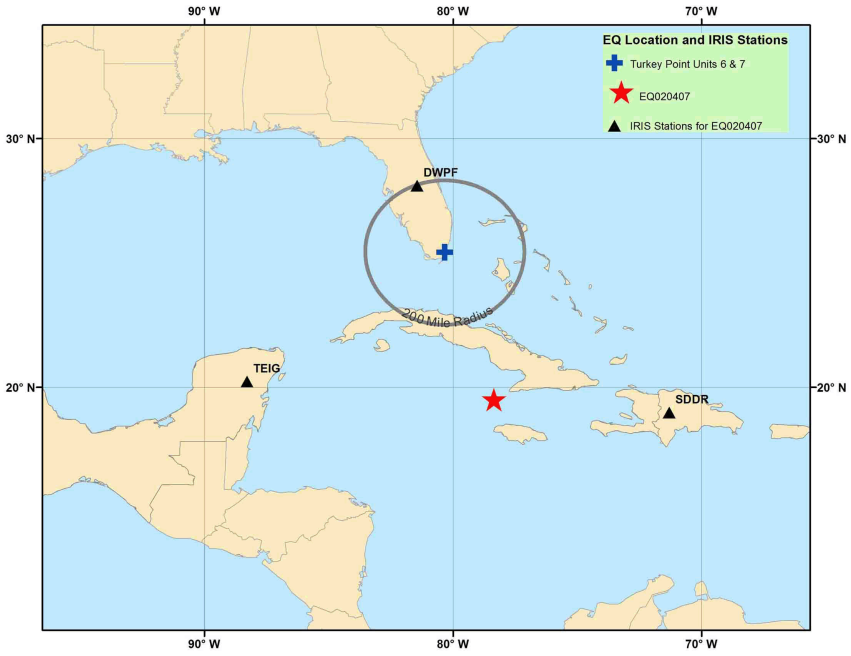

Figure 2.5.2-260a Map Showing the Earthquake Location for the 02/04/2007 Cuba Region Earthquake (M_w 6.2), the IRIS Station Locations Used in the Analysis, and Turkey Point Units 6 & 7 Site Location

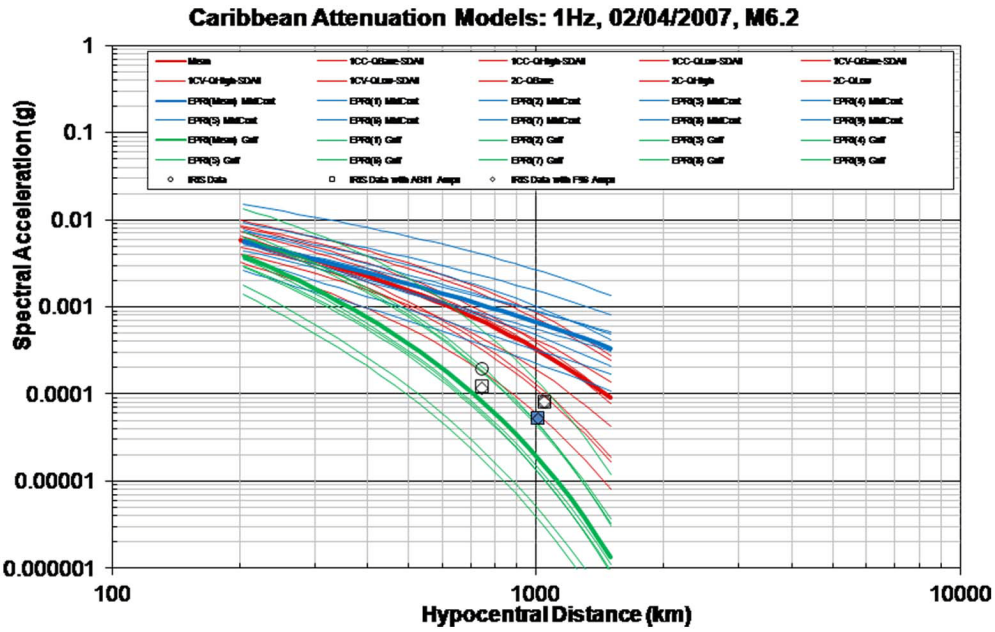

Figure 2.5.2-260b Comparison of Caribbean (Red), EPRI (2004) (Reference 242), Mid-Continent (Blue), and Gulf Coast Region (Green) GMPEs with Raw Empirical IRIS Data (Open Circle), IRIS Data with Atkinson and Boore (2011) (Reference 359) Amplification Factor Corrections (Open Squares) and IRIS Data with Frankel et al. (1996) (Reference 252) Amplification Factor Corrections (Open Diamonds) for a Spectral Frequency of 1 Hz

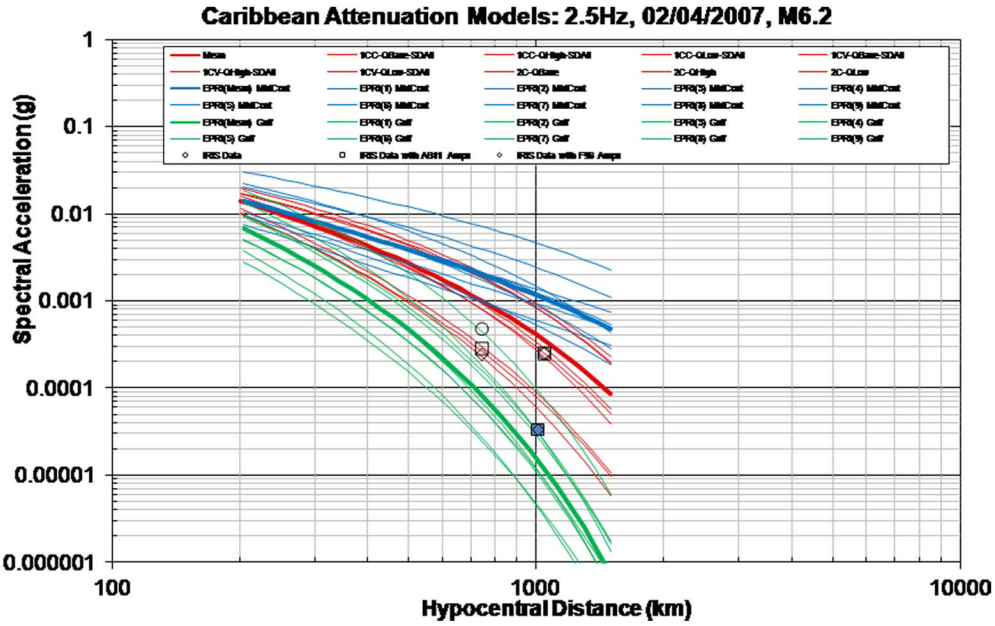

Figure 2.5.2-260c Comparison of Caribbean (Red), EPRI (2004) (Reference 242), Mid-Continent (Blue), and Gulf Coast Region (Green) GMPEs with Raw Empirical IRIS Data (Open Circle), IRIS Data with Atkinson and Boore (2011) (Reference 359) Amplification Factor Corrections (Open Squares) and IRIS Data with Frankel et al. (1996) (Reference 252) Amplification Factor Corrections (Open Diamonds) for a Spectral Frequency of 2.5 Hz

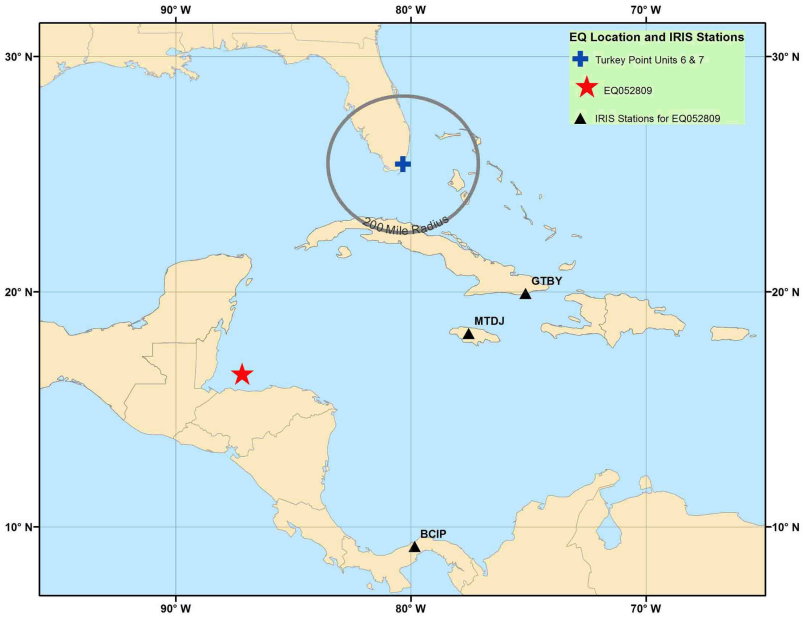

Figure 2.5.2-261a Map Showing the Earthquake Location for the 05/28/2009 North of Honduras Earthquake (M_W 7.3), the IRIS Station Locations Used in the Analysis, and Turkey Point Units 6 & 7 Site Location

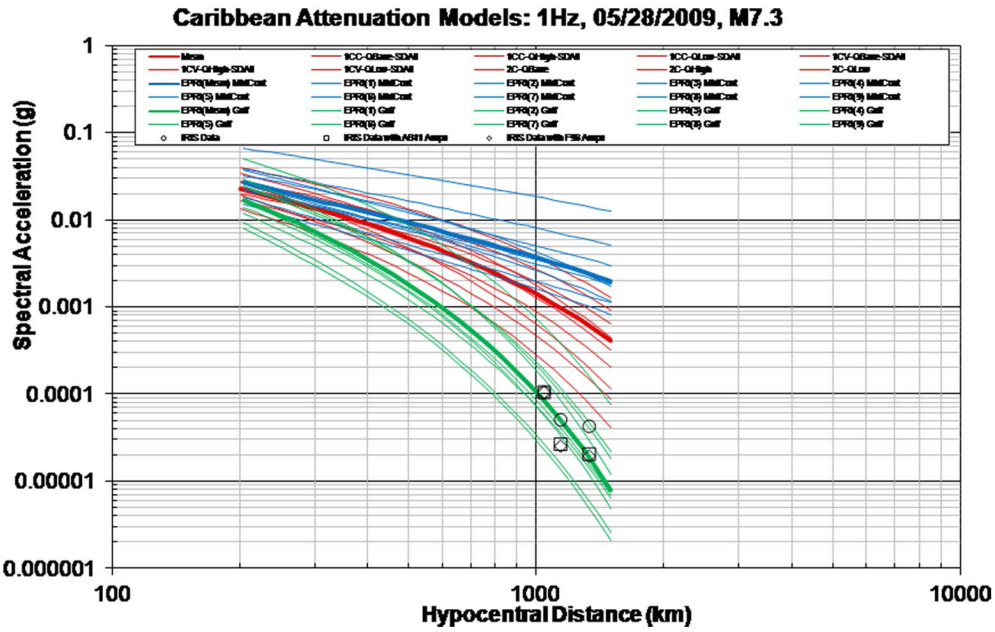

Figure 2.5.2-261b Comparison of Caribbean (Red), EPRI (2004) (Reference 242), Mid-Continent (Blue), and Gulf Coast Region (Green) GMPEs with Raw Empirical IRIS Data (Open Circle), IRIS Data with Atkinson and Boore (2011) (Reference 359) Amplification Factor Corrections (Open Squares) and IRIS Data with Frankel et al. (1996) (Reference 252) Amplification Factor Corrections (Open Diamonds) for a Spectral Frequency of 1 Hz

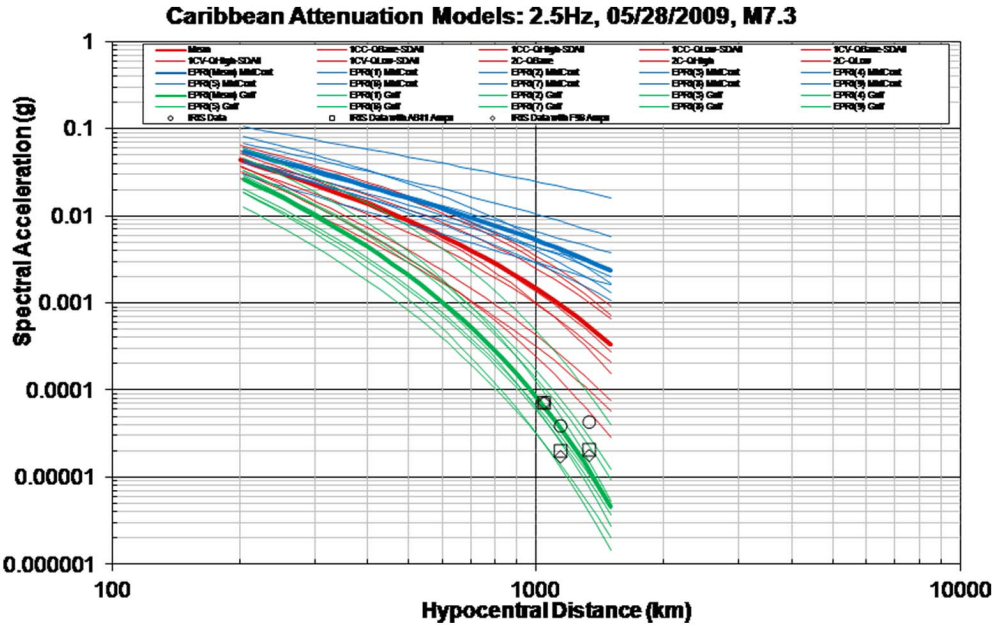

Figure 2.5.2-261c Comparison of Caribbean (Red), EPRI (2004) (Reference 242), Mid-Continent (Blue), and Gulf Coast Region (Green) GMPEs with Raw Empirical IRIS Data (Open Circle) IRIS Data with Atkinson and Boore (2011) (Reference 359) Amplification Factor Corrections (Open Squares) and IRIS Data with Frankel et al. (1996) (Reference 252) Amplification Factor Corrections (Open Diamonds) for a Spectral Frequency of 2.5 Hz

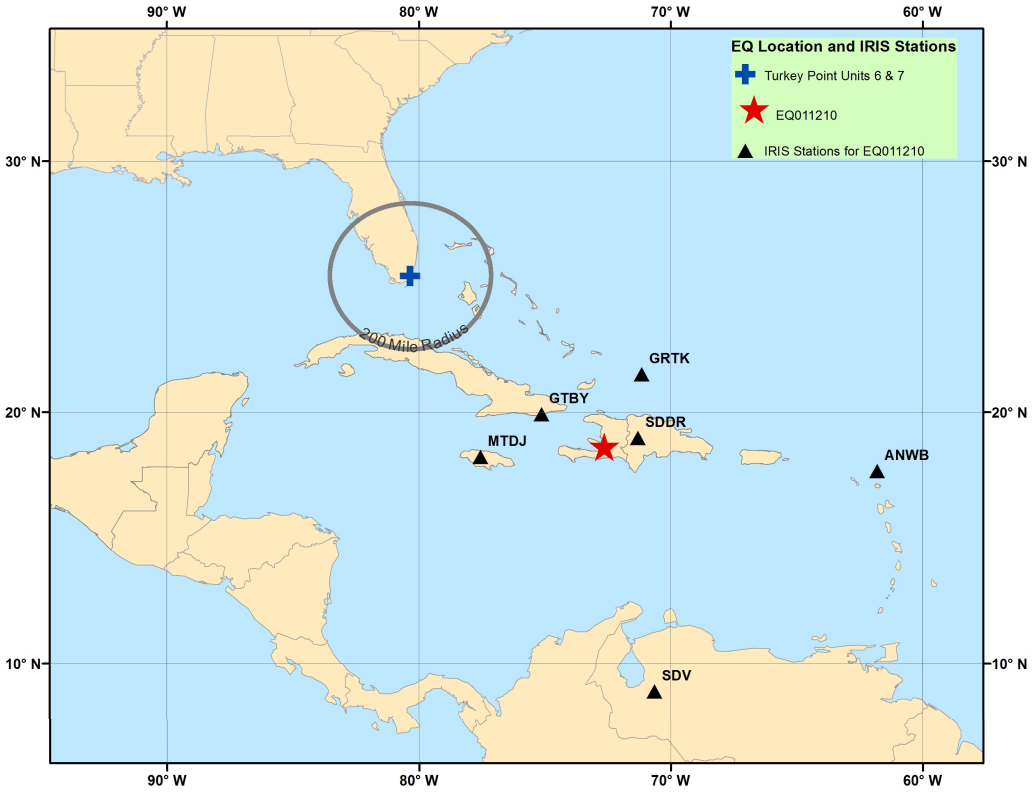

Figure 2.5.2-262a Map Showing the Earthquake Location for the 01/12/2010 Haiti Earthquake (M_w 7.0), the IRIS Station Locations Used in the Analysis, and Turkey Point Units 6 & 7 Site Location

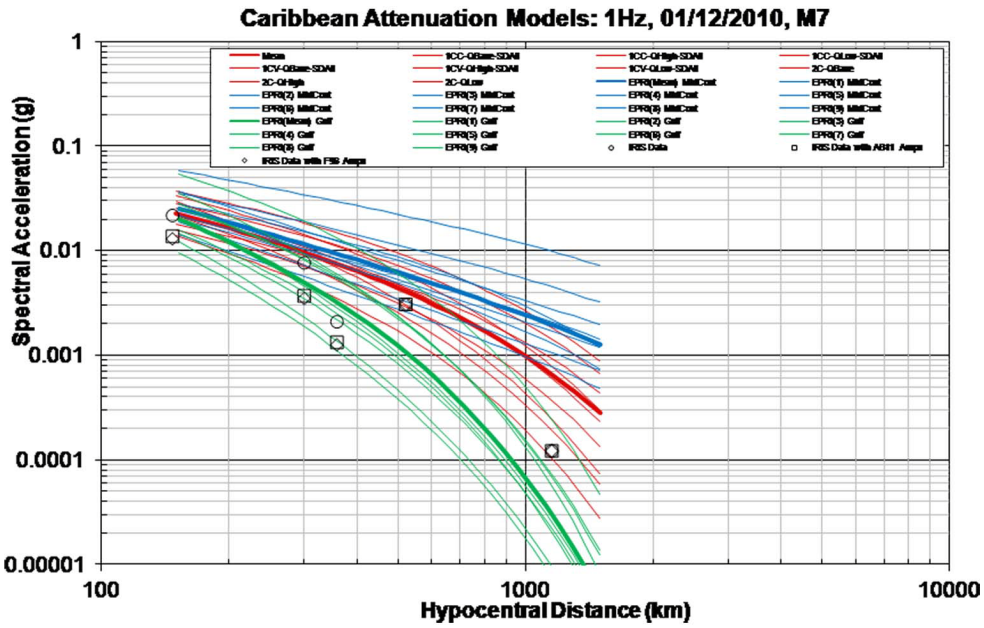

Figure 2.5.2-262b Comparison of Caribbean (Red), EPRI (2004) (Reference 242), Mid-Continent (Blue), and Gulf Coast Region (Green) GMPEs with Raw Empirical IRIS Data (Open Circle), IRIS Data with Atkinson and Boore (2011) (Reference 359) Amplification Factor Corrections (Open Squares) and IRIS Data with Frankel et al. (1996) (Reference 252) Amplification Factor Corrections (Open Diamonds) for a Spectral Frequency of 1 Hz

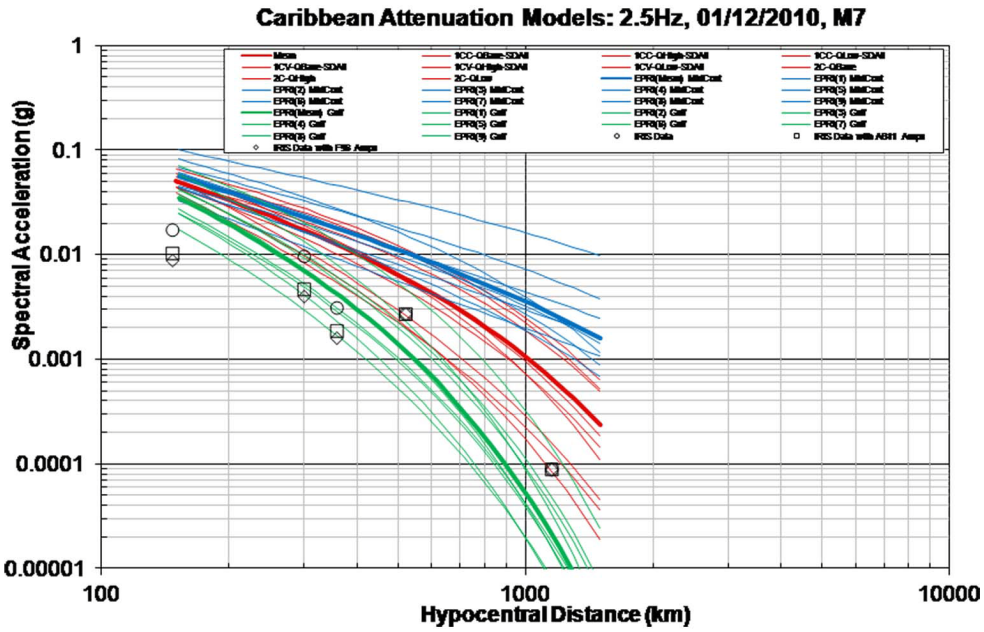

Figure 2.5.2-262c Comparison of Caribbean (Red), EPRI (2004) (Reference 242), Mid-Continent (Blue), and Gulf Coast Region (Green) GMPEs with Raw Empirical IRIS Data (Open Circle), IRIS Data with Atkinson and Boore (2011) (Reference 359) Amplification Factor Corrections (Open Squares) and IRIS Data with Frankel et al. (1996) (Reference 252) Amplification Factor Corrections (Open Diamonds) for a Spectral Frequency of 2.5 Hz

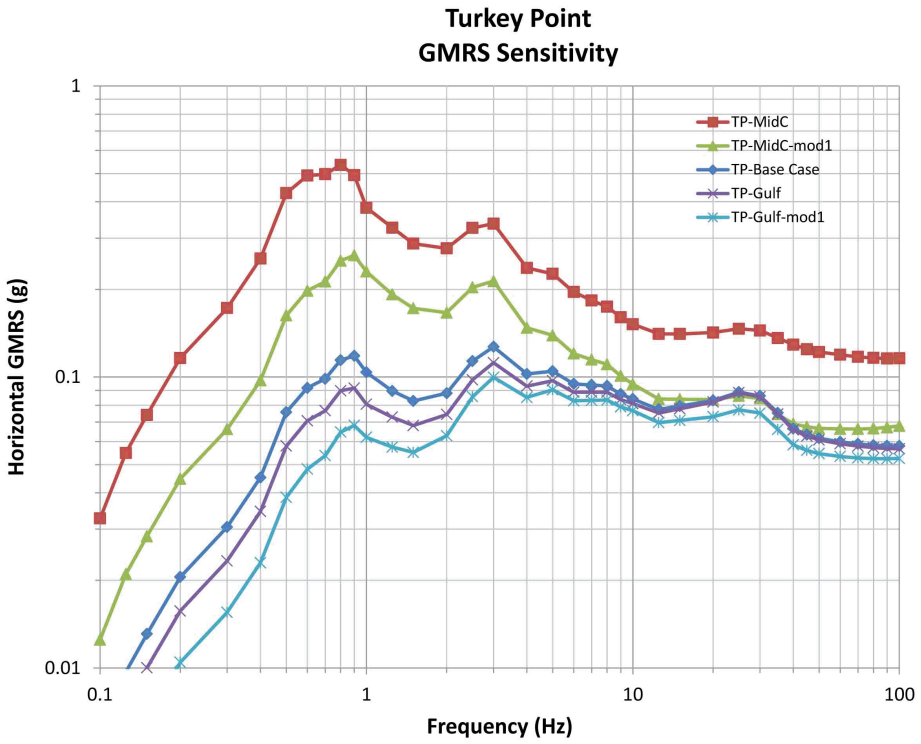

Figure 2.5.2-263 Horizontal GMRS for Caribbean Sources for Five GMPE Models for the Turkey Points Units 6 & 7 Site

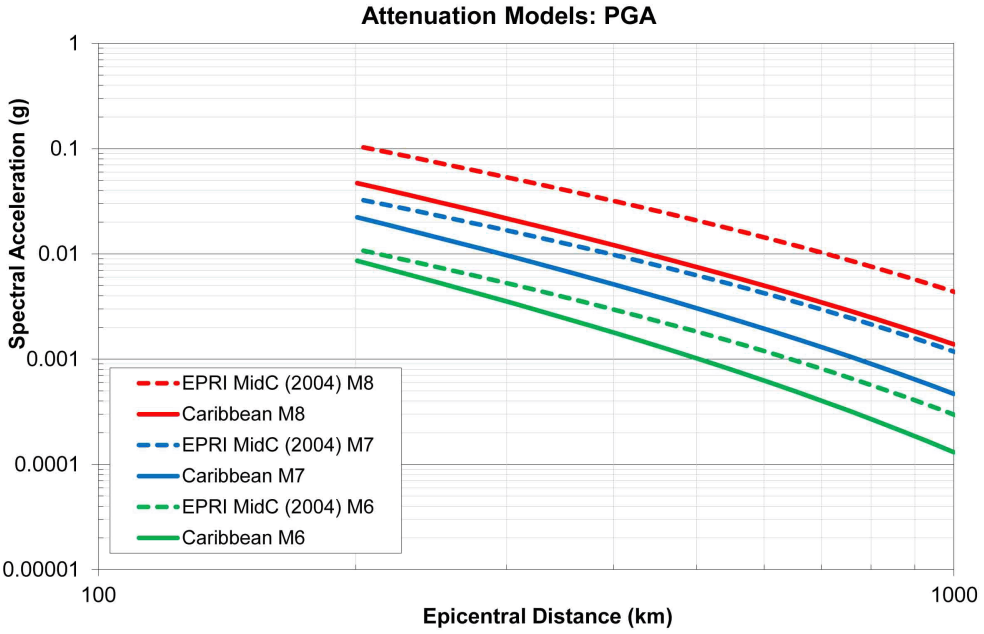

Figure 2.5.2-264 Comparison of EPRI Mid-Continent (Reference 242) Mean (dashed lines) and Caribbean Mean (solid lines) Attenuation Curves for Magnitudes 6, 7, and 8 for PGA

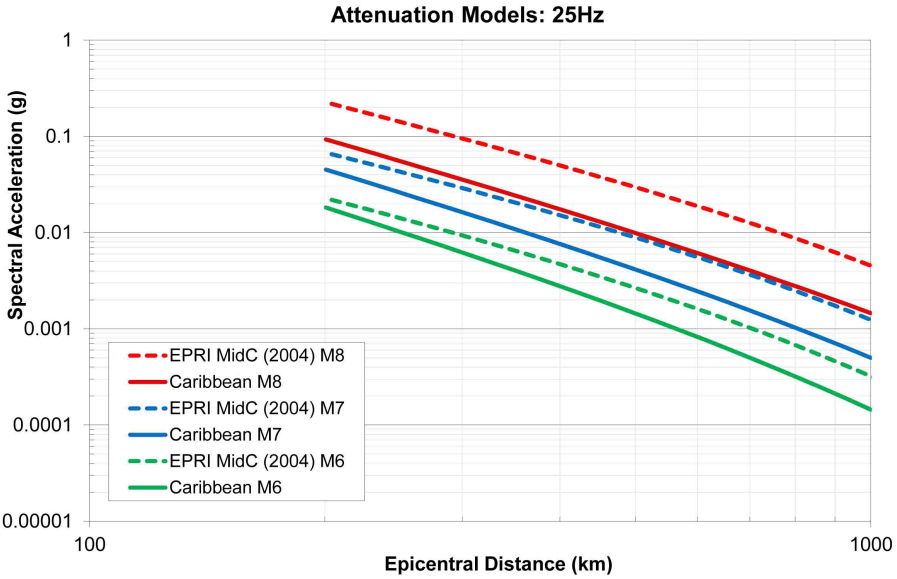

Source: Reference 242

Figure 2.5.2-265 Comparison of EPRI Mid-Continent Mean (dashed lines) and Caribbean Mean (solid lines) Attenuation Curves for Magnitudes 6, 7, and 8 for 25 Hz

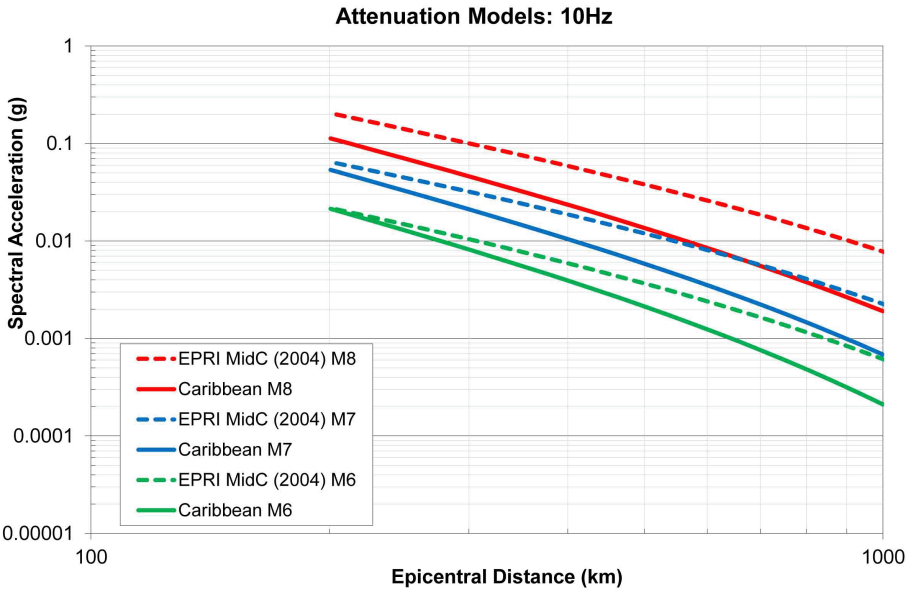

Source: Reference 242

Figure 2.5.2-266 Comparison of EPRI Mid-Continent Mean (dashed lines) and Caribbean Mean (solid lines) Attenuation Curves for Magnitudes 6, 7, and 8 for 10 Hz

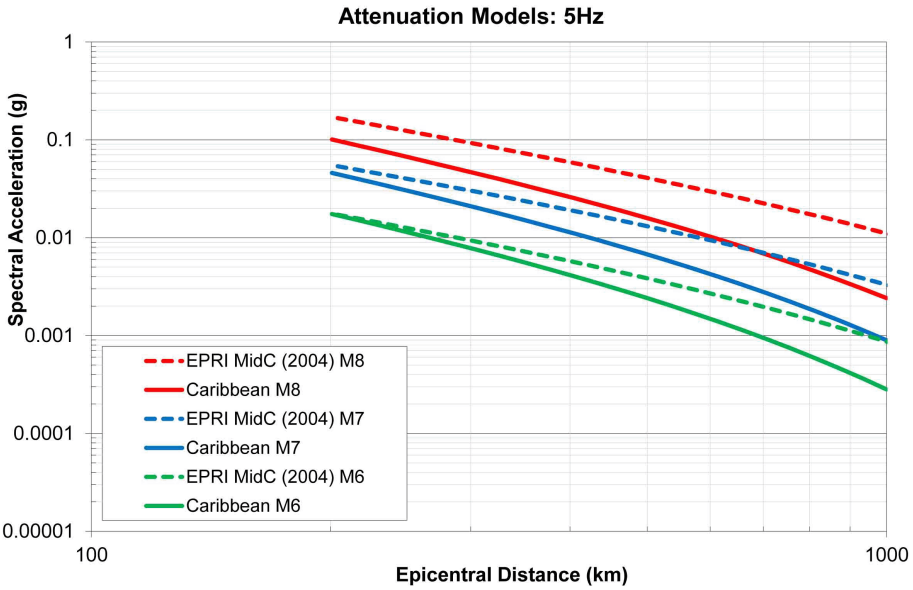

Source: Reference 242

Figure 2.5.2-267 Comparison of EPRI Mid-Continent Mean (dashed lines) and Caribbean Mean (solid lines) Attenuation Curves for Magnitudes 6, 7, and 8 for 5 Hz

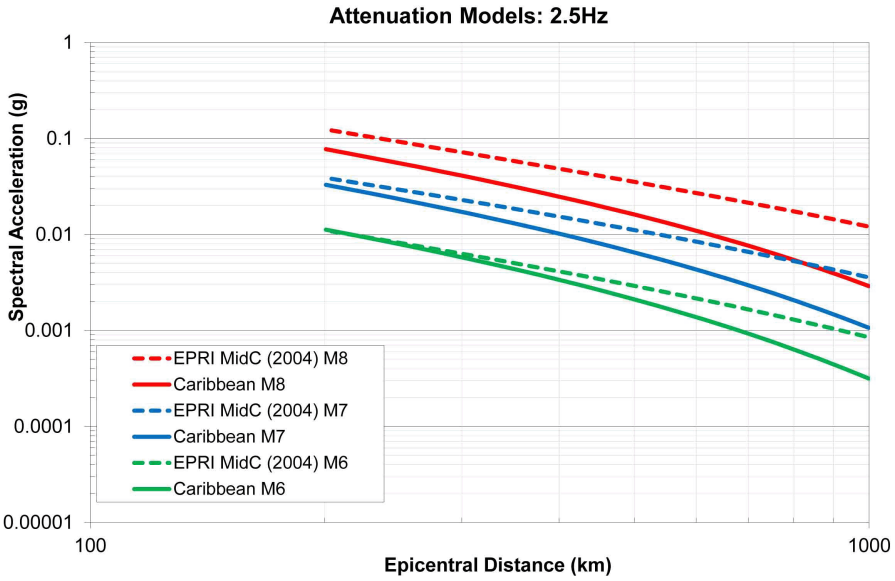

Source: Reference 242

Figure 2.5.2-268 Comparison of EPRI Mid-Continent Mean (dashed lines) and Caribbean Mean (solid lines) Attenuation Curves for Magnitudes 6, 7, and 8 for 2.5 Hz

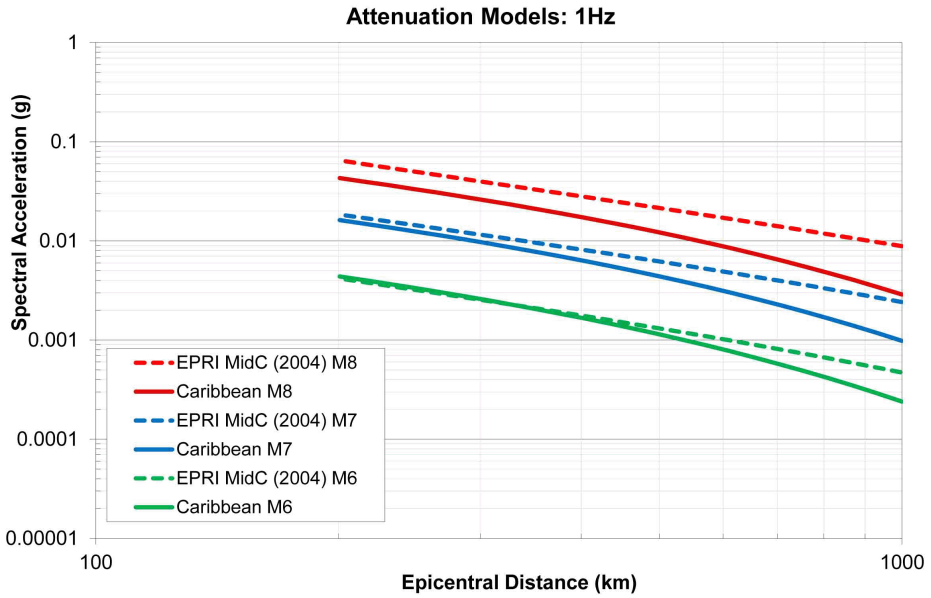

Source: Reference 242

Figure 2.5.2-269 Comparison of EPRI Mid-Continent Mean (dashed lines) and Caribbean Mean (solid lines) Attenuation Curves for Magnitudes 6, 7, and 8 for 1 Hz

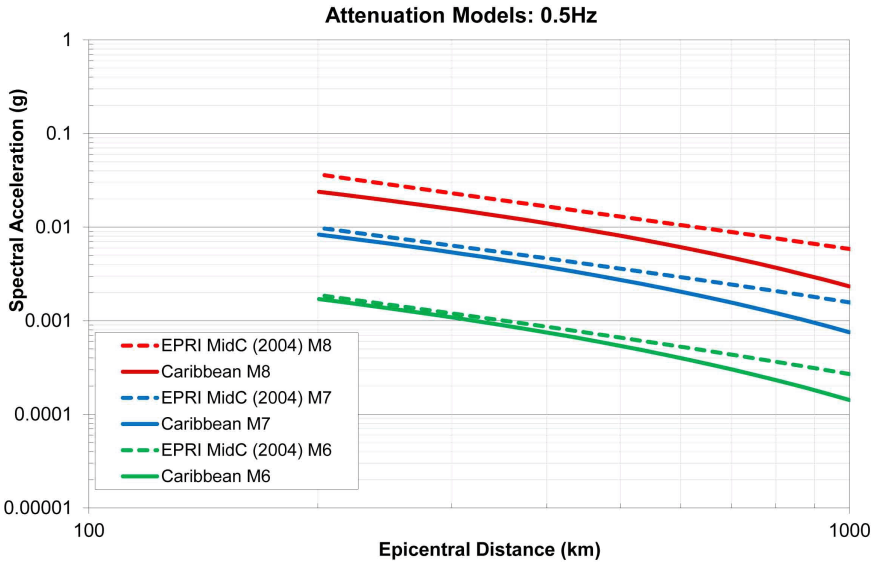

Source: Reference 242

Figure 2.5.2-270 Comparison of EPRI Mid-Continent Mean (dashed lines) and Caribbean Mean (solid lines) Attenuation Curves for Magnitudes 6, 7, and 8 for 0.5 Hz

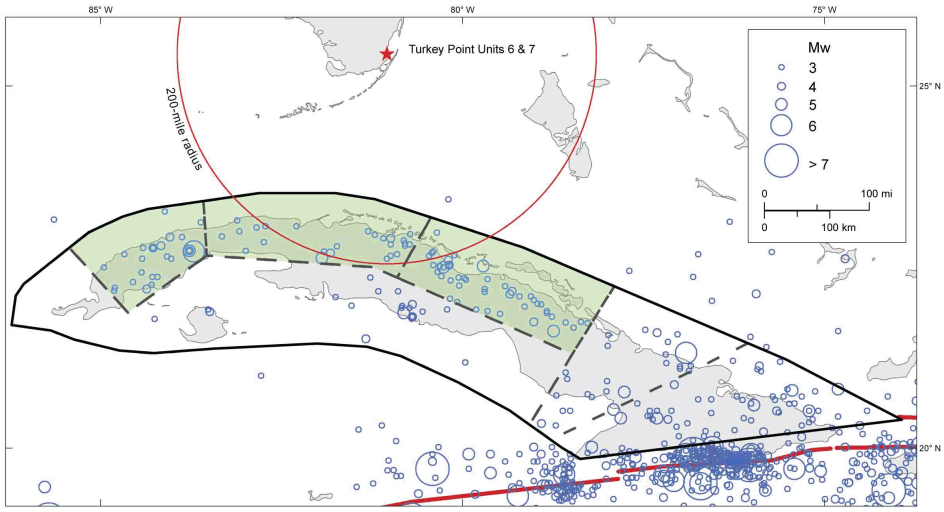

Figure 2.5.2-271 Map Showing Cuba Single Areal Source Zone (solid black line), Six Sensitivity Areal Source Zones (dashed black lines), and Northern Cuba Subzone Used in Hazard Sensitivity Calculation (green shading). Seismicity (blue circles) is from the Phase 2 Earthquake Catalog. Thick Red Lines Show Plate Boundary Fault Sources Included in PSHA.

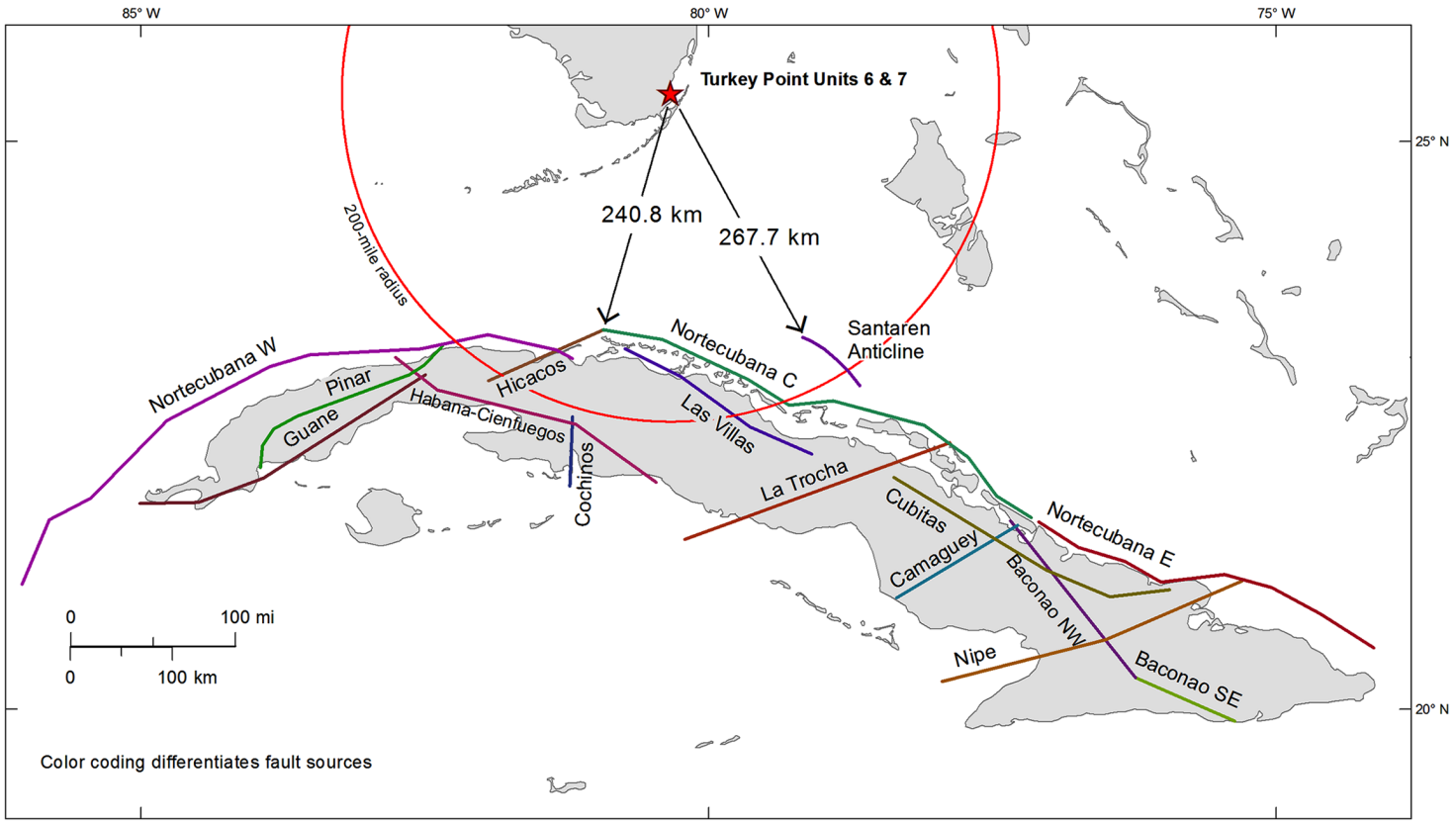

Figure 2.5.2-272 Map of Cuba Fault Sources and Santaren Anticline Fault Source for Hazard Sensitivity Calculations

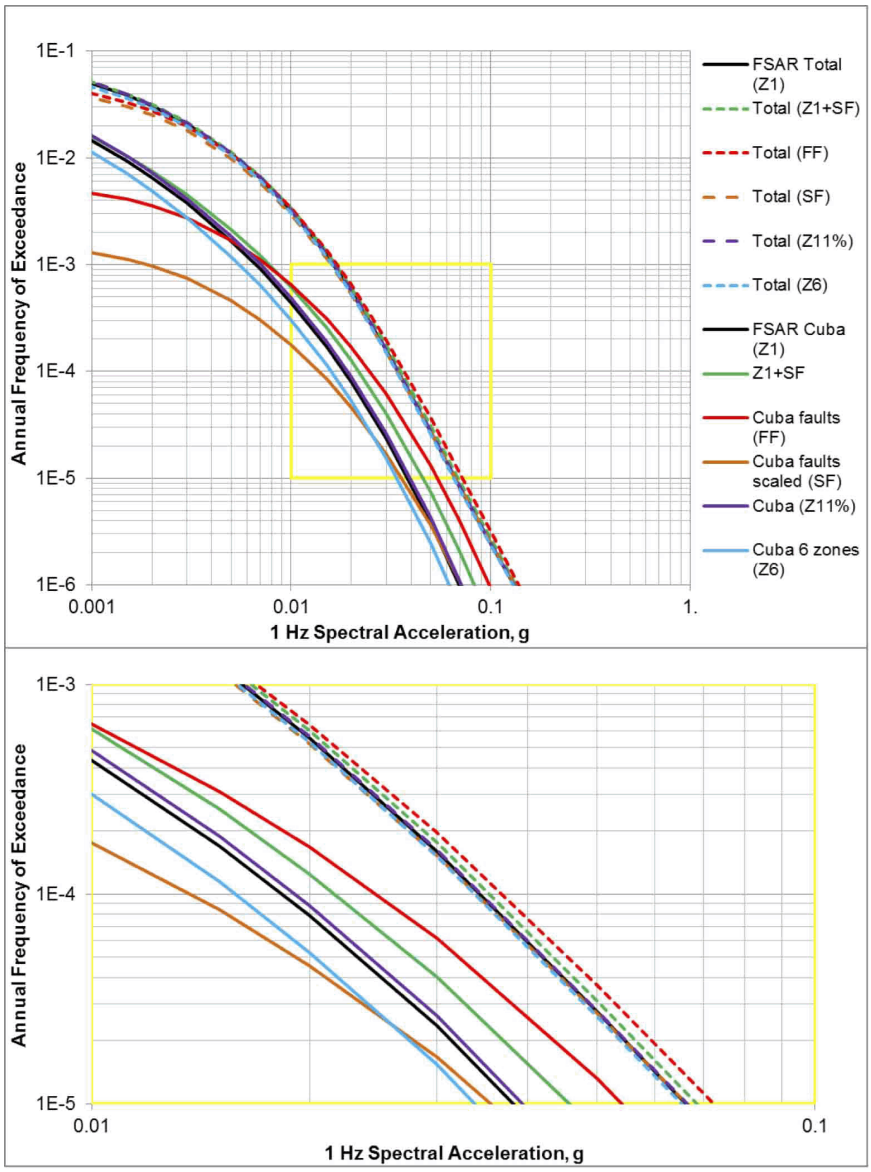

Figure 2.5.2-273 1 Hz Mean Hazard Curves Showing Sensitivity to Cuba Source Scenarios. Lower Panel is Expanded View of Yellow Box in Upper Panel.

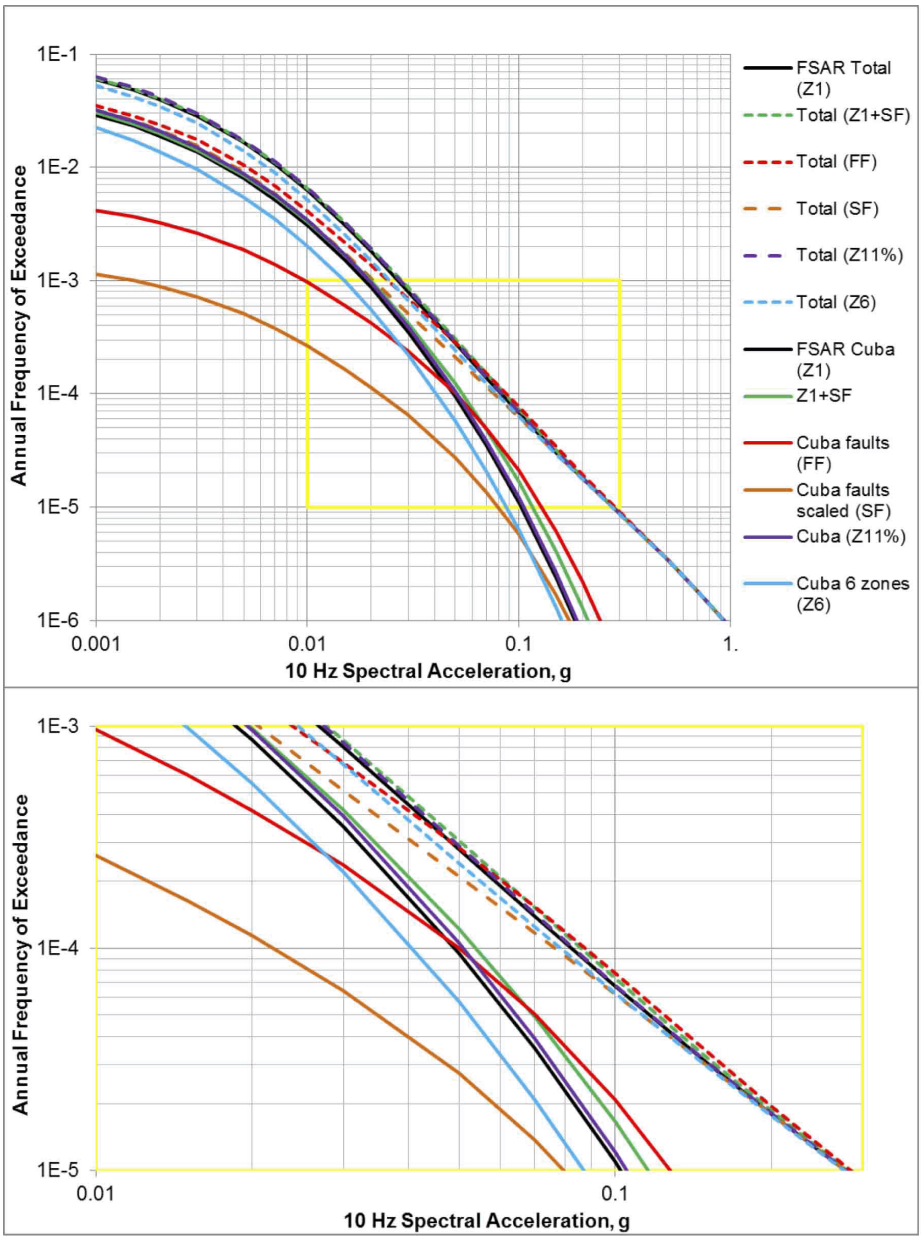

Figure 2.5.2-274 10 Hz Mean Hazard Curves Showing Sensitivity to Cuba Source Scenarios. Lower Panel is Expanded View of Yellow Box in Upper Panel.

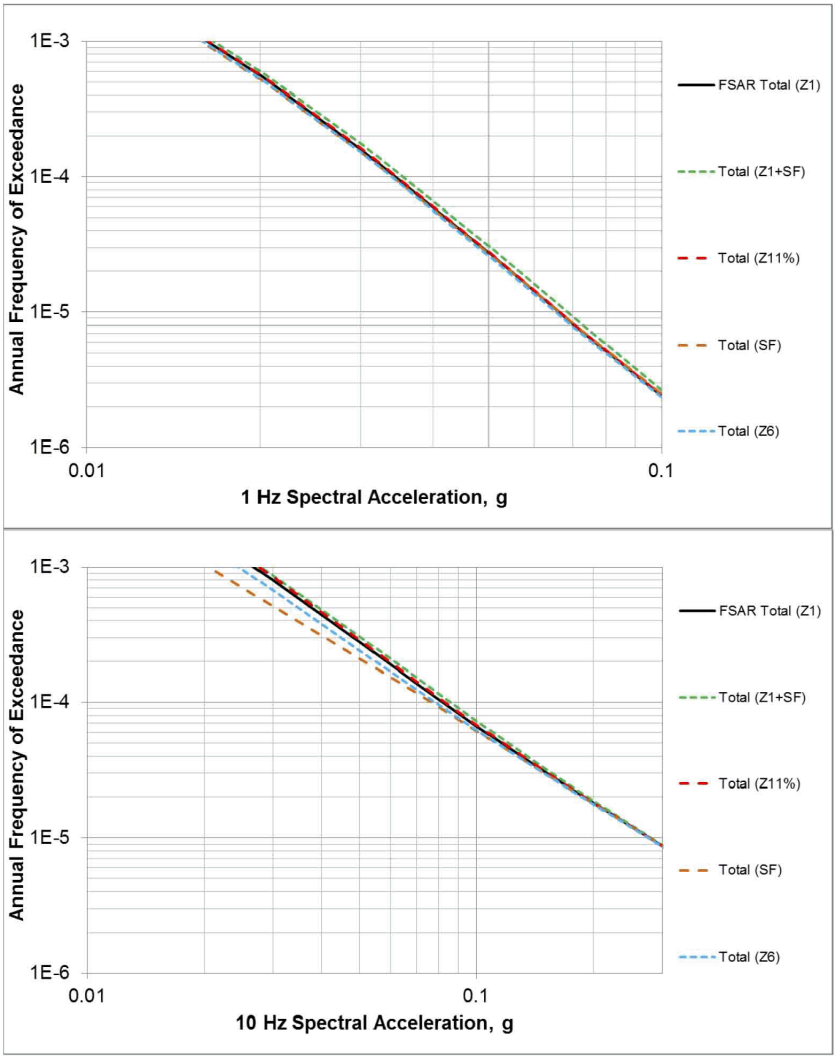

Source: Reference 242

Figure 2.5.2-275 Total Mean Hazard Curves for 1 Hz (Upper) and 10 Hz (Lower) Showing Sensitivity to Four Cuba Source Scenarios

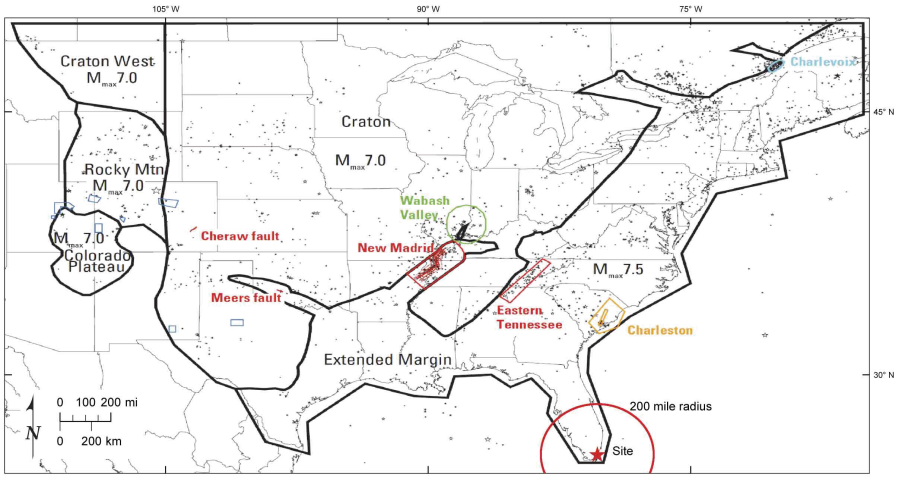

Source: Reference 300

Figure 2.5.2-276 Seismic Sources from the U.S. Geological Survey's 2008 National Seismic Hazard Mapping Project

Figure 2.5.2-277 Not Used

Figure 2.5.2-278 Not Used

Figure 2.5.2-279 Not Used

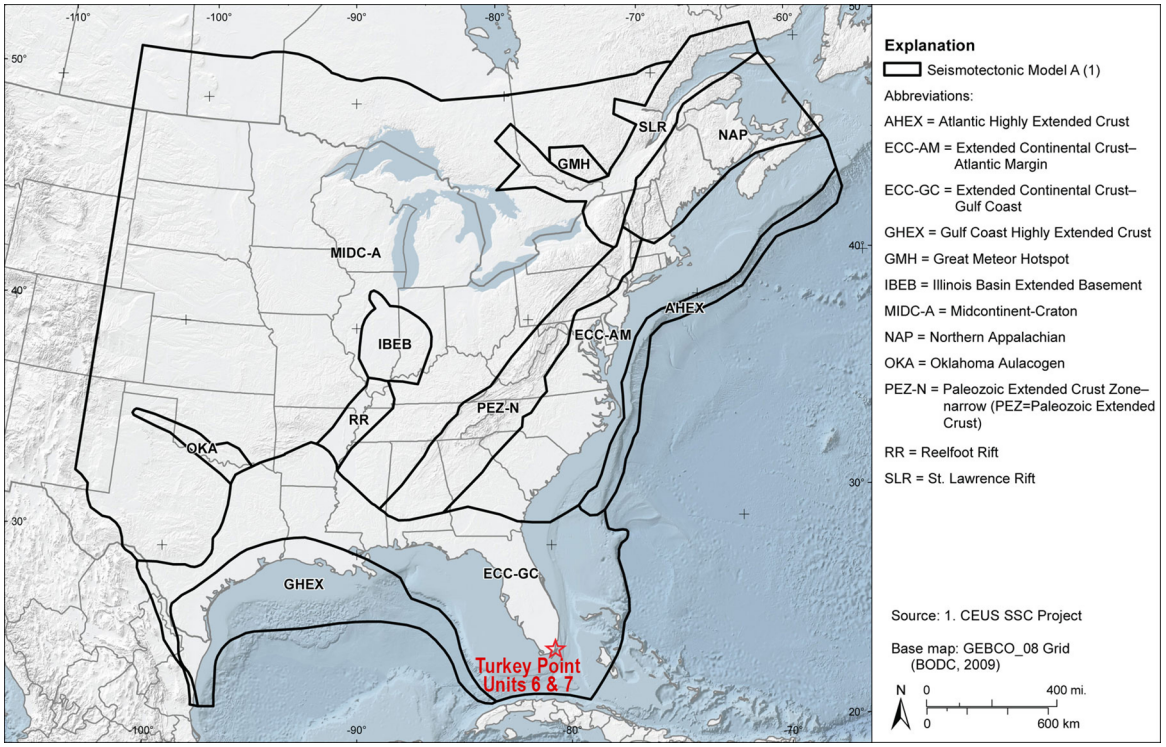

Note: Seismotectonic source zones for the “narrow” interpretation of PEZ and the Rough Creek Graben not included as part of the Reelfoot Rift (RR) source (Figure 4.2.4-2 of NUREG-2115). Approximate location of the Turkey Point Units 6 & 7 site is shown by the red star.

Figure 2.5.2-280 Seismotectonic Source Zones in the CEUS SSC Model

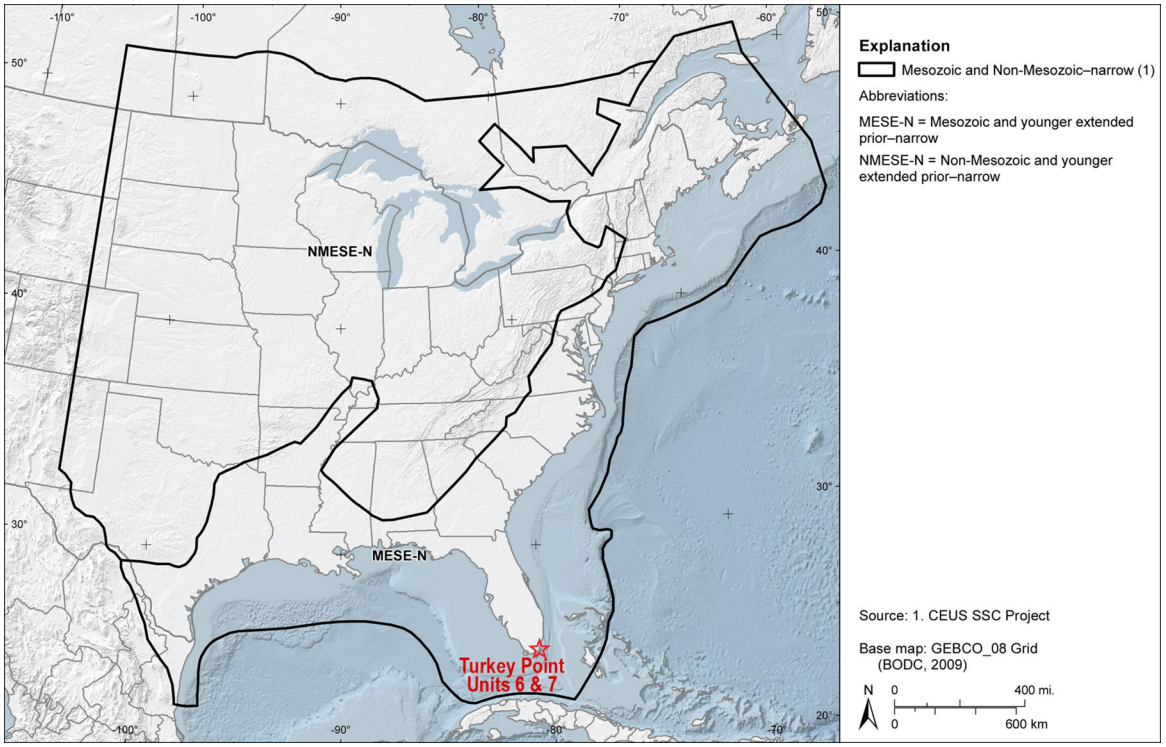

Note: Mmax source zones from the CEUS SSC model for the “narrow” interpretation (Figure 4.2.3-2 of NUREG-2115). Approximate location of the Turkey Point Units 6 & 7 site is shown by the red star.

Figure 2.5.2-281 Mmax Source Zones in the CEUS SSC Model

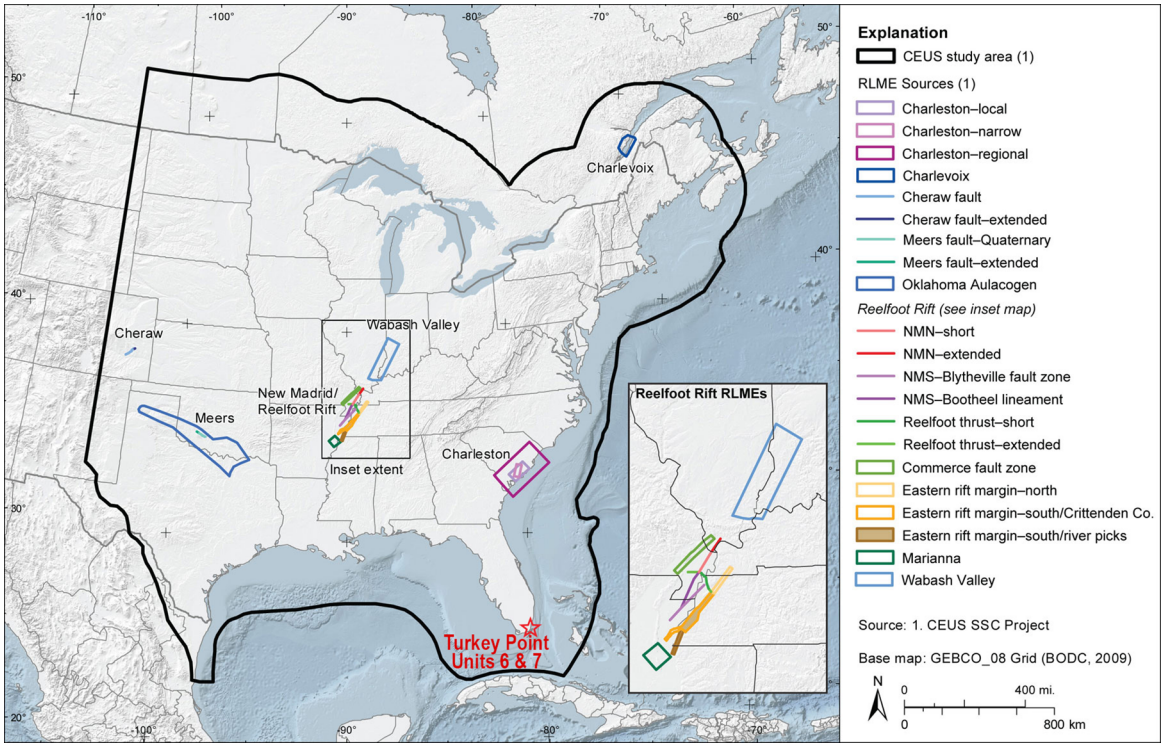

Note: Location of RLME sources in the CEUS SSC model (Figure 4.2.2-2 of NUREG-2115). Approximate location of the Turkey Point Units 6 & 7 site is shown by the red star.

Figure 2.5.2-282 RLME Sources in the CEUS SSC Model

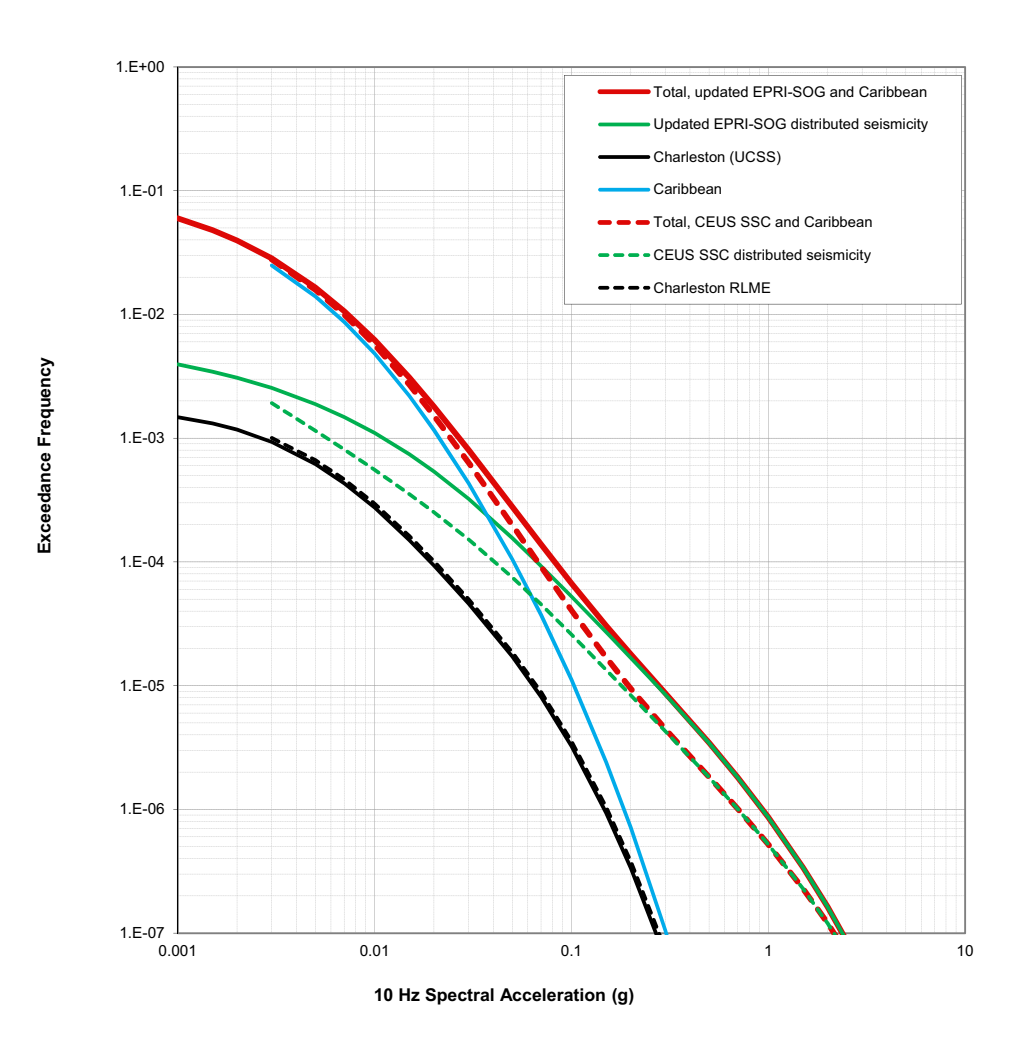

Note: Contributions of various source types to total hazard. Solid curves show hazard based on updated EPRI-SOG. Dashed curves show hazard based on CEUS SSC model.

Figure 2.5.2-283 Contributions of Various Source Types to Hard Rock Hazard for 10 Hz

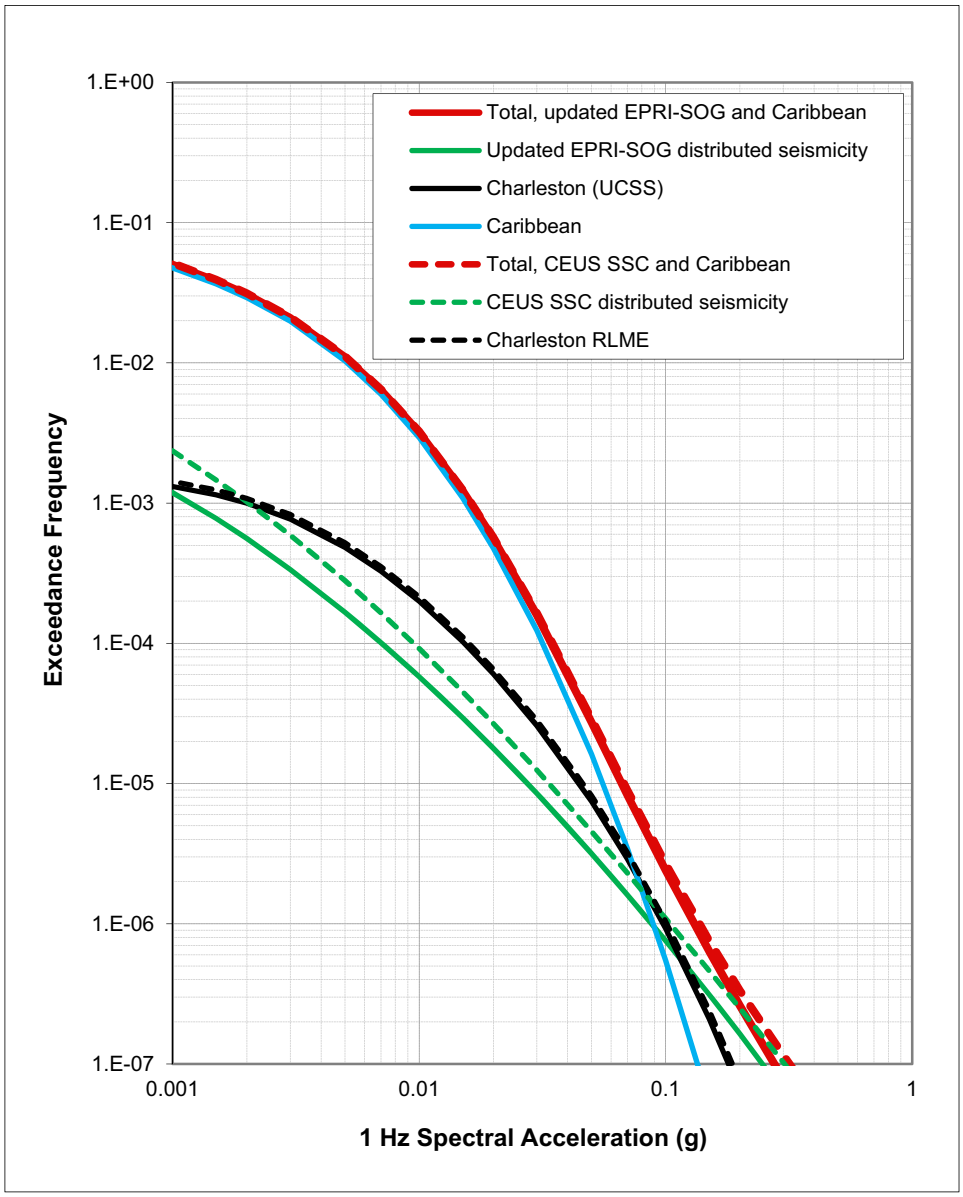

Note: Contributions of various source types to total hazard. Solid curves show hazard based on updated EPRI-SOG model. Dashed curves show hazard based on CEUS SSC model.

Figure 2.5.2-284 Contributions of Various Source Types to Hard Rock Hazard for 1 Hz

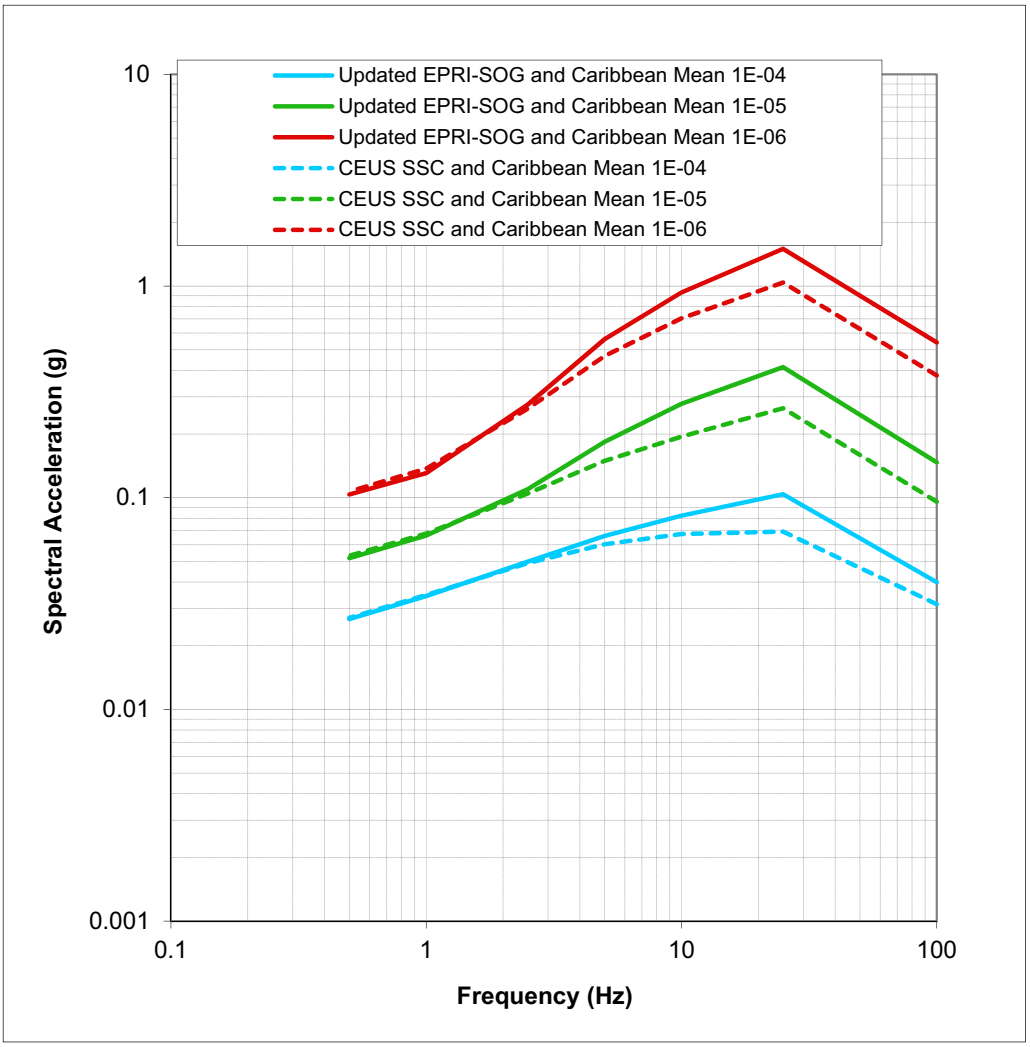

Note: Comparison between the hard rock UHRS based on the updated EPRI-SOG model plus Caribbean Sources, and the UHRS computed using the CEUS SSC model plus Caribbean sources.

Figure 2.5.2-285 Comparison of Hard Rock UHRS

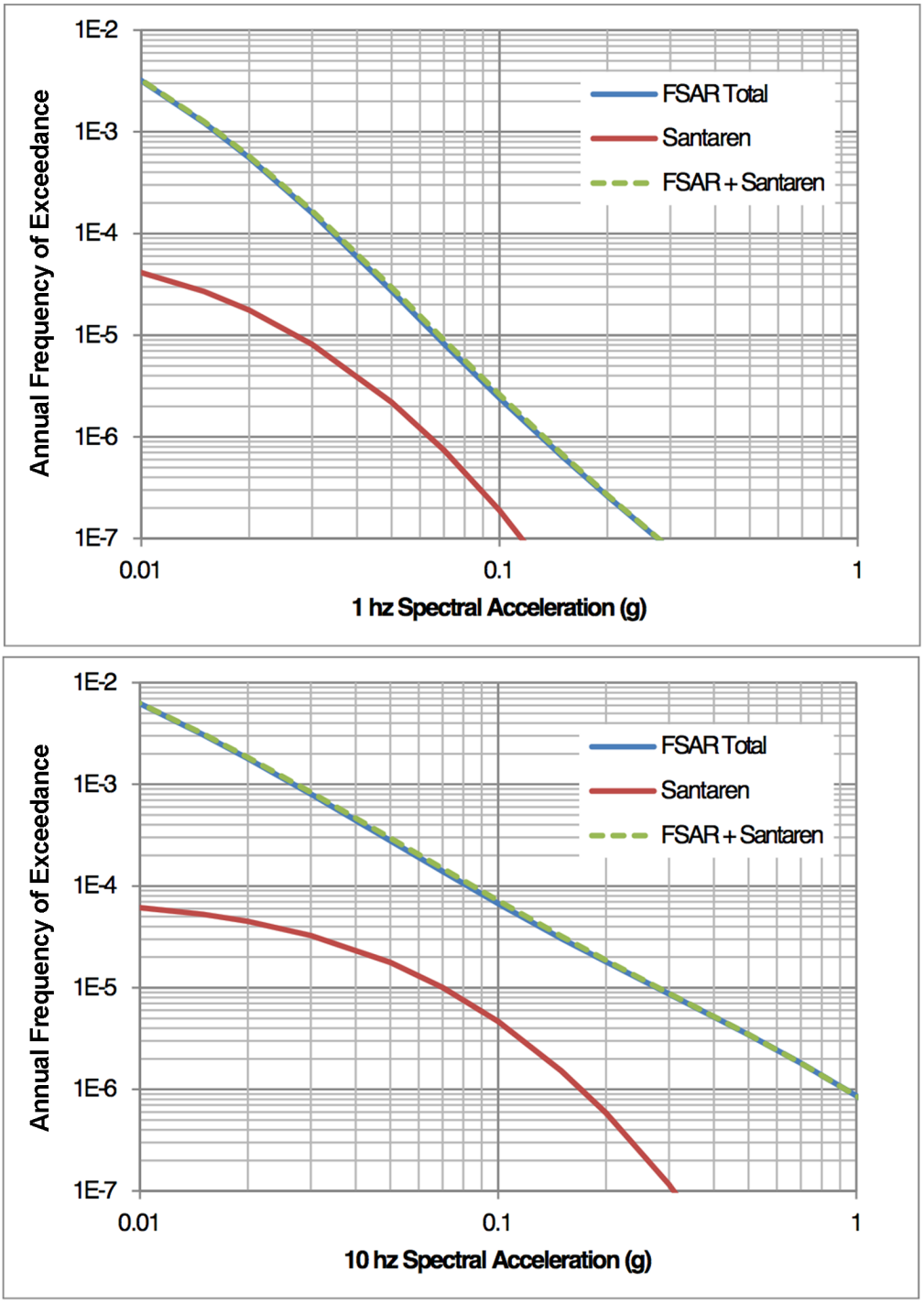

Figure 2.5.2-286 1 Hz and 10 Hz Mean Hazard Curves Showing Sensitivity to Santaren Anticline Fault Source